Dissertation

Environmental use of volcanic soil as natural adsorption material

erstellt am

Department of Sustainable Waste Management and Technology, University of Leoben, Austria

Vorgelegt von:

Dipl. Ing. Rodrigo Navia

0135208

Betreuer:

O. Univ. Prof. Dipl.-Ing. Dr. Karl E. Lorber

Gutachter:

O. Univ. Prof. Dipl.-Ing. Dr. Karl E. Lorber

Prof. Dr.-Ing. Martin Jekel

Leoben, November 2004

EIDESSTATTLICHE ERKLÄRUNG

Ich erkläre an Eides statt, dass ich die vorliegende Dissertation selbständig und ohne fremde Hilfe verfasst, andere als die angegebenen Quellen und Hilfsmittel nicht benutzt und die den benutzten Quellen wörtlich und inhaltlich entnommenen Stellen als solche erkenntlich gemacht habe.

To Francisca and Aitana

ACKNOWLEDGEMENTS

Abstract

Environmental use of volcanic soil as natural adsorption material

In this work, three possible environmental applications of a volcanic soil have been tested: adsorption of wastewater pollutants from bleached Kraft mill effluent, adsorption of chlorophenols from synthetic groundwater and adsorption of heavy metals from a synthetic landfill leachate. The evaluated adsorption capacities of the volcanic soil are comparable with natural zeolites. Moreover, the physico-chemical and mineralogical characteristics of the volcanic soil suggest a possible use as a full-scale sanitary landfill mineral liner.

For wastewater and groundwater remediation processes, a porous ceramic material was developed from natural volcanic soil, based on a patented foaming-sintering process that uses recycled PET as the main raw material. This material was developed for resisting hydraulic loads, as well as to prevent attrition losses and sludge formation during contaminated water treatment. The obtained ceramic material has a very stable structure and batch adsorption experiments show an enhanced adsorption capacity compared with natural soil.

Finally, two sustainable waste management ways for the spent volcanic soil, i.e., contaminated with chlorophenols or heavy metals, were also studied. The main sound alternatives include bioremediation (for chlorophenols) and immobilization (for heavy metals). Therefore, a natural attenuation process, including the chlorophenols-contaminated soil biological activity, and the possible use of the heavy metal-contaminated volcanic soil in the clinker/cement production were evaluated. In the case of chlorophenols-contaminated soil, the soil biological activity and bioremediation capacity indicates that the microorganisms present in this soil are able to degrade the adsorbed chlorophenols. In the case of contaminated soil use in the clinker/cement production, the metal oxides content of the volcanic soil (SiO_2, Al_2O_3 and Fe_2O_3) can be used for the substitution of clay and/or correction materials in the primary clinker mixture. It was concluded that only some small emission problems would occur in the worst-case scenario, while using pet-coke and scrap-tires as alternative fuel in the clinker kilns. In this case, the Pb and Zn content in the flue gas can surpass the maximum level described in the draft project of the new Chilean emission law for incineration and co-incineration of wastes.

Contents

1   Introduction

In some South American countries, like Chile for example, new environmental regulations have been worked out in the last ten years. These regulations are now the new framework for international and national investors, and are forcing these countries to make investments in wastewater and solid waste management and treatment facilities, as well as in groundwater remediation processes.

In the case of industrial wastewater treatment facilities, primary physico-chemical treatments and secondary aerobic biological processes have been commonly used, basically due to their simplicity and economical attractiveness, as they rapidly treat biodegradable wastewater pollutants. Nevertheless, these new regulations are forcing treatment technologies to be more efficient, looking for the avoidance of environmental impacts from the wastewater discharges and, when possible, to reuse the treated wastewater. Many industrial effluents are composed of a fraction of non-easily biodegradable pollutants (e.g. pulp and paper industry, chemical industry, textile industry and others), therefore needing advanced or tertiary treatment units. Adsorption is one of the most common technologies used in advanced (waste)water treatment facilities, where activated carbon has been used as the main important adsorption material for the removal of trace organic compounds, such as mutagenic and toxic compounds [1]. Nevertheless, the high cost of this adsorption material (between 2 and 7 €/kg) and its low selectivity has pushed the technologists to continue investigating on alternative cheaper and more selective adsorbents. New research work regarding non-conventional adsorption materials has been focused mainly on waste material [2]; carbonized coconut shell, wood, coal, straw and rubber [3]; cucurbituril [4]; ion exchange resins [5],[6]; aluminun oxide and ferric hydroxide [7]; organoclays [8],[9] and volcanic soils [10],[11].

Regarding groundwater remediation processes, since the late 70´s the on-site pump & treat process has been extensively used for groundwater depuration. The groundwater is pumped, treated normally in a filter/adsorbent system and returned to the ground. Sand filters, granular activated carbon adsorbers, biofilters and advanced oxidation processes have been commonly used as treatment systems. A novel process, the reactive walls in-situ process (e.g. "funnel & gate" system), is also an interesting technology developed for groundwater remediation in the last ten years. This technology relies upon an in-situ installation of a reactive barrier to allow physico-chemical adsorption of the pollutants presents in the groundwater plume. Activated carbon, minerals and zero-valent metals are the most used adsorbent materials with interesting application as reactive walls for contaminant compounds adsorption [12],[13].

In the case of solid wastes, in Europe they are normally separated at source, recycled, treated and finally disposed in sanitary landfills. Sanitary landfills are commonly designed under the "multibarrier system" concept in which clay mineral layers play an important role as constituents of landfill barriers, preventing the breakthrough of hazardous contaminants

[14],[15]. Typical mineral landfill barriers are clays, bentonite and zeolites, which are the main natural adsorption materials marketed in Europe.

1.1   Problem description

New cheaper and selectively adsorption materials are needed to be developed for their use in wastewater treatment facilities (tertiary/advanced processes), groundwater remediation processes (e.g., as reactive wall) and in sanitary landfills (as mineral clay liners), particularly in developing countries, where the costs of these adsorption materials could be prohibitive in certain cases.

1.2   Objectives and goals

The following objectives and goals are envisaged in this work:

➢   To evaluate the possible use of volcanic soil as a natural adsorption material in wastewater treatment facilities, especially in the pulp and paper industry.

➢   To evaluate the possible use of volcanic soil as a natural adsorption material in groundwater remediation processes, especially regarding chlorophenols remediation.

➢   To evaluate the possible use of volcanic soil as a mineral liner in sanitary landfills, especially regarding heavy metals retention.

➢   To evaluate the development of a stable ceramic porous material based on volcanic soil for its use in wastewater and groundwater treatment facilities.

➢   To evaluate the most suitable waste management options for spent contaminated volcanic soil, especially regarding bioremediation and its possible use in clinker/cement facilities as an alternative raw material.

2   Theoretical background

2.1   Adsorption and adsorbent materials

Adsorption is an interfacial phenomenon resulting from the differential forces of attraction or repulsion occurring among molecules or ions of different phases at their exposed surfaces. As a result of cohesive and adhesive forces coming into play, the zones of contact among phases may exhibit a concentration or a density of material different from that inside the phases themselves. A distinction should be made between adsorption, which is a surficial attachment or repulsion, and absorption, which refers to cases in which one phase penetrates or permeates another. In reality, it is often impossible to separate the phenomenon of adsorption from that of absorption, particularly in the case of highly porous systems, thus the noncommittal term sorption is frequently employed [16]. As different phases come in contact, various types of adsorption can occur: adsorption of gases on solids, of gases in liquid surfaces and of liquids as well as solutes on solids. In adsorption processes, a distinction has been attempted between physical and chemical adsorption. Physical adsorption involves mainly Van der Waals forces characterized by low energies of adsorption (less than 20 kJ/mol), while chemical adsorption involves the formation of stronger and more permanent bonds of a chemical nature (between 80 and 400 kJ/mol) [16]. To interpret these two kinds of adsorption mechanisms and the adsorption data, the Freundlich and Langmuir isotherms models are mainly used. As the Freundlich isotherm is in fact an empirical model, the Langmuir equation was the first theoretical one that introduced a clear concept of the monomolecular adsorption on energetically homogeneous surfaces. The statement proposed by Langmuir was applied to chemisorption and with some restrictions to physical adsorption [17].

As follows from the aforementioned considerations, the development and application of adsorption cannot be considered separately from the development and manufacture of adsorbents. These adsorbents can take a broad range of chemical forms and different geometrical surface structures and can be applied selectively for the removal of different environmental pollutants. In Table 1, the basic types of industrial adsorbents used nowadays are described. Activated carbons, zeolites, and clay minerals are the most applied adsorbent materials in environmental technology. Moreover, waste-derived adsorbents, zero-valent metals and natural soil are promising novel adsorbent materials with interesting environmental applications.

2.1.1   Activated carbon

Activated carbon is mainly used in drinking and wastewater treatment facilities, as well as in groundwater remediation and it is capable to adsorb a wide range of organic and inorganic pollutants present in water systems. Its amphoteric character governs adsorption onto activated carbon. In fact, in response to pH changes, the carbon surface develops coexisting electric charges of opposite sign, whose prevalence depends on the chemistry of the

solution. Therefore, attractive or repulsive electrostatic interactions between the adsorbate and the adsorbent must be taken into consideration [18]. Activated carbon can adsorb heavy metals like Cr(III), Cr(VI), Mo, Co, Ni, Cu, Zn, Cd, Hg, Pb, U, Au and As, as well as phosphates [18], phenols [3], substituted phenols and benzenes [19],[20], dyes [21], natural organic matter (NOM) [18], and other organics like trihalomethanes, amines, chlorinated organic compounds, alcohols, carboxylic and fatty acids, amino acids and others [18]. Due to its wide range of adsorption spectra, activated carbon is considered a non-selective adsorption material. In addition, the high cost of this adsorption material (between 2 and 7 €/kg) has pushed the technologists to search for other cheaper and selectively adsorption materials, as mentioned before.

Table 1: Basic types of industrial adsorbents (adapted from [17])

Carbon adsorbents	Mineral adsorbents	Others
Activated carbons	Silica gels	Synthetic polymers
Activated carbon fibers	Activated alumina	Composite adsorbents
Molecular carbon sieves	Metal oxides	Mixed sorbents
Mesocarbon microbeds	Metal hydroxides	
Fullerenes	Zeolites	
Heterofullerenes	Clay minerals	
Carbonaceous nanomaterials	Pillared clays	
	Porous clay hetero-structures	
	Inorganic nanomaterials	

2.1.2 Zeolites

Only in recent years increasing attention has been directed towards natural zeolites, whose status changed from that of museum curiosity to an important mineral commodity. Several thousand tons of natural zeolite bearing materials are mined in the United States, Japan, Italy, Germany, Czech Republic, Turkey, Bulgaria, Cuba, Mexico, Korea, and other countries but only those containing chabazite, clinoptilolite, erionite, ferrierite, philippsite, mordenite and analcime are available in sufficient quantity and purity to be considered as exploitable natural resources [22]. Zeolites are one of the main natural adsorption materials of the European market, with a current price of around 0.1 €/kg. Clinoptilolite is the most abundant zeolite in nature because of its wide geographic distribution and large size of deposits [23].

Zeolites have a three-dimensional structure constituted by (Si, Al)O_4 tetrahedra connected by all their oxygen vertices forming channels where H_2O molecules and exchangeable cations are present counterbalancing the negative charge generated from the isomorphous substitution [24]. The isomorphous replacement of Si^{4+} by Al^{3+} in its structure, gives rise to a deficiency of positive charge in the framework, which is in fact balanced by mono and divalent exchangeable cations like Na^+, Ca^{2+}, K^+ and Mg^{2+}. These cations are coordinated

with the defined number of water molecules, located on specific sites in framework channels. The sorption on zeolitic particles is a complex process because of their porous structure, inner and outer charged surfaces, mineralogical heterogeneity, existing of crystal edges, broken bonds and the imperfections on the surface, but cation exchange due to isomorphous replacement of Al^{3+} by Si^{4+} in the structure is the main mechanism involved [25]. The advantages of zeolites are their low cost and ion selectivity generated by their rigid porous structure. Zeolites have also a wide range of application, mainly based on their structural characteristics, sorbent properties and high specific surface area. Zeolites have been used as molecular sieves, as water softeners, as removers of ammonium from urban, agricultural and industrial wastewaters [26], and of toxic gases from gaseous emissions, as well as filters for odor control [24]. Zeolites are capable to adsorb heavy metals like Zn, Cu, Pb, Cr(III), Ni, Cd and Fe [23],[24],[27]. In addition, aluminum-loaded zeolite is able to adsorb arsenic(V) from drinking water [28]. Moreover, the application of zeolites as landfill mineral liners to prevent the breakthrough of various environmental pollutants is also becoming a common practice [29],[30].

2.1.3   Clay minerals

Clay minerals, which comprise the smallest particles in the soil, are defined as the fraction with particles smaller than a nominal diameter of 2 µm. They are usually classified into two main groups, structured and amorphous. The most common clay mineral of the structured type is kaolinite, which is part of the 1:1 subgroup, and montmorillonite, which is part of the 2:1 clay structured minerals subgroup. In Table 2 the typical properties of selected clay minerals are shown.

In the case of kaolinite, from the subgroup 1:1 (which signifies the silica/alumina ratio), the basic layer crystal structure is a pair of silica-alumina sheets, which are stacked in alternating fashion and held together by hydrogen bonding in a rigid multilayered lattice that often forms a hexagonal platelet. Because of this rigidity, only the outer faces and edges of the platelets are exposed, and therefore kaolinite has a rather low specific surface [16]. The unit layer formula of kaolinite is $Al_4Si_4O_{10}(OH)_8$. At the opposite end of the spectrum of aluminosilicate clay minerals is montmorillonite. The lamellae of montmorillonite are stacked in loose assemblages called tactoids. As the montmorillonite crystals expand, their internal as well as external surfaces come into play, thus increasing the specific surface area several fold. One of the most common clay minerals from the montmorillonite family is bentonite, which swelling properties are due to its content of montmorillonite [31]. A typical unit layer formula of montmorillonite is $NaAl_5Mg(Si_4O_{10})_3(OH)_6 \cdot nH_2O$. A clay mineral with intermediate properties between kaolinite and montmorillonite is illite. It belongs to a group of clay minerals called hydrous micas, which have a 2:1 silica/alumina ratio but are nonexpanding. Isomorphous substitution of aluminum ions for silicon ions in the tetrahedral sheets (rather than Mg^{2+} for Al^{3+} in the octahedral sheets, as in montmorillonite), to the extent of about 15%, accounts for the relatively high density of negative charges in these sheets. This attracts potassium ions and fixes them tightly between adjacent lamellae. As a result, the layers

bound together, so the expansion of the lattice is effectively prevented. A typical layer formula of illite is $KAl_4(Si_7AlO_{20})(OH)_4$. An example of a 2:2-type mineral is chlorite, wherein magnesium rather than aluminum ions predominate in the octahedral sheets, which are in combination with tetrahedral silica sheets. Its typical unit formula is $Mg_6Si_4O_{10}(OH)_8$, with $Mg_6(OH)_{12}$ occurring between the layers.

The clay fraction may also contain quantities of non-crystalline (amorphous) mineral colloids. Allophanes, for instance, are random combinations of poorly structured silica and alumina components expressible in the general formula $Al_2O_3 \cdot 2SiO_2 \cdot H_2O$, where the mole ratio of alumina to silica ranges between 0.5 and 2.0 [16]. Allophane is considered a non-crystalline hydrous aluminosilicate characterized by a short-range ordered nature and by the presence of Si-O-Al bonds [32]. Its main characteristics are a high specific surface, between 310 and $672 m^2/g$ [33], and its capacity to develop a pH-variable charge [34].

Another important constituent of the clay fraction is the group of hydrous oxides of iron and aluminum. These are prevalent mainly in tropical and subtropical regions and their composition can be formulated as $Fe_2O_3 \cdot nH_2O$ and $Al_2O_3 \cdot nH_2O$ in which the hydration ratio is variable. Hematite (α-Fe_2O_3), maghemite (β-Fe_2O_3), goethite (α-FeOOH) and lepidocrocite (β-FeOOH) are typical iron oxides, and gibbsite ($Al(OH)_3$) and boehmite (β-AlOOH) are frequently encountered aluminum oxides. These mineral oxides are partly crystallized and partly amorphous [16],[35].

Table 2: Typical properties of selected clay minerals (adapted from [16],[33])

Property	Clay mineral				
	Kaolinite	Illite	Montmorillonite	Chlorite	Allophane
Planar diameter [µm]	0.1-4.0	0.1-2.0	0.01-1.0	0.1-2.0	-
Basic layer thickness [Å]	7.2	10.0	10.0	14	-
Particle thickness [Å]	500	50-300	10-100	100-1000	-
Specific surface [m^2/g]	5-20	80-120	700-800	80	310-672
CEC [cmol+/kg]	3-15	15-40	80-100	20-40	40-70
Area per charge [$Å^2$]	2.5	50	100	50	120

CEC: Cation exchange capacity

Clay minerals have a wide range of environmental applications and are able to adsorb several pollutants. Cation exchange as well as complex surface reactions are recognized as the main mechanisms involved in clay adsorption processes [36]. For instance, as landfill liner materials in laboratory columns, clay minerals are able to attenuate BTEX (benzene, toluene, ethylbenzene and xylene), pesticides, chloro-aromatic and chloro-aliphatic compounds, inclusively degrading some of them into the clay structure [37],[38]. Some phenols and chlorinated phenols have been found to adsorb onto modified montmorillonites [39],[40] as well as some heavy metals like Cd, Cr(III), Cu, Mn, Ni, Pb and Zn [41]. In

addition, arsenic, as As(III) and (V), has been found to adsorb strongly onto amorphous iron oxide, goethite and modified montmorillonites [42].

2.1.4   Waste-derived adsorbents

Extensive research regarding non-conventional low-cost adsorption materials has been undertaken mainly to identify the possible reuse of some organic and inorganic wastes. Inorganic waste materials act as pure adsorbents, while organic waste materials could act as adsorbents as well as biosorbents, because of the microbiological flora present in them.

Fly ash from thermal power stations and dried activated sludge were used to adsorb and biosorb 2- and 3-chlorophenol, respectively, with satisfactory results [20]. Furthermore, chlorophenols and nitrophenols were found to adsorb strongly onto a cheap carbonaceous material obtained from the waste slurry generated in fertilizer plants [2], while cheaper activated carbons based on coconut shell, wood, coal, straw and tires were tested successfully for the removal of phenol and p-chlorophenol from contaminated water [3].

Bagasse fly ash, a sugar industry waste, has been recently investigated for the removal of some specific toxic and carcinogenic compounds such as pesticides based on a chlorobiphenyl structure [43]. This same residue is also capable to remove Cd and Ni from wastewater streams [44].

Low-cost adsorbents obtained from organic residues have also been developed for the removal of hexavalent chromium, which is often found in the wastewater discharges from electroplating, metal finishing and chrome preparation, and is considered to be highly toxic with a potential carcinogenic effect. At acidic pH, sawdust, sugar cane bagasse, sugar beet pulp and corn cob, which are naturally occurring cellulosic waste materials, are able to adsorb Cr(VI) present in contaminated water [45]. Moreover, Cu and Cd ions have been found to adsorb successfully onto bone char [46], while Al, Ca, Cd, Cu, Fe, Mg, Ni, Pb and Zn ions (especially Pb) were efficiently removed from an acidic leachate by cocoa shells and, to a lesser degree, by cedar bark [47].

Regarding colored effluents, these wastewaters are not only aesthetically displeased, but they also impede light penetration, thus upsetting biological processes within a stream. In addition, many dyes are toxic to some organisms and may cause direct destruction of aquatic communities, needing some form of advanced treatment. Adsorption of acid and basic dyes present in aqueous solutions onto low-cost adsorbents such as bagasse pith, peat, corn cob, bean waste, sugar-industry-mud have presented very successful results [48], as well as onto low-cost sewage sludge-based activated carbon [49].

2.1.5   Zero-valent metals

Zero-valent metals are one of the most promising adsorbent materials with an interesting application for pollutants adsorption in in-situ groundwater remediation processes and are

partially displacing the on-site groundwater treatment processes like "pump & treat". In this process, the groundwater is pumped, treated normally in a filter/adsorbent system and returned to the ground, but the growing tendency is moving to in-situ remediation technologies [13]. Fe^0, Al^0, Zn^0, Ni^0, Cu^0, Pd^0/C and combinations of them have been tested successfully for organochlorides removal from groundwater. Moreover, it has been demonstrated that zero-valent iron is capable to produce the reductive dechlorination of a great spectra of chlorinated organic compounds [50] (see Chapter 2.6.2).

2.1.6   Natural soils

The development and research regarding abundant, cheap and selectively natural adsorbents has been mainly focused on special soils. Such kinds of soils have been recently investigated for their pollutants adsorption and remediation capacity. As they are normally present in an abundant form in the environment, they could consequently present interesting costs advantages. Historically, the porosity and pore size distribution of soil were of interest primarily for their effects on water retention and flow, advection and diffusion of gases and transport of nutrients. With the emergence of concern about environmental pollution, the pore structure of soils has come to be recognized as a critical factor in the sorption of pollutants. Sorption is of underlying influence on the transport, chemistry and biological activity of pollutants.

Soil is composed of individual minerals and organic matter grains that are cemented together to form particles. These particles, in turn, may agglomerate to form higher ordered structures [51]. Mainly the association of its mineral and organic parts control the porosity of the soil system, having soil water a strong effect. From the point of view of potential interactions with various pollutants, the constituents of the soil solid phase should be grouped according to their surface area. The fate of pollutants is affected by all the components of the soil solid phase. The soil constituents with low surface area could, however, mainly affect the transport of the pollutants as solutes, as immiscible with water liquids, or as vapors. The soil solid phase can also indirectly induce the degradation of the organic pollutants in the soil medium, through its effects on the water/air ratio in the system and, consequently, on the biological activity of the soil. The group of constituents with high surface area controls, besides the transport of pollutants, their retention, and release on and from the soil surface, as well as their surface-induced chemical degradation [35].

In their clay fraction, soils could contain a variety of minerals, e.g., oxide minerals (as discussed before as clay minerals), calcium carbonates and calcium sulphates. Many soils formed from the appropriate parent materials contain significant quantities of relatively high surface, soluble calcium carbonate ($CaCO_3$) or calcium sulphate ($CaSO_4$). Some agricultural soils may contain more than 50% $CaCO_3$ and almost the same percentage could characterize the sulphated soils from an arid and semiarid region [35].

Soil organic matter (SOM) is defined as the nonliving portion of the soil organic fraction, and is formed by decomposed plant and microbial material. Except in the litter zone, the bulk

SOM consists of humic substances that bear little physical and chemical resemblance to their precursor biopolymers [52]. SOM also contains smaller amounts of lipid-soluble materials and recognizable protein and carbohydrate fragments. Humic substances are composed of fulvic acid (water soluble), humic acid (water soluble only at alkaline pH) and humin (insoluble at all pH), all of which are structurally related [51]. These dark-colored pigments extracted from the soil are produced as a result of multiple reactions; the major pathway being through condensation reactions involving polyphenols and quinones. Polyphenols derived from lignin are synthesized by microorganisms and enzimatically converted to quinones, which undergo self-condensation or combine with amino compounds to form N-containing polymers [35]. The major components of SOM and their definitions are presented in Table 3.

Table 3: Definitions of SOM components of soil (adapted from [51],[52])

Term	Definition
Litter	Macroorganic matter that lies on the soil surface (e.g., plant residues)
Light fraction	Undecayed plant and animal tissues and their partial decomposition products that occur within the soil proper and that can be recovered by flotation with a liquid of high density
Soil biomass	Organic matter present as live microbial tissue
Humus	Total of the organic compounds in soil exclusive of undecayed plant and animal tissues, their partial decomposition products and the soil biomass
Humic substances	A series of relatively high molecular weight, yellow to black colored substances formed by secondary synthesis reactions. The term is used as a generic name to describe the colored material or its fractions obtained on the basis of solubility characteristics. These materials are distinctive to the soil environment in that they are dissimilar to the biopolymers of microorganisms and higher plants (including lignin)
Nonhumic substances	Compounds belonging to known classes of biochemistry, such as amino acids, carbohydrates, fats, waxes, resins, organic acids, and others. Humus probably contains most, if not all, of the biochemical compounds synthesized by living organisms
Humin	The insoluble fraction of SOM or humus
Humic acid	The dark-colored organic material that can be extracted from soil by dilute alkali and other reagents and that is insoluble in dilute acid
Fulvic acid	Fraction of SOM that is soluble in both, alkali and acid
Generic fulvic acid	Pigmented material in the fulvic acid fraction

The soil solid phase surface is heterogeneous and is characterized by multicomponent association among humic substances, clays, metal oxides, $CaCO_3$ and other minerals. In some cases, up to the 90% of the soil organic matter could be found to be associated with the mineral fraction of the soil. The most extended interactions between components of the soil solid phase are those between clay minerals and organic matter, forming the so-called clay-humate or metal-humate complexes [32],[35]. This association between organic (humic) substances and clay surface may be controlled by the properties of both components and various mechanisms can contribute to it (see Table 4). All these adsorption mechanisms are

expected to operate when dissolved organic matter reacts with the clay surfaces. Like clay, at typical natural pH, humic molecules are polyanionic due to acid dissociation of some of the carboxylic (-COOH) and phenolic (-OH) groups. Since the cation exchange process depends on replacement of the hydrogen in these groups, it is pH dependent, with the cation exchange capacity generally increasing at higher pH values [16].

Table 4: Mechanisms of adsorption of organic (humic) compounds to clay surface in soil (adapted from [35])

Mechanism	Principal organic functional group involved
Cation exchange	Amines, ring-NH, heterocyclic N
Protonation	Amines, heterocyclic N, carbonyl, carboxylate
Anion exchange	Carboxylate
Water bridging	Amino, carboxylate, carbonyl, alcoholic OH
Cation bridging	Carboxylate, amines, carbonyl, alcoholic OH
Ligand exchange	Carboxylate
Hydrogen bonding	Amines, carbonyl, carboxyl, phenylhydroxyl
Van der Waals interactions	Uncharged, nonpolar organic functional groups

As described, humic substances, clays, clay-humate and metal-humate complexes, metal oxides, and other minerals present in the soil solid phase will participate in the sorption process of environmental pollutants. The adsorption mechanisms involved in pollutants adsorption onto soil are supposed to be similar to those described in Table 4. Furthermore, during hydration, each humic "particle" forms a micelle and act as a giant, composite anion, capable of adsorbing various organic and inorganic compounds, including cations [16].

In addition, some specific soil and environmental properties may affect this sorption of pollutants onto the soil matrix, as described in Table 5. It is well established that hydrophobic pollutants sorb predominantly to the SOM component. In fact, the affinity of non-hydrogen bonding compounds for the surfaces of hydroxylated, non-microporous minerals, such as SiO_2, α-Al_2O_3 and α-Fe_2O_3, is extremely small in the presence of water. Sorption of weakly polar hydrophobic compounds to SOM predominates as long as the fraction of organic carbon is above 0.01% of the total soil mass [53]. The cation exchange capacity (CEC) of humic substances is much greater, per unit mass, than that of clay and consequently the sorption per unit mass of SOM is several orders of magnitude higher than per unit mass of mineral fraction [54]. Therefore it is established that SOM provides an organophilic medium for escape of hydrophobic molecules from water.

Regarding water in the soil matrix, it can influence the soil sorbent properties. At high relative humidity (> 70%) the hydroxylated surfaces of metal oxide particles - which provide the bulk of mineral surface area in soils - are coated with multiple layers of water molecules, the first one or two of which are strongly adsorbed. In addition, the micropores and many of the mesopores of the fixed pore system are water filled and SOM is swollen with water. Thus,

pollutant molecules must travel through water or a water-swollen phase to reach sorption sites [51].

Table 5: Parameters affecting sorption of contaminants to soil (adapted from [55])

Parameter	General effect on sorption
Soil type	
Organic matter	Sorption increasing with increasing organic matter
Clay	Sorption increasing with increasing clay content
Sand	Sorption decreasing with increasing sand content
Soil properties	
Surface area	Adsorption increasing with increasing the surface area
CEC	Adsorption increasing with increasing the CEC
Environmental parameters	
Temperature	Sorption decreasing with increasing temperature
Soil moisture	Sorption decreasing with increasing soil moisture
pH	Sorption can vary with pH, often showing a plateau within a certain range

CEC: Cation exchange capacity

In general, sorption of inorganic and organic pollutants onto the soil solid phase is a complex process, but it its well established that both, sorption on the SOM and clay fraction of the soil will participate in this process. The distribution coefficient K_d derived from linear isotherms has been applied to describe this sorption behavior, as shown in Equation 1.

$$(x/m) = K_d * C^*$$ (1)

Where (x/m) is the adsorbed amount of the pollutant onto the soil [mg/g], C^* is the equilibrium concentration of the pollutant in the liquid phase [mg/L] and K_d is the global distribution coefficient in [L/g]. Many authors have suggested that hydrophobic non-ionic pollutants may adsorb only in the SOM of the soil, neglecting the adsorption processes on the clay fraction [54],[56],[57]. However, in clay rich soils with an extremely low organic fraction, the adsorption onto the mineral fraction cannot be neglected. Neglecting the adsorption onto the clay fraction, K_d could be expressed as a function of the organic carbon fraction present in the soil (f_{oc}) and a carbon-normalized partition coefficient (K_{oc}), as shown in Equation 2 [54].

$$K_d = f_{oc} * K_{oc}$$ (2)

As discussed before, this expression will be valid for $f_{oc} > 0.0001$ (or for an organic carbon content of above 0.01% from the total soil mass). Based on linear free energy relationship, the log K_{oc} has been well linearly correlated with the logarithm of the octanol/water partition coefficient of hydrophobic chemicals, K_{ow}, where a_1 and a_2 are regression constants [54],[56] (Equation 3).

$$\log K_{oc} = a_1 + a_2 \log K_{ow}$$ (3)

Combining Equations 1, 2 and 3, Equation 4 is obtained as a linear partitioning relationship for hydrophobic organic pollutants onto the SOM of soils with more than 0.01% organic carbon.

$$(x/m) = f_{oc} * 10^{a_1} * K_{ow}^{a_2} * C^* \qquad (4)$$

In the case where the soil content of organic matter is low, and where high water soluble polar ions are involved in the adsorption process, correlations between the CEC of the sorbent material and the pollutant adsorption capacity have been investigated. For soils with low organic carbon (< 0.01%), the linear distribution coefficient K_d for the adsorption of polar contaminants was correlated as indicated in Equation 5, where a_3 and a_4 are the regression constants [57].

$$K_d = a_3 + a_4 * CEC \qquad (5)$$

Combining Equation 1 with 5, a linear adsorption relationship based on the CEC is obtained (Equation 6).

$$(x/m) = (a_3 + a_4 * CEC) * C^* \qquad (6)$$

In the case of non-hydrophobic pollutants, i.e. heavy metal cations and high water soluble, dissociable, polar compounds, their adsorption process onto soil will be mainly governed by cationic exchange (or anionic exchange in some specific cases) and chemical linkage. Both, SOM and the clay fraction of the soil solid phase will contribute to these cationic exchange capacity and chemical linkage as discussed previously, and the cationic exchange capacity (CEC) of humic substances will be some orders of magnitude higher, per unit mass, than that of the clay fraction. Nevertheless, there is a lack of correlations between the distribution coefficient K_d and the soil properties for the adsorption of polar and hydrophilic compounds onto soils with organic carbon content higher than 0.01%. In these cases, empirical data is needed (isotherms) for evaluating the K_d value from Equation 1.

2.2   Volcanic soils

The term volcanic soil (or volcanic ash-derived soil) is commonly used to designate the soil produced by pyroclastic volcanic eruption materials. Volcanic soil covers more than 1.2 million km^2, about 1% of the total earth surface [58]. Important presence of volcanic soil has been studied and reported in Mexico, Costa Rica, Nicaragua, Chile, Azores Islands, Canaries Islands, Germany, France, Italy, Iceland, Japan and some other countries where different types of volcanic soils can be distinguished.

2.2.1   Chilean volcanic soils

The formation processes of volcanic soils in Chile have been mainly influenced by both the chemical composition of the parent volcanic ashes and the climate of the southern

hemisphere beyond a latitude 35°S (Chillán City), characterized by high annual rainfall (1,500-3,000 mm) and low temperature regimes (12-15°C) [59]. Soil formation resulted in acidic volcanic-derived soils, whose clay fractions are composed of allophane or allophane-like minerals [60]. About two third of the agricultural land in Chile, approximately 0.4 million km^2, is derived from volcanic ash, which are mainly volcanic soils of the Dystrandepts and Palehumult series. Andisols are typical Dystrandep series soils, while Ultisols belong to the Palehumult series [61].

2.2.2   Andisols

Andisols develop themselves preferentially from laxly stored volcanic output material with different chemical composition as volcanic ashes, as well as from lava streams, tuff and ignimbrite. Andisols occur also as volcanic eruptions in all ecological zones [62]. In the horizon sequence, the topsoil is very laxly and mostly colored from brown to black. The clay fraction prevalent consists on spherical close-grained allophane, imogolite and, by advanced development, also on halloysite, which are all originated by weathering of volcanic glasses. In the rest fractions, fresh glasses prevail in young andisols, while in old andisols stable decomposed silicates (from non-volcanic origin) have enriched. Andisols are due to their high water retention capacity and their stable pore rich microstructure, considered as excellent locations for plant growth. They are characterized by a high variable charge and therefore dispose by alkaline pH values a high cationic exchange capacity and by acidic pH a strong phosphor bond and fixation capability [63].

In general, it is possible to distinguish two types of andisols: vitric and andic. The very young and relative not weathered vitric andisols consist in up to 60% (vol.) of volcanic glasses, while strong weathered andic andisols distinguish themselves by allophane abundance or aluminum-humus complexes. The aluminum present in the volcanic output material dissolves through weathering processes and forms stable aluminum-complexes with organic substances. These immobile complexes gather themselves on the surface and build a dark and humic rich horizon (called A horizon). The soil solution can also contain high quantities of dissolved Si, which in contact with Al leads to the formation of secondary minerals (like allophane) from the saturated soil solution. Only increasingly weathering leads to a depletion of the glass fraction and to silicon decrease in the soil solution, which results in the conversion of meta-stable in stable crystalline minerals [58]. Under the mineralogical properties of andisols it is possible to distinguish between allophanic andisols and non-allophanic andisols. The general average composition of these two types of andisols is shown in Figure 1. Particular characteristic from these types of andisols are the non-crystalline components, such as allophane, imogolite and others like opal and non-crystalline ferrous oxides. The chemical composition of these mineral components is not fixed and they do not have a regular three-dimensional grid structure. The mineralogical composition of the colloid fraction from andisols varies depending on the chemical, mineralogical and physical properties of the volcanic output material and on the soil-forming state.
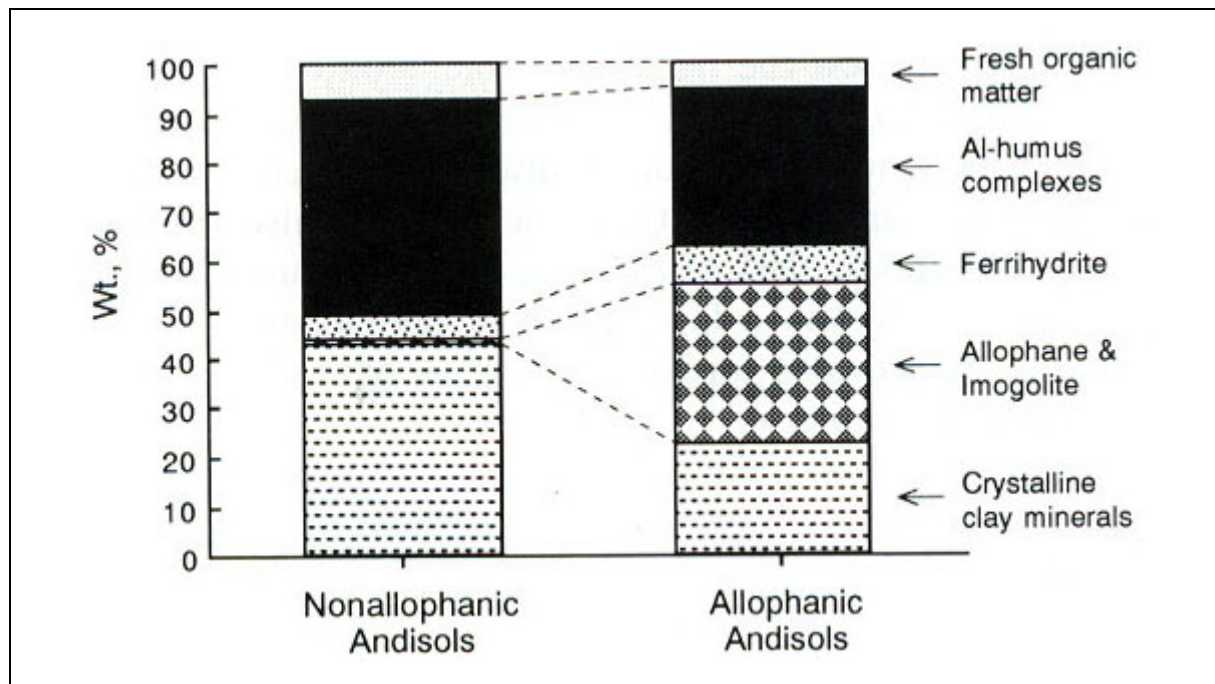
Figure 1: Average composition of allophanic ad non-allophanic andisols (Wt.: Weight) [64]

2.2.3 Chilean andisols

The Temuco Andisol (also known as "Trumao" soil) is one of the most common soils in Chile, with a total covered surface of about 33,000 km^2. Allophane is the main component of the clay fraction of andisols of Southern Chile and is considered a non-crystalline hydrous aluminosilicate characterized by a short-range ordered nature and by the presence of Si-O-Al bonds [32]. Its main characteristics are a high specific surface, between 310 and 672 m^2/g [33], and its capacity to develop a pH-variable charge [34]. Furthermore, the high organic matter content in these soils suggests that a substantial portion of the organic matter forms stable complexes with allophane through its binding to Fe and Al hydroxide active sites [32]. Therefore, the volcanic soil works as a dual adsorbent; the organic matter present in the soil has a great affinity with pollutants that have a high log K_{ow} value, because of the presence of humic and fulvic acids (i.e. –COOH and phenolic –OH reactive groups). In addition, the clay reactive sites can also be involved in fixing organic pollutants onto the soil matrix, as it is known that the organic matter adsorption on clay occurs by ligand exchange with the surface hydroxyl groups, and therefore it follows that the Fe-humate and Al-humate complexes can influence the soil reactivity [32]. In addition, ions (like heavy metals) can be adsorbed by ion exchange and chemical linkage to the soil surface, as discussed before.

2.3 Chlorophenols in the environment

The Cluster Rule, recently introduced by the United States Environmental Protection Agency (US EPA) [65], regulates the level of 12 chlorophenols in the environment (Figure 2). In addition, other chlorophenols that have been found frequently in the surrounding environment and have some important toxicity are presented in Figure 3.
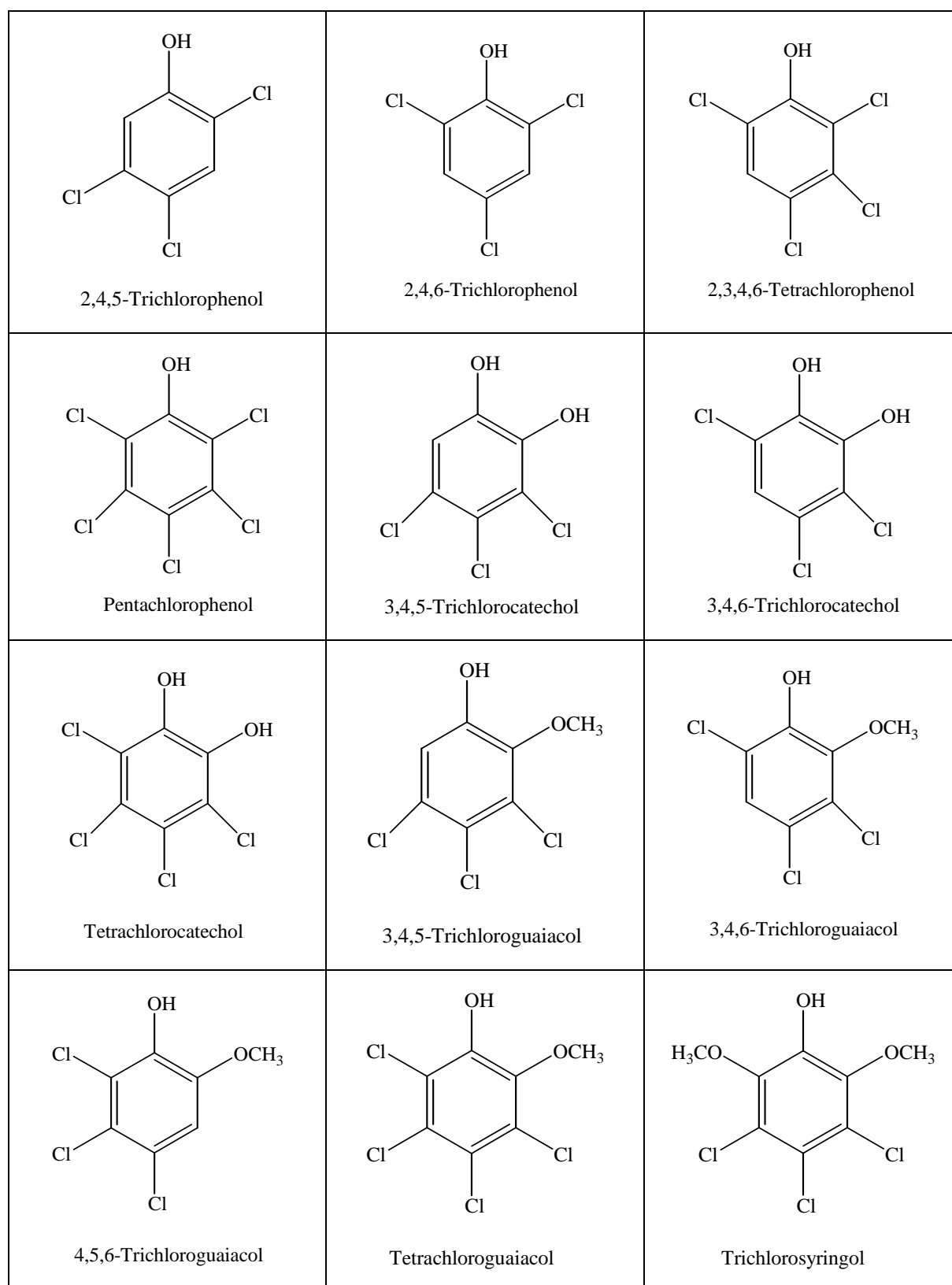
Figure 2: Chlorophenols regulated by the Cluster Rule (adapted from [65])

In fact, the most important chlorophenols present in groundwater streams in the USA and Germany are 2,4,5-trichlorophenol, 2,4,6-trichlorophenol, 2,4-dichlorophenol, 2-chlorophenol, 3-chlorophenol and pentachlorophenol [66]. Moreover, these six compounds are in the list of the most common contaminants present in groundwater streams at contaminated sites. In

addition, although 2,4,5-trichlorophenol, 2,4,6-trichlorophenol, 2,4-dichlorophenol, 2-chlorophenol and pentachlorophenol are in the third group of priority contaminants, 3-chlorophenol and 2,6-dichlorophenol could join the first or the second group as its toxicity is not jet well established [66]. The physico-chemical properties of chlorinated phenols present in the soil-aquifer media and the environmental conditions will determinate the fate of these compounds. The adsorption and desorption kinetics of chlorophenols to soil depends primarily on the number of chlorine substitutions, and to a lesser degree the position on the phenol ring [67].
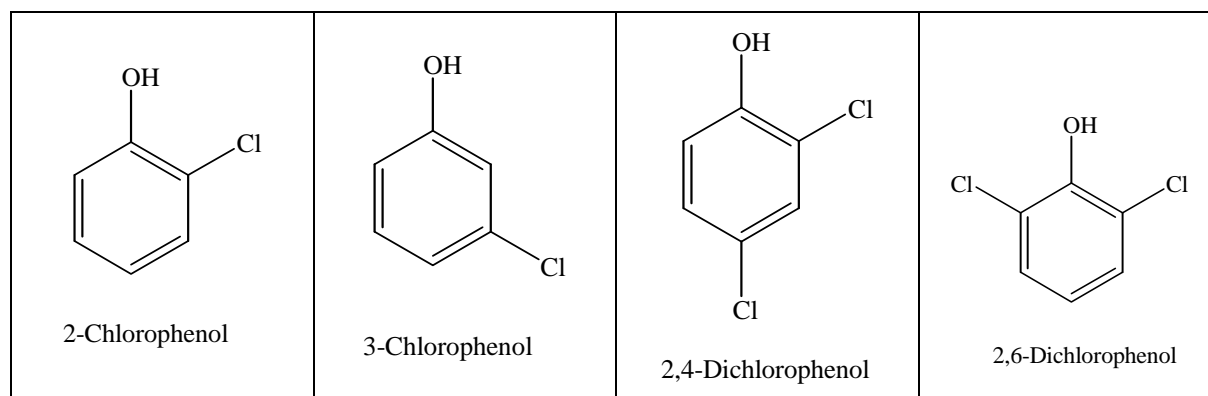
Figure 3: Other cholorophenols with important toxicity present in the soil-aquifer environment

Table 6: Physico-chemical properties of relevant chlorinated phenols (adapted from [68])

Contaminant	MW [g/mol]	log K_{ow}	Solubility[a] [mg/L]	Boiling Point[b] [°C]	pK$_a$	Vapor Pressure[a] [mmHg]	Henry's Constant[a]
2-CP	128.6	2.17	$2.3 * 10^4$	175	8.5	1.00	$3.0 * 10^{-4}$
3-CP	128.6	2.50	$2.2 * 10^4$	214	9.1	0.32	$1.0 * 10^{-4}$
2,4-DCP	163.1	3.08	$4.5 * 10^3$	210	7.9	0.14	$2.7 * 10^{-4}$
2,6-DCP	163.1	2.86	$2.6 * 10^3$	219	6.8	0.24	$8.1 * 10^{-4}$
2,4,5-TCP	197.5	3.72	$7.2 * 10^2$	249	7.2	0.05	$7.4 * 10^{-4}$
2,4,6-TCP	197.5	3.69	$7.1 * 10^2$	246	6.5	0.03	$4.5 * 10^{-4}$
2,3,4,6-TeCP	232.0	4.10	$1.8 * 10^2$	150	5.4	$5.9 * 10^{-3}$	$4.1 * 10^{-4}$
PCP	266.3	5.01	$1.8 * 10^1$	310	4.7	$9.4 * 10^{-4}$	$7.5 * 10^{-4}$

CP: chlorophenol, DCP: dichlorophenol, TCP: trichlorophenol, TeCP: tetrachlorophenol PCP: pentachlrophenol, MW: molecular weight, [a]: in water at 25°C, [b]: at 760 mmHg

From Table 6 and looking the log K_{ow} values, it is clearly stated that non-ionic PCP has a great affinity with organic matter and will remain probably adsorbed onto the soil organic matter (SOM) in the unsaturated zone. Moreover, non-ionic PCP has a relative low solubility and also a very low vapor pressure, which means a low Henry constant. Therefore, it will be very difficult to find PCP in the vapor phase. Sorption of both ionic and non-ionic chlorophenols can occur. However, at low ionic strength and at pH values exceeding the pK$_a$ by more than 1 log unit, the sorption of the ionic form is insignificant [69]. Chlorophenols,

especially the one with few chlorine atoms, must generally be considered rather mobile in neutral and alkaline mineral soils and the opposite in acidic soils with high amounts of organic matter. In addition to adsorption, covalent binding to soil humic material may incorporate chlorophenols into the soil organic matter. Enzymes produced by fungi, bacteria, and plants found in the surface of the soil catalyze this oxidative coupling. Covalently bound chlorophenol residues are strongly immobilized against biodegradation [67]. Nevertheless, all these considerations may change depending on the pH value of the water and soil system, and will affect the dissociation state of each compound in dependence with its pK_a value. This dissociated species may have different behaviors in the surrounding environment and will of course have different solubility, Henry's constants and vapor pressures. Considering that the pH value controls the presence of the dissociated species in a soil-water environment, it will be important to know the dissociation curve for each pollutant and its dependence with pH. Taking for example a pH value of 7 in the soil/water system, PCP would be preferentially in the anionic form and its solubility will increase from $1.4*10^1$ (non-ionic PCP) to 10^4 mg/L (anionic PC-phenolate) (Figure 4). For 2,4,5-TCP and 2-CP, for example, the situation will be quite different, because at pH 7, the 2,4,5- TCP would be present at about 50% in the anionic form and 50% in the non-ionic form, while 2-CP will be mainly present in the non-ionic form in the aqueous phase. Therefore, there will be only some small quantities of non-ionic 2,4,5-TCP and 2-CP remaining adsorbed onto the soil pores.
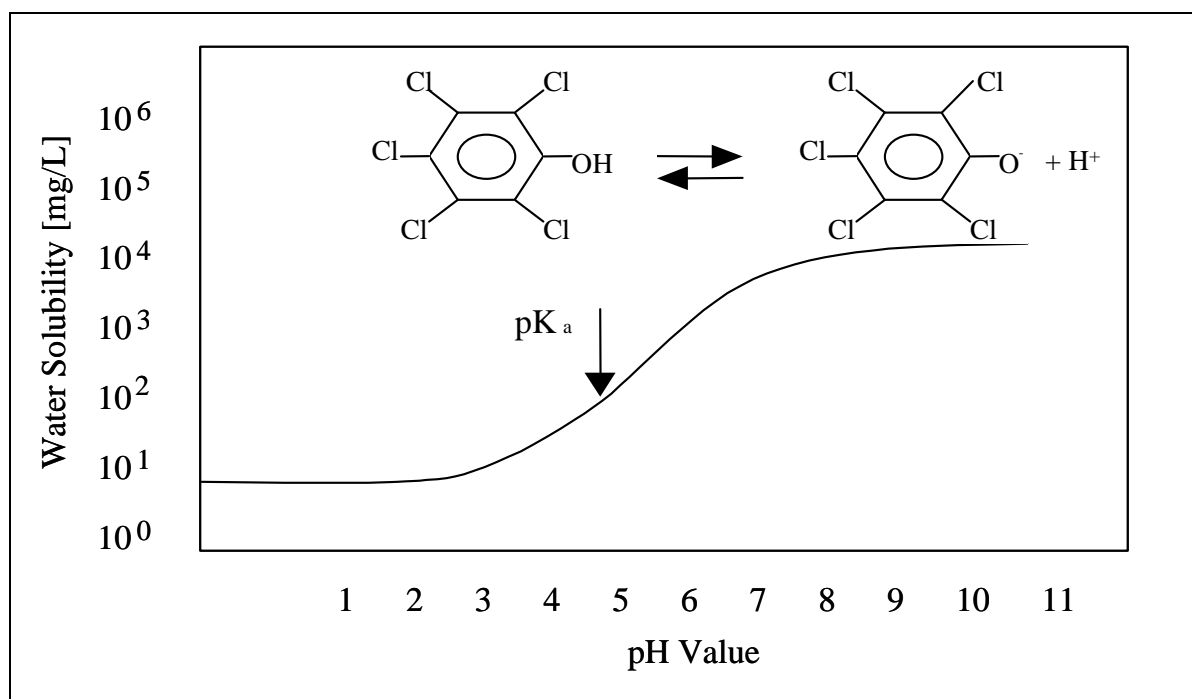
Figure 4: Solubility and dissociation dependence of PCP from pH-value (adapted from [70])

2.4   Heavy metals in the environment

Heavy metals are introduced into the environment through natural phenomena and human activities, such as agricultural practices, transport, industrial activities and waste disposal.

Although many heavy metals are necessary in small amounts for the normal development of the biological cycles, most of them become toxic at high concentrations. The concentration and mobility of heavy metals in soils and sediments have been widely studied in the last decades [41]. The toxicity of these anthropogenic compounds has become a large problem. It is very important to remove or reduce the presence of these contaminants to lower the possibility of their assimilation by plants, where they would eventually accumulate in the food chain [47]. In addition, it is important to prevent the dissolution and dispersion of these toxic compounds to underground and surface waters [71]. In Table 7, the main heavy metals produced in different industrial, agricultural and domestic activities are presented. In addition, metal ions can be discharged in effluents from other industries including pulp and paper, chemicals manufacturing and electronics [46]; and could be also present in sewage sludge [45].

Table 7: Heavy metals produced in different industrial, agricultural and domestic activities

Heavy metal	Activity	References
Arsenic (As^{3+}/As^{5+})	Medicine and cosmetic	[72]
	Agriculture (as insecticide, rodenticide and herbicide)	[72]
	Coal and coal combustion (by-product)	[72]
	Mining (naturally occurring)	[42],[72]
Zinc (Zn^{2+})	Metal finishing	[24]
Copper (Cu^{2+})	Metal finishing	[24]
Iron (Fe^{3+})	Fertilizer, metal industry	[73]
Chromium	Metal finishing, electroplating, chrome preparation (Cr(VI))	[24],[45]
	Fertilizer (Cr(III))	
Cadmium (Cd^{2+})	Metal finishing	[24]
	Plating, cadmium-nickel battery, phosphate fertilizer, stabilizer, alloy	[44],[73],[74]
Nickel (Ni^{2+})	Metal finishing	[24]
	Plating, cadmium-nickel battery, phosphate fertilizer, stabilizer, alloy	[44]
Mercury (Hg^{2+})	Domestic garbage (from thermometers, fluorescent lamps, mercury batteries) leaching and incineration	[75]
Lead (Pb^{2+})	Metal finishing	[24]

There are important differences between the toxicity of these heavy metals. Cadmium (Cd^{2+}) and chromium (in the hexavalent oxidation state) show high toxicity to humans as well as to animals, while copper, nickel and zinc show moderate toxicity to humans and animals. All these metals are also toxic to plants, being nickel and cadmium the strongest phytotoxic elements [24]. Hexavalent chromium is of considerable concern because it is known to have also a potential carcinogenic effect. Therefore it always has to be reduced to the trivalent form, followed by a lime precipitation process [45].

2.5   Wastewater treatment in the pulp and paper industry

World paper and pulp production is estimated at ca. 300 million ton/a [76], while the Chilean production reaches about 2.2 million ton/a [77]. In Chile, pulp and paper mills are located preferentially in the South (regions VII and VIII) and the pulp production is mainly based on the Kraft process with an elemental chlorine-free (ECF) bleaching stage. Considering the production of 1 ton of final product as calculus basis, the wastewater generation for this process is in the range of 10 to 110 m^3/ton [76],[78]. The pulp industry in Chile discharges large volumes of brown-colored effluents. The effluent impacts depend on the different pulp products, which normally involve two types: standard, with four steps (bleaching sequence: D/C EO D_1 D_2) for bleaching softwood pulp with 50% chlorine-dioxide substitution in step one, and elemental chlorine free (ECF) pulp (bleaching sequence: Do EOP D_1 D_2). D and C denotes ClO_2 and Cl_2 bleaching stage, respectively, EO indicates oxygen-reinforced alkaline extraction stage and EOP denotes oxygen and hydrogen peroxide reinforced alkaline extraction stage. This pulp wastewater stream could produce three kinds of impacts [10]: biological oxygen demand (BOD), toxicity and color (Figure 5). BOD is originated because of the presence of easily biodegradable compounds. Toxicity has mostly been attributed to wood resin, chlorinated phenols [79] and tannins [80], while brown color results from the presence of lignin or polymerized tannins in the wastewater [81]. The organic load of this effluent (measured as chemical oxygen demand, COD) ranges between 4 and 90 kg/ton and the adsorbable organic halides (AOX) content moves between 0 and 2 kg/ton [78].
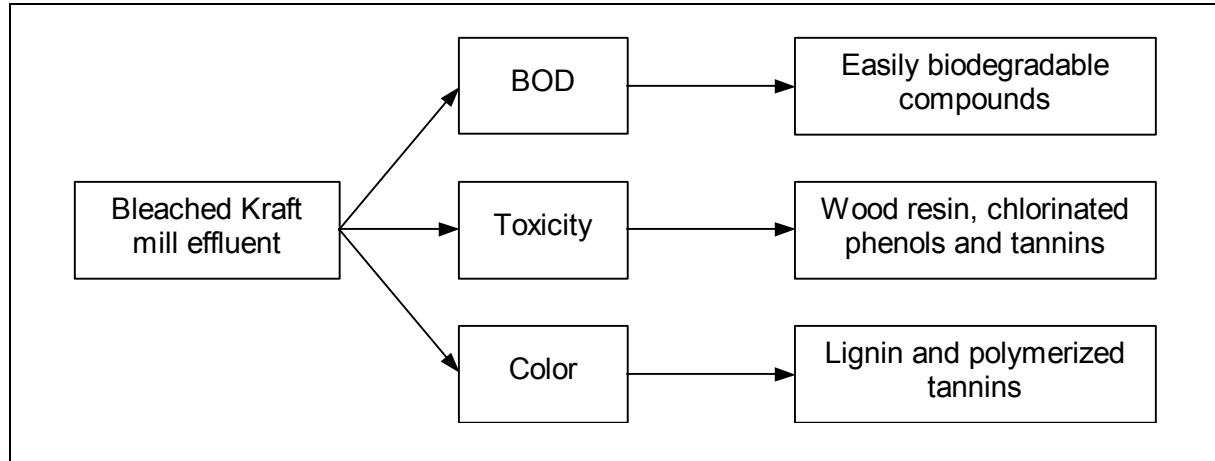
Figure 5: Impacts of bleached Kraft mill effluents

Aerated lagoons remove between 30 and 40% of the organic-linked chlorine and about 50% of the chlorinated phenolic compounds, while activated sludge treatments remove around 50% of the chlorinated organic compounds and about 60% of the chlorinated phenolic compounds [82]. Nevertheless, both treatments are not able to remove the color present in the Kraft pulp industry effluent [83].

The most recent bleaching technologies involve ozone, oxygen and/or oxygen peroxide as bleaching agents. These processes are known as total chlorine free (TCF) and have the advantage that no chlorinated organic compounds are produced in the bleaching step.

Nevertheless, in these modern bleaching pulp and paper mills, the used chelating compounds such as ethylenediamine tetraacetic acid (EDTA) are poorly degraded by biological processes, are scarcely degradable by chlorine, hardly retained by activated carbon filters and resistant to ozone treatment [84].

2.6   Groundwater remediation processes

2.6.1   Chlorophenols-contaminated groundwater

Chlorophenols-contaminated groundwater can be remediated by biological and/or physico-chemical processes. Bioremediation has a great potential in chlorophenol contaminants treatment, but is limited by possible low ambient aquifers temperatures. This effect is very important in northern and southern countries. For instance, in Finland the groundwater temperature is below 10°C throughout the year [85] and the mineralization processes of these chlorophenols can be seriously affected by this factor (Table 8).

Table 8: Effect of low groundwater temperature in the mineralization of chlorophenols

Compound	Conditions	References
PCP	Batch incubation. Enrichment culture from a lake sediment mineralized PCP at 28°C. No mineralization was observed at 8°C	[86]
	Flavobacterium sp. mineralized PCP between 24 and 35°C. No mineralization was observed at 12°C.	[87]
	Half-life of PCP in soil (500 mg/kg) increased from 60 to 179 days for a temperature decrease from 25 to 5°C	[88]
TCP	By an *Azotobacter sp.* at 20°C degradation rate was reduced by 40% from optimal rate and no degradation was observed at 4°C.	[89]

PCP: Pentachlorophenol, TCP: Trichlorophenol

Biological on-site treatment of chlorophenols-contaminated groundwater could require inclusively heating [90]. In the environment, chlorinated phenols are normally recalcitrant due to the inadequate conditions for biodegradation or the absence of chlorophenol-degrading organisms. In on-site treatment systems, chlorophenols can be degraded at ambient temperatures under aerobic and anaerobic conditions (see Chapter 2.8). Aerobic fluidized-bed biodegradation using *Flavobacterium* and *Rhodococcus* bacteria produces an effluent with chlorophenol concentrations close to drinking water [91]. There has been very little experience with in-situ biological treatment of chlorophenols-contaminated groundwater. Ex-situ systems could be more controllable and predictable and less complex than in-situ treatments [92].

Regarding physico-chemical processes, the electron-beam irradiation process relies upon the production of free H· and OH· radicals during water irradiation. These radicals have been tested to react with chlorinated compounds like trichloroethylene and carbon tetrachloride,

producing CO_2, H_2O, salts and other harmless compounds [92]. The possible application as an on-site remediation process for chlorophenols has not yet been studied.

2.6.2   The reactive wall in-situ process

The reactive walls in-situ process is also an interesting technology developed for groundwater remediation. This technology relies upon an in-situ installation of a reactive barrier to allow physico-chemical adsorption of the pollutants present in the groundwater plume (Figure 6).
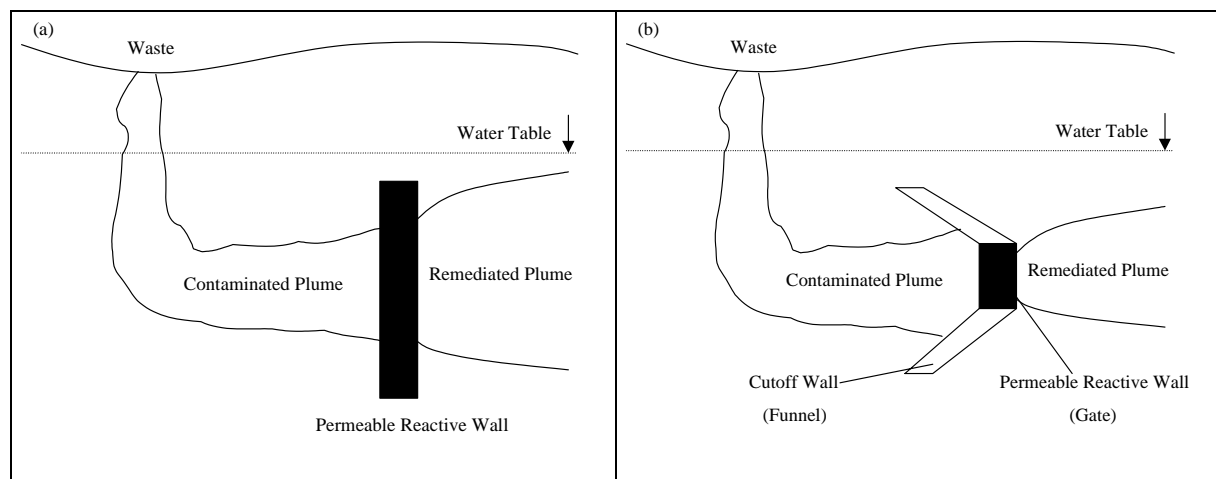
Figure 6: The reactive wall (a) conventional process and (b) funnel and gate process

Activated carbon, minerals and zero-valent metals are the most used adsorbent materials for groundwater remediation [13]. Different zero valent metals have demonstrated a great field of application as permeable reactive walls. In fact, Fe^0, Al^0, Zn^0, Ni^0, Cu^0, Pd^0/C and combinations of them have been tested successfully as permeable barrier for organochlorides removal from groundwater [50]. In addition, it has been demonstrated that zero-valent iron is capable to promote the reductive dechlorination of a great spectra of chlorinated organic compounds, but the treatment of chlorophenols remains still unknown or poorly understood. As indicated in Table 9, there are some unknown Fe^0 treatable organochlorides, but some of them have recently been carefully studied. Particularly, polychlorinated biphenyls (PCBs) reductive dechlorination may also occur in the presence of zero-valent iron while extracting PCBs from soil and sediments. In fact, the higher chlorine-substituted PCB homologues were completely reduced to their lower-substituted counterparts, as the lower-substituted congeners were subsequently nearly-completely dechlorinated [93]. From the chlorophenols group, the electrochemical dechlorination of 4-chlorophenol to phenol was determined to occur rapidly on palladized carbon cloth and palladized graphite electrodes. In this case, the reactions on the palladized carbon cloth and graphite depend on the adsorption of 4-chlophenol on the carbon surface and the reaction with hydrogen as catalyst at the palladium/carbon interface [94].

Moreover, reductive dechlorination of lindane was achieved in aqueous solution using Zn-modified carbon cloth cathode. In this case, lindane was adsorbed first from water on the carbon cloth and then reduced by metallic Zn on the carbon cloth surface. The metallic Zn islands were regenerated by the electrochemical reduction of Zn^{2+} [95]. In addition, at laboratory scale, complete dechlorination of PCP was observed in a Pd/Mg reactive wall, while the dechlorination of less substituted chlorinated phenols by different metallic systems was found to be more facile [96].

Table 9: Organochlorinated compounds treatability with Fe^0 as reactive wall (adapted from [50],[97])

Treatable organochlorinated compounds	
Methanes	trichloromethane
	tetrachloromethane
Ethanes	1,1-dichloroethane
	1,1,2-trichloroethane
	1,1,1-trichloroethane
	1,1,1,2-tetrachloroethane
	1,1,2,2-tetrachloroethane
	hexachloroethane
Ethenes	vinyl chloride
	1,1-dichloroethene
	trans-1,2-dichloroethene
	cis-1,2-dichloroethene
	trichloroethene
	tetrachloroethene
Propanes	1,2-dichloropropane
	1,2,3-trichloropropane
Other	hexachlorobutadiene
Not treatable organochlorinated compounds	
Methanes	chloromethane
	dichloromethane
Ethanes	chloroethane
	1,2-dichloroethane
Organochlorinated compounds with unknown treatability	
Chlorobenzenes	-
Chlorophenols	-
Certain Pesticides	-
PCBs	-

Institut für nachhaltige
Abfallwirtschaft u. Entsorgungstechnik

In organochlorine contaminated groundwater, three oxidants could drive corrosion of zero-valent iron: water, oxygen and the organochlorinated pollutant [98]. The water corrosion reaction (Equation 7) is slow but ubiquitous, whereas the reaction of Fe^0 with dissolved oxygen is very quick as long as oxygen is available (Equation 8). The presence of organochlorinated pollutants in a Fe^0-H_2O system could provide the third corrosion reaction (Equation 9, R: hydrocarbon radical) that can contribute to the overall corrosion rate.

$$Fe^0 + 2\ H_2O \leftrightarrow Fe^{2+} + H_2 + 2\ OH^- \tag{7}$$

$$2\ Fe^0 + O_2 + 2\ H_2O \leftrightarrow 2\ Fe^{2+} + 4\ OH^- \tag{8}$$

$$Fe^0 + RCl + H^+ \leftrightarrow Fe^{2+} + RH + Cl^- \tag{9}$$

On the other hand, passivation of iron surface is also possible, because of the solid reaction products of Fe^{2+} under different environmental conditions [98]. The presence of bicarbonate (in carbonate rich groundwater) will lead to siderite production ($FeCO_3$), and goethite (α-FeOOH) is an expected product in an oxidant excess environment (O_2 and H_2O). Moreover, the production of green rust precipitate is also feasible under specific situations. The environmental site conditions and passivation products should be taken into account carefully while designing a Fe^0 reactive wall and determining the shelf-life of the reactive metal.

The reaction pathways involved in the reductive dechlorination with Fe^0 could explain and provide future applications of this process as a chlorophenol remediation technology. As discussed by [99], three pathways for reductive dechlorination in anoxic Fe^0-H_2O systems could be possible. In the direct electron transfer pathway, the organochloride pollutant adsorbs first on the Fe^0 surface and a subsequently electron transfer occurs at the surface. This same mechanism has also been analyzed as a possible one for the dechlorination of 4-chlorophenol to phenol on palladized carbon cloth and palladized graphite electrodes and was found to be unsuccessfully, indicating that this route is not important in this case. On the other hand, the dechorination of 4-chlorophenol seemed to be dependent on the hydrogen catalysis at the metal surface, making this pathway the most suitable for 4-chlorophenol [94]. For the trichloroethene (TCE) reductive dechlorination with granular Fe^0, only about 3.0 to 3.5% of the initial TCE appeared in the dechlorination products, including the three dichloroethene isomers and vinyl chloride. Based on the low concentrations of TCE degradation products in the water phase, [100] proposed that the most of the TCE could remain sorbed onto the iron surface until complete dechlorination is achieved. Therefore, a sequential dechlorination pathway for highly chlorinated compounds (like PCP or TCP) should be studied carefully, and the possibility of complete dechlorination in the metal surface remains uncertain.

Considering that chlorophenols adsorption and H_2 catalytic reaction at the metal surface would play a key role in the reductive dechlorination process, a high surface area of the zero-valent metal would be required to enhance the dechlorination process in a reactive wall in-

situ reactor. In fact, there is a direct relationship between the available surface of the metal and the dechlorination rate, and the treatment of the surface with HCl could also enhance the dechlorination reaction further [99],[101]. Finally, the use of zero-valent iron (Fe^0) could have some advantages compared with activated carbon in field applications. This comparison is presented in Table 10 for the case of a possible chlorophenol polluted groundwater.

Table 10: Fe^0 and activated carbon as reactive barrier for cholorophenols reduction in groundwater remediation

Reactive material	Advantages	Disadvantages
Activated carbon	Adsorbs chlorophenols strongly	Expensive material
		Chlorophenols remain in the surface
		Material must be regenerated or disposed
Zero valent iron (Fe^0)	Cheap Material	Dechlorination chemistry not known
	Should react and dechlorinate the pollutants selectively	

2.7   Mineral liners in sanitary landfills

Sanitary landfills are commonly designed under the "multibarrier system"-concept, in which clay mineral layers play an important role as constituents of landfill barriers, preventing the breakthrough of hazardous contaminants like heavy metals or organic pollutants. The geo-technical barrier consists normally of a subsoil barrier, a soil sealing layer, a geomembrane, a protective layer, a drainage blanket and a transition layer before the waste body itself [102]. The so-called composite liner is a combination of successive natural clay liners (soil sealing layer) with a total thickness of 0.5-1.5 m and a superficial geomembrane, 2.5-3.0 mm thick, depending both on the type of waste to be disposed and on the environmental regulations of each country [103]. The geomembrane itself is made of a high-density polyethylene or polypropylene, and is covered with a geosynthetic sheet in order to protect it against damages caused by the overlying coarse gravel drainage layer [102]. Therefore, in order to prevent leaching of environmental pollutants into the subsoil and groundwater bodies in landfills, the basal liner is constructed with a redundant design: if the geomembrane fails after years or decades of operation, the clay liner should be still able to take over its task of retaining the pollutants. The geomembrane is an absolute barrier against convection and the pollutants can only permeate it by diffusion. The rate of diffusion will depend on the pollutant nature. For heavy metal ions and other inorganic compounds the geomembrane is virtually a perfect barrier and though water can diffuse through it to some small extent, thus is not considered to be harmful [102]. Mineral clay liners are generally assumed to maintain their efficiency over geological periods of time even under chemical attack. The permeability of the mineral layer of basal liners must be between to $5*10^{-9}$ and $5*10^{-10}$ m/s to avoid permeability by convection processes [102]. Under this condition, the effective diffusion (which considers

also the adsorption processes of the pollutant onto the clay surface) through the clay liner will be the main pollutant transport mechanism.

The transport through mineral liners can be divided in two main processes: advection and dispersion. The advection process (or convection process) refers to the liquid phase flow that depends naturally on the linear velocity of the liquid phase through the liner. The term dispersion (or hydrodynamic dispersion) includes the mechanical dispersion and molecular diffusion. Mechanical dispersion represents the mixing effect in the mineral soil column, which results from local variations in velocity, due to porous medium non-ideality [104],[105]. On the other hand, molecular diffusion represents the contaminants movement due to a concentration gradient in the soil column [104]. The adsorption processes that occur in the soil organic matter (SOM), as well as in the soil mineral fraction, can retard the advective and dispersive movement of contaminants in soil.

The advective and dispersive processes can be separated clearly depending on the soil type used as mineral liner. In non-compacted and non-clayed soils, with a hydraulic conductivity (K_f) normally higher than $3*10^{-6}$ m/s, the liquid flow or the linear velocity of the liquid phase will be the variable that will control the contaminant mobility through the soil [15],[106]. On the other hand, in compacted and clayed soils with a K_f value lower than $3*10^{-6}$ m/s, the dispersion will be the process controlling the contaminants mobility through the soil [15]. In addition, in this case the mechanical dispersion is normally negligible and therefore, the molecular diffusion will be the main process controlling the mobility of pollutants through the soil matrix [14],[15],[107].

2.8   Contaminated soil waste managing options

The soil properties have to be considered and analyzed carefully while looking after spent soil waste management and remediation options. The most important properties of soil to take in account for remediation technologies assessment are the soil type, the hydraulic conductivity K_f and the organic matter content [92],[106].

Table 11: Geohydrological parameters of different soil types (adapted from [108],[109])

Soil type	Particle size [mm]	K_f [m/s]	In-situ (IS) or Ex-situ (ES) treatment
Gravel	> 2.0	$1.2*10^{-3}$	IS
Coarse sand	0.6 - 2.0	$1.2*10^{-4}$ - $1.2*10^{-3}$	IS
Middle sand	0.2 - 0.6	$5.8*10^{-5}$ – $1.2*10^{-4}$	IS
Fine sand	0.06 - 0.2	$3.0*10^{-6}$ - $5.8*10^{-5}$	IS
Silt	0.002-0.06	$< 3.0*10^{-6}$	ES
Clay	<0.002	$< 3.0*10^{-6}$	ES
Peat	-	$< 3.0*10^{-6}$	ES

As presented in Table 11, soil types like gravel and sands could be remediated utilizing in-situ technologies because of their adequate K_f values (normally > 3.0*10^{-6} m/s). It is obvious that the natural soil environment is composed of heterogeneous mixtures of different soil types and the average K_f value should be determined empirically for each particular case. The organic matter content in soil is also an important parameter while analyzing possible remediation processes. In fact, according to [108], in-situ remediation technologies could be applicable only on soils with an organic matter content under 5%, as depicted in Figure 7.
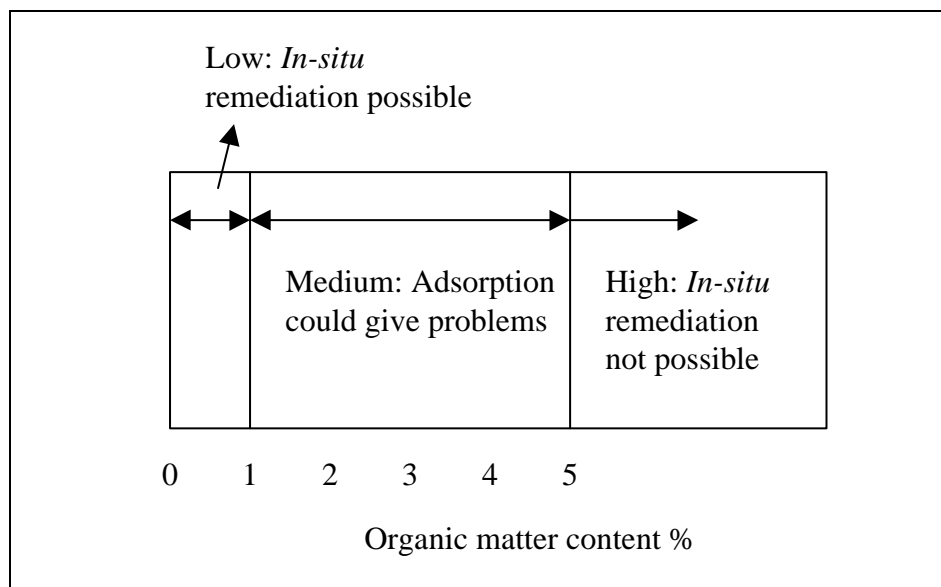
Figure 7: Effect of organic matter content in soil remediation possibilities

2.8.1   Chlorophenols-contaminated soil

Different processes have been investigated and tested for the remediation of soils contaminated with chlorophenols. Physical, chemical and biological processes have been the most useful techniques depending on the physico-chemical parameters of the soil and the kind and concentration of chlorinated pollutants [92],[106],[110]. Biological in-situ remediation is only possible if the chlorophenols concentration lies below the toxicity level of 200 mg/kg dry weight. For highly chlorophenols-contaminated soil, incineration seems to be the only feasible solution. For moderately contaminated soils, windrow composting in bio-piles, thermal desorption and deposition have been proposed as remediation options, while low contaminated soils should be treated with in-situ remediation [111].

In biological processes, the chlorophenols distribution in the soil matrix is very important for the application of a remediation technology at an industrial scale. It is known from the literature that aerobic biological remediation processes are highly dependent on the bioavailability of the pollutant, oxygen and nutrients (nitrogen and phosphor). This means that the pollutant, oxygen and nutrients must be dissolved in the water phase, which becomes very difficult. A biological degradation process could be suitable for chlorophenols in its ionic form, while the non-ionic form will remain mostly adsorbed. The air stream would be capable to strip the most volatile pollutants like 2-CP. This means that an ulterior gas

treatment for this air stream should be used to degrade the most volatile clorophenols. The main problems with biological in-situ treatments are that normally they require long process times (years), the microorganisms should be very specific and the products of the biochemical reactions involved should be determined to be innocuous. The soil is a natural environment for a large number of microorganisms that could play a key role in the remediation process of cholorophenols. Bacteria (*Agrobacterium, Athrobacteri, Bacillus, Flavobacterium* and *Pseudomonas*) constitute the most important group, but the presence of actinomicetes and fungi is also relevant. Bacteria grow faster than fungi and are also easier to culture, appear to metabolize chlorinated organic compounds better and mineralize these compounds and use them as carbon and energy sources. The use of fungi in the bioremediation of chlorophenols has been questioned because of the possible production of chloroanisols as metabolites in the degradation process, but some important fungi have been used successfully in the degradation of lignin (*P. crysosporium, Phebia radiata and Trametes versicolor*) without producing chloroanisols [112]. Moreover, their non-specific enzymatic system presents some advantages for the treatment of mixtures of xenobiotics.
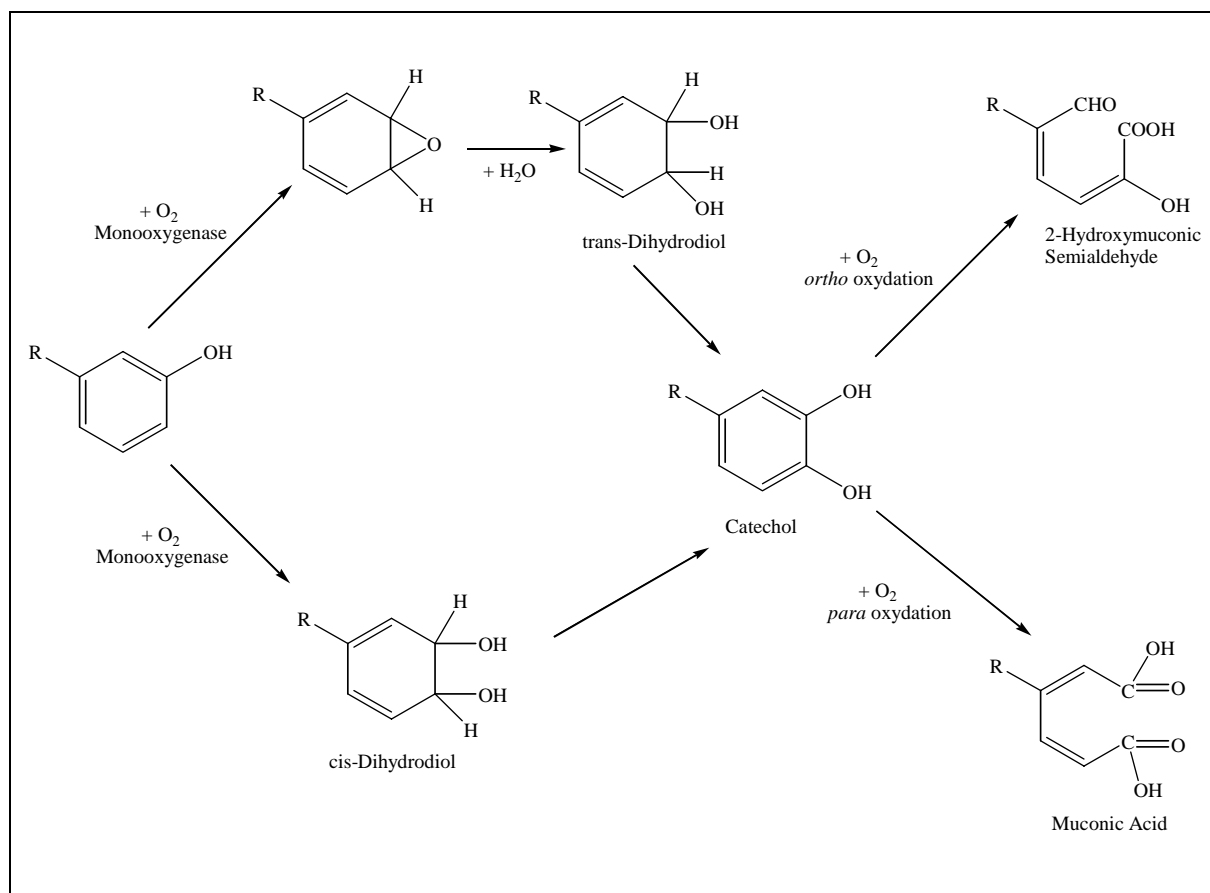
Figure 8: Aerobic degradation of chlorophenols, R: Cl in this case (adapted from [113],[114])

Chlorophenols could be degraded aerobically by activation and cleavage of the aromatic ring (Figure 8). This chemical activation involves the incorporation of molecular oxygen in the ring, which occurs because of the action of enzymes like oxygenases. In this case, monooxygenases from fungus and other eukaryots could catalyze the incorporation of a simple oxygen atom into the cholorophenolic ring while dioxygenases from bacteria could

catalyze the incorporation of two molecular oxygen atoms forming a cis-dihydrodiol [115]. Both ways can produce finally catechol, which could be oxidized via *ortho*, or *para* to form 2-hydroxymuconic semialdehyde and muconic acid respectively. The acid and semialdehyde products are finally used and degraded by microorganisms to form CO_2 and biomass. As an example, the aerobic degradation of 4-CP in a pure culture of *Alcaligenes A7-2,* with an initial concentration in soil of 0.3 mM was successfully performed after a maximum of 35 h under different degradation conditions [116].
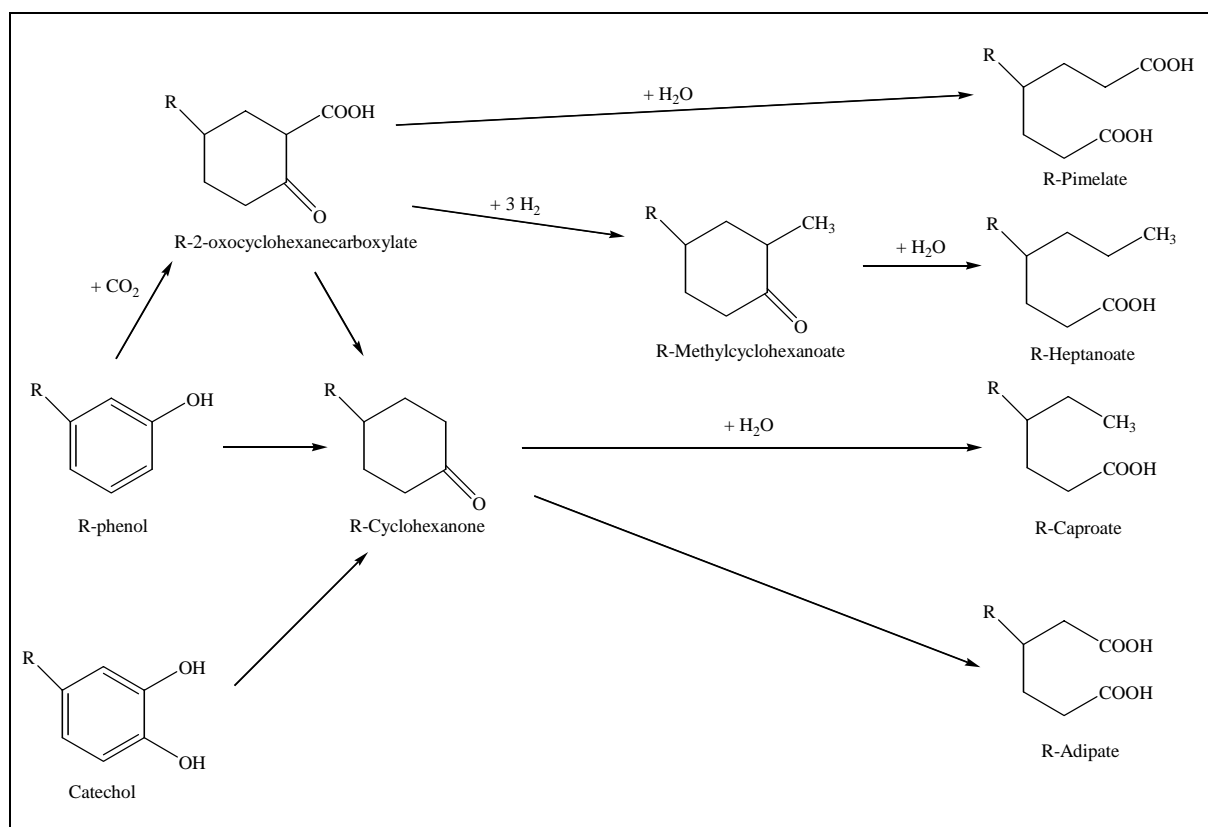
Figure 9: Anaerobic degradation of chlorophenols and catechols, R: Cl in this case (adapted from [113])

Anaerobically, the chlorophenols ring is not oxidized, but reduced, and the key intermediate product is in this case cyclohexanone. The ring could be opened by hydration of this intermediate product (Figure 9). In the case of aromatic compounds with more than one chlorine substitution (PCP for example), these compounds are reductively dehalogenated before the ring is reduced [113]. Microorganisms could perform reductive dechlorination from high substituted chlorinated aromatics through four different pathways: hydrogenolysis, dichloro-elimination, coupling and hydrolytic reaction [113],[114]. The hydrogenolysis mechanism relies upon replacing a chlorine substituent with hydrogen. In the dichloro-elimination pathway, two chlorine subtituents are eliminated simultaneously from the aromatic compound and parallel a double bond is formed in the aromatic ring. The coupling reaction normally occurs when free radicals are involved and the hydrolytic reduction involves a two-electron reduction of a polychlorinated carbon to carbenoid followed by hydrolysis. For highly substituted phenols the hydrogenolysis mechanism is the most

common anaerobic dehalogenation pathway (Figure 10a). In fact, the reductive dechlorination of TCP was found to be 100% successfully with *Azotobacter GP1* after 4 days with a pollutant concentration in soil of 5 mM [117]. Moreover, an oxidative dechlorination with a direct chlorine substitution by a hydroxyl group could also occur in PCP. The enzyme PCP-dehalogenase from *Athrobacter sp. ATCC 33970* was found to be responsible for the degradation of PCP forming tetrachloro p-hydroquinone [117]. This product can only be degraded and mineralized under anaerobic conditions (Figure 10b) [118].
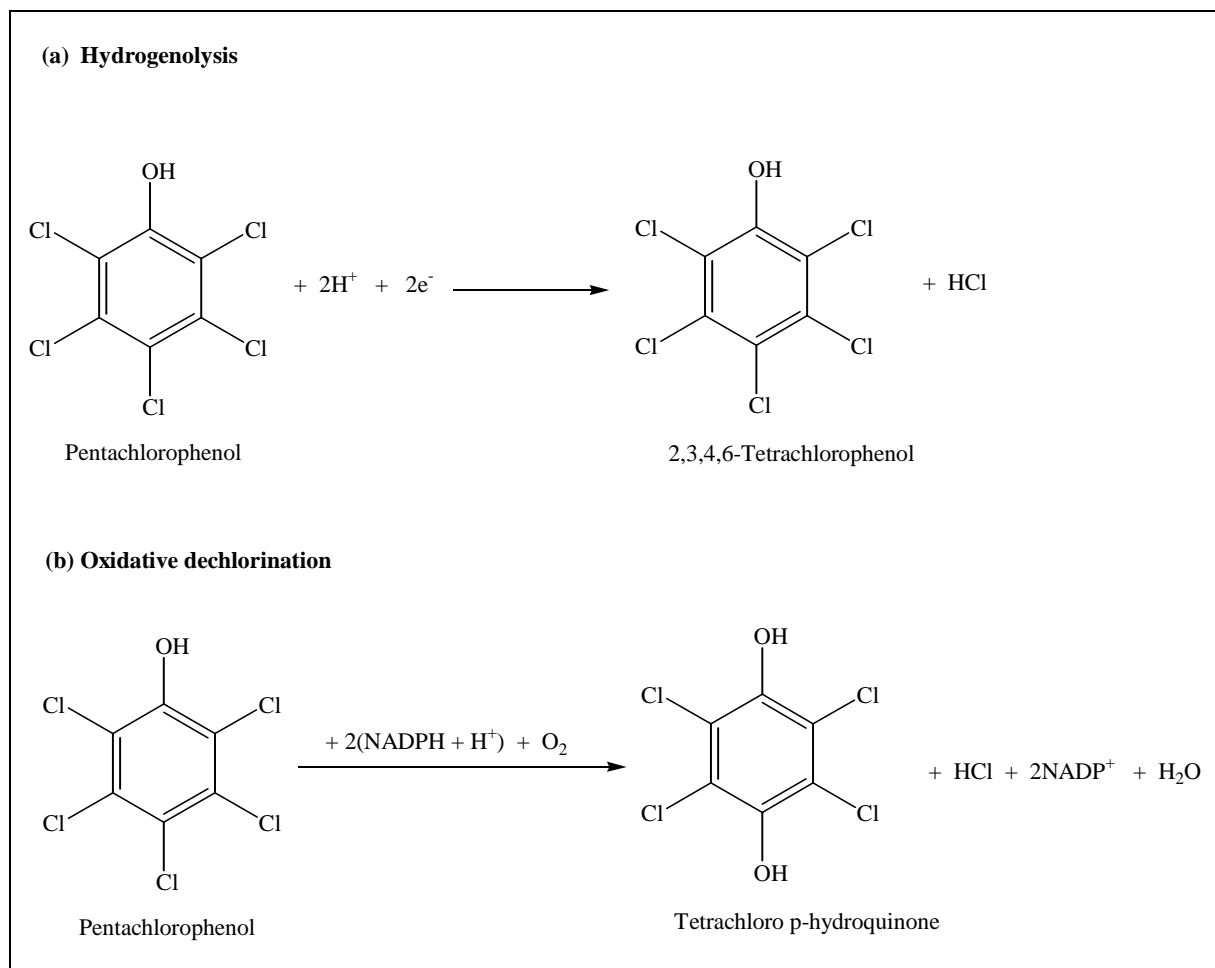
Figure 10: Dechlorination processes of PCP (a) hydrogenolysis and (b) oxidative dechlorination

Different types of microorganisms are able to degrade chlorophenols in the soil environment. The position and substitution grade is important for determining the biological degradability from these compounds. In fact, for highly chlorinated phenols (like PCP), there is a great possibility that reductive dechlorination occurs. On the other hand, the products of this dechlorination process contain fewer chlorine atoms in the ring and are probably less reductively dechlorinated (2-CP for example). These compounds could be oxidized under aerobic conditions and the dechlorination would occur after cleavage from the aromatic ring [118].

One of the most used full-scale soil remediation technologies is the in-situ bioventing process, but it hasn't been used to remediate chlorophenols-contaminated soil so far. It relies upon an increase in the flow of air (oxygen) through the vadose zone, which provides oxygen in the subsurface to optimize natural aerobic biodegradation, which becomes the dominant remedial process [119]. The humidity in the soil matrix should be intensive to allow pollutants, oxygen and nutrients solubilization [120],[121] and the air permeability should be higher than $3*10^{-6}$ m/s. In addition, temperature, C/N relationship and pH should allow normal bacteria growth [122]. The bioventing technology has been used successfully in the remediation of sites contaminated with organic and organohalogenated compounds. It relies upon changing the anaerobic condition of a contaminated site to an aerobic one, in which the biochemical degradation processes from organic pollutants are accelerated, producing finally water, CO_2 and biomass [123]. In the air stream, the oxygen content is enhanced with pure oxygen until it reaches 28-40%. This air stream is pumped through the contaminated site at pressures up to 6 bar. At the same time, gas-suctioning lances operate to collect around a 30% higher flow rate compared with the pumped air. This stream passes through a biofilter where any volatile pollutant and also the landfill gases are cleaned [124]. In the case of chlorinated phenols, an aerobic degradation process could be induced with this enhanced oxygen air stream, while simultaneously a biofilter could clean the gas stream. Moreover, the exothermic aerobic process will produce a temperature increment in the soil, which in field cases could rise up to 70°C. This factor could be determinant to biologically degrade some organohalogenated compounds, which can be degraded satisfactory with hyperthermophilic bacteria. In addition, in some cases the natural attenuation process could also have some incidence in the biodegradation of pollutants by the native soil microorganisms.

A simulation of the in-situ bioremediation of chlorophenols in a sandy aquifer at pilot plant scale has been recently performed [125]. The intrinsic microbial development was enhanced by adding the necessary nutrients for obtaining biodegradation yields between 87% (PCP) to 100% (2-CP and 2,4,6-TCP).

The possibility of ex-situ biological treatment is also feasible in this case, and will depend particularly on the soil properties, as discussed before, and on the time needed for remediation. In ex-situ processes, remediation times are around one year, while in in-situ technologies the remediation times range normally between one and five years or more. Moreover, in ex-situ processes, optimal aerobic conditions could be achieved, while adding support materials for optimal aeration and surface for bacteria growth. In this process the soil is arranged in a pile and normally the aeration occurs through a vacuum pump. The contaminated air passes through a biofilter and is returned to the pile. In addition, the percolate water is collected and cleaned in an aerated treatment plant and recirculated with nutrients to the pile to maintain the optimal humidity content of the soil [126]. Different investigations regarding the composting of chlorophenols-contaminated soils and wastes have been performed. Chlorophenol-contaminated pulp and paper mill fly ash was successfully composted with wastewater treatment sludge, obtaining chlorophenol concentrations below the levels stipulated by local regulations [127]. In addition,

chlorophenol-contaminated soil was composted with straw compost and bioremediated soil as inocula, obtaining mineralization yields between 24 and 56% for PCP, depending on the process conditions [128]. During a pilot and a full scale composting process of chlorophenol-contaminated soil, over 90% of the chlorophenols were removed during the composting period. Frequent mixing and control of the nutrient level enhanced the chlorophenol degradation activity of the indigenous microbes in the contaminated soil [129],[130].

Regarding physico-chemical processes, the soil wash process (SWP) relies upon the help of water as fluid medium and energy for the separation of pollutants present in non-saturated media. The SWP is able to break loose the pollutants from the soil pores through mechanical energy, forming a pollutant suspension or an emulsion in the wash fluid medium. An ulterior pollutant separation is required to recover concentrated pollutants and a clean wash fluid. Normally pure water is used as the fluid medium, but some process changes include the addition of organic solvents, complexing agents and high-pressure soil wash [131]. The use of this remediation technology is normally ex-situ, but there are also some cases of in-situ application, depending principally on the soil characteristics. In the case of chlorophenols, some interesting ex-situ applications have been studied by [132], obtaining a mechanical removal of chlorophenols of around 70% from contaminated soil. Different ex-situ soil wash processes were tested (drum screen, vibratory screen, shaking table, mixer, hydrocyclone and press filter), but the fine reactive fraction of the soil (normally under 63 µm) that remains contaminated needs further remediation by incineration or a biological process.
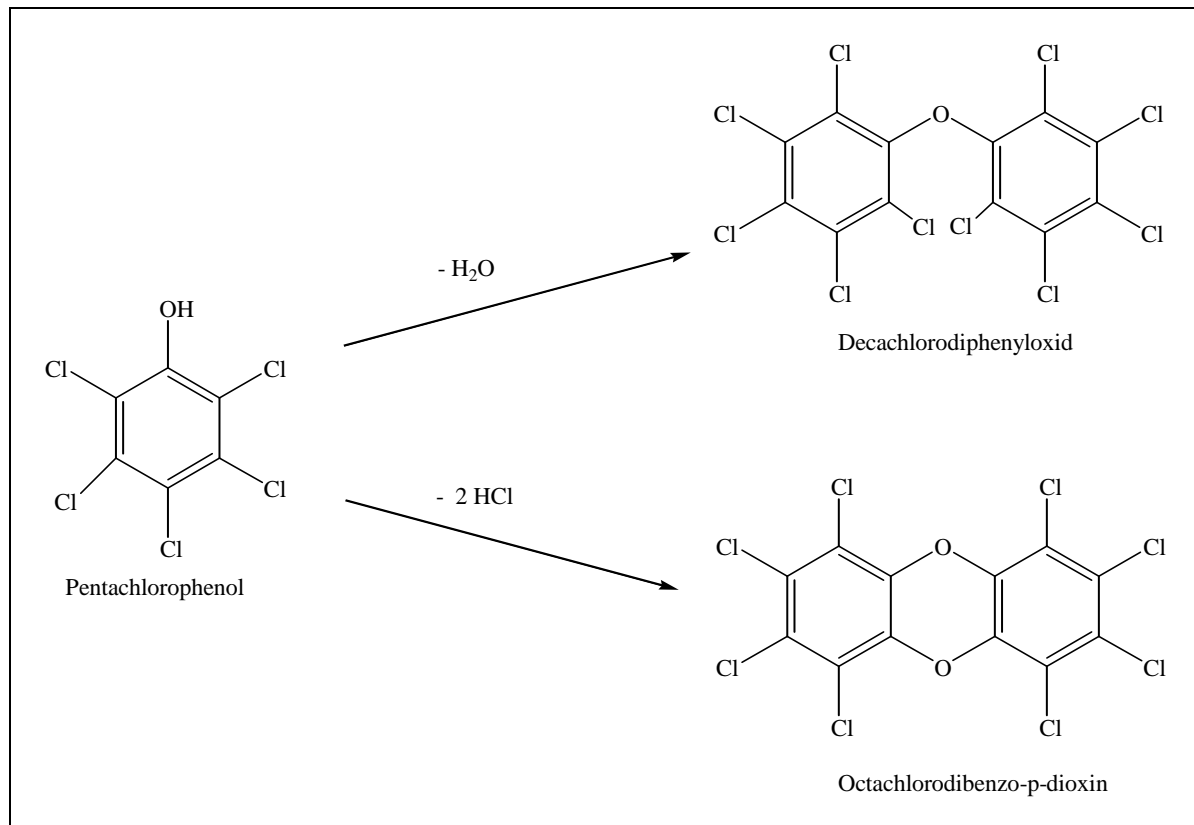
Figure 11: Thermal behavior of PCP, 1: Decachlorodiphenyloxid, 2: Octachlorodibenzo-p-dioxin

Thermal treatment is normally used as a remediation technique for organochlorides in soil, but it could produce some new pollutants, if we consider the thermal reaction products for pentachlorophenol at 300°C (Figure 11) [70]. For instance dioxins are known to be toxic and carcinogenic pollutants. Because of this, a thermal treatment of the soil and the formation of new pollutants should be studied carefully to assess the environmental safety of the process.

2.8.2   Heavy metals-contaminated soil

Several remediation techniques are available for the treatment of soil contaminated by heavy metals, including: isolation and containment, mechanical separation, pyrometallurgical separation, chemical treatment, permeable treatment walls, electrokinetics, biochemical processes, phytoremediation, soil flushing and washing, among others [92],[133].

Contaminants can be isolated and contained, to prevent further movement, by reducing the permeability of the waste to less than 10^{-7} m/s, and to increase the strength or bearing capacity of the waste [134]. Physical barriers made of steel, cement, bentonite and grout walls can be used for capping vertical and horizontal containment. Capping is a site-specific proven technology to reduce water infiltration. Synthetic membranes can be used for this purpose [133]. Solidification/stabilization technologies contain the contaminants, not the contaminated area like physical barriers. Solidification is the physical encapsulation of the contaminant in a solid matrix while stabilization includes chemical reactions to reduce contaminant mobility. Some metals such as arsenic, chromium (VI) and mercury are not suitable for this type of treatment since they do not form stable hydroxides and are not highly soluble. Normally, liquid monomers that polymerize, pozzolans, bitumen, fly ash and cement are injected to encapsulate the soils [92],[133].

In mechanical separation processes the main objective is to remove the larger cleaner particles from the smaller, more polluted ones. To accomplish this objective, different processes are used. Hydrocyclones separate larger particles greater than 20 µm by centrifugal force from the smaller particles. Fluidized bed separation can also be used. In this case a cut-off of 50 µm can be achieved. In addition, gravimetric settling and flotation are also useful processes [133].

The pyrometallurgical process relies upon the use of high temperature furnaces to volatilize metals in contaminated soil. The typical temperature range moves between 200 and 700°C. After the volatilization, metals are recovered or immobilized. This method is most applicable to mercury since it is easily converted to its metallic form at high temperatures. Other metals including lead, arsenic, cadmium and chromium may require pretreatment with reducing or fluxing agents to assist melting and provide a uniform feed [133].

Chemical treatment by reductive as well as oxidative mechanisms may be used to detoxify or decrease the mobility of metal contaminants [135]. Oxidation reactions, which detoxify, precipitate or solubilize metals, involve the addition of potassium permanganate, hydrogen peroxide, hypochlorite or chlorine gas. Reduction reactions are induced through the addition

of alkali metals such as sodium, or sulfur dioxide, sulfite salts and ferrous sulfate. Sometimes chemical treatment is used to pretreat the soil for solidification or other treatments. For instance, chemical reduction of Cr(VI) is performed during solidification/stabilization. Mercury, lead, selenium and silver are also applicable for reduction. Arsenic is most applicable for chemical oxidation since As(V) is less toxic than As(III). These chemical treatments can be performed in-situ, by injection into the groundwater level [133].

Permeable treatment walls have been already described in Chapter 2.6.2. In the case of heavy metal contamination, preliminary results indicate that zero-valent iron is capable to reduce chromium while limestone can precipitate lead [133].

Electrokinetic processes involve passing a low intensity electric current between a cathode and an anode imbedded in the contaminated soil. An electric gradient initiates movement of ions by electromigration (charged chemicals movement), electro-osmosis (fluid movement), electrophoresis (charged particle movement) and electrolysis (chemical reactions due to electric field) [136]. The metals can be removed by electroplating or precipitation/co-precipitation at the electrodes, using ion exchange resins or recovering the metals by pumping the waste to the surface [92],[133]. Metals as soluble ions and bound to the soil as oxides, hydroxides and carbonates are removed by this method, while other non-ionic components can also be transported due to the flow. Unlike soil washing, this process is effective in clayed soils with low permeability and it has been used for treating Cu, Zn, Pb, As, Cd, Cr and Ni-contaminated soils [133].

The main biochemical remediation processes include bioleaching and oxidation/reduction reactions. Bioleaching involves *Thiobacillus sp.* bacteria under aerobic and acidic conditions at temperatures between 15 and 55°C, depending on the bacteria strain. Leaching can be performed by direct means, or oxidation of metal sulfides to produce sulfuric acid, which then can desorb the metals in the soil by proton substitution. Indirect leaching involves conversion of Fe^{2+} to Fe^{3+}, which in turn oxidizes sulfur minerals (e.g. FeS_2) to Fe^{2+}, producing acidity (H_2SO_4) [133]. Microorganisms are also known to oxidize and reduce metal contaminants. Mercury and cadmium can be oxidized, while microorganisms can reduce arsenic and iron. Bacteria such as *Bacillus subtilis* and sulfate reducing bacteria in the presence of sulfur can perform these reactions [133].

Phytoremediation involves the use of plants for the remediation of contaminated soil. Plants such as *Thlaspi, Urtica, Chenopodium, Polygonum sachalase* and *Alyssim* have the capability to accumulate cadmium, copper, lead, nickel and zinc and can therefore be considered as an indirect method of treating contaminated soils [137]. This method is limited to a shallow depth of contamination. Rhizofiltration, the adsorption by plant biomass, can be used to remediate metal-contaminated groundwater. Phytoextraction involves the uptake of metals by trees, herbs, grasses and crops, and can be used for soil treatment. Once contaminated, the plants have to be disposed of in an appropriate manner. Some safe techniques include drying, incineration, gasification, pyrolysis, acid extraction, anaerobic digestion, or safety disposal [138]. Phytostabilization is a process to excrete components

from the plant to decrease the soil pH and form metal complexes. Phytoremediation will be most applicable in shallow soils with low levels of contamination (2.5 - 100 mg/kg).

By the in-situ soil flushing process, extracting solutions are infiltrated into the soil by using surface flooding, sprinklers, leach fields, basin infiltration systems, surface trenches and horizontal or vertical drains. Water with or without additives is used to solubilize contaminants. The efficiency of the extraction depends on the hydraulic conductivity of the soil (see Table 11) and the solubility of the pollutant. Chemical enhanced flushing includes the addition of organic and inorganic acids, sodium hydroxide, which can dissolve the soil organic matter (SOM), water soluble solvents such as methanol, the displacement of toxic cations with non-toxic cations, and the addition of complexing agents such EDTA, or oxidizing/reducing agents [133].

2.9   Stable ceramic adsorption materials

For a possible large-scale industrial application of natural soils, clays and minerals as adsorbent materials, a stable form or matrix would be necessary, capable to resist hydraulic loads and to prevent attrition losses and sludge formation. Therefore it was intended to develop a stable ceramic material based on the chemical composition and physical properties (i.e. sintering temperature) of this natural Chilean volcanic soil. For this purpose, a novel process has already been patented [139]. The process basically consists on the foaming of the raw material (i.e. the natural adsorbent) mixed with reactants for forming rigid polyurethane foam, and a subsequent thermal treatment of the foam at the sintering temperature range of the raw material. The main foam reactants are aromatic polyester-polyols obtained under a patented process by the glycolysis of recycled polyethylene terephthalate (PET) bottles [140], therefore reducing the projected foaming costs of the process and solving partially the problem of managing PET residues.

Polyurethane foams are made using a prepolymer, which is the reaction product of an organic polyisocyanate and a polyol. This prepolymer is reacted at specified volume ratios and isocyanate indices with a polyol component that includes at least one polyol. The foam is made in the presence of a blowing agent and a catalyst as shown in Figure 12 (adapted from [141]). Preferred blowing agents are water and chemical blowing agents that generate carbon dioxide in the reaction. Preferred catalysts have primary or secondary amino-groups that allow them to interact with the resulting polymer structure, thus decreasing the level of volatile components. Moreover, some polyurethane foams also need a stabilization agent in their formula [142].

With the suggested process, a porous ceramic material can be obtained. Moreover, during the thermal treatment, the sites of the original raw material are activated, because of the combustion and elimination of the organic matter. Previous works have demonstrated a successful use of this process in the production of solid ceramic filters based on zeolites and aluminum oxide as raw material.
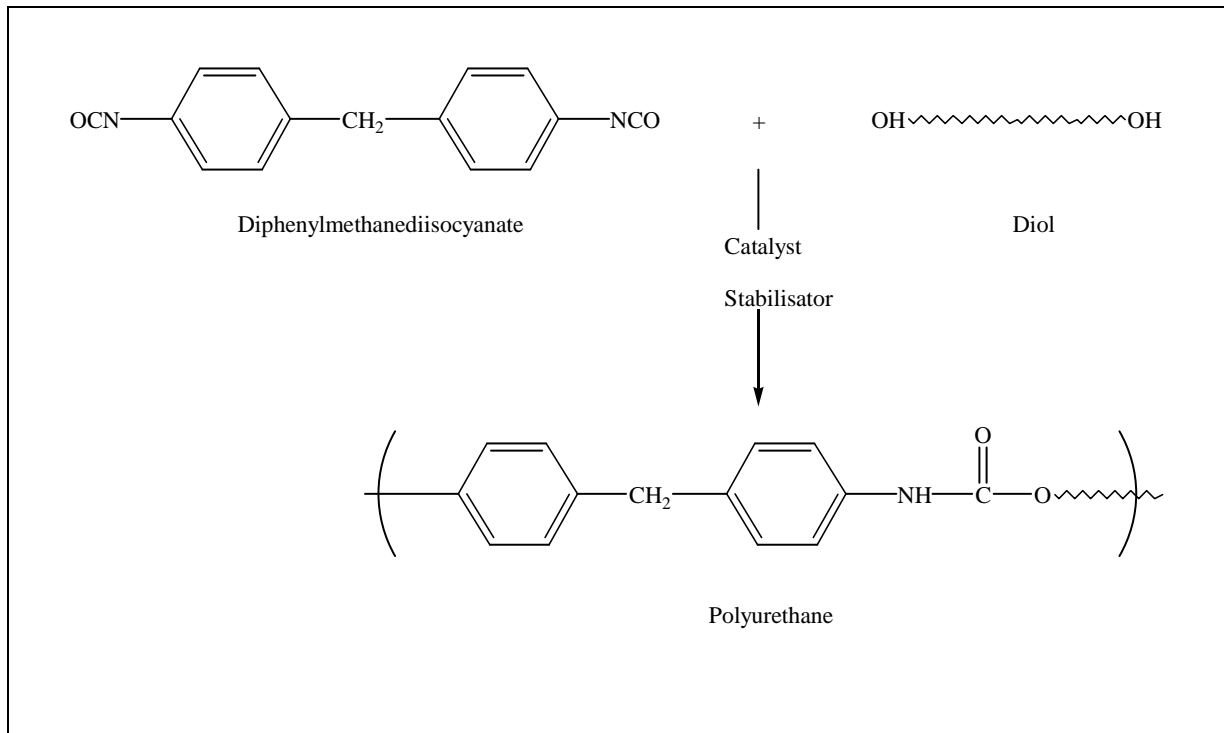
Figure 12: Polyurethane formation from Diphenylmethane-4,4`-diisocyanate and polyol (diol)

3   Materials and methods

3.1   Volcanic soil

The volcanic soil selected for this study was collected in the "Estación Las Encinas", Temuco, IX Region, Chile. This farm is owned by the University of La Frontera and is used as an agricultural experimental station.

3.2   Adsorption kinetics for color and phenolic compounds

For the determination of color and phenolic compounds (from Kraft mill effluent) adsorption kinetics onto vocanic soil, 2.0 g air-dried and sieved volcanic soil (through 2 mm mesh) from the 20-40 cm profile were weighed in plastic flasks. After that, 29 mL Kraft mill effluent (aerobically pretreated) and 1 mL of a KCl 0.1 M solution were added as a background electrolyte. The soil-solution suspension pH was adjusted to 4.5, using HCl or NaOH 1 M solutions. The samples were kept at 20°C in an incubator for 5 min, 15 min, 30 min 45 min, 1 h, 2 h, 6 h, 8 h, 24 h, 36 h, 48 h and 72 h, respectively. Finally, the supernatant was filtered through 0.45 μm membranes for color and phenolic compounds quantification [143].

3.3   Adsorption isotherms

3.3.1   Color and phenolic compounds

0.5 g air-dried and sieved (through 2 mm mesh) volcanic natural and acidified soil from the 20-40 cm profile were weighed in polycarbonate centrifuge tubes. The volcanic soil acidification was done by H_2SO_4 washes, as described by [10]. After that, 29 mL of Kraft mill effluent (aerobically pretreated) and 1 mL of a KCl 0.1 M solution were added as a background electrolyte. The soil-solution suspension pH was adjusted to 4.5, using HCl or NaOH 1 M solutions. The samples were maintained at 25°C under continuous stirring in a shaker for 24 h. Then, the samples were centrifuged for 10 min at 10,000 rpm and filtered through 0.45 μm membranes for color and phenolic compounds quantification [143].

The Langmuir (Equation 10) and Freundlich (Equation 11) models were fitted to the isotherms experimental data. In the Langmuir model, x/m is the adsorbed mass of the pollutant [mg/g soil], k_L is the equilibrium constant (affinity term) [L/mg], b represents the maximum amount that can be adsorbed [mg/g] and C^* is the equilibrium concentration of the pollutant in the liquid phase after adsorption in [mg/L]. In the Freundlich model, the k_F units will depend on the n value and will be expressed as $[(L/mg)^{(1/n)} * (mg/g)]$. k_F and n [-] are empirical constants, which correlate to the maximum adsorption capacity and adsorption intensity, respectively.

Langmuir:
$$\frac{x}{m} = \frac{k_L b C^*}{1 + k_L C^*}$$
(10)

Freundlich:
$$\frac{x}{m} = k_F (C^*)^{1/n}$$
(11)

3.3.2 Chlorophenols

2,4-dichlorophenol (2,4-DCP) and pentachlorophenol (PCP) were selected as reference pollutants. The chlorophenols were of analytical grade from the chemical company Sigma (USA).

0.5 g (for 2,4-DCP) and 0.1 g (for PCP) of air-dried and sieved volcanic soil (through 2 mm mesh) from the 0-20 cm profile were weighed in plastic flasks. 20 mL of 2,4-DCP (0, 5, 10, 15 and 20 mg/L), or PCP (0, 2, 4, 5 and 6 mg/L) solution, with KCl 0.1 M as a background electrolyte were added to the flasks. The soil-solution suspension was adjusted to pH 6.0 and the flasks were maintained at 25°C under continuous shaked in a shaker for 24 h. After that, the supernatant was filtered through 0.45 μm membranes for further chlorophenols quantification with high performance liquid chromatography (HPLC) [144]. The Langmuir and Freundlich models were fitted to the isotherm's experimental data.

3.3.3 Heavy metals

The heavy metals used in this work were Cr(VI) (as CrO_4^{2-} anion from K_2CrO_4), Cu^{2+} (from $CuCl_2$), Zn^{2+} (from $ZnCl_2$) and Pb^{2+} (from $Pb(NO_3)_2$). All the compounds were of analytical grade from the company Merck.

The adsorption isotherms were determined for the four specific heavy metal ions mentioned before: CrO_4^{2-}, Cu^{2+}, Zn^{2+} and Pb^{2+}. The heavy metal solutions were prepared according to the observed concentration ranges of these heavy metals in landfill leachates; therefore solutions of 0, 25, 50, 75 and 100 mg/L of each heavy metal were tested. The adsorption tests were made for three different soil depth levels (0-20, 20-40 and 40-60 cm), which may differ in their organic matter content, and at two different pH values (4.5 and 7.5) at a constant temperature of 25°C. The Cu^{2+}, Zn^{2+} and Pb^{2+} adsorption isotherms were performed in plastic flasks previously washed with nitric acid (1:1, 50% HNO_3 and 50% distilled water). From the fraction with particle size less than 2 mm of all soil profiles, a sample of 0.5 g was taken. Then, 20 mL of the correspondent heavy metal solution prepared in KCl 0.1 M with deionised water were added to the flasks. The soil-solution pH value was adjusted using HNO_3 0.1 M and NaOH 0.1 M. The samples were kept at 25°C and were shaken for 24 h. After that, the supernatant was filtered through a 20-25 μm membrane filter and analyzed for soluble metals (Cu, Zn and Pb) with flame atomic absorption spectroscopy (AAS) [145].

The CrO_4^{2-} adsorption isotherms were performed in plastic flasks previously washed with nitric acid (1:1, 50% HNO_3 and 50% distilled water). From the fraction with particle sizes less than 2 mm of all soil profiles, a sample of 1.0 g was taken. Then, 40 mL of the correspondent heavy metal solution prepared in KCl 0.1 M with deionised water were added to the flasks. The soil-solution pH value was adjusted using HNO_3 0.1 M and NaOH 0.1 M. The samples were kept at 25°C and were shaken for 24 h. After that, the supernatant was filtered through a 20-25 µm membrane filter and analyzed colorimetrically for chromate [145]. The Langmuir and Freundlich models were fitted to the isotherms experimental data, as mentioned above.

3.4 Kraftmill effluent column trials

3.4.1 Breakthrough curves

Wastewater from a modern bleached Kraft mill located in the south of Chile was sampled and analyzed. This mill produces two types of pulp: standard and elemental chlorine free (ECF) pulp. Inside the mill, the wastewater undergoes a primary treatment in a settling tank to reduce its fiber and suspended solids content; this is followed by an aerobic treatment. The analyzed samples correspond to the aerobically treated wastewater. The samples were taken periodically (approximately once a month) throughout a one-year period. Samples were cooled for one day and analyzed immediately for the physical and chemical characteristics shown in Table 12 [146].

Table 12: Kraft mill wastewater characterization

Parameter	Unit	Aerobically treated wastewater	
		Range	Average
pH	[-]	6.8-7.7	7.3
Color	[mg/L]	670-1320	830
Phenolic compounds	[mg/L]	134-332	246
COD	[mg/L]	248-574	351
Tannins & Lignin	[mg/L]	24-44	33

Glass columns (32 cm length and 5 cm internal diameter) were used for breakthrough curve determination. The used adsorptive packing consisted of a mixture (1:4 to 1:1) of the adsorbent material (natural or acidified volcanic soil, 20-40 cm profile) with the structure material (sand). This configuration was used in all the performed experiments (Table 13). The soil acidification procedure was carried out according to [10], washing the soil with a H_2SO_4 0.1 M solution. The sand was washed with distilled water, dried at 100°C and stored in a vacuum desiccator. The columns were filled with 400 g (total mass of the adsorptive packing) and were fed with the aerobically treated wastewater with two different flow rates. The pH of the aerobically treated wastewater was kept constant at 4.5 by dosing a 0.1 M HCl or NaOH solution.

Table 13: Breakthrough experiment conditions

Experiment	Volcanic soil fraction α[a]	Sand fraction	Total mass [g]	Bulk density ρ [g/mL]	Porosity ε	Effluent flow rate [mL/min]
1	0.2	0.8	400	1.26	0.55	1.5[b]
2	0.2	0.8	400	1.26	0.55	2.5[c]
3	0.5	0.5	400	1.03	0.59	1.5

[a]: using natural and acidified soil, linear flow velocity u_o = [b]: $1.25 * 10^{-5}$ m/s and [c]: $2.12 * 10^{-5}$ m/s

3.4.2   Molecular weight distribution of the effluent pollutants

The determination of the molecular weight distribution of the pollutants present in the input and output streams of one soil column was made using tangential ultrafiltration at ambient temperature (20 ± 3°C). The splitting was made using Pellicon XL membranes with a cut-off size of 30,000, 10,000 and 5,000 Da, and a peristaltic pump which gave a flow rate between 30 and 50 mL/min. Previously to the tangential ultrafiltration, the effluent was passed through a cellulose filter with a cut-off size of 5 µm, in order to avoid a quick obstruction of the ultrafiltration membranes. Moreover, each membrane was cleaned with distilled water and pre-conditioned with a $NaHCO_3$ buffer solution, previous to the ultrafiltration process [147].

3.4.3   Fixed bed adsorption rate

For fixed bed adsorption rate calculation, several models have been developed and applied. Some models simply estimate the main design parameters regarding pollutants adsorption and transport in a fixed-bed reactor (filled with soil or an adsorption material) [2]. Other more elaborated models try to determine separately the external film resistance and the internal pore diffusion of the pollutant in a soil or adsorbent column [148]. Nevertheless, due to its simplicity, one the most used models in fixed-bed systems is the empirical model developed by Bohardt y Adams [36],[46],[48],[49],[147], which determines the service time (or the bed length) and the adsorption rate. Although the application of this this model is very simple, its empirical and non-phenomenological character makes it less suitable for possible explanations regarding the adsorption process. Phenomenological models are more suitable for those objectives as the global mass transfer coefficient is the main indicator for adsortion processes. Moreover, phenomenological models with an analytical solution are of great interest, as they combine both, the understanding of the process phenomena and the simplicity of using a final equation for the parameters calculation.

A simple phenomenological model for color and phenolic compounds adsorption was used for predicting analytically the adsorption breakthrough. This model was based on the solute mass balance through the column proposed by [149],[150],[151]. The theoretical results were compared with the experimental data, evaluating the overall mass transfer coefficients between the effluent and the adsorbed phase and the fixed bed adsorption rates. The overall

mass transfer coefficients and the adsorption rates were obtained by the numerical optimization of the solution of the differential equations system involved in the mass balance.

3.5   Heavy metals diffusion trials

3.5.1   Column diffusion trials

Plastic columns (10 cm length and 2.5 cm internal diameter) were filled with ca. 55 g of raw volcanic soil (without sieving) from the 5-20 cm, 20-40 cm and 40-60 cm profile, respectively. The bulk density of the volcanic soil columns was 1.17 ± 0.03 g/cm^3. The columns were saturated with distilled water and sealed at the bottom. Each column was fed with 12,5 mL synthetic leachate at pH 4.5 for a maximum of 50 days. A 2 cm leachate level was maintained on the top of each soil column to promote contaminants diffusion through the soil. The synthetic leachate contained 50 ppm Zn, 2.5 ppm Pb and 5 ppm Cu. After 50 days, the columns were "opened" and cut in slices at five different levels. The heavy metals were extracted from the soil and quantified by flame AAS. Chloride was used as a non-adsorptive indicator and was measured by a colorimetric procedure [152].

3.5.2   Diffusion of pollutants through a mineral liner

A column diffusion model based on Fick's second law and the models proposed by [14],[107],[153],[154] was used for the determination of the heavy metals diffusion coefficients and breakthrough times in a volcanic soil landfill liner.

3.6   Bioremediation   of   soil   contaminated   with   specific chlorophenols

The chlorophenol-contaminated soil biological activity and natural bioremediation capacity was estimated. Respirometric assays were carried out coupled with bacteria, actinomicetes and fungi plate counts and chlorophenols soil concentration measurements through the time.

3.6.1   Respirometric assays

Respirometric assays were carried out according to the methodology of [155]. The assays were done using 50 g of volcanic dry soil, moistened to 60 % of its water-holding capacity, placed in hermetically sealed 1 L flasks and incubated for 115 days at 25ºC. The flasks contained vials with 10 mL distilled water for maintaining a humid atmosphere and 10 mL 0.5 M NaOH for absorbing the produced CO_2. The assays were done in triplicate by adding to the soil 2.5 mL of distilled water as control 1 (M0), a 10 mM KOH solution as control 2 (M0`) and 2,4-DCP or PCP 800 (M1), 80 (M2) and 8 (M3) mg/L solutions, respectively. The flasks were closed hermetically and were stored at 25°C. The produced CO_2 (absorbed in the NaOH solution) was measured by tritiation with a 0.5 M HCl solution.

3.6.2 Bacteria, actinomicetes and fungi plate counts

From the same respirometric assay flasks, soil samples were taken on the days 0, 15, 30, 60, 90 and 115 for bacteria, actinomicetes and fungi determination. In the case of bacteria plate counts, 10^{-3} and 10^{-4} dilutions were used. The plate culture media was casein peptone-glucose-yeast extract agar (Merck), using 50 mg/L cyclohexamide as fungi inhibitor [156]. The plates were incubated for a 48 h period at 28°C [157].

For actinomicetes plate counts, 10^{-3} and 10^{-4} dilutions were used. The plate culture media was actinomicetes agar. The plates were incubated for a 48 h period at 28°C [157]. In the case of fungi plate counts, 10^{-2} and 10^{-3} dilutions were used. The plate culture media was potato-glucose agar (Merck) using 14 mL/L (10%) of tartaric acid as bacteria inhibitor. The plates were incubated for five days at 20°C [157].

### 3.6.3 Development of chlorophenols concentration in soil through time

From the same flasks of the respirometric assays, approximately 8 g of contaminated soil were separated for each time sample and stored at 25°C for 12 h. Then, the humidity was determined at 105°C in each sample. The chlorophenols extraction was made as described by [158]. 4 g of Na_2SO_4 (anhydride) and 4 g of dried soil were mixed and deposited in filter paper. The filter paper was introduced in a Butt tube, which was connected to an extraction balloon adding 70 mL hexane. The extraction was done at a temperature between 140 and 165°C for 16 h. Then, the mixture was evaporated in a rotating evaporator until dryness. HPLC grade methanol (5 mL) was used to suspend the sample again. The sample was then sonicated for 0.5 h. After that, the methanol solution was filtered in a 0.45 µm membrane and leveled to 5 mL. This solution was then injected into the HPLC equipment.

3.7   Analytical methods

3.7.1 Total organic carbon

The total organic carbon (TOC) determination was based on the methodology described by [159]. The TOC value is determined indirectly from the difference between the total carbon (TC) and the total inorganic carbon (TIC) content of the soil sample. The equipment for TOC determination basically consists of a combustion unit, a TIC determination unit, a CO_2 analyzer and a computer for controlling the whole system (Figure 13).

The combustion unit consists of two in-series connected ovens: an infrared oven and a resistance oven. In the infrared oven the heat is produced by radiation, which reflects on the gold surface and focuses on the combustion tube. In about 30 s the oven reaches a temperature of 950°C. The in-series connected resistance oven operates at a steady-state temperature of 850°C to produce a complete oxidation of the combustion gases thanks to a prolonged residence time.
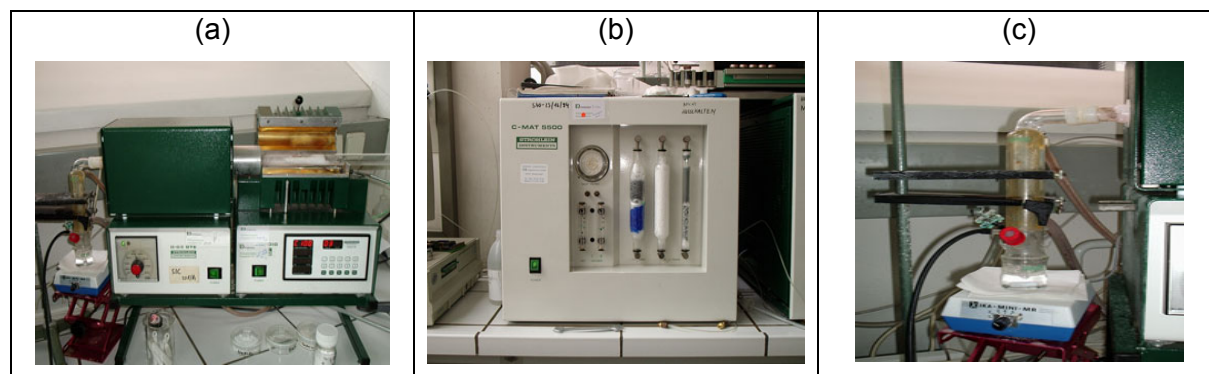
Figure 13: (a) Combustion unit (b) CO_2 analyzer and (c) TIC determination unit of the TOC equipment

For the TC-determination, the sample passes in a quartz receptacle through a quartz tube to the infrared oven, where the sample is combusted at 950°C and all the carbon present in the sample is transformed into CO_2. The combustion gases then enter the CO_2 analyzer through a cooling trap. Before the gases reach the infrared detector for determining the CO_2 concentration, halogenated compounds, water and dust have to be eliminated from the gas stream. Halogenated compounds are adsorbed in a zinc column, water is absorbed in magnesium perchloride and dust is eliminated with a filter. Moreover, the first column from the CO_2 analyzer (Figure 13b) consists of sodium hydroxide and silica, for cleaning the O_2 used in the combustion stage. An infrared radiator, an infrared sensor and a cell compose the infrared detector. The cell is an internally clothed gold tube, which is closed by optical glasses at both ends. While the combustion gases pass through this tube, the infrared radiator emits a wide spectral ray to the cell that reaches the surface of the infrared sensor. The CO_2 concentration in the gas is based on the Lambert-Beer law. Therefore, the CO_2 concentration depends on the transmittance by a logarithmic relationship (Equation 12), where E is the optical density (or extinction), I_i is the initial intensity and I is the measured intensity [160].

$$E = \ln\left(\frac{I_i}{I}\right) \tag{12}$$

The analyzer is able to detect (with two different sensors) two different CO_2 levels. The lower level ranges between 50 to 400 ppm and the higher level ranges between 400 and 500 ppm. Finally the computer integrates the signal and the result is given as TC in %.

For the TIC determination, a known weight of the original sample is put into the stripping column (Figure 13c). The hermetic glass equipment is cleaned with oxygen until no more CO_2 from the surrounding air is present. The inorganic carbon from the sample reacts by the injection of H_3PO_4 forming CO_2. The analyzer detects the CO_2 and the result is given as TIC %. H_3PO_4 does not attack the organic carbon, but remains in the sample.

3.7.2   Cationic exchange capacity (CEC)

The cationic exchange capacity determination was based on the methodology described by [161]. The effective cationic exchange capacity (CEC_{eff}) is the exchange capacity from the soil at each pH value. The potential cationic exchange capacity (CEC_{pot}) is the measured exchange capacity at pH 7. The CEC_{eff} will be lower than the CEC_{pot} as the pH value of the measurement decreases, and is higher, as the variable charge fraction of the soil increases. Therefore, the CEC_{eff} was measured at the pH value of the soil sample, as well as the exchangeable cations Na^+, K^+, Ca^{2+}, Mg^{2+}, Mn^{2+}, Fe^{3+} and Al^{3+}.
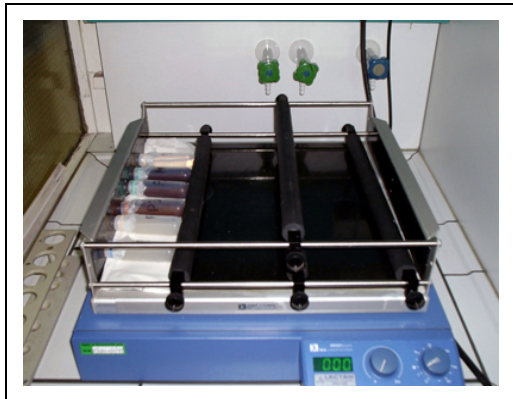
Figure 14: Shaking chamber

For the CEC_{eff} and exchangeable cations determination, 2.5 g dry soil were weighed in centrifuge tubes and saturated with a 0.1 M $BaCl_2$ solution. For a successful barium (Ba) saturation of the soil samples, the mixtures were shaked for 1 h in a shaking chamber (Figure 14) and after that centrifuged at 15,000 rpm. The supernatant was decanted and collected in a 100 mL flask. This procedure was repeated three times until the soil was completely saturated with barium. After that, the 100 mL flask was leveled with the 0.1 M $BaCl_2$ solution. This liquid sample served also for determining the exchangeable cations content by flame atomic absorption spectroscopy (AAS). The determination of the exchange equilibrium from the soil was then started with a 0.0025 M $BaCl_2$ solution. The samples were shaken over night and then centrifuged at 15,000 rpm. The supernatant was decanted while the soil was mixed with 30 mL of a 0.02 M $MgSO_4$ solution and shaken over night. This procedure allows for the total barium, present in the liquid phase as well as adsorbed in the soil, to precipitate in the form of barium sulfate; while magnesium occupies the free exchangeable cation places. After this procedure, the samples were centrifuged at 15,000 rpm again. The collected supernatant was then filtered through a paper filter in an Erlenmeyer flask. A blank sample was also measured by doing the procedure already described in a sample tube without soil. The determination of the CEC_{eff} was done through the measurement of the magnesium concentration in the filtered supernatant solution by flame AAS. The measured magnesium concentration in the supernatant of the samples has to be corrected, as some liquid volume is left in the soil sample after the centrifugation process. The correction formula is expressed in Equation 13:

$$C_2 = \frac{C_1 * (m_{MgSO4} + m_2 - m_1)}{m_{MgSO4}}$$

(13)

Where C_1 is the measured magnesium concentration of the sample [mmol/L], C_2 is the corrected magnesium concentration of the sample [mmol/L], m_1 is the mass of the centrifuge tubes with the dried soil sample [g], m_2 is the mass of the centrifuge tubes with the humid soil sample [g] after the 0.0025 M $BaCl_2$ solution treatment and m_{MgSO4} is the added mass of the 0.02 M $MgSO_4$ solution (30 g). The CEC_{eff} of the soil sample is then the difference between the magnesium concentration of the blank supernatant and the magnesium concentration of the filtered soil supernatant according to Equation 14:

$$CEC_{eff} = \frac{V_{MgSO4} * (C_b - C_2)}{m_s}$$

(14)

Where V_{MgSO4} is the added volume of the 0.02 M $MgSO_4$ solution (30 mL), C_b is the magnesium concentration in the blank solution [mmol/L] and m_s is the mass of the dried soil sample [g].

The determination of the Na, K, Ca, Mg, Mn, Fe and Al content in the soil sample was done by flame AAS, as described in Chapter 3.7.3.1. The computer of the equipment did the evaluation of the measured data, where the software directly gave the concentration in [mg/L] for each measured element. The measured concentration of the blank was subtracted from the concentration measured in the soil solutions. The final result of the exchangeable cations expressed as cmol+/kg was obtained according to Equation 15:

$$X_C = \frac{(C_X - C_b) * V * 100}{MW * m_s}$$

(15)

Where X_C is the measured exchangeable cation [cmol+/kg], C_X is the cation concentration [g/L], C_b is the blank concentration [g/L], MW is the molecular weight of the cation [g/mol], m_s is the soil mass [kg] and V is the solution volume [L].

3.7.3   Heavy metals as specific elements

3.7.3.1   Volcanic soil characterization and exchangeable cations determination

The measurement of specific elements (metals) during the volcanic soil characterization and exchangeable ions determination was made by flame atomic absorption spectrometry (AAS). The procedure was based on the protocols of the Laboratory for Environmental and Process Analyses at the University of Leoben. The specific elements determined were Na, K, Ca, Mg, Mn, Fe, Al and Si, in the case of the soil characterization and Na, K, Ca, Mg, Mn, Fe and Al,

in the case of exchangeable cations determination. First, the samples were put into a microwave oven. For this purpose, 0.2 g of the samples were weighed in teflon receptacles and then reacted with 6 mL HNO_3, 2 mL HCl and 2 mL HBF_4. Each main sample was split into three parts (triplicates). The teflon receptacles were closed and introduced to the microwave oven. The microwave oven computer program was then started and after cooling (around 3 h) the samples were taken from the microwave oven and leveled with distilled water to 50 mL. The split and diluted samples were analyzed for the specific elements mentioned before. For the Al and Si determination a N_2O/acetylene flame was used. In the case of all other elements, an acetylene flame was applied. In a first step, the standard elements were measured for the elaboration of a calibration curve. Then, each element was measured in a GBC Avanta AAS equipment, as shown in Figure 15.

Figure 15: Flame AAS equipment used

The computer of the flame AAS equipment directly gives the concentration of each specific element in [g/L]. The calculation of the content in [mg/kg] of each specific element was done according to Equation 16:

$$X_E = \frac{C_E * V * 100}{m_s}$$

(16)

Where X_E is the measured content of the specific element in the soil [mg/kg], C_E is the specific element concentration [mg/L], V is the solution volume [L] and m_s is the soil mass [kg]. The final value stored in the data system was the average of triplicate determinations.

### 3.7.3.2 Adsorption isotherms and diffusion trials

Soluble Cu, Zn and Pb were also measured by flame atomic absorption spectrometry (AAS). The equipment used was a GBC Scientific Equipment Pty Ltd., serial number 838 (Australia). The lamps used were a Photron Pty Ltd. (Australia) for Zn and Perkin-Elmer (USA) for Cu and Pb. No suppressor was used in the measurements. The flame used for the

measurement of all metals was an air-acetylene one [152]. The soluble Cr (i.e. CrO_4^{2-}) determination was performed by colorimetry using a Hach Colorimeter DR/2000 (USA). The determination was done at a wavelength of 540 nm with a detection limit of 0.02 mg/L [152].

3.7.4   Anionic exchange capacity

The determination of the anionic exchange capacity (AEC) was based on the procedure described by [162]. Syringes doted with a capillary hose were filled with 4 g of dry soil samples as described in Figure 16.
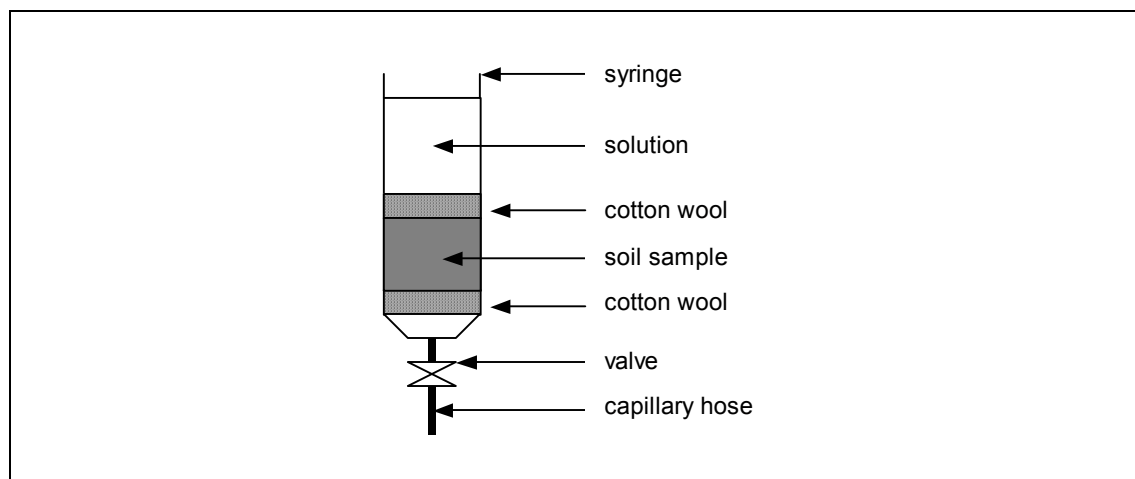
Figure 16: Equipment employed for the determination of the anionic exchange capacity

The soil sample was secured in between cotton wool walls, to avoid sample loses while doing the extraction procedure. After the compaction of the sample with the syringe piston, 5 mL of a 2 mM NH_4Cl solution was added to the system. With the valve closed, the system was left under these conditions overnight. The soil-solution mixture was expected to be in equilibrium by the next day. Then, during the next day, the sample was rinsed up to 10 times with 5 mL of 2 mM NH_4Cl solution, for a total time of 3 h. Such, the soil sample became saturated with chloride. The syringe with the humid sample was then weighed, for determining the water fraction of the humid sample. The chloride present in the saturated sample was then displaced by washing the soil 10 times with 5 mL of a 20 mM KNO_3 solution for 3 h. The resulting extraction solution was weighed and analyzed by ion chromatography for its chloride content.

For the calculation of the AEC, first of all, the dry and humid soil samples in the syringes were weighed to determine the difference in quantities of the 2 mM NH_4Cl solution volume (or mass) retained in the soil. Then, with the calculated mass [mg] of NH_4Cl present in the 2 mM solution retained in the soil, the chloride mass was calculated, knowing that 66% of Cl^- is present in one molecule of NH_4Cl. After that, the chloride concentration of the displaced soil solution was determined by ion chromatography. The results given by the chromatograph were in [mg/L], therefore the mass of chloride is obtained by knowing the displaced solution

volume. The difference between the chloride mass in the displaced solution and the retained solution is namely the AEC, expressed as [cmol/kg].

3.7.5   pH value

The determination of the pH value of the soil was based on the methodology described by [163]. Basically, 10 g of dry soil were weighed for the pH value determination in 90 mL of distilled water and 25 mL of a 0.01 M KCl solution. The suspension was mixed with a magnetic stirrer for about 10 min. After calibrating the pH-meter with standard buffer solutions, the measurement was performed taking the average pH value for every three measurements.

3.7.6   Buffer capacity

The determination of the buffer capacity of the soil was based on the methodology described in [162]. 10 g dry soil and 25 mL of a 0.1 M KCl solution were put in a 100 mL glass beaker. The suspension was mixed with a magnetic stirrer and after that, the pH value was measured. Then, 0.5 mL of a 0.1 M HCl solution were added and the suspension was stirred again. The new pH value was measured. The HCl dosage was repeated until the desired acid pH range was covered. The same experiment was repeated adding NaOH (0.1 M solution) for covering the alkaline pH range.

The determination of the specific buffering capacity of Al and Fe was also determined. Al and Fe were determined in the solution at an acid and at an alkaline pH value. The soil solution was filtered prior to the determination of Al and Fe content by flame AAS. For the determination of Al and Fe at the acid and alkaline pH values, 8 mL of a 0.1 M HCl solution and 12 mL of a 0.1 M NaOH solution were added to the soil sample, respectively.

3.7.7   Particle size distribution

The determination of the particle size distribution of the soil was based on the methodology described in [164]. The particle size distribution was performed by means of wet sieving and sedimentation. The wet sieving procedure was used for determining the particle size distribution for particles with a size higher than 0.063 mm, whereas the sedimentation method supplied the particle size distribution less than 0.063 mm. The size limit for the sedimentation procedure was established at 0.001 mm. In the first step, the wet sieving process took place with the following sieves dispositions: 4 mm; 2 mm; 1 mm; 0.5 mm; 0.25 mm; 0.125 mm and 0.063 mm. The sample mass for each measurement was about 150 g. Before the wet sieving, the samples were deliberately not dried at 105°C in the drying oven to avoid changes in the clay fraction of the samples. Such changes would make the complete separation of the fraction under 0.063 mm very difficult and questionable, and would make the subsequent sedimentation process almost impossible. Therefore, the determination of the dry mass of the samples was based on the water content, which was determined

previously at 105°C for 24 h in the dry oven. Before wet sieving, the samples were treated in an ultrasound bath for 15 min, to dissolve any possible particle aggregates. The wet sieving process happened subsequently by means of a Retsch sieve machine in step by step operation (Figure 17). The sieving duration was established based on the turbidity of the particle size fraction less than 0.063 mm passage and took ca. 25 min for each sample. After finishing the wet sieving, the remnants of each particle size fraction were dried in the drying oven at 105°C until constant weight was obtained. The particle size fraction less than 0.063 mm was caught in receptacles and was then analyzed by the following sedimentation experiment.

Figure 17: Wet sieving process applied

The particle size fraction of less than 0.063 mm was allowed to settle in the glass receptacles (Figure 18); the water level was then rised up and the samples were dried at 35°C in the drying oven for several days until constant weight was obtained. Higher temperatures were deliberatly not selected because of possible clay changes. Each hydrometer and test-tube was weighed. Before the experiment started, it was very important to correct the hydrometer's reading. During the experiment, the hydrometer's reading was made at the upper meniscus limit, however the scale of the hydrometer is valid only for a flat water level. Therefore it was important to do the mentioned correction. In addition, the distilled water density is lower than that of the water-dispersant mixture and thereby another correction is to taken into account. To ascertain the calibration of these two deviations and for the correction of a possible zero point error, 25 mL dispersant ($Na_4P_2O_7 \cdot 10H_2O$) were added to a test-tube and leveled to 1000 mL with distilled water. The hydrometer was immersed in the solution and the reading was done at the upper meniscus limit, which corresponded to the correction factor C_m.

Figure 18: Settlement of the fraction < 0.063 mm

After drying, the samples were mixed with 25 mL of dispersant and ca. 100 mL of distilled water to avoid flocks formation. Subsequently, the samples were cleaned completely with distilled water in a test-tube and filled to the 1000 mL mark. The suspension was shaken for some minutes in the test-tube, whereby the test-tube was reiteratively totally overturned. After that, the test tubes with the suspensions were placed on the table. The hydrometer was immediately immersed in the suspension to permit a free swimming of it (Figure 19). The hydrometer measurements were made after 0.5, 1, 2 and 5 min. Then, the hydrometer was carefully removed from the suspension and cleaned with distilled water. New measurements were made after 15 and 45 min and after 2, 6 and 24 h. The temperature was immediately registered after each measurement.

Figure 19: Sedimentation procedure applied

The particle size distribution results were presented as percentage of the dry mass. The mass difference (sieving loss) between the initial weighed soil mass and the total collected particle size fractions cannot be more than 1%, as described in [164]. In the case of the sedimentation experiment, the different particle size fractions were determined based on the sedimentation velocity of each fraction in still water. Particles with different sizes settled with different velocities in water medium, and therefore the distribution of the particle sizes as well

as the suspension density is expected to change with the height of the test-tube. Stokes law, as described in Equations 17 and 18, determines the relationship between particle size, density and sedimentation velocity.

$$\text{Stokes law:} \qquad d = \sqrt{\frac{18 * \eta * v}{g * (\rho_p - \rho_w)}} \qquad\qquad (17)$$

$$\text{with:} \qquad v = \frac{h_p}{t} \qquad\qquad (18)$$

Where d is the particle diameter [cm], η is the dynamic viscosity of the suspension [g/cm s], v is the particle sedimentation velocity [cm/s], ρ_p is the particle density [g/cm^3], ρ_w is the water density [g/cm^3], g is the acceleration of gravity [cm/s^2], h_p is the hydrometer's reading level [cm] and t is the time [s]. In addition, h_p was determined with the following relationship (Equation 19):

$$h_p = h_1 + \frac{1}{2} * \left(h - \frac{V_H}{A_C} \right), \qquad\qquad (19)$$

where h_1 is the distance between bottom of the rod of the hydrometer and the reading level (cm), h is the height of the hydrometer's body until the bottom of the rod [cm], V_H is the volume of the hydrometer's body [cm^3] and A_C is the transversal area of the cylindrical test-tube [cm^2] (Figure 20).

The water density and the dynamic viscosity of the suspension, as described in [164], are related to the temperature (T in °C) as indicated in Equations 20 and 21, respectively.

$$\rho_w = \frac{1}{1 + \left((2.32 * T - 2.0)^2 - 182 \right) * 10^{-6}} \qquad\qquad (20)$$

$$\eta = \frac{0.00178}{1 + 0.0337 * T + 0.00022 * T^2} \qquad\qquad (21)$$

The sieve passage corresponds to the mass fraction a, and is described analitically in Equation 22.

$$a = \frac{100}{m_d} * \frac{\rho_p}{\rho_p - 1} * (R + C_T) \qquad\qquad (22)$$

Where m_d is the sieve passage dry mass [g], R is the corrected auxiliar value [g] and C_T is the temperature correction factor (taked from [164]). The factor R is calculated according to Equations 23 and 24.

$$R = R` + C_m \tag{23}$$

$$R` = (\rho`- 1) * 10^3 \tag{24}$$

Where $R`$ is the auxiliar value calculated from the hydrometer's reading [g], $\rho`$ is the hydrometer's reading [g/cm^3] and C_m is the correction factor for the hydrometer's reading.
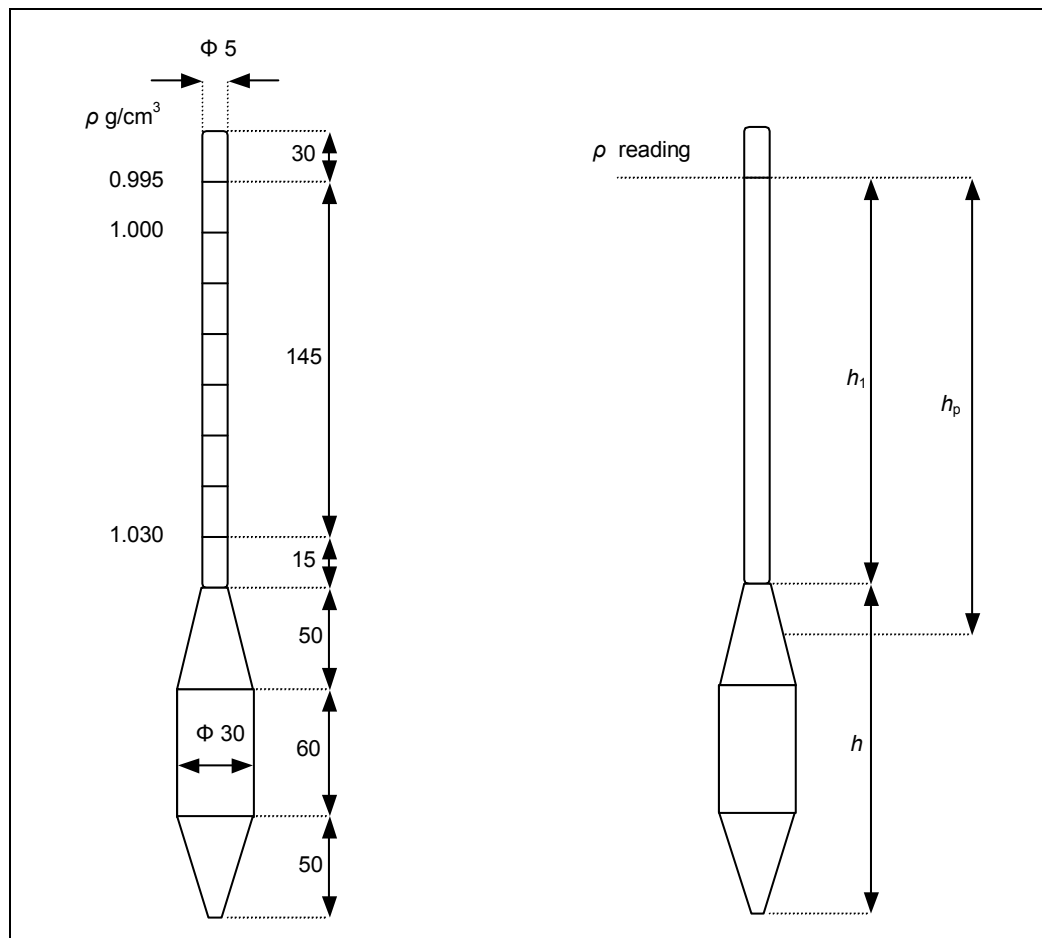
Figure 20: Hydrometer used (dimensions in mm)

The determination of the particle density (ρ_p) was performed through a capillary pycnometer, as described in [165]. First of all, the mass of the capillary pycnometer with the stuff was registered. Then, the pycnometer was filled with distilled water and closed. No air bubbles can remain in the stuff, and the capillary tube has also to be completely filled with water. In the next step, the mass of the water filled capillary pycnometer including the stuff was registered. Knowing the density of the distilled water at the experiment conditions, the volume of the capillary pycnometer was determined. After that, as the pycnometer was already dry, ca. 20 g dry soil sample were weighed in it. Then, the pycnometer was filled with distilled water until 3 cm below its upper level and the sample air was eliminated. Finally, the

pycnometer was totally filled with distilled water and then weighed. The particle density was estimated according to Equations 25 and 26.

$$\rho_p = \frac{m_d}{V_b} = \frac{m_d}{V_c - V_w} \tag{25}$$

$$V_W = \frac{m_w}{\rho_w} = \frac{m_t - (m_c + m_d)}{\rho_w} \tag{26}$$

Where ρ_p is the particle density [g/cm^3], m_d is dry soil sample mass [g], V_b is the bulk volume occupied by the soil sample in the pycnometer [cm^3], V_c is the volume of the pycnometer [cm^3], V_w is the water volume in the pycnometer [cm^3], m_w is the water mass in the pycnometer [g], ρ_w is the water density [g/cm^3], m_t is the total mass including the pycnometer, the soil sample and the water [g], and m_c is the mass of the capillary pycnometer [g].

3.7.8   Loss on Ignition (LOI)

The loss on ignition (LOI) of a soil sample is a measurement of the total soil organic matter (SOM). It is the difference between the initial and the final (after ignition) soil sample mass. The procedure was carried out according to [166]. A dry soil sample of about 2 g was weighed in a platinum pan and completely burned in the oven at 1000°C for 1 h. Then, the sample was cooled in a desiccator and the mass after ignition was registered. After that, the sample was burned for another hour, to secure a final constant mass, and weighed again. Samples were treated in duplicate.

3.7.9   Proctor density

The Proctor density is the highest possible density of a dry soil sample under defined experimental conditions. For a possible soil density enhancement, its porosity has to be reduced. At the same time the shear strength and stiffness of the soil are enhanced. This is achieved by adding water to the soil sample. Until specific water content in the soil sample, the density of the dry soil sample is enhanced, as the development of water pore pressures because of the presence of water pores in a non-saturated soil sample provokes the disorder of the soil particles. After this specific water content in the soil sample, the dry soil density decreases again, as the water pores cannot flow quickly into the remaining free-pores, because of the dynamic forces produced during the enhancement of the soil density. In a totally water saturated soil, no possible dynamic density enhancement is taking place. Moreover, the absolute limit is the soil particle density, when no more water and air are present in the soil sample. The relationship between water content and dry soil density is known as Proctor curve and the maximum density at the specific water content will be the Proctor density.

The determination of the Proctor density of the soil was based on the methodology described in [167]. The sample compaction was done in a steel cylinder (Figure 21).
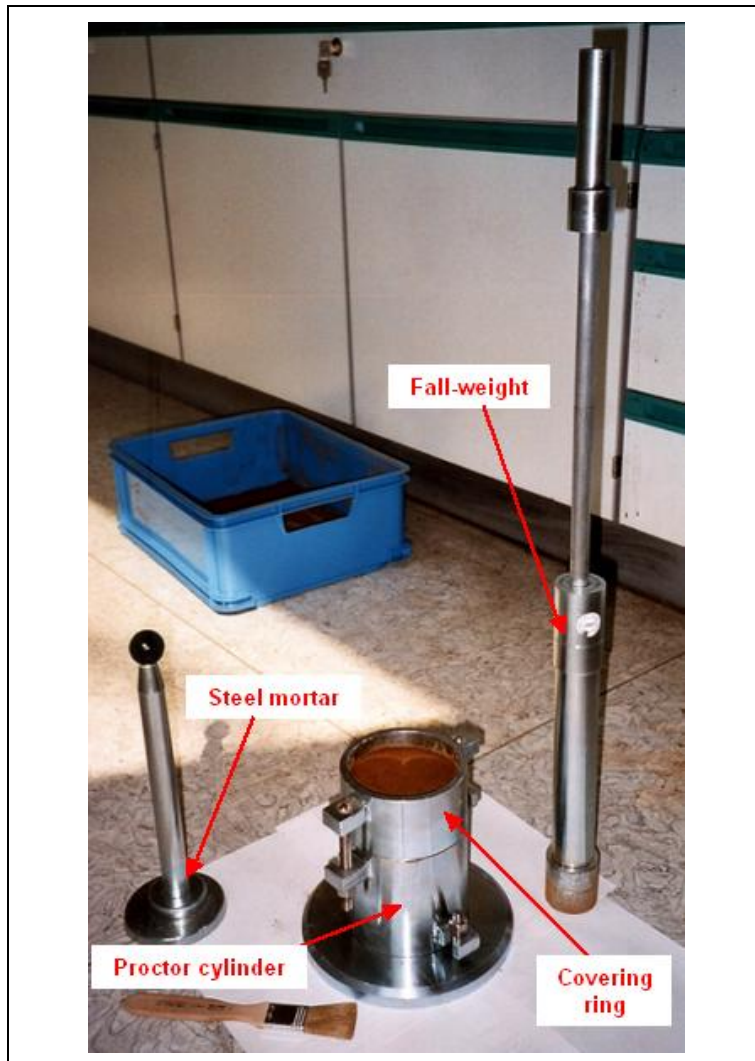
Figure 21: Proctor density determination equipment used
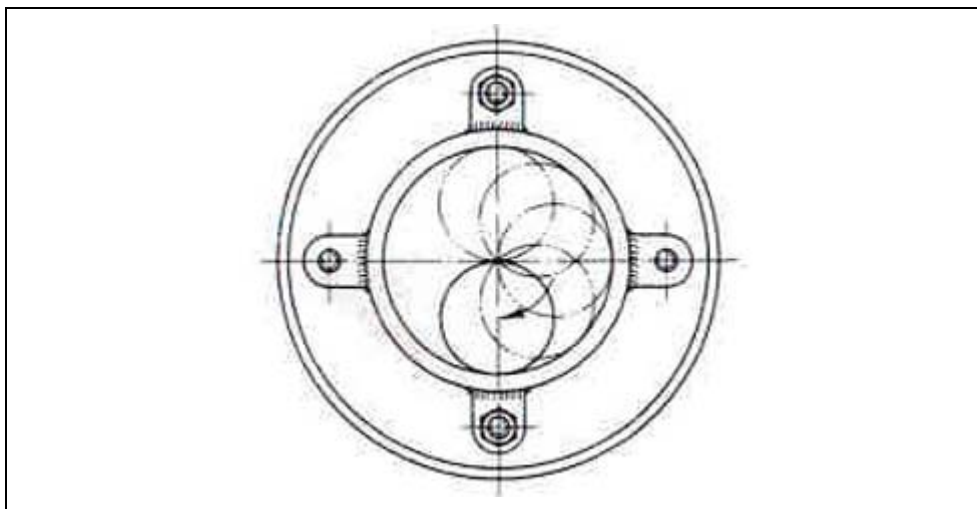
**Figure 22:** Compression of the soil sample in the Proctor cylinder

The diameter of this cylinder depends on the maximum particle size fraction of the soil sample. In this case, for volcanic soil and zeolites the maximum particle size fractions are 2 and 4 mm, respectively. This requirement makes the 100 mm cylinder to be the most suitable for the Proctor density determination. The soil quantity also depends on the maximum particle size fraction of the soil sample, as well as on the Proctor cylinder diameter. The sample has to be compacted between the half and the quarter part of the original volume. Therefore, 2 kg soil was used for the Proctor density determinations. First, the sample was dried at 80°C until constant mass. Then, a known water quantity was added to the soil sample. The initial water quantity selected was far from the supposed optimal water content. After that, the samples were introduced into the Proctor cylinder with a shovel and separated in three layers with same thickness. Each layer surface was then slightly pressurized with a steel-mortar, and subsequently compacted with 25 beats of a 2.5 kg fall-weight from a height of 30 cm in a circular way of compression (Figure 22). The initial sample layer thickness selected allowed the compacted sample to completely fill the Proctor cylinder, with a maximum 10 mm level difference in the covering ring. The beats were done without any break time (2 s between each beat). When the three layers were already compacted, the covering ring was retired and the remaining sample part over the Proctor cylinder was carefully put away. The sample surface was exactly leveled at the Proctor cylinder top level with a steel ruler. Finally, the cylinder was weighed with the sample. After this first experiment, the other experiments with different water content were performed in the same way. To obtain an homogeneous water content in the soil sample, the humid sample was left for 10 min in the covered Proctor cylinder and was mixed after that. The water content was determined after each experiment, by weighing the humid mass of each soil sample after the Proctor experiment. Subsequently the complete samples were dried after each experiment and the dry mass was determined. The difference between the humid and the dry mass resulted in the water fraction expressed as the water mass/dry soil mass ratio.

3.7.10 Hydraulic conductivity

The hydraulic conductivity (K_f) value describes the resistance of a particular soil to the flow of a fluid and can be only exactly determined in the Reynolds range between 1 and 10. The K_f value of a water-saturated soil can be determined using Darcy's law. Under the condition that the water flow through the soil is in a laminar regime, Equation 27 can be applied.

$$\text{Darcy's law:} \quad \frac{Q}{A} = K_f * i \tag{27}$$

Where Q is the water flow rate [m³/s], A is the cross section of the soil [m²], K_f is the hydraulic conductivity [m/s] and i is the hydraulic gradient [m/m] expressed as $\Delta h/L$ (Figure 23). Measuring the flow rate that passes through the soil sample (Q) and knowing the cross section of the soil sample (A) and the $\Delta h/L$ value (i), the K_f value can be determined from Equation 27.
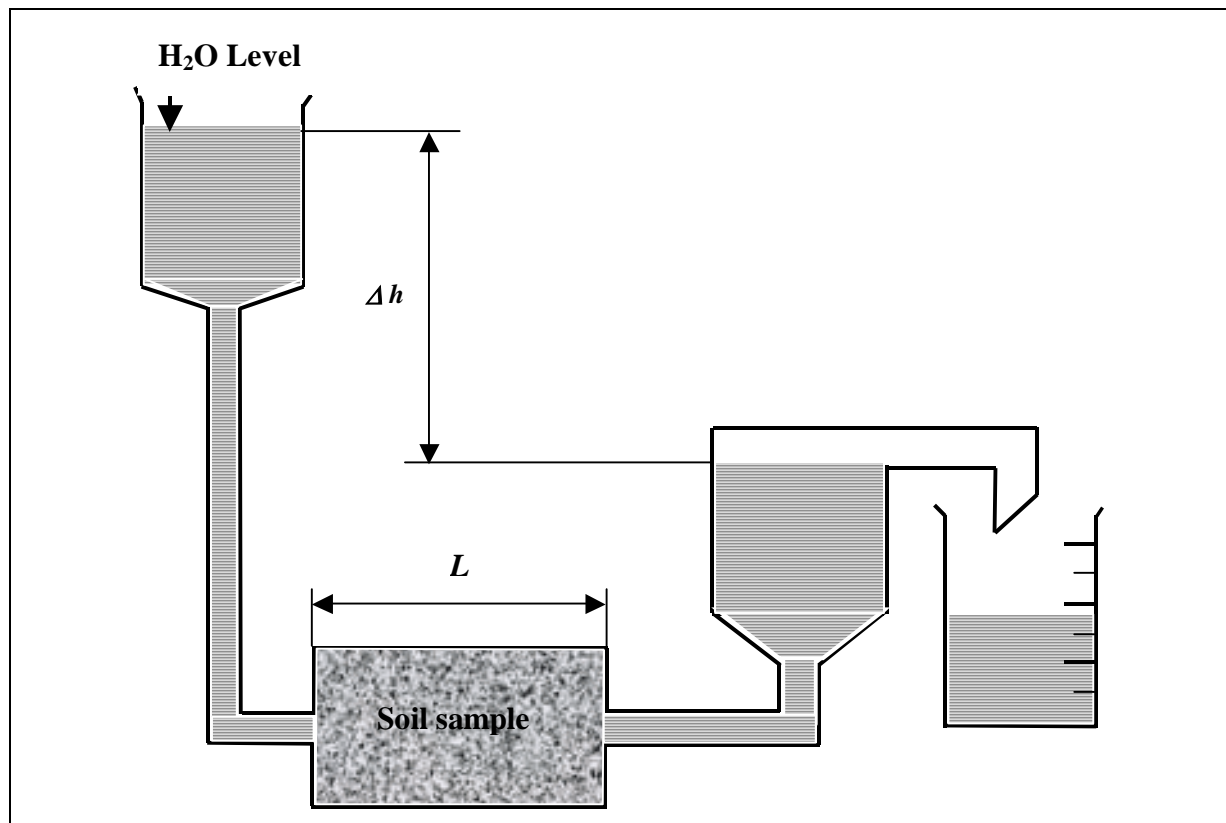
Figure 23: Darcy's law principle used for K_f determination

In addition, the standardized K_f values at 10°C (K_{f10}) were calculated using the K_f values determined at the measured water temperature (T) with the Poiseuille formula [168], presented in Equation 28.

$$K_{f10} = \frac{1.359}{1 + 0.0337 * T + 0.00022 * T^2} * K_f \tag{28}$$

The determination of the hydraulic conductivity of the soil was based on the methodology described in [168]. A hydraulic conductivity cell with changeable i gradient was chosen for determining the K_f values. Three standing glass tubes with a 4, 6 and 8 cm internal diameter were used for the supply of different water flow rates (Q) and hydraulic gradients (i) (Figure 24). The highest input of the standing tubes used was 220 cm and for the determination of the water flow rate, the water level in the tubes was measured through the experiment times.

The K_f value determination was performed at the maximum dry density of the soil, i.e., at the Proctor density. The samples were compressed in the Proctor cylinder prior to building the hydraulic conductivity cell. The hydraulic conductivity cell had three connections; for water input, water output and air drainage (Figure 25). In addition, for a homogeneous water distribution through the soil, a filter stone was put in the upper coverage and the bottom of the hydraulic conductivity cell. The water flow was supplied from the bottom to the top of the cell. First, the system was filled with water, while draining the air. As soon as the sample was free from air bubbles, the experiment and measurements began.
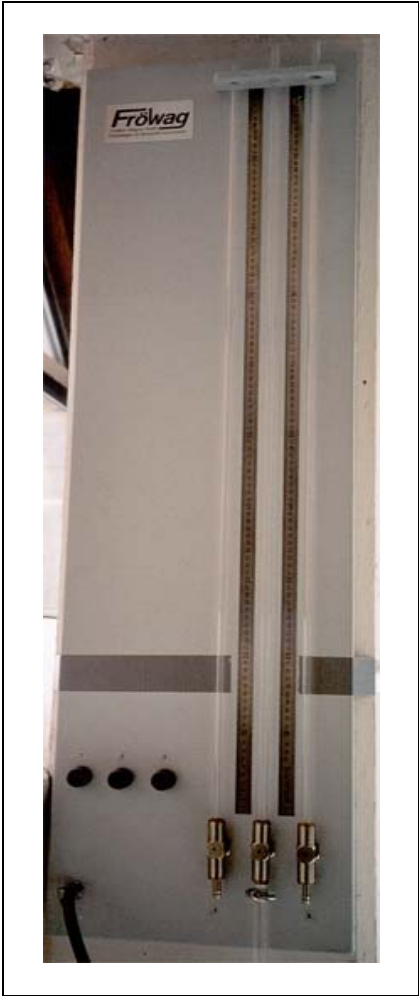
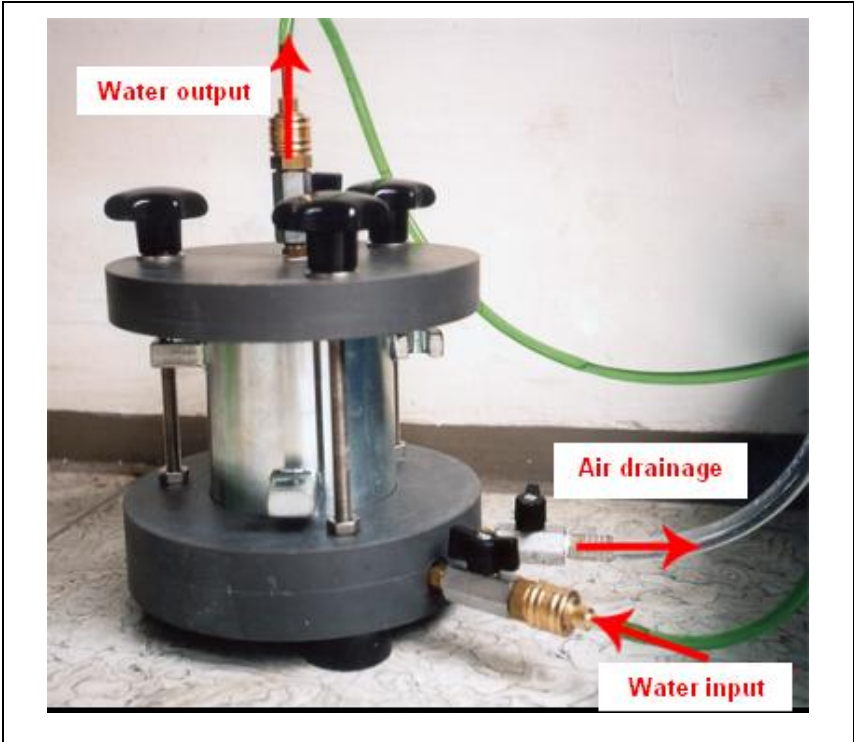**Figure 24:** Standing glass tubes

Figure 25: Hydraulic conductivity cell

In all the experiments the samples were completely saturated. For achieving this aim, water was supplied until the input and output flow rates were equalized. The changeable hydraulic gradient (*i*) was obtained by making experiments with different water levels in the input glass tube and a constant water level in the output glass tube. The level difference in the input glass tube was measured through a specific time for the flow rate calculation. The water temperature was also measured in each experiment and each trial was repeated four times.

3.7.11 X-Ray fluorescence spectrometry (XRFS)

The X-Ray (Roentgen) fluorescence analysis was carried out according to the procedure given by [169]. This method allows for the quantitative determination of chemical elements with an atomic number $Z \geq 5$ down to trace level concentrations. It is mainly used to determine the content of principal and secondary elements like Si, Al, Mg, Ca, Fe, K, Na, Ti, S and P in silicate rocks, as well as trace compounds like the heavy metals Pb, Zn, Cd, Cr and Mn. The X-Ray fluorescence spectrometry (XRFS) is a quick and non-destructive method, appropriate for the evaluation of solid and liquid samples. The X-Ray fluorescence equipment is presented in Figure 26. This equipment is a Philips PW 1410 wavelength dispersive system. Using this method (Figure 27), the sample is radiated with X-rays, which are produced in the Roentgen tube. Thus, the emitted fluorescence radiation, which depends directly on the composition of the soil sample, passes through the first collimator and reaches the crystal analyzer. The radiation is diffracted at the crystal analyzer and then reaches the detector system by passing through a second collimator. The collimators have the task to preserve the radiation geometry before and after the crystal analyzer. In addition, a goniometer allows for the detector to always pivot exactly at a double angle (2θ) position, when the crystal analyzer rotates at a single angle (θ) position, regarding to the incident radiation over the crystal [170]. At the end, the detector finally records the energy and fluorescence radiation values.
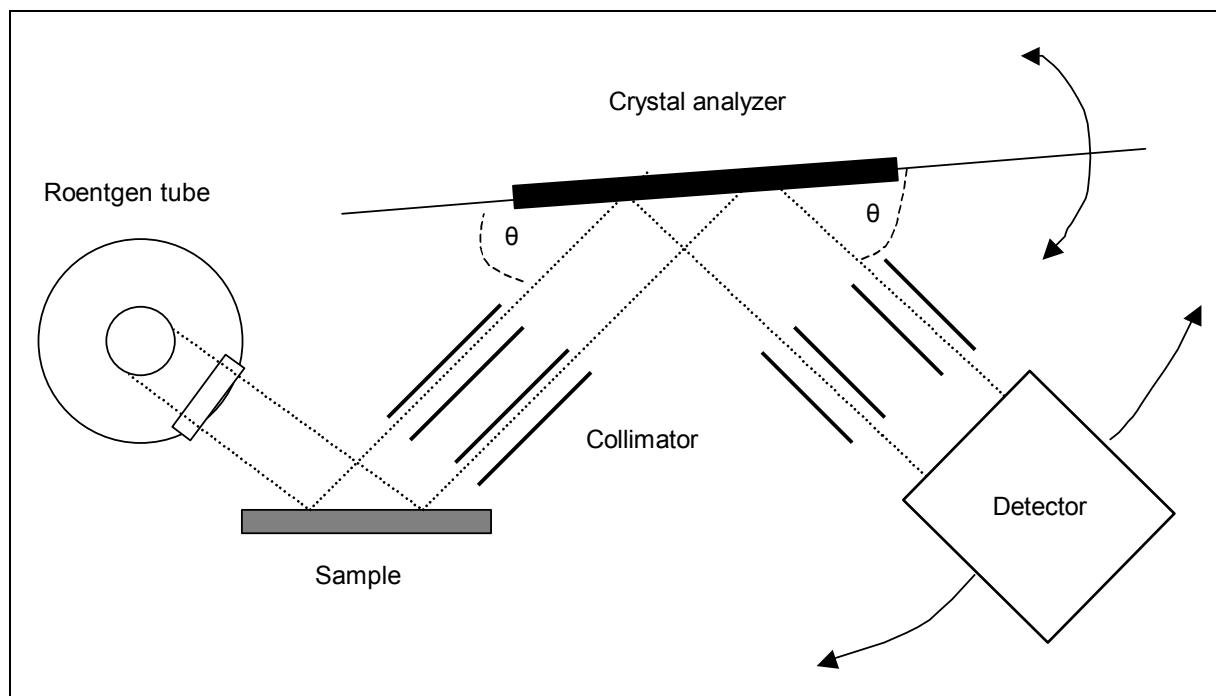

Figure   26: Wavelength   dispersive   X-Ray fluorescence equipment used

The task of the Roentgen generator is to supply, with high stability, a discrete tension between 20 and 200 kV and an electric current between 5 and 80 mA to the Roentgen tube. The sample receptacle serves for taking the sample in the form of pressed dust pills, melting pills, solid and liquid state. In the case of soil samples, the particle size influences the homogeneity of the sample surface and therewith the radiation intensity. Therefore, melting pills are the most suitable sample form for determining the principal elements in the soil sample. The melting pills originated by fusing the sample in a lithium tetra-borate molten mass, producing thereby a homogeneous sample. Effects including particle size and compaction pressure were minimized with this sample preparation procedure.

The physical law that represents the diffraction at the crystal analyzer of the fluorescence radiation emitted from the soil sample is known as the Bragg formula (Equation 29).

$$n_o * \lambda = 2 * d_g * \sin(\theta) \tag{29}$$

Where n_o is the order of diffraction (n=1,2,3, etc.), λ is the element specific wavelength of the X-Ray fluorescence radiation [nm] or [Å], d_g is the grid surface distance in the crystal analyzer [Å] and θ is the diffraction angle. Due to the fact that the crystal analyzer has a known d_g factor, the element specific fluorescence wavelength λ can be calculated from the measured diffraction angle θ.

Figure 27: Principle of the wavelength dispersive XRFS

3.7.12 X-Ray diffractometry (XRD)

The X-Ray (Roentgen) diffractometry (XRD) is a method used for determining the mineralogical composition of soil and rock samples. The main advantage of this technique is

the automatic and rapid measurement obtained and the exactitude of the results. The diffractometer used was a Philips X-pert System as shown in Figure 28. Approximately 1 g dry soil was milled to a particle size less than 2 µm in an agate mortar. Two kinds of sample preparations were applied, texture-free and texture preparations. In texture-free samples, all the particle directions have to be statistically distributed to preserve a real effect of all intensity relationships of the reflexes. For not getting any favored kind of particle orientation, a rough glass plate covered an aluminum carrier and the sample was filled from above. Through the rough glass surface and a repeated jog, the particles fell strewn at large in the deepening of the aluminum carrier. After the measurement of quartz standards, the texture-free preparations were measured continuously in an angle range between 2° and 65°.

For making the texture sample preparations, 4x4 cm glass plates with a 1 cm wide gap (1 µm deep) were required. For raising the reproducibility, a constant water/soil ratio was preserved in the sample. For this purpose, 0.045 g of distilled water and 0.085 g of soil were weighed and mixed with a spatula, obtaining finally a paste that was laid in the gap of the glass plate. After drying, the preparation was transfered to a 3x1 cm glas plate by means of a razor blade. A favored particle orientation of the texture preparation was obtained by the lay on of the sample paste. The analyses of this preparation took place at an angle range between 2° and 37°.

Figure 28: X-Ray diffractometer used

To properly detect the clay minerals, the texture preparations were vaporized with ethylenglycol at 60°C at the end of the analyses and analyzed again in an angle range between 2° and 37°. After that, thermal treatments of the samples were performed at 350°C and 550°C and analyses done at the same angle range. In this procedure the Bragg formula (Equation 29) is used again, but in this case the results are expressed as Roentgen emission intensity v/s the 2θ angle measured. Equation 29 determines the unknown d_g factors from the different minerals of the soil sample. These d_g factors are characteristic for each mineral present in the soil sample.

3.7.13 Light microscopy

A thin section was made by grinding down a slice of the soil, which was glued to a glass slide until it reached a thickness of about 0.03 mm. At this thickness most minerals become more or less transparent and can therefore be studied by a microscope using transmitted light. The used microscope was a Leitz DMRXP.

3.7.14 Scanning electron microscopy (SEM)

Scanning electron microscopy (SEM) is used to depict rough mineral surfaces with a considerable augmentation. In this case, 30-, 50- and 200-fold enlargements were used. Especially the large resolution of this microscopy enables very good quality 3D pictures. With this technique, pictures and energy dispersive spectra (EDS) coupled with a semiquantitative chemical analysis of the samples were obtained. The volcanic soil 20-40 cm profile and the zeolite Agro Clino samples were analyzed with a Jeol JSM-6400 scanning electron microscope.

3.7.15 Specific chlorophenols determination by HPLC

The 2,4-DCP and PCP concentration in liquid media was measured by high performance liquid chromatography (HPLC) using a Merck-Hitachi pump, model L-7100, coupled with a Rheodyne injector, model 7725i with an injection loop of 20 µL. The analytical column used was a reverse phase Lichrophere 60RP select B (5 µm), 250 mm long and 4 mm diameter. The flow of the system was maintained at 1 mL/min and the detection was done with a diode array Merck-Hitachi model L-7455 detector. The mobile phase consisted in a mixture of acetonitrile and phosphoric acid. The 2,4-DCP was detected at a wavelength of 205 nm in a 1:1 acetonitrile/phosphoric acid mixture. The PCP was detected at a wavelength of 215 nm in a 1.5:1 acetonitrile/phosphoric acid mixture as mobile phase [158].

3.7.16 Color and phenolic compounds

The total phenolic compound concentration was measured by UV absorbance in a 1 cm quartz cell at 215 nm and pH 6.0 (0.2 M KH_2PO_4 buffer). Color was measured at 440 nm in a Hach DR-2000 spectrophotometer and expressed as mg platinum chloride/L, as described in [10].

3.7.17 Other analyses

Humic and fulvic acids were purified according to [171]. The organic fraction of the soil was first extracted with a NaOH 0.5 M solution. The mixture was shaked for 24 h at room temperature and then centrifuged for 15 min at 10,000 rpm. The separated supernatant was acidified (pH = 2) with a 4 M HCL solution for precipitating the humic acid phase. The fulvic acids remained dissolved in the solution. Both phases were then separated by centrifugation

for 15 min at 10,000 rpm. The precipitated humic acid phase was redissolved in a NaOH 0.1 M solution and centrifuged for 10 min at 10,000 rpm. The supernatant was eliminated. After that, humic acids were suspended in a HCl/HF solution and centrifuged again to eliminate the Si presence. This procedure was repeated three times. Furthermore, humic acids were washed with distilled water for chloride elimination. Finally, the cleaned humic acids were liofilized and stored in dark flasks. The fulvic acid phase (i.e. previous dissolved phase) was passed through a Superlite XAD-8 adsorption column with a flow rate of 200 mL/h and washed with distilled water for eliminating chloride excess. The column was eluted first with a NaOH 0.1 M solution and then with distilled water. The eluted fulvic acids were finally purificated in a Dowex 50-X8 cationic exchange column. The purificated fulvic acids were liofilized and stired in dark flasks.

Tannins and lignins were measured according to [152]. 25 mL sample were filtered through a 0.45 μm membrane. Then, 0.5 mL of the commercial reactive TanniVer 3 and 5 mL of a sodium carbonate solution were added to the filtered sample. The mixture reacted for 25 min. Then, tannins and lignins were measured in a Hach DR-2000 spectrophotometer at 700 nm.

All other physico-chemical parameters (e.g. BOD, COD) were measured according to [152].

4   Results and discussion

4.1   Volcanic soil characterization and comparison with zeolites

The particle size distribution is an important physical parameter that characterizes a soil sample. Normally, the most reactive particles of a soil are the particles with a size less than 63 µm, which are also the most capable to retain environmental pollutants [172]. Moreover, the description of the particle size fractions will indicate a tendency for the capacity of the soil to retain some specific pollutants. The general particle size fraction description is presented in Table 14 [173]. The most reactive particle size fractions are therefore silt and clay.

Table 14: Description of soil in relationship to the particle size fractions

		Description	Particle size [mm]
Not cohesive soil	Gravel	Coarse	>20 to 63
		Middle	>6.3 to 20
		Fine	>2 to 6.3
	Sand	Coarse	>0.6 to 2
		Middle	>0.2 to 0.6
		Fine	>0.06 to 0.2
Cohesive soil	Silt	Coarse	>0.02 to 0.06
		Middle	>0.006 to 0.02
		Fine	>0.002 to 0.006
	Clay	Fine	<0.002

In Figure 29, the particle size distributions are presented for volcanic soil (three profiles) and two common zeolites from the European market (Agro Clino and Nat Min 9000), for comparison purposes. It is clear stated that for the volcanic soil, the clay and silt fractions, which are the most reactive ones, ranged between 38% (40-60 cm profile) and 54% (5-20 cm profile), while for the zeolites these values reached only 13% for Agro Clino and 38% for Nat Min 9000. This result clearly showed that the volcanic soil clay and silt fractions together are higher than that of the zeolites analyzed. In addition, the zeolite Agro Clino presented also a particle size fraction higher than 2.0 mm. This fine gravel fraction reached about 42% of the total mass of the mentioned zeolite. The clay and silt fractions together normally range, in some allophanic soils, between 27 and 78% [174], while the clay and silt fractions content in mineral landfill liners usually range between 52 and 92% [15],[107]. In this case, the clay and silt fractions of the investigated allophanic volcanic soil samples are near to the average value of allophanic soils and near the lower ranges of mineral landfill liners.
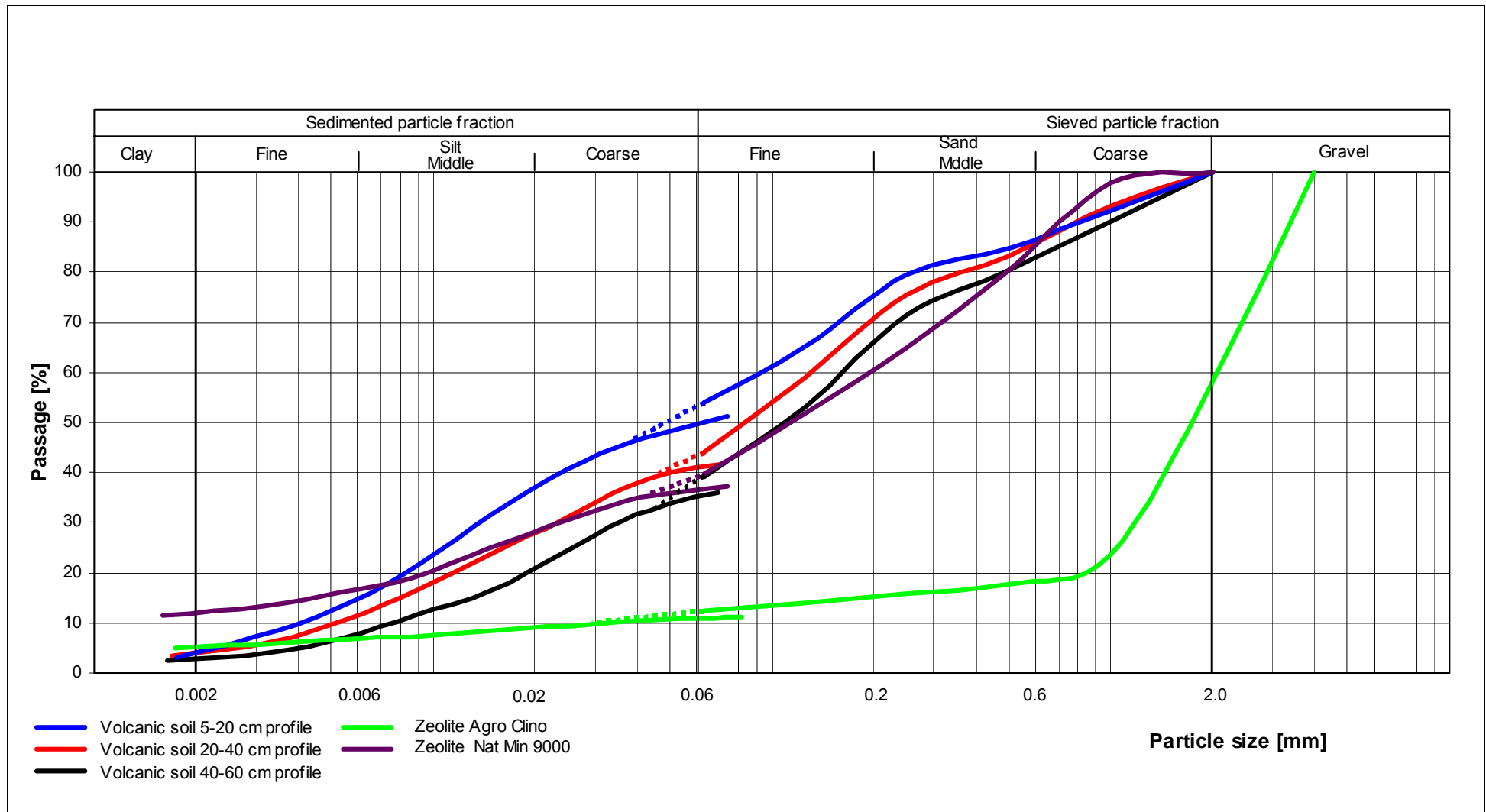
Figure 29: Volcanic soil and zeolites particle size distribution (adapted from [175],[176])

Total organic carbon (TOC) and soil organic matter (SOM) are also important parameters while characterizing a soil sample. As expected, the TOC content in the volcanic soil samples decreased with the depth; this occurred with the SOM as well (Table 15), since both values a directly related. This is a logical result, as in the upper soil profile (5-20 cm), decomposed roots and plants and non-decomposed matter are expected to increase this value. This effect is less important in the deepest (40-60 cm) volcanic soil level. No total inorganic carbon (TIC) was found in the volcanic soil samples. This result indicates that there was no presence of carbonate, bicarbonate and soluble carbon dioxide in the investigated soil samples. The SOM results are comparable with other allophanic soils, were the SOM content varies between 15 and 34% [177]. In the case of the zeolites samples, no TIC and no TOC were detected. The absence of TOC was expected, as both samples are mineral final products of the European market. Nevertheless, an ignition loss of 6.7 and 7.0% was obtained for the zeolite Agro Clino and Nat Min 9000 samples, respectively. As it is not possible to relate this values with any organic matter present in the zeolites, the ignition loss was attributed to the loss of crystallized water present in the zeolites matrix.

Table 15: TC, TIC, TOC and SOM content in volcanic soil and zeolite samples [176]

Sample	TC [%]	TIC [%]	TOC [%]	SOM [%] (LOI [%])
Volcanic soil 5-20 cm profile	8.5	<0.08	8.5	20.2
Volcanic soil 20-40 cm profile	4.6	<0.08	4.6	14.6
Volcanic soil 40-60 cm profile	2.6	<0.08	2.6	11.1
Zeolite Agro Clino	<0.08	<0.08	<0.08	(6.7)
Zeolite Nat Min 9000	<0.08	<0.08	<0.08	(7.0)

TC: Total carbon, TIC: Total inorganic carbon, TOC: Total organic carbon, SOM: Soil organic matter, LOI: Loss on Ignition

Specific elements (metals) and metal oxides were also determined during the volcanic soil characterization. As described in Chapters 3.7.3.1 and 3.7.11, two methods were used for this purpose, i.e., flame atomic absorption spectrometry (flame-AAS) and X-Ray fluorescence spectrometry (XRFS). The zeolite Nat Min 9000 sample was selected for comparison purposes, because of its similar particle size distribution compared with volcanic soil. The characterization results obtained by flame-AAS and XRFS are presented in Table 16 and Table 17, respectively. The AAS results from Table 16 clearly indicate, that although the metal oxides analyzed were the main components of the volcanic soil and zeolite samples these components didn't completely fulfill the mass balance. In fact, the accountable mass balance for the volcanic soil profile samples ranged between 80.0 and 88.0%, while the zeolite mass balance reached only 54.6% of total mass. With the flame-AAS method, the results obtained for the Al_2O_3 or Al content in the volcanic soil and zeolite samples were significantly lower than expected, as well as the SiO_2 or Si content in the zeolite sample. The XRFS results from Table 17 clearly showed a more satisfactory mass balance. These results confirmed the previous expectation, assuming higher contents of SiO_2 and Al_2O_3 in the sample.

Table 16: Chemical characterization of volcanic soil and zeolite samples by flame-AAS. Content of metal oxides and elemental composition ( ) [176]

[%]	Volcanic soil profile			Zeolite
	5-20 cm	20-40 cm	40-60 cm	Nat Min 9000
SiO_2	40.4	40.0	38.5	37.7
(Si)	(18.9)	(18.7)	(18.0)	(17.6)
Al_2O_3	7.6	7.6	8.1	1.8
(Al)	(4.0)	(4.0)	(4.3)	(0.9)
Fe_2O_3	11.8	12.7	13.2	1.3
(Fe)	(8.3)	(8.9)	(9.2)	(0.9)
CaO	3.6	3.5	3.8	2.5
(Ca)	(2.6)	(2.5)	(2.7)	(2.8)
MgO	1.1	1.2	1.5	0.5
(Mg)	(0.7)	(0.7)	(0.9)	(0.3)
Na_2O	2.4	2.5	3.1	0.7
(Na)	(1.8)	(1.9)	(2.3)	(0.5)
K_2O	0.6	0.6	0.5	3.1
(K)	(0.5)	(0.5)	(0.4)	(2.6)
MnO	0.3	0.2	0.2	0.03
(Mn)	(0.2)	(0.1)	(0.1)	(0.02)
LOI	20.2	14.6	11.1	7.0
Total	88.0	82.9	80.0	54.6

LOI: Loss on ignition

In general, apart from SiO_2 (Si) and Al_2O_3 (Al) all the other values for the investigated compounds are quite similar, comparing both analytical methods. Nevertheless, due to the excellent mass balance obtained with the XRFS technique, it was decided to use these values (Table 17) for further investigations. In fact, looking at the main metal oxides present in the volcanic soil profile samples, i.e., SiO_2, Al_2O_3 and Fe_2O_3, it was observed that the content of them increased with the soil depth. These increments of mineralogic compounds are logically related with the decrease in the soil organic matter (SOM) content with increasing soil depth. Typical values for the Si, Al and Fe contents in some andisols in Costa Rica range between 7.4 and 14.4% for Si, 8.9 and 20.1% for Al and 2.5 and 5.5% for Fe [178], making the investigated Chilean allophanic soil to be richer in Si and Fe. Regarding the zeolite Nat Min 9000 sample, the SiO_2 content was found to be very high, reaching a value of 71.5% compared with values between 41.6 to 45.0% for the volcanic soil profile samples. On the other hand, as expected for allophanes, the Al_2O_3 content was much higher in the volcanic soil samples (between 18.6 and 21.6%) compared with 12.3% only in the zeolite Nat Min 9000. In addition, the Fe_2O_3 content was much higher in the volcanic soil samples too (10.5 to 12.4%), compared with zeolite Nat Min 9000 sample (only 1.4%). In

allophanic soils, the reactive sites are mainly related with Si, Al and Fe oxides/hydroxides. Therefore, these parameters became a key point while analyzing the volcanic soil adsorption and ions exchange capacity. The content of all the other metal oxides was found to be quite similar when comparing the volcanic soil with zeolite samples. Only the K_2O content appears to be important in the case of the zeolite Nat Min 9000 sample, with a relative high value of 3.7%.

Table 17: Chemical characterization of volcanic soil and zeolite samples by XRFS. Content of metal oxides and elemental composition ( ) [176]

[%]	Volcanic soil profile			Zeolite
	5-20 cm	20-40cm	40-60 cm	Nat Min 9000
SiO_2	41.6	43.7	45.0	71.5
(Si)	(19.4)	(20.4)	(21.0)	(33.4)
Al_2O_3	18.6	20.8	21.6	12.3
(Al)	(9.8)	(11.0)	(11.4)	(6.5)
Fe_2O_3	10.5	11.7	12.4	1.4
(Fe)	(7.3)	(8.2)	(8.7)	(0.9)
CaO	3.4	3.3	3.6	2.0
(Ca)	(2.4)	(2.4)	(2.6)	(1.4)
MgO	1.8	2.0	2.3	0.9
(Mg)	(1.1)	(1.2)	(1.4)	(0.5)
Na_2O	1.5	1.6	1.8	0.3
(Na)	(1.1)	(1.2	(1.3)	(0.2)
TiO_2	1.3	1.5	1.6	0.1
(Ti)	(0.8)	(0.9)	(1.0)	(0.05)
P_2O_5	0.8	0.6	0.5	0.01
(P)	(0.4)	(0.3)	(0.2)	(0.005)
K_2O	0.5	0.4	0.4	3.7
(K)	(0.4)	(0.35)	(0.35)	(3.1)
MnO	0.3	0.2	0.2	0.04
(Mn)	(0.2)	(0.15)	(0.15)	(0.03)
LOI	20.2	14.6	11.1	7.0
Total	100.5	100.4	100.5	99.3

LOI: Loss on Ignition

The effective cationic exchange capacity (CEC_{eff}) is also an interesting parameter for evaluating the possible adsorption mechanisms and capacity of the volcanic soil, compared with zeolites (Table 18). The volcanic soil profile's CEC_{eff}, decreased with the soil depth from 6.5 cmol+/kg for the 5-20 cm profile to 5.2 cmol+/kg for the 40-60 cm profile. This result is a direct consequence of the decrease in the SOM (Table 15). In fact, as discussed in Chapter

2.1.6, it was established that the cation exchange capacity of humic substances is much greater, per unit mass, than that of clay. Compared with andisols derived from volcanic ashes in Nicaragua, higher CEC_{eff} values between 15.4 and 44.4 cmol+/kg were obtained in these soils [174], while in andisols from the Azores Islands (Portugal) the CEC_{eff} values ranged between 0.71 and 21.3 cmol+/kg [179]. Regarding the zeolites studied, the CEC_{eff} obtained were slightly higher than that of the volcanic soil profiles, but in the same order of magnitude. In addition, the CEC_{eff} can normally vary between 4 and 80 cmol+/kg in clay mineral landfill liners [14],[15].

Table 18: CEC_{eff} and exchangeable cations in volcanic soil and zeolite samples [176]

		Volcanic soil profile			Zeolite	
		5-20 cm	20-40 cm	40-60 cm	Agro Clino	Nat Min 9000
CEC_{eff} [cmol+/kg]		6.5	6.1	5.2	11.4	9.7
Exchangeable cations [cmol+/kg]	**Ca^{2+}**	10.5	8.0	6.5	13.6	14.8
	Mg^{2+}	0.71	0.66	0.64	2.7	2.1
	K^+	0.85	0.20	0.12	7.3	8.4
	Na^+	0.06	0.08	0.11	4.5	4.7
	Al^{3+}	0.10	0.0	0.0	0.0	0.0
	Fe^{3+}	0.0	0.0	0.0	0.0	0.0
	Mn^{2+}	0.0	0.0	0.0	0.0	0.0

CEC_{eff}: Effective cationic exchange capacity

The main exchangeable cations measured in the volcanic soil profiles were Ca^{2+}, Mg^{2+} and K^+, while in zeolites were the three before mentioned cations and Na^+. On the one hand, in acid soils (like volcanic soil, see Table 20) the main exchangeable cations are normally Ca^{2+}, Mg^{2+}, K^+ and Na^+, as obtained in the volcanic soil profile samples. This fact was corroborated by [177],[179],[180], where in different andisols from Azores Islands, Portugal; Mexico and Tenerife, Spain; the same cations, i.e., Ca^{2+}, Mg^{2+}, K^+ and Na^+, were determined to be the main exchangeable. In volcanic soil and zeolites the different cations are competing for the exchangeable sites and therefore the properties of the cations and the matrix-material will influence the final CEC. In general, the exchange capacity will depend mainly on the cation valence (charge) and diameter. Cations with higher valence will have a higher exchange capacity and at same valence, the exchange capacity will increase with increasing cation diameter. Naturally, as shown for volcanic soil, these properties can be affected, by the soil pH value.

The anionic exchange capacity (AEC) is only important in soils with variable charge, e.g, in presence of allophanes and Fe- and Al-oxides. The non-variable surface charge mineral soils (like zeolites) have mainly a negative surface, being able only to exchange cations. The zero point charge pH (pH_{ZPC}) of the volcanic soil was determined to range between 3.2 and 6.2 [33], with an average value of 5.5 [145]. As the pH values of the volcanic soil profiles are

near the pH_{ZPC}, it was expected that part of the soil surface being positively charged, enhancing a possible anion exchange compared with zeolites. The AEC of volcanic soil and zeolites are presented in Table 19. It was clearly shown that the AEC in volcanic soil, found close to the surface (i.e. 5-20 cm and 20-40 cm profile) is higher than in zeolites. Typical exchangeable anions are Cl^- and NO_3^-, as well as PO_4^{3-}, SO_4^{2-} and HCO_3^-. AEC values for different andisols from the Azores Islands, Portugal were determined to range between 1.44 and 7.04 cmol/kg, values that are quite comparable with those obtained for the Chilean volcanic soil.

Table 19: AEC of volcanic soil and zeolites [176]

Sample	AEC [cmol/kg]
Volcanic soil 5-20 cm profile	2.7
Volcanic soil 20-40 cm profile	1.6
Volcanic soil 40-60 cm profile	0.5
Zeolite Agro Clino	0.5
Zeolite Nat Min 9000	0.6

AEC: Anionic exchange capacity

The pH values of the volcanic soil profiles and zeolites are presented in Table 20. The investigated volcanic soil profiles are in the acid pH region. The uppers profile (5-20 cm) had a pH value of 5.9 (in water) and 5.3 (in KCl), while the deepest profile (40-60 cm) presented values of 6.8 (in water) and 5.9 (in KCl). The more acidic pH value in the upper soil profile can be explained by the presence of SOM, the influence of acidic precipitations and the liberation of H^+ protons during the cation exchange processes in plant roots. In addition, the possible hydrolysis of Al^{3+} ions in the soil solution will contribute to the soil acidity. Acidic volcanic soils of Chile have normally pH values between 4.8 and 6.0 [60],[61], which is the pH range of the volcanic soil samples measured in KCl solution. The investigated zeolites presented higher pH values, i.e. 6.2 for the Agro Clino and 6.7 for the Nat Min 9000 samples, respectively.

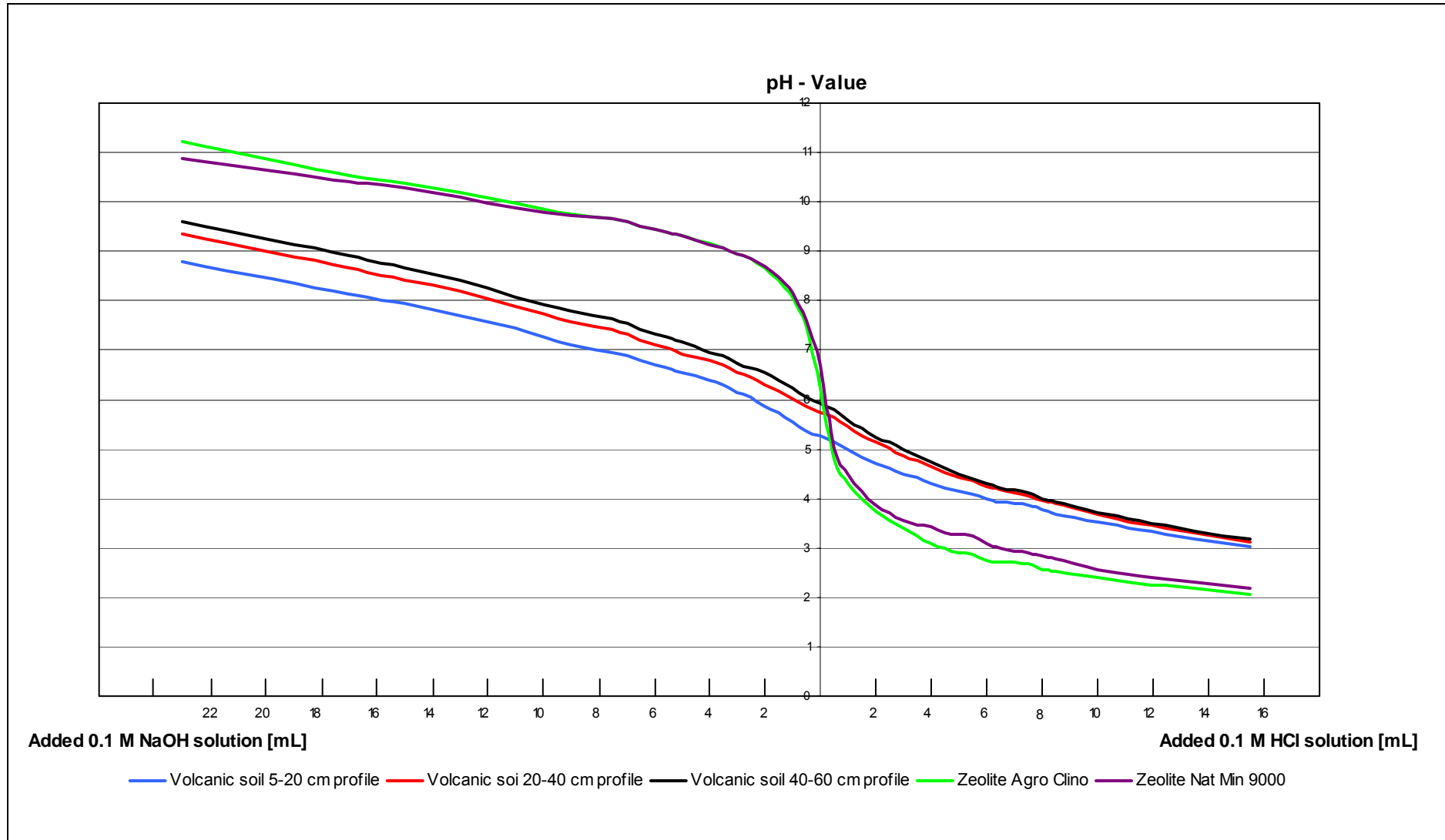**Table 20:** pH values of volcanic soil and zeolites [176]

Sample	pH-value (in H_2O)	pH-value (in KCl)
Volcanic soil 5-20 cm profile	5.9	5.3
Volcanic soil 20-40 cm profile	6.7	5.7
Volcanic soil 40-60 cm profile	6.8	5.9
Zeolite Agro Clino	7.6	6.2
Zeolite Nat Min 9000	7.8	6.7

The buffer capacity of a natural adsorption material is an important parameter, especially in the case of treating very acidic or alkaline effluents or leachates. Different buffering systems can participate in the soil for binding H^+ and/or OH^- ions, in a reversible or irreversible manner. The pH value is therefore maintained at a relatively constant level until the buffering substance of the soil has completely reacted. The buffering capacity of the volcanic soil profiles and zeolites is presented in Figure 30.

As shown, the buffering capacity of the three volcanic soil profiles was higher than that of the zeolite samples. For the volcanic soil profiles the pH value changed up to a maximum value of only 9.6 (40-60 cm profile), while the zeolites pH changed up to 11.2 (Agro Clino), when adding 22 mL of a 0.1 M NaOH solution. On the other hand, when adding 16 mL of a 0.1 M HCl solution, the volcanic soil profiles pH values decreased to a minimum of 3.0 (5-20 cm profile), while the zeolite samples reached a minimum pH value of 2.1 (Agro Clino). In addition, the shape of the zeolites buffering capacity curves showed a strong change when adding only small amounts (< 2 mL) of the acid and the alkaline solutions, indicating that no sufficient buffering compounds were present in this material to neutralize these acidic and alkaline initial loads.

As observed, the volcanic soil profile's buffering capacity curves showed a slightly change only under acidic and alkaline initial loads. This fact suggests that sufficient buffering substances are present in the investigated volcanic soil, binding the H^+ (from the HCl solution) and OH^- (from the NaOH solution) ions until almost to the end of the experiment. Different systems can act as buffering substances in soil. In Table 21, the main H^+ buffering substances are summarized.

The presence of carbonate (CO_3^{2-}) and bicarbonate (HCO_3^-) is not relevant in the case of volcanic soil and zeolites, as no inorganic carbon was found in both natural adsorbents (see Table 15). Clay minerals, primary silicates and oxides/hydroxides are present in both naturals adsorbents and are responsible for the buffering capacity of zeolites in the acidic pH range. In addition, the presence of humin is only relevant in the volcanic soil samples, as the SOM fraction was found to be important in all soil profiles (Table 15). This fact can explain the much higher buffering capacity of the volcanic soil compared with natural zeolites in the acidic pH range. The role of aluminum and iron, present in volcanic soil and zeolites, was determined. After the addition of 8 mL 0.1 M HCl solution and 12 mL 0.1 M NaOH solution, both metals were measured in the soil solution respectively (Table 22). In the case of the 8 mL HCl solution addition, only Al was detected in the volcanic soil solutions, suggesting that the reactions of $Al(OH)_3$ and $AlO_2^-]Me$ (Table 21) are the main buffering mechanisms involved in the mineral soil fraction. In the case of zeolites, the additional reactions of FeOOH as a buffering compound should be also assumed, as the presence of iron was found to be relevant in the zeolites solution. In the case of addition of 12 mL 0.1M NaOH solution, no metal (neither aluminum nor iron) was detected in the volcanic soil and zeolites solutions.

Figure 30: Volcanic soil and zeolites buffer capacity (adapted from [176])

Table 21: H^+ buffering substances in soil (adapted from [181],[182])

Soil type	Buffering substance		Reaction example	pH range
Alkaline carbonated	Carbonate	$CaCO_3$	$CaCO_3 + H^+ \leftrightarrow HCO_3^- + Ca^{2+}$	6.5 - 8
	Bicarbonate	HCO_3^-	$HCO_3^- + H^+ \leftrightarrow CO_2 + H_2O$	4.5 - 7
With variable charge	Clay minerals	Cm-OH]Me	Cm-OH]Me + H^+ $\leftrightarrow$ Cm-OH$_2$] + Me$^+$	<5 - 8
		Cm-OH	Cm-OH + H^+ $\leftrightarrow$ Cm-OH$_2$$^+$	<3 - 6
		$-(SiO_3)Al$	$-(SiO_3)Al + 3H^+ \leftrightarrow -Si(OH)_3 + Al^{3+}$	< 4.5
		Mg(O,OH)$^-$]Me	Mg(O,OH)$^-$]Me + 3H$^+$ $\leftrightarrow$ Mg^{2+} + Me$^+$ + 2H$_2$O	< 4.5
		AlO_2^-]Me	AlO_2^-]Me + 4H$^+$ $\leftrightarrow$ Al^{3+} + Me$^+$ + 2H$_2$O	<4.5
	Humin	R-(COO)Me	R-(COO)Me + H^+ $\leftrightarrow$ R-(COO)H + Me$^+$	<3 - 6
		$R-NH_2$	$R-NH_2 + H^+ \leftrightarrow R-NH_3^+$	4 - >7
With oxides/ hydroxides	Primary silicates	-(SiO)Me	-(SiO)Me + H^+ $\leftrightarrow$ -(SiOH) + Me$^+$	<7
	Al-hydroxide	$Al(OH)_3$	$Al(OH)_3 + 3H^+ \leftrightarrow Al^{3+} + 3H_2O$	3 - 4.8
	Al-OH-sulphate	$AlOHSO_4$	$AlOHSO_4 + H^+ \leftrightarrow Al^{3+} + SO_4^{2-} + H_2O$	3 - 4.5
	Fe-oxide/hydroxide	FeOOH	$FeOOH + 3H^+ \leftrightarrow Fe^{3+} + 2 H_2O$	<3
		FeOOH	$4FeOOH + CHOH + 8 H^+ \leftrightarrow 4Fe^{2+} + CO_2 + 7H_2O$	<7
	Mn-oxide/hydroxide	MnO_2	$2MnO_2 + 4H^+ + CHOH \leftrightarrow 2Mn^{2+} + CO_2 + 3H_2O$	<8

Cm: Clay mineral, Me: Metal,]: Adsorptive bond, R: Hydrocarbon radical

Table 22: Aluminum and iron content in the soil solution after addition of NaOH and HCl

| Sample	0.1 M NaOH (12 mL)		0.1 M HCl (8 mL)	
	Al [%]	Fe [%]	Al [%]	Fe [%]
Volcanic soil 5-20 cm profile	n.d.	n.d.	0.026	n.n.
Volcanic soil 20-40 cm profile	n.d.	n.d.	0.017	n.n.
Volcanic soil 40-60 cm profile	n.d.	n.d.	0.016	n.n.
Zeolite Agro Clino	n.d.	n.d.	0.049	0.018
Zeolite Nat Min 9000	n.d.	n.d.	0.055	0.022

n.d.: not detected

The **Proctor densities** were also determined for all the volcanic soil profiles and zeolites. The results are presented in Table 23 and Figure 31. The different volcanic soil profiles had a similar Proctor density and are comparable to zeolite Agro Clino but smaller than zeolite Nat Min 9000, which presented the highest Proctor density. This result was expected as zeolite Nat Min 9000 also presented the highest clay particle size fraction (see Figure 29), which normally contributes to higher Proctor densities. Although the volcanic soil Proctor densities are smaller than that of zeolites, all the Proctor curves are in the range known for clay minerals (Figure 32). In fact, the densities in the Proctor curve of clay minerals vary between 1.15 to 1.35 g/mL, which is almost the same range obtained for volcanic soil and zeolites. The Procotor curves of silt, fine sand, coarse sand, and gravel are in a higher range

compared with clay minerals. For instance, the fine sand Proctor curve values range between 1.5 and 1.6 g/mL, while the coarse sand Proctor curve values can range between 1.6 and 1.7 g/mL. In addition, the silt procotor curve values range between 1.7 and 1.9 g/mL, while the Proctor curve values of gravel vary between 1.9 and 2.9 g/mL [183].

Table 23: Measured Proctor densities of volcanic soil and zeolites

Sample	Proctor density [g/mL]	Particle density [g/mL]*	Water fraction [w/w]
Volcanic soil 5-20 cm profile	1.11	2.45	0.409
Volcanic soil 20-40 cm profile	1.13	2.56	0.410
Volcanic soil 40-60 cm profile	1.15	2.66	0.418
Zeolite Agro Clino	1.19	2.40	0.365
Zeolite Nat Min 9000	1.34	2.42	0.273

* Maximum possible density evaluated from Equation 25
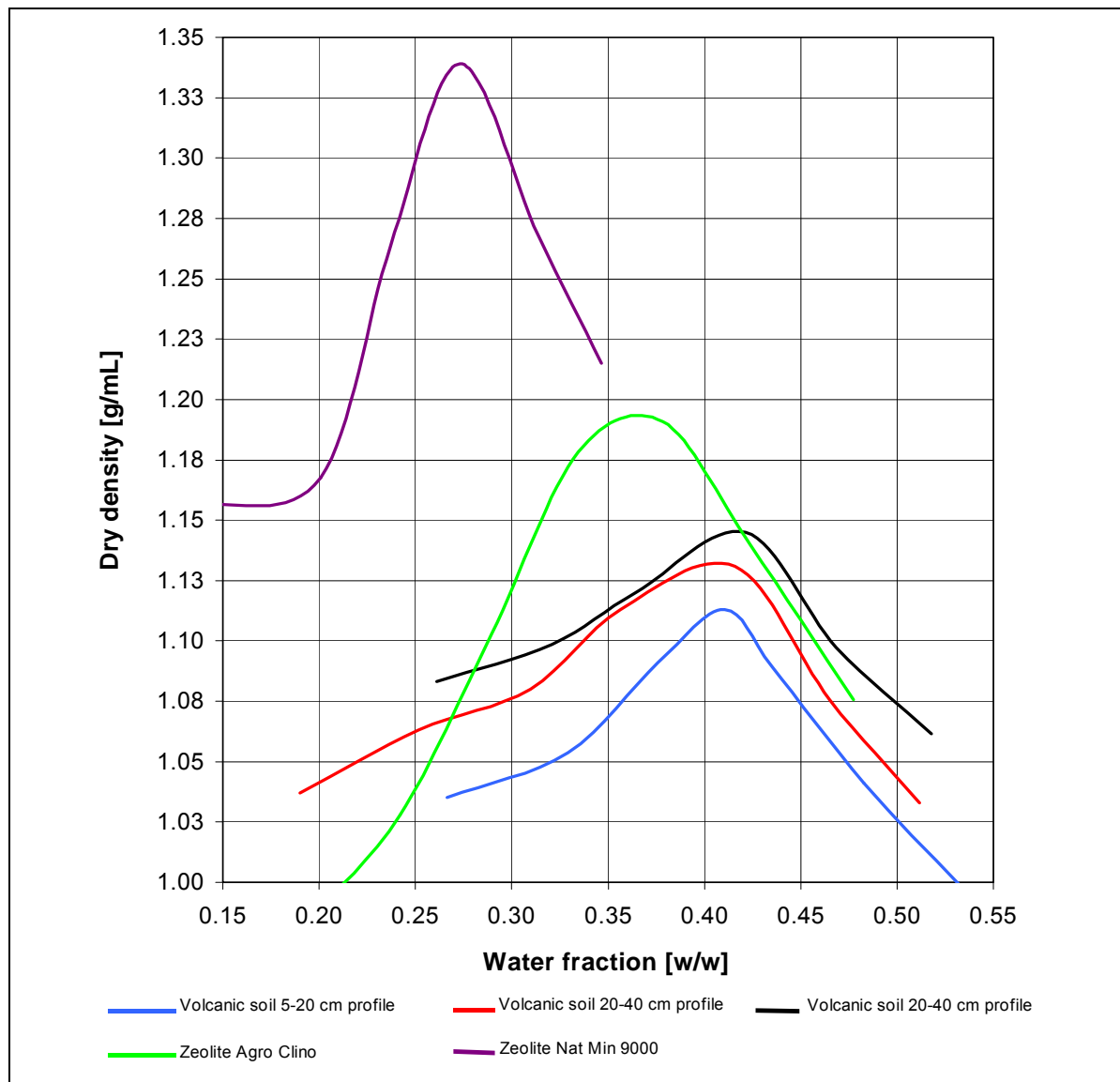
Figure 31: Proctor density curves of volcanic soil and zeolites (adapted from [176])
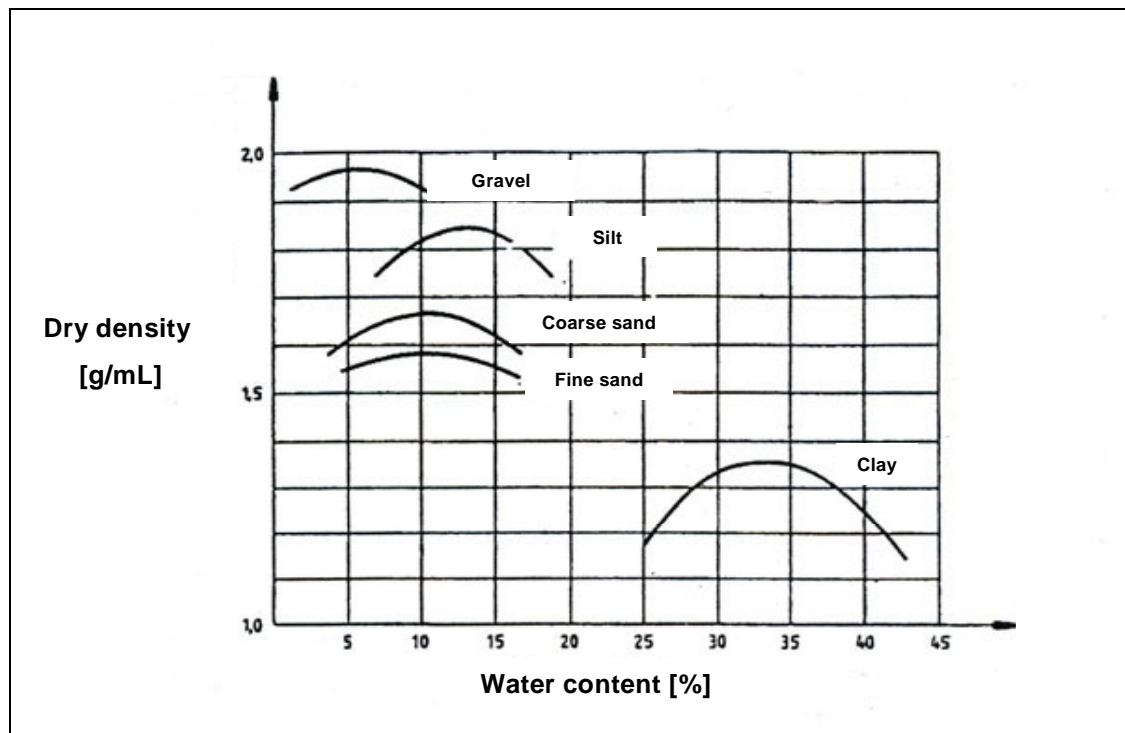
Figure 32: Procotor curves of different soil types (adapted from [183])

The **hydraulic conductivity (K_f)** of the three volcanic soil profiles and zeolite Nat Min 9000 were also determined. The zeolite Nat Min 9000 was chosen because of its similar particle size distribution compared with volcanic soil. The results are presented in Table 24.

Table 24: K_f values for volcanic soil and zeolites [176]

Sample	Water temperature [°C]	K_f [m/s]	K_{f10} [m/s]
Volcanic soil 5-20 cm profile	23.0	$7.18*10^{-9} \pm 4.27*10^{-11}$	$5.16*10^{-9} \pm 3.32*10^{-11}$
Volcanic soil 20-40 cm profile	20.5	$7.76*10^{-9} \pm 2.22*10^{-11}$	$5.91*10^{-9} \pm 1.83*10^{-11}$
Volcanic soil 40-60 cm profile	26.0	$9.66*10^{-9} \pm 2.89*10^{-11}$	$6.48*10^{-9} \pm 2.06*10^{-11}$
Zeolite Nat Min 9000	21.3	$6.03*10^{-9} \pm 2.38*10^{-11}$	$4.51*10^{-9} \pm 2.06*10^{-11}$

It clearly can be seen that the volcanic soil's K_f values are quite similar to that of zeolite Nat Min 9000. For the volcanic soil profiles, the K_f values increased with the soil depth, correlating with the higher clay fraction of the upper soil profiles (Figure 29). This fact explains also the case of zeolite Nat Min 9000, where a slightly higher K_f value was obtained.

X-Ray diffractograms (XRD) were performed with volcanic soil and zeolite samples for determining the mineralogical characteristics of both natural adsorbents (Annex I) [175]. The

volcanic soil profiles did not differ in their mineralogical composition. Plagioclase, quartz, magnetite and maghemite were determined as the main minerals present in the three profiles. Comparing the reflexes intensity, it was observed that the plagioclase fraction was slightly higher in the 5-20 cm volcanic soil profile. On the other hand, quartz content was much higher in the 40-60 cm profile. The presence of magnetite and maghemite was quite surprising, as, to our knowledge, the magnetic property of the volcanic soil was not known before. Zeolites X-Ray diffractograms indicated the presence of the same mineralogical composition for both zeolite samples. Zeolite (clinoptilolite), cristobalite, tridymite, quartz, feldspar, illite, chlorite and smectite were detected as the main minerals present in the zeolite samples. The analysis regarding swelling clay minerals was positive in the case of zeolites. By thermal treatment at 350°C, a smectite peak was observed. The smectite amount was estimated to be ca. 5-10%.

Light microscopy pictures were recorded for the identification of the main minerals present in the volcanic soil and zeolite samples [175]. In the 5-20 cm volcanic soil profile, a high weathering grade was found, indicated by the brownish colored oxidized compounds. Especially, the presence of andesite fragments evinces an advanced conversion grade. The present plagioclase showed polysinthetic unification (Figure 33). The andesite fragments present in the 20-40 cm soil profile presented a lesser weathering grade compared with the upper profile. Plagioclase and quartz were identified (Figure 34).
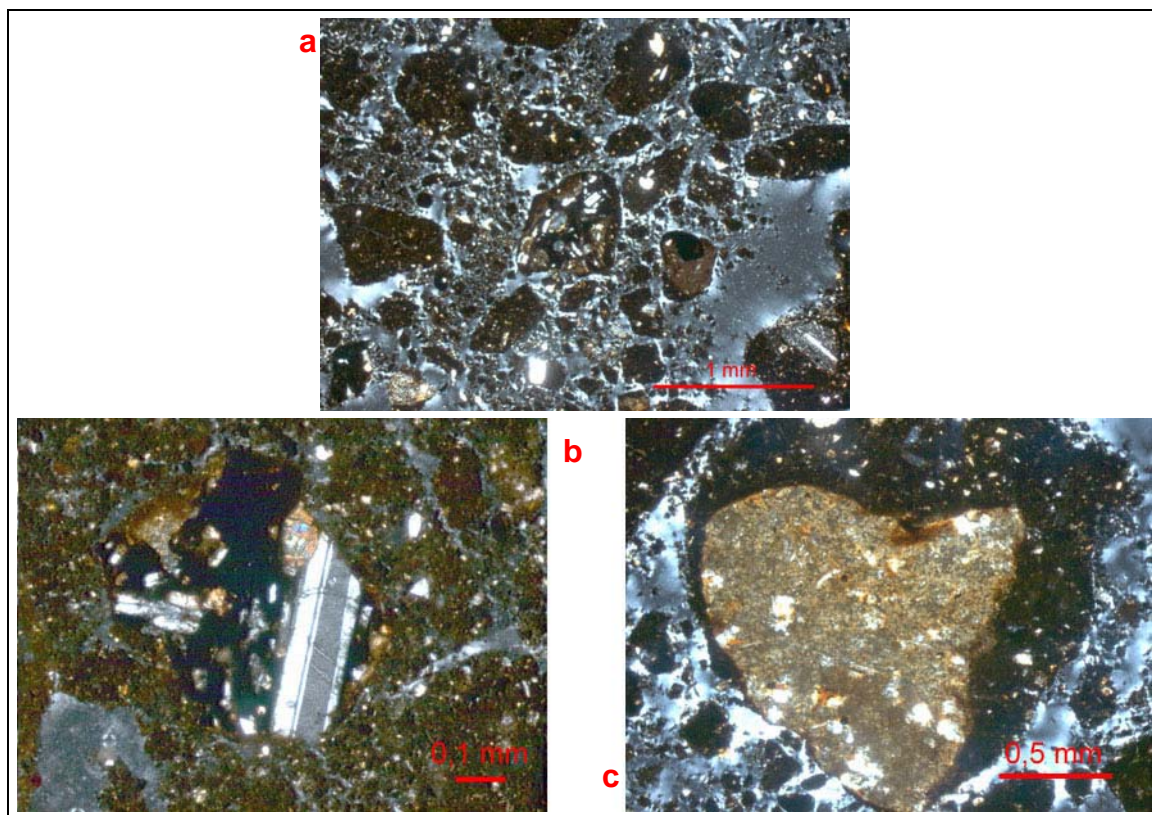
Figure 33: Volcanic soil 5-20 cm profile (a) clastic compounds (b) plagioclase and (c) oxidized andesite fragment (crossed polarization)
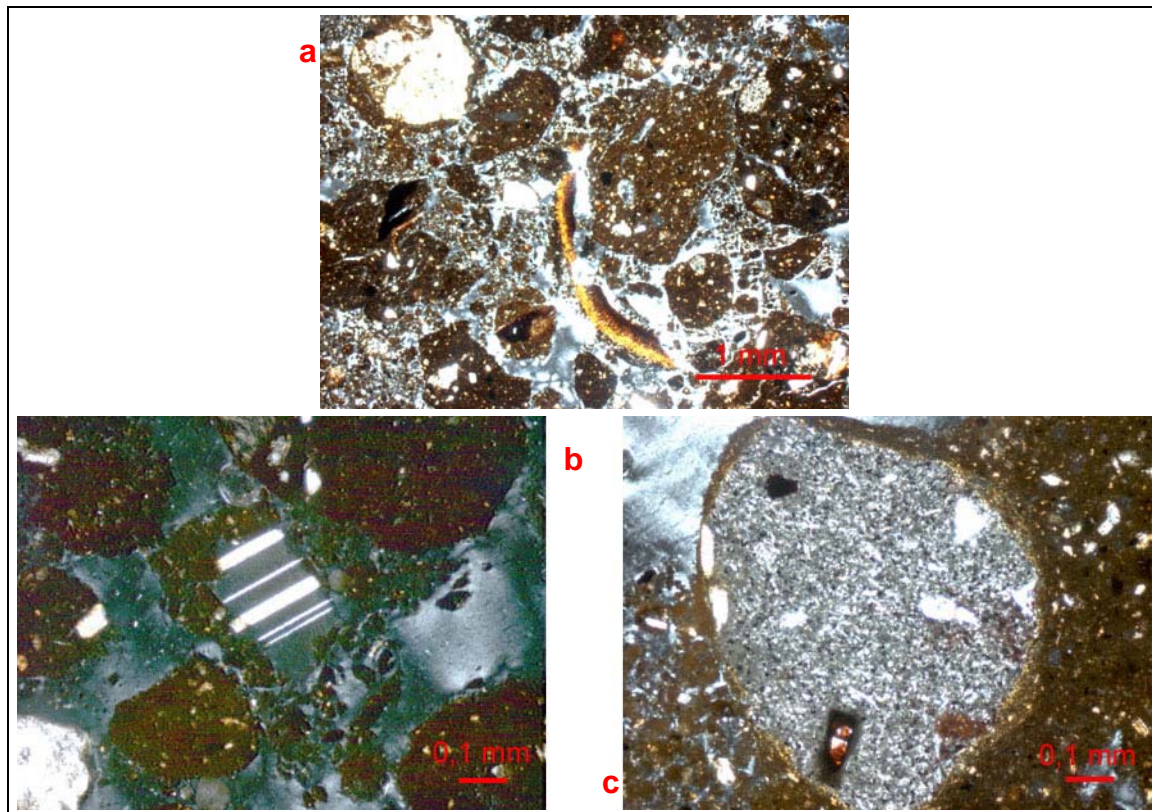
Figure 34: Volcanic soil 20-40 cm profile (a) clastic compounds and longish organic matter (b) plagioclase and (c) andesite with oxidized border (crossed polarization)

In the deepest volcanic soil profile (40-60 cm), andesite fragments, plagioclase and quartz were identified. As well as in the other two soil profiles, volcanic glass was also identified in form of transparent white surfaces (Figure 35).
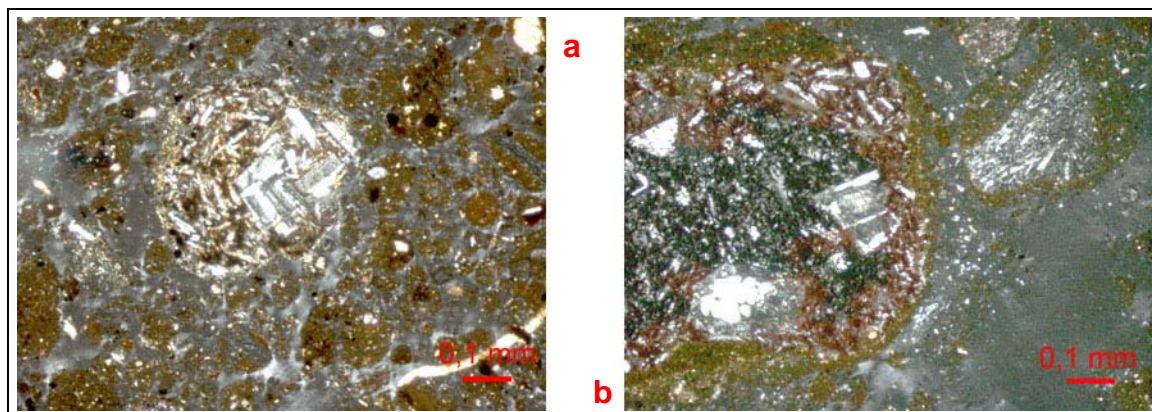

Figure 35: Volcanic soil 40-60 cm profile (a) detailed plagioclase and (b) quartz (crossed polarization)

The two analyzed zeolite samples differed only in their granularity. In both, clinoptilolite, small quantities of quartz and feldspar were identified (Figure 36 and Figure 37). It was observed, that quartz was able to change its color very quickly (from black to white) and wasn't unified. These facts suggest a volcanic origin and a development from volcanic glasses.
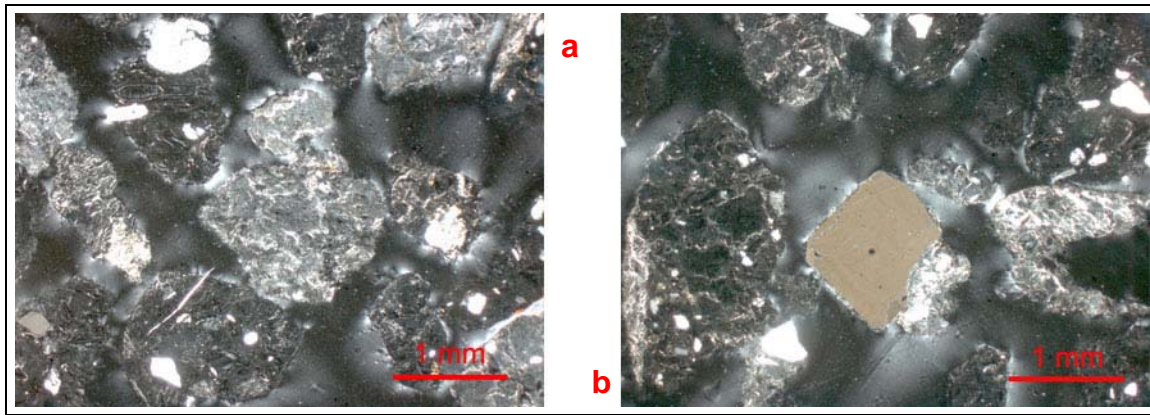
Figure 36: Zeolite Agro Clino (a) clinoptilolite rough grain mass and (b) quartz
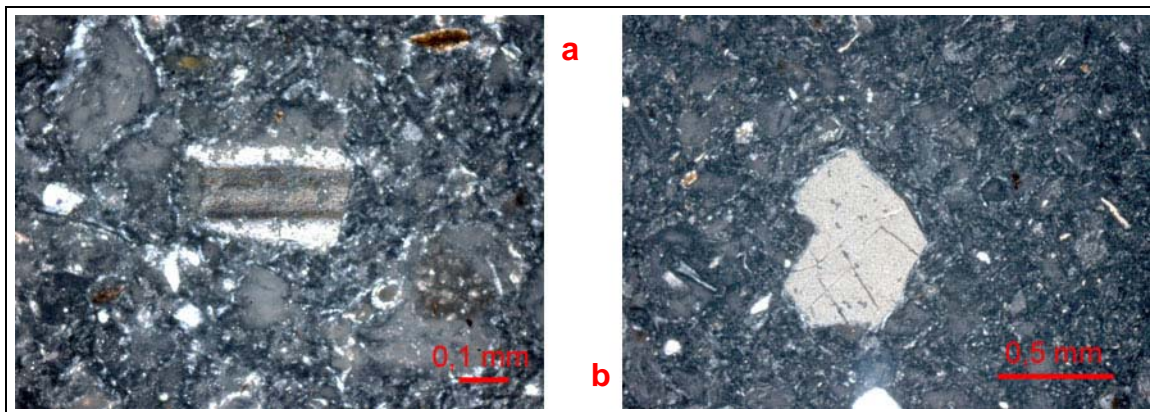
Figure 37: Zeolite Nat Min 9000 (a) feldspar and (b) quartz

Scanning electron microscopy (SEM) was performed to determine the chemical composition of feldspars and allophane phases present in the soil samples, by recording the pictures and energy dispersive spectra (EDS) [175].

Table 25: Chemical composition of feldspars [184]

		SiO_2 [%]	Al_2O_3 [%]	Na_2O [%]	CaO [%]	K_2O [%]
A. F.	**Sanidine**	64.7	18.3	-	-	16.9
Plagioclase	**Albite**	68.7	19.5	11.8	-	-
	Oligoclase	63.6	22.9	9.5	4.0	-
	Andesine	58.5	36.3	7.1	8.1	-
	Labradorite	53.4	29.8	4.7	12.1	-
	Bytownite	48.3	33.2	2.4	16.1	-
	Anorthite	43.3	36.6	-	20.1	-

A.F.: Alkali feldspars

Feldspars are normally divided in two main groups: alkali feldspars and plagioclase. On the one hand, the alkali feldspars spectra range from the sodium rich albite ($NaAlSi_3O_8$) to the

sodium poor and potassium rich sanidine ($KAlSi_3O_8$). On the other hand, the plagioclase spectra range from albite to the sodium poor and calcium rich anorthite ($CaAl_2Si_2O_8$) [185]. The typical feldspars compositions are presented in Table 25.

For the SEM identification of feldspars and allophanes, selected points and surfaces of the volcanic soil 20-40 cm profile (and the zeolite Agro Clino) were recorded and analyzed by means of EDS and compared with Table 25. In the case of the 20-40 cm volcanic soil profile, SEM pictures with a 30-, 50- and 200-fold augment were recorded. The results are summarized in Annex II.

In Figure 38, SEM pictures of the 20-40 cm volcanic soil profile with a 30-fold augment and a detailed picture with a 200-fold augment are shown. The correspondent EDS plots of the point-analyses are shown in Figure 39.
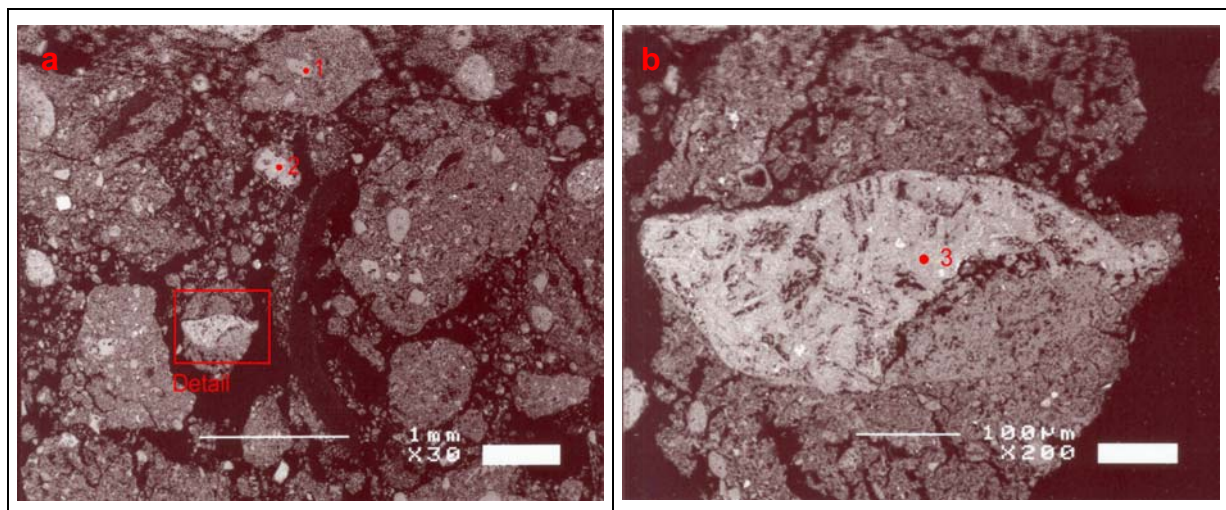
Figure 38: SEM pictures of the 20-40 cm volcanic soil profile (a) with a 30-fold augment (b) detail with a 200-fold augment
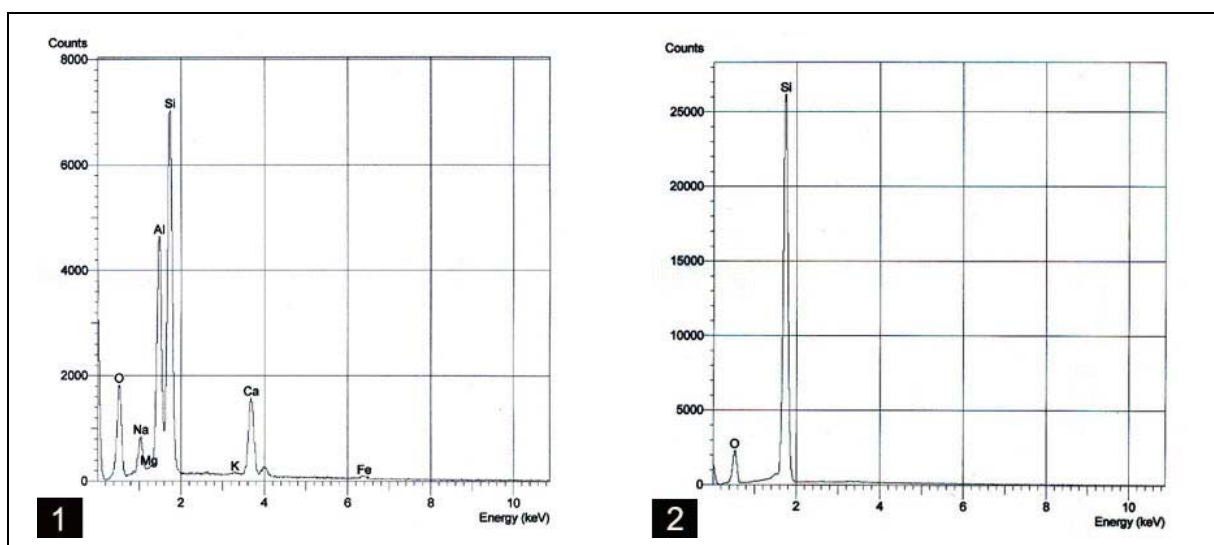
Figure 39: Energy dispersive spectra (EDS), point-analyses of (1) and (2) in Figure 38a

The point (1) quantitative analysis gave the following percentual composition:

SiO_2: 54.09%, Al_2O_3: 28.41%, Na_2O: 7.21%, CaO: 9.55% and Fe_2O_3: 0.74%. Comparing this result with the typical plagioclase compositions presented in Table 25, it seems that the point (1) analysis corresponds to a plagioclase in between andesine and labradorite. The point (2) EDS plot shows only oxygen and Si, which clearly indicates quartz presence. In Figure 40, the surface-analyses of point (3) (Figure 38b) and point (4) (Figure 41) are presented. The quantitative surface analysis of (3) indicated a percentual composition of:

SiO_2: 57.75%, Al_2O_3: 9.66%, Na_2O: 4.98%, CaO: 2.04%, K_2O: 2.38%, Fe_2O_3: 12.13%, MgO: 8.87% and Ti_2O: 2.19%. It seems that this complex grain was not a pure plagioclase and could not be identified exactly.
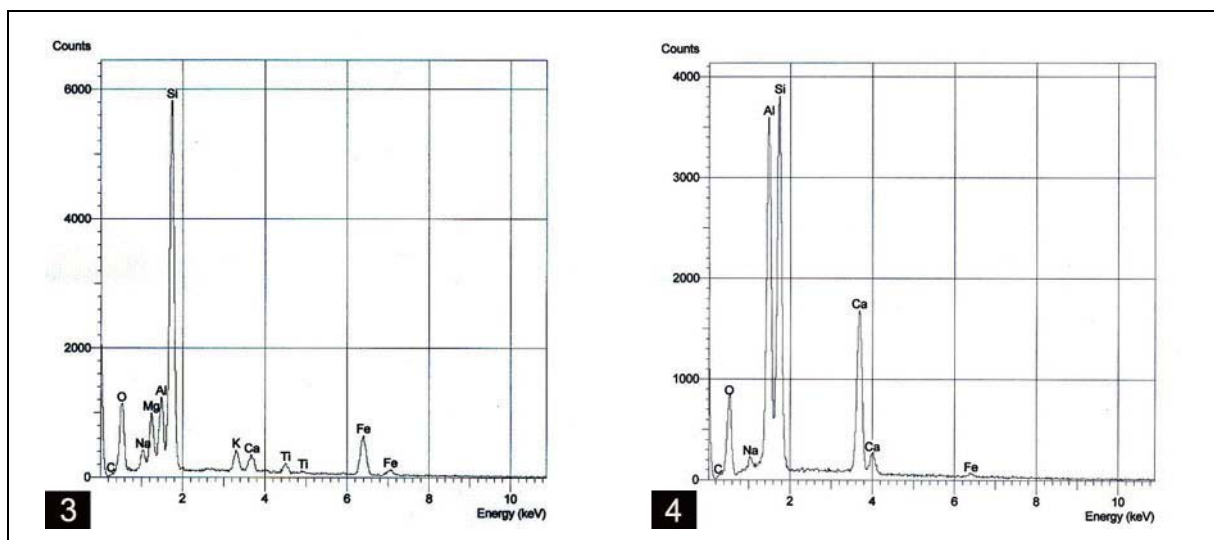
Figure 40: Energy dispersive spectra (EDS), 20x30 µm surface-analyses of point (3) (Figure 38b) and point (4) (Figure 41)
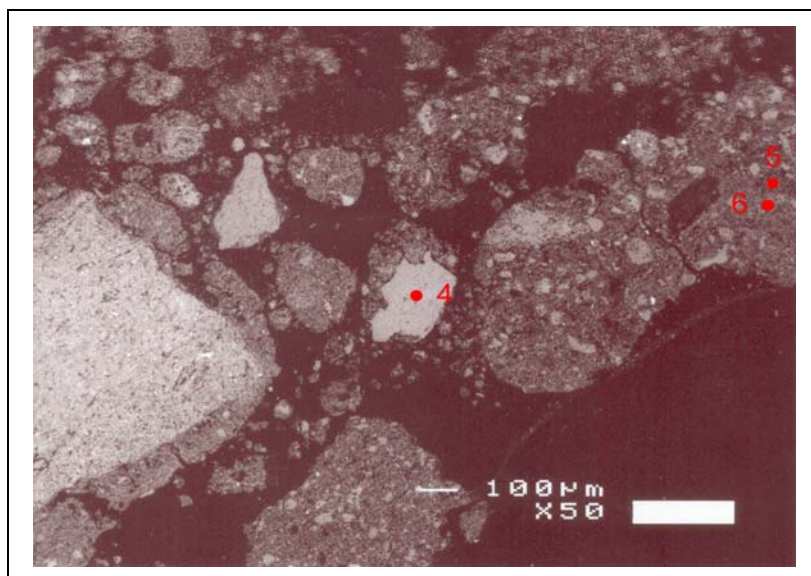
Figure 41: SEM picture of the 20-40 cm volcanic soil profile with a 50-fold augment

The quantitative surface analysis of point (4) indicated the following percentual composition:

SiO_2: 46.24%, Al_2O_3: 34.15%, Na_2O: 2.54%, CaO: 16.38% and Fe_2O_3: 0.69%. Comparing this result with Table 25, it becomes obvious that this investigated surface matches almost exactly with bytownite.
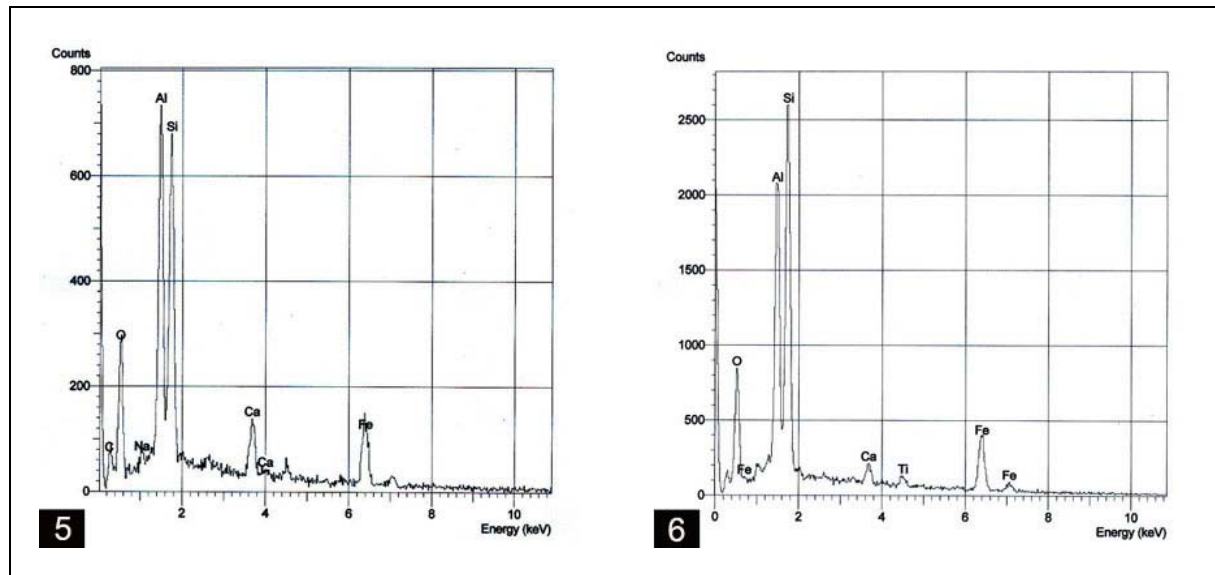
Figure 42: Energy dispersive spectra (EDS), point-analyses of (5) and (6) in Figure 41

In Figure 42, the EDS plots of the point-analyses for point (5) and (6) of Figure 41 are presented. The dark range in which points (5) and (6) lay, suggests the presence of aluminum rich soil particles, indicating a possible allophane presence. In fact, the quantitative analysis of point (6) expressed in percentual content was:

SiO_2: 48.31%, Al_2O_3: 31.17%, Na_2O: 3.40%, CaO: 1.98%, Fe_2O_3: 12.97% and TiO_2: 1.81%. This composition is typical for allophane, and comparing with point (5), a higher aluminum and calcium content were found to be the only differences.

The zeolite Agro Clino was also analyzed with SEM technique. In Figure 43, the SEM picture of zeolite Agro Clino with a 30-fold augment is presented. The points (1) to (6) were processed as point-analyses, while the points (7) to (10) were processed as surface-analyses for homogeneity determination.
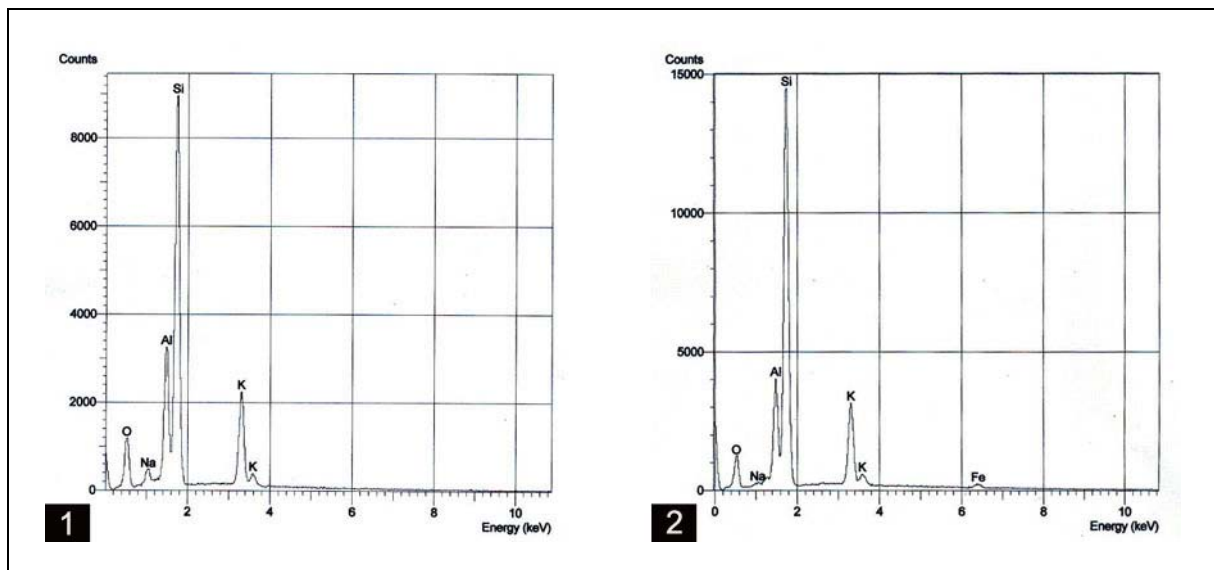
The energy dispersive spectra (EDS) of point (1) and (2) are presented in Figure 44. The quantitative analysis of point (1) revealed the following percentual composition:

SiO_2: 65.66%, Al_2O_3: 19.05%, Na_2O: 3.32% and K_2O: 11.96%. This result is matching with a sodium–poor sanidine. The quantitative analysis of point (2) showed following composition:

SiO_2: 71.98%, Al_2O_3: 14.31%, Na_2O: 0.87%, K_2O: 11.55% and Fe_2O_3: 1.29%. This speakes for a slightly iron-contaminated sanidine.
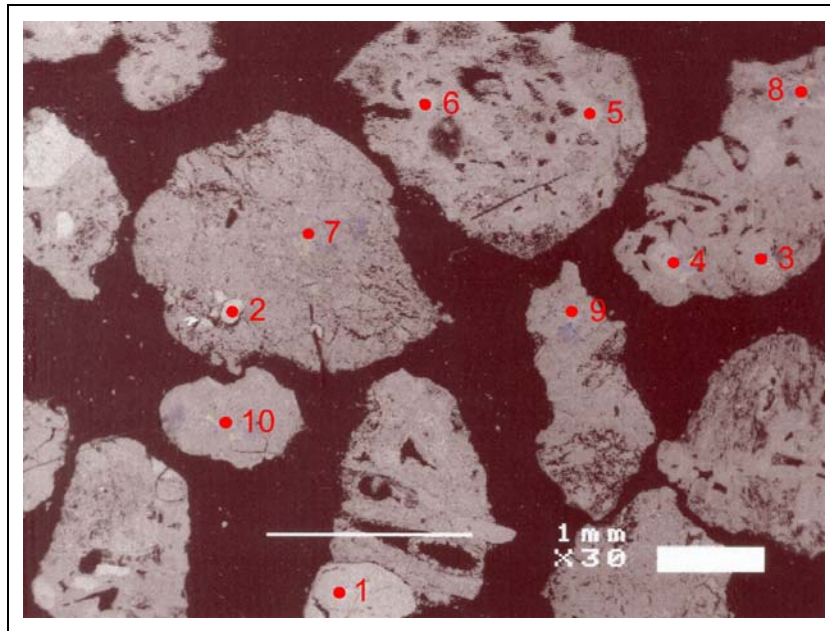
Figure 43: SEM picture of the zeolite Agro Clino with a 30-fold augment
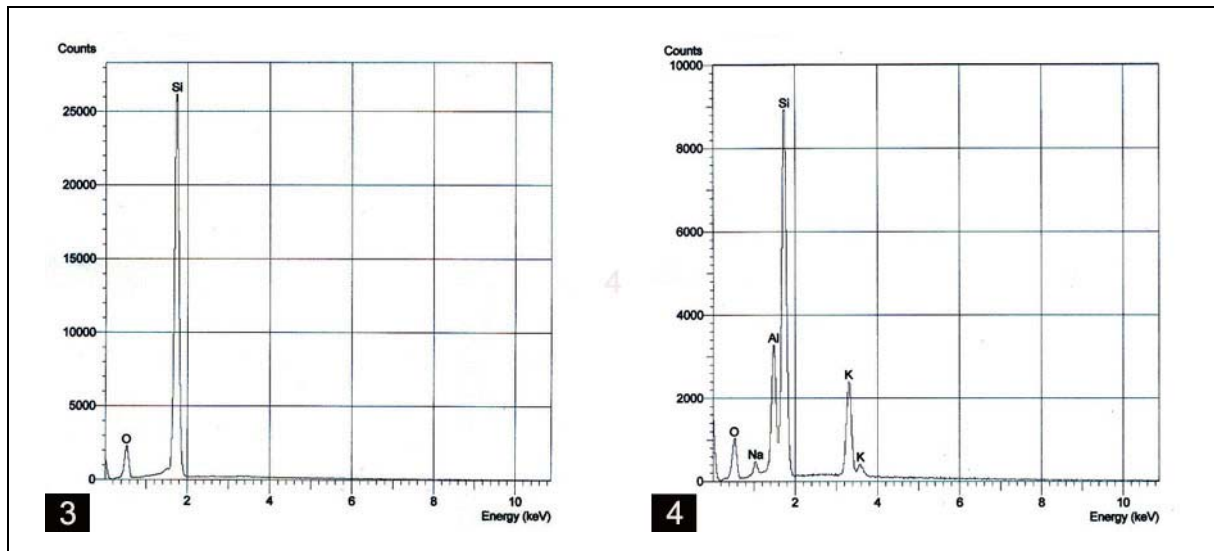

Figure 44: Energy dispersive spectra (EDS), point-analyses of (1) and (2) in Figure 43
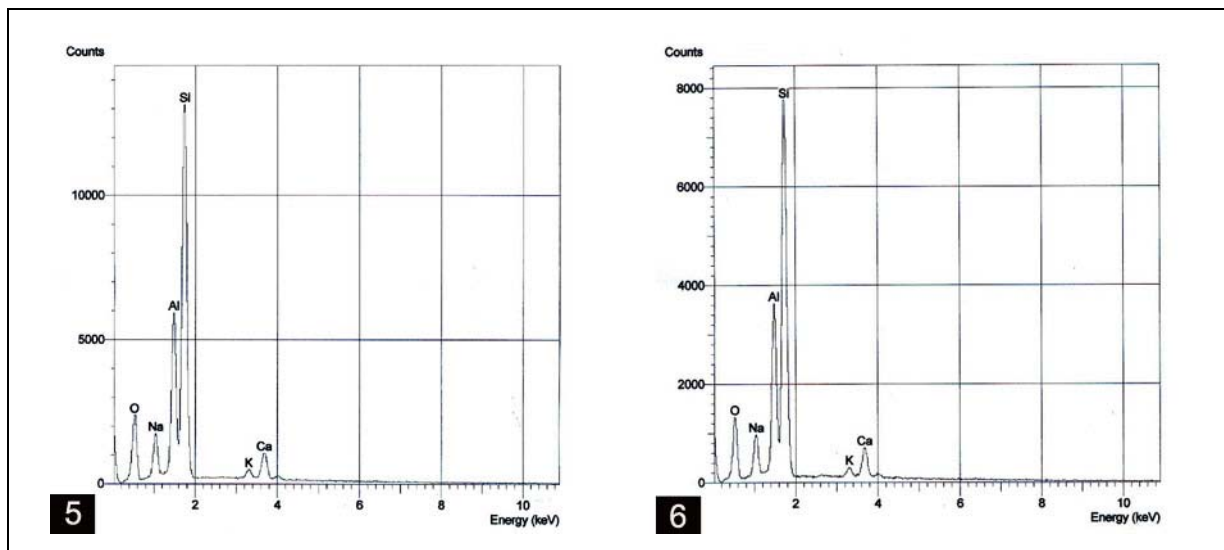
From the energy dispersive spectrum (EDS) of point (3) in Figure 45, quartz was identified. Moreover, the quantitative analysis of the EDS plot for point (4) in Figure 45 gave the following percentual composition:

SiO_2: 65.65%, Al_2O_3: 18.57%, Na_2O: 3.03% and K_2O: 12.75%. This mineral phase is assumed to be sanidine, with a very similar composition as point (1).

In Figure 46, the EDS spectra of point (5) and (6) are presented. The quantitative analyses of both points, indicated the presence of the same main compounds, as summarized in Table 26. In both cases the presence of oligoclase can be assumed.

**Figure 45:** Energy dispersive spectra (EDS), point-analyses of (3) and (4) in Figure 43

Figure 46: Energy dispersive spectra EDS, point-analyses of (5) and (6) in Figure 43

Table 26: Quantitative EDXRF analysis of point (5) and (6) from Figure 43

Point	Composition [%]				
	SiO_2	Al_2O_3	Na_2O	CaO	K_2O
(5)	63.32	22.70	8.99	3.91	1.08
(6)	63.43	22.82	8.54	4.12	1.09

The EDS diagrams for the SEM surface analyses (7) to (10) are presented in Figure 47. All these spectra show a similar composition, as summarized in Table 27. In agreement with the XRFS results of Table 17, the presence of clinoptilolite can be assumed.
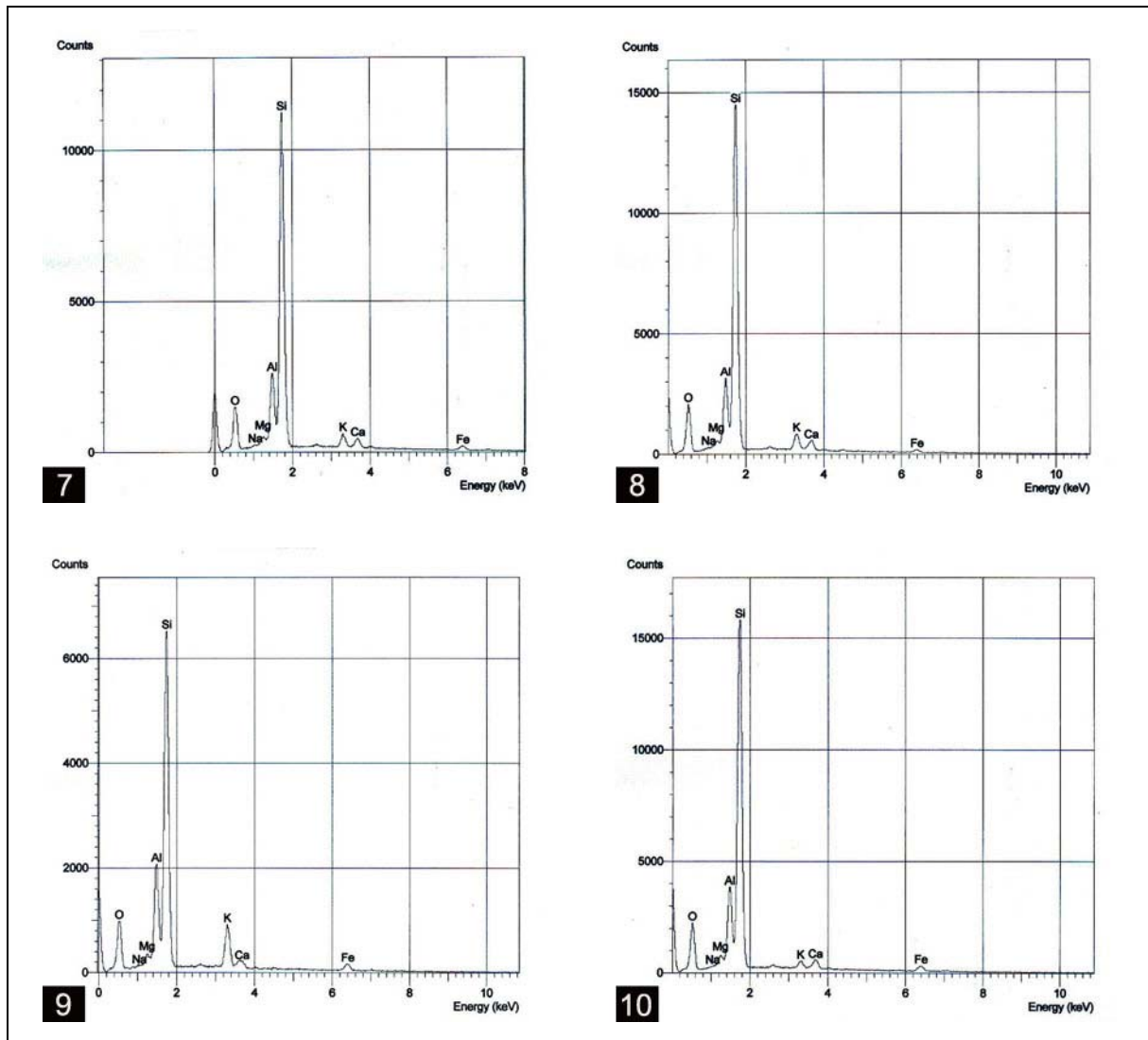
Figure 47: EDS diagrams of SEM surface analyses: 200x300 μm (7), 100x150 μm (8), 100x150 μm (9) and 200x300 μm (10) in Figure 43

Table 27: Quantitative EDXRF analysis of surface (7) to (10) from Figure 43

| Surface	Composition [%]						
	SiO_2 (%)	Al_2O_3 (%)	Na_2O (%)	CaO (%)	K_2O (%)	Fe_2O_3 (%)	MgO (%)
(7)	77.84	13.60	0.92	1.95	2.43	2.13	1.12
(8)	79.92	12.07	0.95	2.02	3.02	1.42	0.60
(9)	69.85	17.37	0.72	1.01	6.84	2.86	1.36
(10)	77.90	14.29	0.80	1.78	1.23	2.52	1.48

4.2   Adsorption of pollutants from bleached Kraft mill effluent

The adsorption capacity of Chilean volcanic soil was first tested with color and phenolic compounds, common pollutants present in bleached Kraft mill effluents. In addition, the capacity of volcanic soil to adsorb some particular pollutants present in these effluents like tannins, lignins and chemical oxygen demand (COD) was also evaluated. Adsorption kinetics and isotherms were determined, as well as breakthrough curves in soil columns. The molecular weight distribution of the input and output effluent of a single column was determined, as an indicator of the molecular size of the pollutants adsorbed onto the soil. Moreover, the main adsorption parameters of the volcanic soil column system (e.g. the linear adsorption isotherm constant (m), the overall mass transfer coefficient ($K_c * a$) and the adsorption rate) were determined using a clasical fixed bed kinetic model (FBKM).

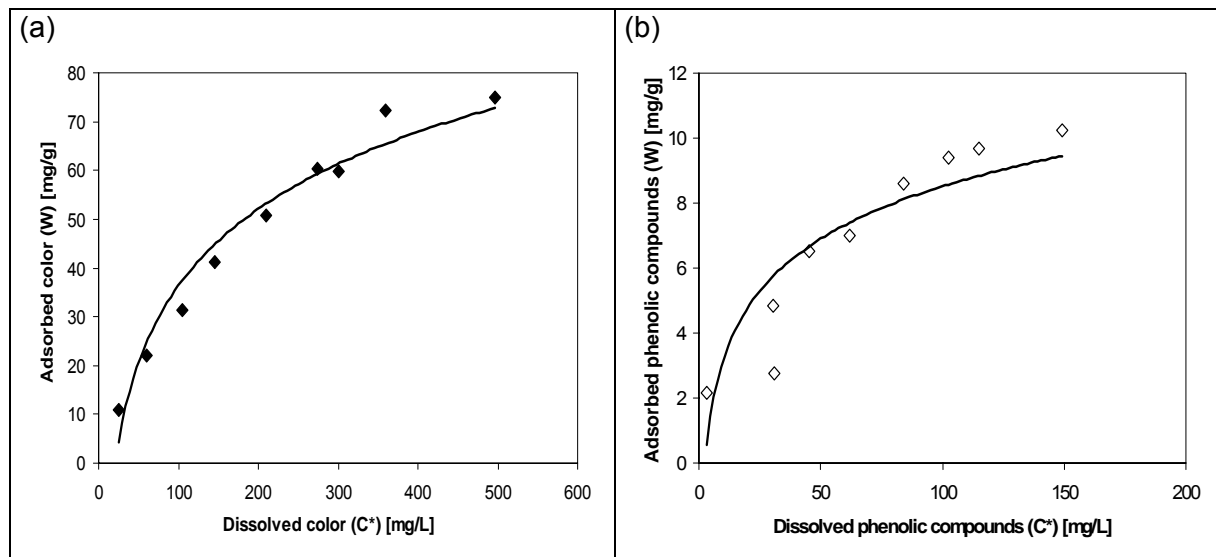### 4.2.1   Color and phenolic compounds adsorption kinetics

Color and phenolic compounds adsorption kinetics onto volcanic soil are presented in Figure 48. It clearly can be seen that after 30 min, 46% of the color and 36% of the phenolic compounds present in the effluent were already adsorbed, respectively. This can be considered as rapid adsorption kinetic that would allow a fixed bed adsorption system to be used for removing such pollutants from effluents. The 20-40 cm soil profile was selected as, in previous works, it proofed as the soil profile capable to adsorb most of color and phenolic compounds [10],[11],[83],[143],[186],[187]
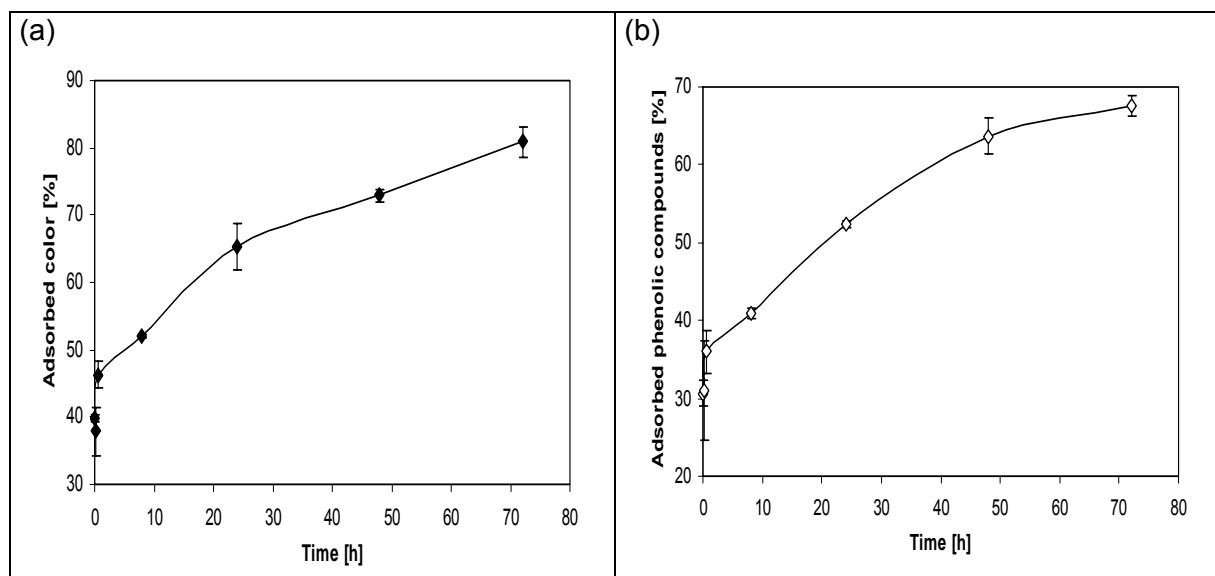
Figure 48: Adsorption kinetics for (a) color and (b) phenolic compounds onto natural volcanic soil 20-40 cm profile (batch trials described in Chapter 3.2)
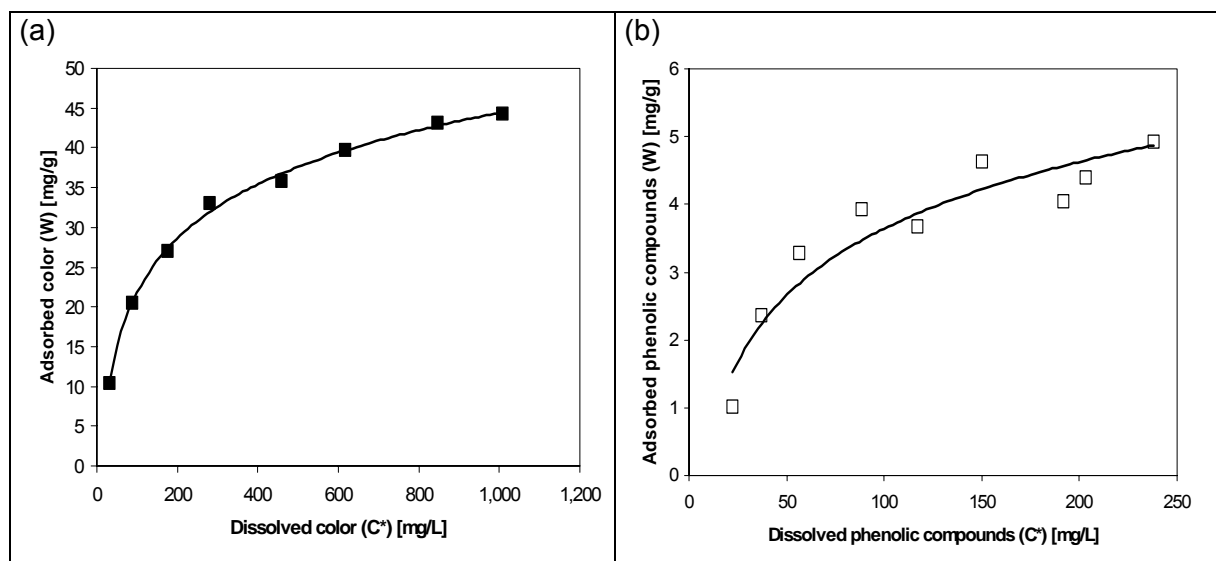
4.2.2   Color and phenolic compounds adsorption isotherms

Adsorption isotherms for color and phenolic compounds onto acidified and natural volcanic soil are presented in Figure 49 and Figure 50.

Figure 49: Adsorption isotherms for (a) color and (b) phenolic compounds onto acidified volcanic soil (the method applied is described in Chapter 3.3.1)

The Langmuir and Freundlich isotherms models were used for representing and interpreting the obtained data. In Table 28 the main parameters calculated using both models are presented for comparison purposes.

Figure 50: Adsorption isotherms for (a) color and (b) phenolic compounds onto natural volcanic soil

The Langmuir *b* value represents the maximum possible amount of pollutant adsorption onto volcanic soil, under the isotherms experiment conditions. First of all, it could be clearly stated that the acidified volcanic soil presented a higher adsorption capacity of both pollutant groups, color and phenolic compounds, compared to natural volcanic soil. In fact, a maximum adsorption capacity of 2,500 mg color/g acidified volcanic soil was obtained compared with 1,429 mg color/g natural volcanic soil. For phenolic compounds, a maximum adsorption capacity of 18.8 mg/g for acidified volcanic soil was obtained compared with 10.8

mg/g for natural volcanic soil. As a comparison, the phenols uptake in activated carbon can vary between 17 and 240 mg/g and for zeolites the adsorption of phenols is about 3.2 mg/g [18]. These results show that the volcanic soil is comparable to natural zeolites as an adsorption material, having even better adsorption uptakes in case of phenolic compounds.

Table 28: Langmuir and Freundlich model parameters (see Chapter 3.3.1) for the adsorption of color and phenolic compounds from bleached Kraft mill effluent onto volcanic soil

Volcanic soil	Pollutant	Langmuir			Freundlich		
		b [mg/g]	k_L [L/mg]	R^2	n [-]	k_F [(L/mg)$^{(1/n)}$*(mg/g)]	R^2
Acidified	Color	2,500	0.0052	0.991	1.90	65.4	0.986
	Phenolic compounds	18.8	0.0055	0.974	1.42	0.25	0.974
Natural	Color	1,429	0.0102	0.989	2.88	131.8	0.873
	Phenolic compounds	10.8	0.0053	0.903	1.75	0.25	0.837

4.2.3   Fixed bed adsorption system trials

The fixed bed adsorption system (FBAS) used for the elaboration of breakthrough curves and model parameters determination is described in detail in Annex III and [11].

4.2.3.1   Total pollutants adsorption capacity

A previous work [11] based on a simple graphic integration of the breakthrough curves (see Annex III) indicated that the total phenolic compounds uptake of volcanic soil in the FBAS at the saturation point ranged between 4.5 and 14.5 mg/g for natural and acidified soil, respectively (experiment 1 of Table 13, Chapter 3.4.1). In the case of color adsorption, the mentioned parameter ranged between 8.0 and 44.6 mg/g for natural and acidified soil respectively, for the same experiment [11].

In the case of phenolic compounds, the adsorption range was quite similar compared with the maximum adsorption value of the isotherms with acidified and volcanic soil, but in the case of color adsorption, the FBAS showed a much lesser uptake. Therefore, the Bohardt & Adams model described in [36],[46],[48],[49],[188] was tested to corroborate these previous results. Phenolic compounds and color adsorption rates onto acidified soil of $2.0*10^{-6}$ and $1.5*10^{-6}$ L/mg*min were obtained, respectively [147]. These adsorption rates were found to be higher than the one obtained with the previous graphical integration model and therefore a **phenomenological model** was used for the final determination of the exact adsorption rate of phenolic compounds and color onto volcanic soil columns.

Moreover, all these previous results [11] suggested that there was no clarity about the competition phenomena in the adsorption columns, regarding the different pollutants present in the bleached effluent. As will be discussed in Chapter 4.2.3.2, later, the molecular weight fraction with a size of more than 30,000 Da was the main fraction adsorbed onto the acidified volcanic soil, suggesting that this factor could explain the preferential color adsorption onto volcanic soil columns.

Phenolic compounds and color are partially responsible for the chemical oxygen demand (COD) present in the effluent, while tannins and lignins are partially responsible for the presence of color in the effluent. The removal efficiencies of these parameters (COD, tannins and lignins) were estimated at the breakpoint and the saturation point in five columns with the same experimental set up as described in Chapter 3.4.1, experiment 1 (Table 13). At the breakpoint, removal efficiencies between 60 and 70% for tannins, lignins and COD were achieved in the volcanic soil columns (see Figure 51 [147]). At the saturation point, COD, tannins and lignin removal efficiencies between 15 and 30% were achieved, indicating that at this point only little adsorption takes place.
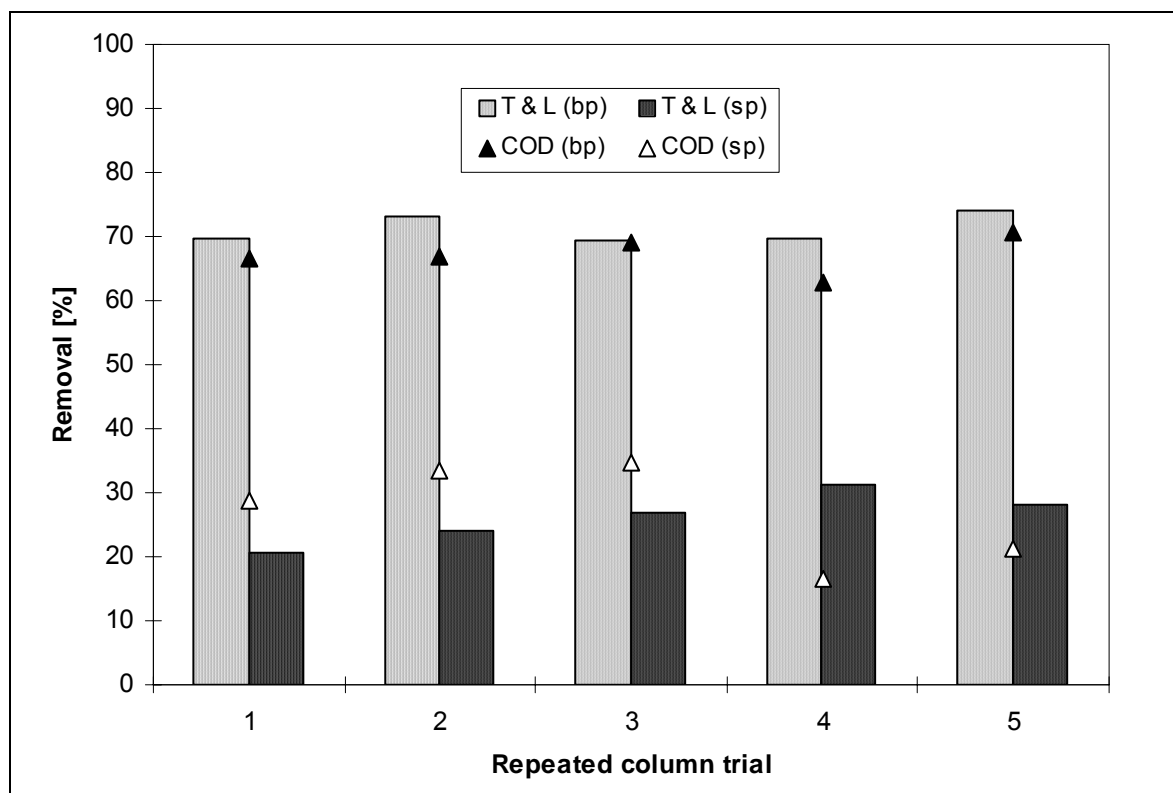

Figure 51: COD and tannins & lignins (T & L) removal efficiencies at the breakpoint (bp) and the saturation point (sp) during the operation of five equal columns filled with acidified volcanic soil

4.2.3.2   Molecular weight distribution (MWD) of the effluent pollutants

The molecular weight distribution (MWD) of the bleached Kraft mill effluent pollutans was also performed as a kind of size indicator for the adsorbed pollutants in the FBAS

experiments. The determination method applied is described in Chapter 3.4.2. In Figure 52, the MWD of the effluent pollutants in the input and output samples of one acidified volcanic soil column is shown. The aerobic treated effluent corresponds to the column input, whereas the initial output, and the samples collected at breakpoint and saturation point indicate the MWD of the effluent pollutants leaving the adsorption column at different times.
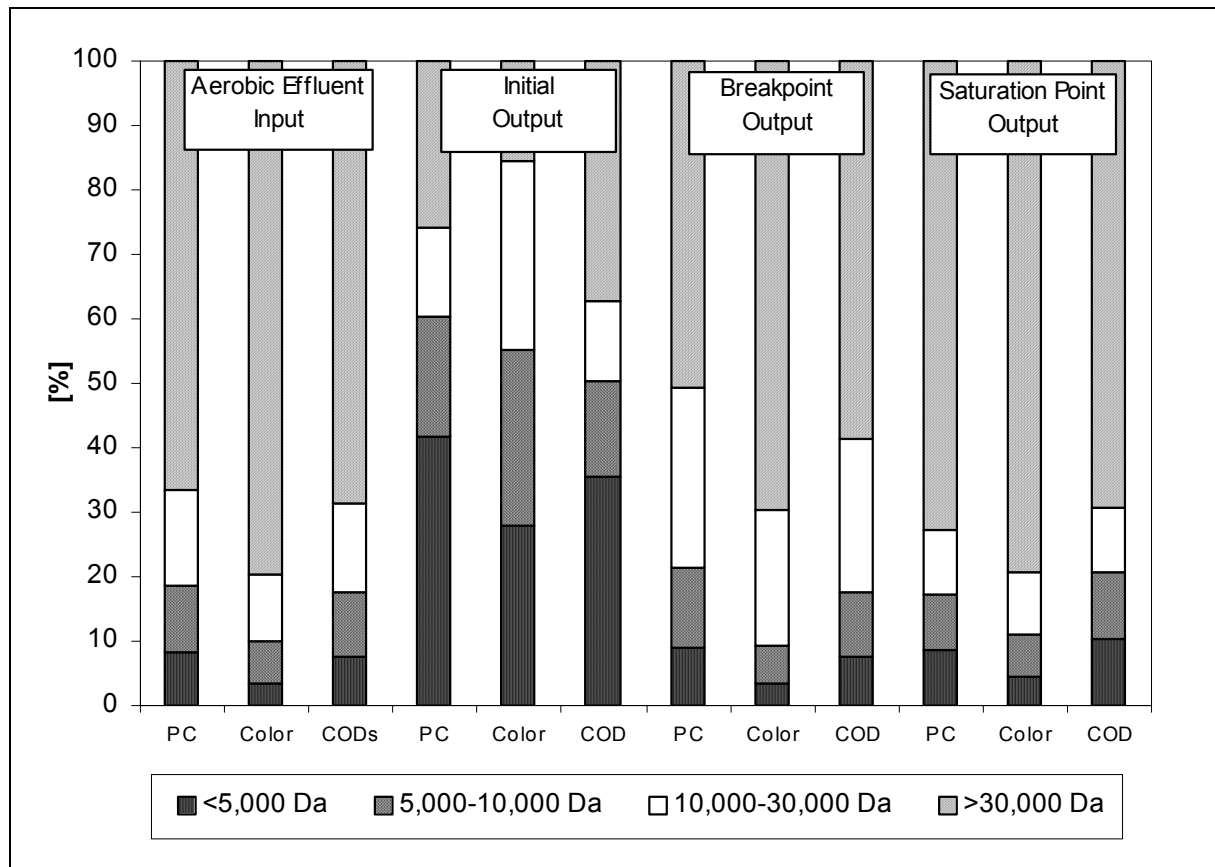
Figure 52: MWD of the effluent input and output in an acidified volcanic soil column experiment (see Chapter 3.4.1, Table 13, experiment 1). PC: Phenolic compounds, COD: Chemical oxygen demand

It was found that in the aerobic effluent (i.e. column input), the most important fraction present was that with molecules size greater than 30,000 Da (for phenolic compounds, color and COD). It is well known that aerobic processes are not able to degrade large and recalcitrant compounds, and therefore it is quite normal that in this case between 70 and 80% of the aerobic treated effluent pollutants had a size of 30,000 Da and higher. Interestingly, the initial output sample had a completely different MWD for phenolic compounds, color and COD as that of the aerobic treated effluent input sample. In fact, in this initial output sample, the fraction > 30,000 Da decreased to a range between 15 and 40%, depending on the analyzed compound (i.e. phenolic compounds, color or COD). This finding indicated that the molecular weight fraction size > 30,000 Da was the main fraction adsorbed onto the acidified volcanic soil. Polymerized (and chlorinated) large organic compounds apparently were preferently adsorbed. Molecules < 5,000 Da were less adsorbed, therefore remaining in the output effluents. Figure 52 clearly shows that, at the

saturation point, practically the same MWD as in the aerobic effluent (column input) was reached, confirming that all the pollutants entering the column at this point, independent of their molecular weight, are leaving the column unadsorbed in the output stream. These results are also suggesting, that larger sized molecules are being adsorbed, practically independent of their presence in the color or phenolic compounds group.

4.2.3.3   Fixed bed adsorption rate

As discussed in Chapter 3.4.3 a simple fixed bed kinetic model (FBKM) was used for the calculation of the adsorption rate of a single pollutant in a soil column, based on the model proposed by [149],[150],[151]. The used model is shortly described in the following steps.

Considering Figure 53, and assuming piston flow regime in the column and an isothermal adsorption process, it is possible to write the following mass balance for the pollutant (Equation 30):
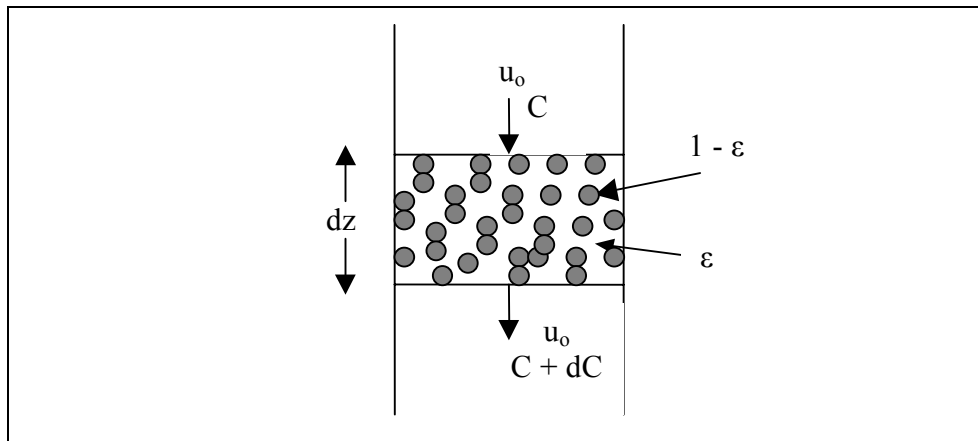
Figure 53: Mass balance model of a pollutant in a column section

$$\varepsilon * dz * \frac{dC}{dt} + dz * \alpha * \rho * \frac{dW}{dt} = u_o * C - u_o * (C + dC) \tag{30}$$

with ε = porosity [-], dz = differential length [m], C = pollutant concentration [mg/L], t = time [s], α = soil fraction [-], ρ = soil/sand bed bulk density [g/L], W = total pollutant amount adsorbed [mg/g soil] and u_o = linear velocity [m/s].

Rearranging Equation 30, will lead to:

$$\varepsilon * \frac{dC}{dt} + \alpha * \rho * \frac{dW}{dt} = -u_o * \frac{dC}{dz} \tag{31}$$

Introducing the global volumetric mass transfer coefficient ($K_c * a$) [s^{-1}] as:

$$\alpha * \rho * \frac{dW}{dt} = K_c * a * \left(C - C^*\right) \tag{32}$$

where C^* is the equilibrium concentration of the pollutant in the liquid phase [mg/L], from Equation 32, it is possible to obtain

$$\frac{dW}{dt} = \frac{K_c * a}{\alpha * \rho} * \left(C - C^*\right) \tag{33}$$

and combining Equation 31 with Equation 33 will give:

$$\frac{dC}{dt} + K_c * a * \left(C - C^*\right) = -\frac{u_o}{\varepsilon} * \frac{dC}{dz} \tag{34}$$

Introducing a new time variable t´ [s] as:

$$t' = t - z * \left(\frac{\varepsilon}{u_o}\right) \quad , \tag{35}$$

the differential expressions would be:

$$dt = dz * \left(\frac{\varepsilon}{u_o}\right) \quad (t' = \text{constant}) \tag{36}$$

and:

$$dt' = dt \quad (z = \text{constant}) \tag{37}$$

Replacing Equations 36 and 37 in Equations 33 and 34 the following equation system is obtained:

$$\frac{dW}{dt'} = \frac{K_c * a}{\alpha * \rho} * \left(C - C^*\right) \tag{38}$$

and:

$$\frac{dC}{dz} = -\frac{K_c * a * \varepsilon}{2 * u_o} * \left(C - C^*\right) \tag{39}$$

With the following border conditions:

$t' = 0 \quad , \qquad W = 0 \qquad z > 0$

$z = 0$, $C = C_o$ $t' > 0$

To solve this equation system, it is necessary to introduce a mathematical relationship between $C*$ and W. As already shown in Figure 49 and Figure 50, an exponential relationship exists between $C*$ and W for both types of pollutants (color and phenolic compounds) and both types of volcanic soils (natural and acidified).

For major simplicity and to obtain an analytical solution of the model, a linear interface equilibrium distribution for these isotherms needs to be assumed. Therefore, it is supposed that $C*$ moves only in a little range during the non-steady-state FBKM experiments.

For a small range of $C*$ the following linear relationship can be assumed:

$C* = m * W$ (40)

where m is the linear relationship parameter [g/L] between $C*$ and W.

The following non-dimensional variables are introduced for simplifying the system:

$$X = \left(\frac{C}{C_o}\right)$$ (41)

$$Y = \left(\frac{C*}{C_o}\right)$$ (42)

and:

$$\phi = z * \frac{K_c * a * \varepsilon}{2 * u_o}$$ (43)

$$\tau = m * t' * \frac{K_c * a}{\alpha * \rho}$$ (44)

where $\varnothing$ is the dimensionless length variable and τ is the dimensionless time variable. Therefore, the system could be expressed as:

$$\frac{dX}{d\phi} = -(X - Y)$$ (45)

$$\frac{dY}{d\tau} = (X - Y)$$ (46)

With the following border conditions:

$\tau = 0$, $Y = 0$ for every value of ϕ

$\phi = 0$, $X = 0$ for every value of τ ,

the analytical solution of the system will be:

$$X = \frac{C}{C_o} = 1 - \int_0^\phi \left[\exp(-(\tau + \phi)) J_o\left(i \sqrt{4 * \tau * \phi}\right)\right] d\phi \tag{47}$$

where $J_o(r)$ is the Bessel function from the first type and order 0. Remembering that the J_n type **Bessel functions** could be written as:

$$J_n(ir) = i^n I_n(r) , \tag{48}$$

Equation 47 will become:

$$X = \frac{C}{C_o} = 1 - \int_0^\phi \left[\exp(-(\tau + \phi)) I_o\left(\sqrt{4 * \tau * \phi}\right)\right] d\phi \tag{49}$$

where $I_o(r)$ is the modified Bessel function from the first type and order 0.

The parameters m and $(K_c * a)$ are the parameters from the model that need to be adjusted. The adjustment was made for each run by minimizing the objective function defined as the error addition over all the experimental data of each breakthrough curve [150]:

$$\Omega = \sum \left[C_{calc}(t,L) - C_{exp}(t,L)\right]^2 \tag{50}$$

where Ω is the objective error function, $C_{calc}(t,L)$ is the calculated pollutant concentration in the column output [mg/L] and $C_{exp}(t,L)$ is the experimental pollutant concentration in the column output [mg/L].

By solving Equation 49 it is possible to obtain the m and $(K_c * a)$ values for the experimental breakthrough curves from phenolic compounds and color adsorption onto volcanic soil (see Table 29). Fitting of the model on the experimental breakthrough curves data for **experiment 1** (see Chapter 3.4.1, Table 13) are presented in Figure 54 to Figure 57. The results clearly indicate that the $(K_c * a)$ values were higher for the adsorption process onto acidified soil, independent of the pollutant and the experimental conditions. This means that the pretreatment by washing the soil with acid has the most positive effect on the adsorption rate for both pollutant groups, color and phenolic compounds, which can be explained by the

activation of the Al and Fe oxide/hydroxide sites present in the soil matrix. These increments ranged from 156% to 372% for color and from 135% to 282% for phenolic compounds.

By increasing the flow rate, from 1.5 mL/min (experiment 1) to 2.5 mL/min (experiment 2), higher (K_c * a) values for both compounds (Table 29) were obtained. In fact, comparing color adsorption onto acidified soil, there is an increment of 43% in the global mass transfer coefficient for experiment 2. For the adsorption of phenolic compounds onto acidified soil, there is a smaller increment of only 4% for the (K_c * a) value. In the case of color and phenolic compounds adsorption onto natural soil, the increments in the (K_c * a) value were 25% and 81%, respectively. Comparing experiments 1 and 3, it its clearly seen that (K_c * a) values for color and phenolic compounds adsorption processes in experiment 3 decrease, indicating that the mass transfer rate is lower than observed in experiment 1.

In fact, for color and phenolic compounds adsorption onto natural soil there was a decrease of 21% and 24% in the (K_c * a) values of experiment 3, respectively. For the adsorption of these pollutants onto acidified soil, the decreases in experiment 3 were 51% and 53%, respectively. These results clearly indicate that both, the effluent flow rate and the soil mass fraction, are affecting the global mass transfer coefficient.

Table 29: Results for m and (K_c * a) values estimated by the model

| Experiment (from Chapter 3.4.1, Table 13)	Pollutant	Volcanic soil	m [g/L]	m range[a] [g/L]	K_c * a [s^{-1}]	Adsorption rate (K_c * a)/m [L/mg*min]
1	Color	Natural	51.8	3.1 – 107.9	$1.14*10^{-4}$	$1.32 * 10^{-7}$
		Acidified	10.7	1.4 – 22.0	$4.67*10^{-4}$	$2.62 * 10^{-6}$
1	Phenolic Compounds	Natural	24.5	11.8 – 148.7	$1.05*10^{-4}$	$2.57 * 10^{-7}$
		Acidified	10.7	3.2 – 48.4	$4.01*10^{-4}$	$2.25 * 10^{-6}$
2	Color	Natural	35.0	3.1 – 107.9	$1.42*10^{-4}$	$2.43 * 10^{-7}$
		Acidified	10.2	1.4 – 22.0	$6.70*10^{-4}$	$3.94 * 10^{-6}$
2	Phenolic Compounds	Natural	22.0	11.8 – 148.7	$1.90*10^{-4}$	$5.20 * 10^{-7}$
		Acidified	13.9	3.2 – 48.4	$4.18*10^{-4}$	$1.80 * 10^{-6}$
3	Color	Natural	23.0	3.1 – 107.9	$9.00*10^{-5}$	$2.35 * 10^{-7}$
		Acidified	5.0	1.4 – 22.0	$2.30*10^{-4}$	$2.76 * 10^{-6}$
3	Phenolic Compounds	Natural	15.0	11.8 – 148.7	$8.00*10^{-5}$	$3.20 * 10^{-7}$
		Acidified	6.1	3.2 – 48.4	$1.88*10^{-4}$	$1.85 * 10^{-6}$

[a]: Evaluated analytically from Figure 49 and Figure 50

On the one hand, the flow rate effect indicates that the external mass transfer coefficient is significant and has a measurable influence on the global mass transfer coefficient. An increment in the flow rate directly enhanced the external mass transfer coefficient (and also the global coefficient), making the pollutants concentration to be higher (and probably close to the bulk concentration of the pollutants in the liquid phase) at the soil surface. This

situation provoked a higher pollutants concentration gradient between the soil surface and the internal pores of it, enhancing the adsorption rate.
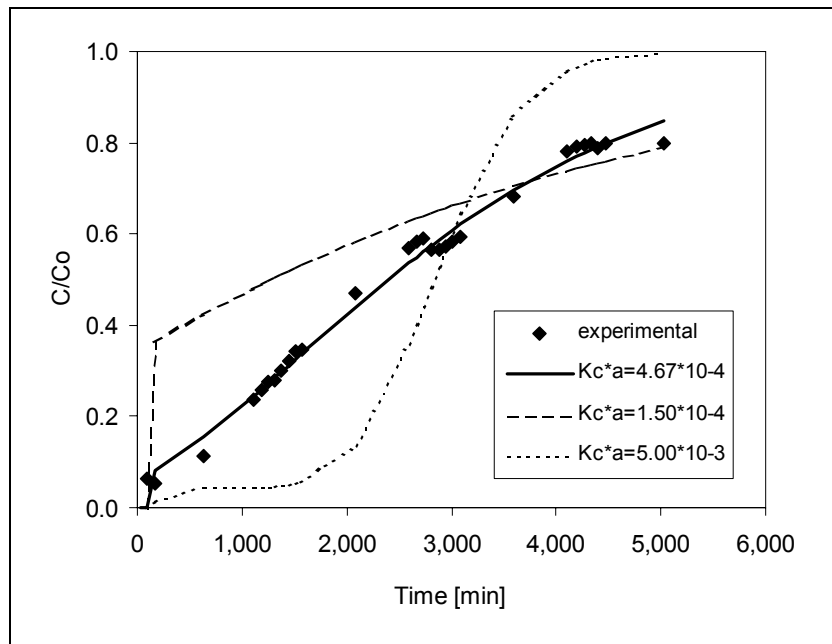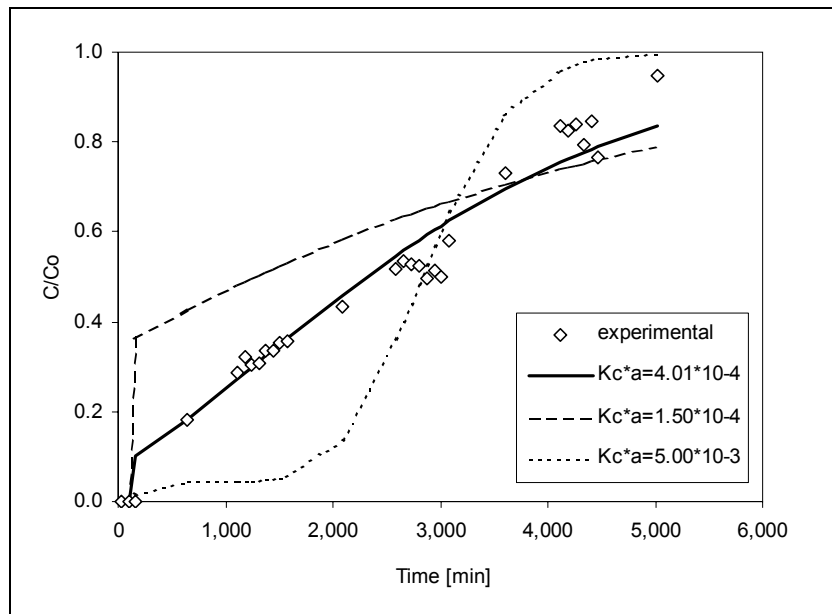

Figure 54: Model fitting for color adsorption onto acidified soil and the effect of ($K_c * a$) variation for experiment 1 in Chapter 3.4.1, Table 13. $K_c * a$ in [s^{-1}]
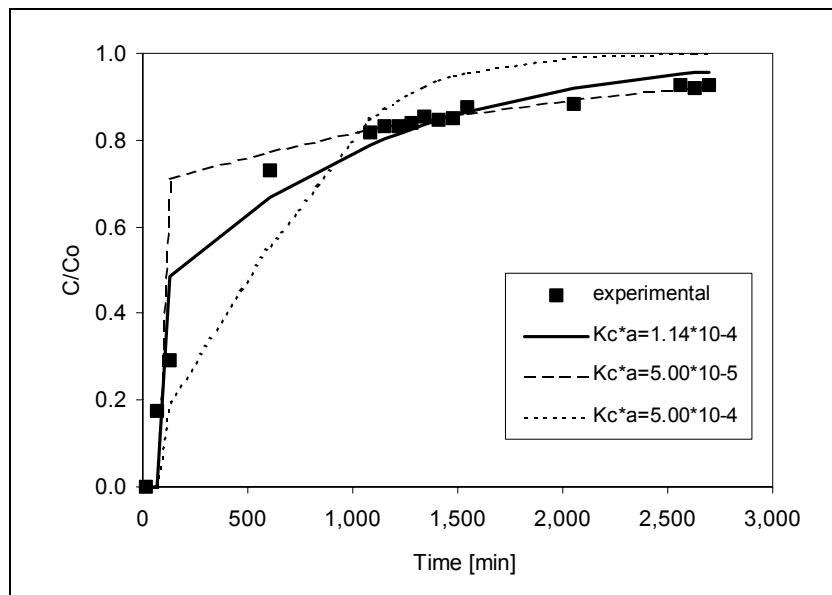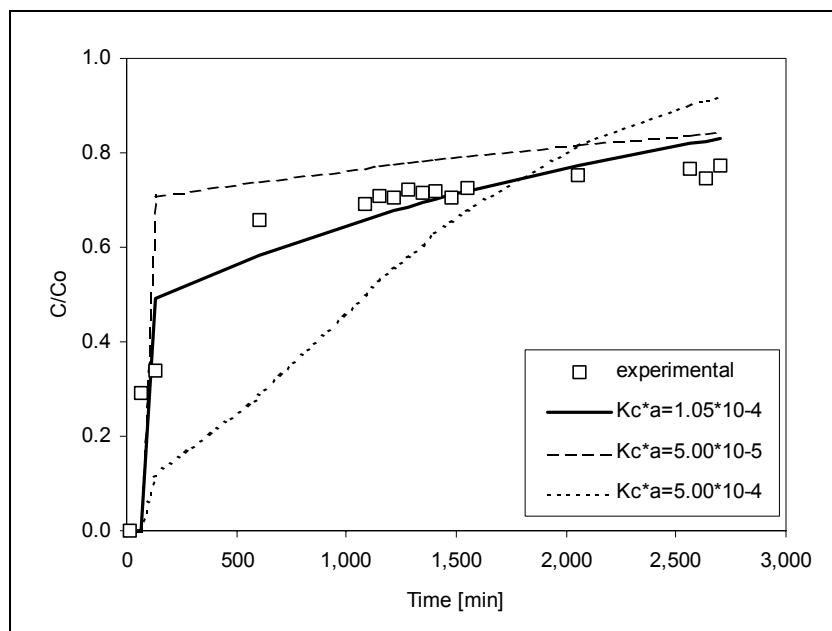

Figure 55: Model fitting for color adsorption onto natural soil and the effect of ($K_c * a$) variation for experiment 1 in Chapter 3.4.1, Table 13. $K_c * a$ in [s^{-1}]

On the other hand, the ($K_c * a$) values had a strong dependence on the soil fraction in the column, indicating the significance of the internal mass transfer resistance. A higher porosity value (e.g. in experiment 3) had a negative effect on the internal mass transfer coefficient (and also on the global mass transfer coefficient at constant flow rate). In this case it's

assumed that a diffusion process takes place in the internal pores of the soil, slowing the adsorption process down.

Figure 56: Model fitting for phenolic compounds adsorption onto acidified soil and the effect of (K_c * a) variation for experiment 1 in Chapter 3.4.1, Table 13. K_c * a in [s^{-1}]

Figure 57: Model fitting for phenolic compounds adsorption onto natural soil and the effect of (K_c * a) variation for experiment 1 in Chapter 3.4.1, Table 13. K_c * a in [s^{-1}]

Analyzing the m values, it is observed that these values were smaller for all the adsorption processes onto acidified soil, independent of the pollutant and the experimental conditions. For a given C^* value, a smaller m value will represent a higher pollutant adsorption capacity, W (see Equation 40). Thus, these higher adsorption capacities for acidified soil compared

with natural soil will range between 343 and 484% for color and between 158 and 229% for phenolic compounds, respectively. Analyzing the adsorption rate constants $(K_c * a)/m$, phenolic compounds and color adsorption rates onto acidified soil of $2.25*10^{-6}$ and $2.62*10^{-6}$ L/mg*min were achieved in experiment 1 (see Table 13 in Chapter 3.4.1 and Table 29 in Chapter 4.2.3.3). These rates are quite similar compared with the ones obtained with the Bohardt & Adams model (i.e. $2.0 * 10^{-6}$ and $1.5 * 10^{-6}$ L/mg*min for phenolic compounds and color respectively) [147]. Moreover, these adsorption rates are comparable with other FBAS. For instance, [48] obtained adsorption rate constants between $4.73*10^{-5}$ and $5.69*10^{-5}$ L/mg*min for dye adsorption onto sugar-industry-mud, which are one and two orders of magnitude higher than the adsorption rates obtained for acidified and natural volcanic soil, respectively. Finally, analyzing the breakthrough experimental curves (see Figure 54 to Figure 57), it seems that all of them were incomplete, i.e., the obtained final C/C_0 values were always less than 1.0, although the experiment times were about 1.7 and 3.5 days for natural and acidified volcanic soil, respectively. This fact is probably attributed to degradation within the column, confirming that degradation is generally an important mechanism (as well as sorption) for the attenuation of organic pollutants in most contaminated aquifers [189].

4.3   Adsorption of chlorophenols from synthetic groundwater

4.3.1   Adsorption isotherms

As described by [11], the adsorption of phenolic compounds was enhanced at low pH values (around pH = 4.0). Appart from an enhanced adsorption capacity, an adequate soil biological activity and bioremediation capacity is needed as well, because the chlorophenols natural biodegradation in volcanic soil will be studied as one of the possible contaminated soil managing options.
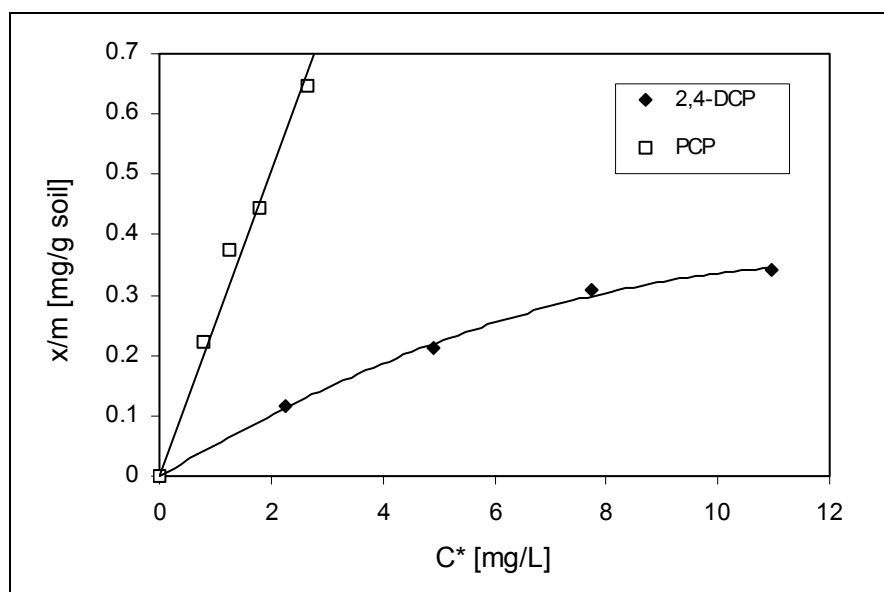
Figure 58: Adsorption isotherms of 2,4-DCP and PCP onto the 5-20 cm profile volcanic soil at pH 6.0

That was the reason why the isotherms were measured at pH 6.0 in the 5-20 cm volcanic soil profile, which is the profile with the highest SOM content, promoting a higher biological activity for the following soil remediation study. In Figure 58, the adsorption isotherms of 2,4-DCP and PCP onto the 5-20 cm volcanic soil profile at pH 6.0 are shown.

The adsorption capacity of PCP onto volcanic soil is higher than that of 2,4-DCP. As suggested by [106], the log K_{ow} value of PCP (5.01) compared to that of 2,4-DCP (3.08) makes PCP to have a greater affinity with the organic matter present in the soil, increasing its adsorption capacity through this mechanism. Moreover, the solubility of non-ionic PCP is only 18 mg/L compared to that of non-ionic 2,4-DCP (4,500 mg/L), which indicates an affinity of 2,4-DCP to remain in the liquid phase, indirectly decreasing its adsorption capacity. Only the pK$_a$ values would suggest that for PCP (pK$_a$ = 4.7) at pH 6.0 the anionic form (phenolate) would be the most important, enhancing its capacity to leach from the soil. In the case of 2,4-DCP (pK$_a$ = 7.9), at pH 6.0 the non-ionic form will be still the most important fraction, suggesting that although the anionic form of PCP is present, the high K_{ow} value of its non-ionic form allows this fraction to get adsorbed more than 2,4-DCP.

The Langmuir and Freundlich model parameters for chlorophenols adsorption onto volcanic soil are presented in Table 30. The obtained Langmuir b values were 0.736 and 2.812 mg/g for 2,4-DCP and PCP, respectively. The adsorption of PCP onto activated carbon is around 160 mg/g at pH 8.5 for C^* values around 10 mg/L [19] which is very high compared with volcanic soil. Moreover, the sorption of phenol and p-chlorophenol onto different cheaper adsorption materials (coal, shell, wood and rubber) ranged between 20 and 80 mg/g or 30 and 110 mg/g, respectively, for C^* values around 10 mg/L [3]. These values are more comparable to those of PCP adsorption onto volcanic soil, looking at the extrapolation of the adsorption isotherm in Figure 58. As discussed before, the adsorption of phenol by zeolites is about 3.2 mg/g [18], which is a very comparable value with the maximum adsorption of 2,4-DCP and PCP onto volcanic soil. The Freundlich model seems to fit properly the experimental data of Figure 58 (se also Table 30). For the adsorption of different substituted phenols onto activated carbon, the Freundlich model k_F constant varies between 0.3 and 2.2, while the n constant varies between 0.06 and 0.3 [18]. In this case, the Freundlich k_F parameter is in the lower range of the previously reported activated carbon, which is an empirical indicator for how much solution (L) is possible to treat with one gram of adsorbent material.

Table 30: Langmuir and Freundlich model parameters for chlorophenols adsorption onto volcanic soil

Chlorophenol	Langmuir			Freundlich		
	b	k_L	R^2	n	k_F	R^2
	[mg/g]	[L/mg]		[-]	[(L/mg)$^{(1/n)}$*(mg/g)]	
2,4-DCP	0.736	0.084	0.953	1.395	0.066	0.984
PCP	2.812	0.111	0.648	1.161	0.280	0.981

4.4   Adsorption of heavy metals from synthetic landfill leachate

4.4.1   Adsorption isotherms

The adsorption isotherms of Cr(VI) (as CrO_4^{2-}), Cu^{2+}, Zn^{2+} and Pb^{2+} are presented in Figure 59 and Figure 60. It is clearly shown that the pH value has an important influence on the heavy metal uptake onto the volcanic soil surface. For the heavy metal cations Cu^{2+} and Zn^{2+}, a higher uptake was obtained at pH 7.5, compared with pH 4.5. This result is related to the pH_{ZPC} (zero point charge pH) of the soil, which was determined to be 5.5. It was therefore expected, that at pH 4.5 the soil surface will be positively charged and at pH 7.5 it will be negatively charged. Anions (CrO_4^{2-}) should then adsorb more at pH 4.5 and cations (Cu^{2+}, Zn^{2+} and Pb^{2+}) at pH 7.5.

This is a very interesting factor for the proposed landfill application as the pH of the landfill leachate varies with time, starting with an acidic value (which is characteristic for the acetogenic stage of the anaerobic biodegradation of wastes) developing further to a neutral to alkaline pH value (which corresponds to the methanogenic phase). Only for Pb^{2+}, this effect wasn't clear and it seemed that Pb^{2+} was capable to adsorb onto the volcanic soil in the whole pH range tested, independent of the soil profile.

The opposite effect was detected for the adsorption of CrO_4^{2-} onto volcanic soil. The uptake of this anion was enhanced at pH 4.5, where the soil surface was supposed to be mainly positively charged. For comparison purposes, the Langmuir and Freundlich adsorption parameters were calculated as shown in Table 31. Acceptable regression factors (R^2) were obtained for both models. Only the Langmuir correlation values for Zn^{2+} seemed to be less acceptable.

The *b* parameter of the Langmuir model, which represents the maximum possible uptake of each heavy metal onto volcanic soil, was higher, in general, for the 5-20 cm volcanic soil profile, confirming therefore the important effect of the SOM (soil organic matter) in the adsorption process onto the soil surface. In fact, for CrO_4^{2-} a maximum Cr(VI) uptake of 2.74 mg/g was determined (5-20 cm profile at pH 4.5). This result is comparable to the adsorption capacity of some mineral clays. For instance, Greek natural zeolites are capable to adsorb Cr^{3+} from $Cr(NO_3)_3$ up to a maximum *b* value of 4.12 mg/g [24]. Moreover, as a directly comparable reference, the maximum Cr(VI) (i.e. CrO_4^{2-}) adsorption capacity of different activated carbons can range between 3.4 and 23.4 mg/g [18].

For Cu^{2+}, a maximum Langmuir *b* value of 5.32 mg/g was obtained in this work. The Cu^{2+} uptake in Greek natural zeolites has been determined to be 5.91 mg/g [24]. Moreover, the Cu^{2+} maximum uptake in Croatian zeolites was estimated to be 26.0 mg/g [23], while the Cu^{2+} uptake onto different activated carbons can move between 15.9 and 27.3 mg/g [18].

In the case of Zn^{2+}, a maximum Langmuir uptake value *b* of 5.86 mg/g was achieved, which is comparable to the maximum value of 3.45 mg/g obtained for Greek zeolites [24]. Croatian

zeolites are capable to retain maximum Zn^{2+} amounts in the range between 13.1 and 13.8 mg/g [23]; while for some specific clay landfill liners, the Zn^{2+} uptake can vary between 0.1 to 0.3 mg/g [14]. In addition, the adsorption capacity of activated carbons for Zn^{2+} ranges between 2.6 and 75.7 mg/g [18].
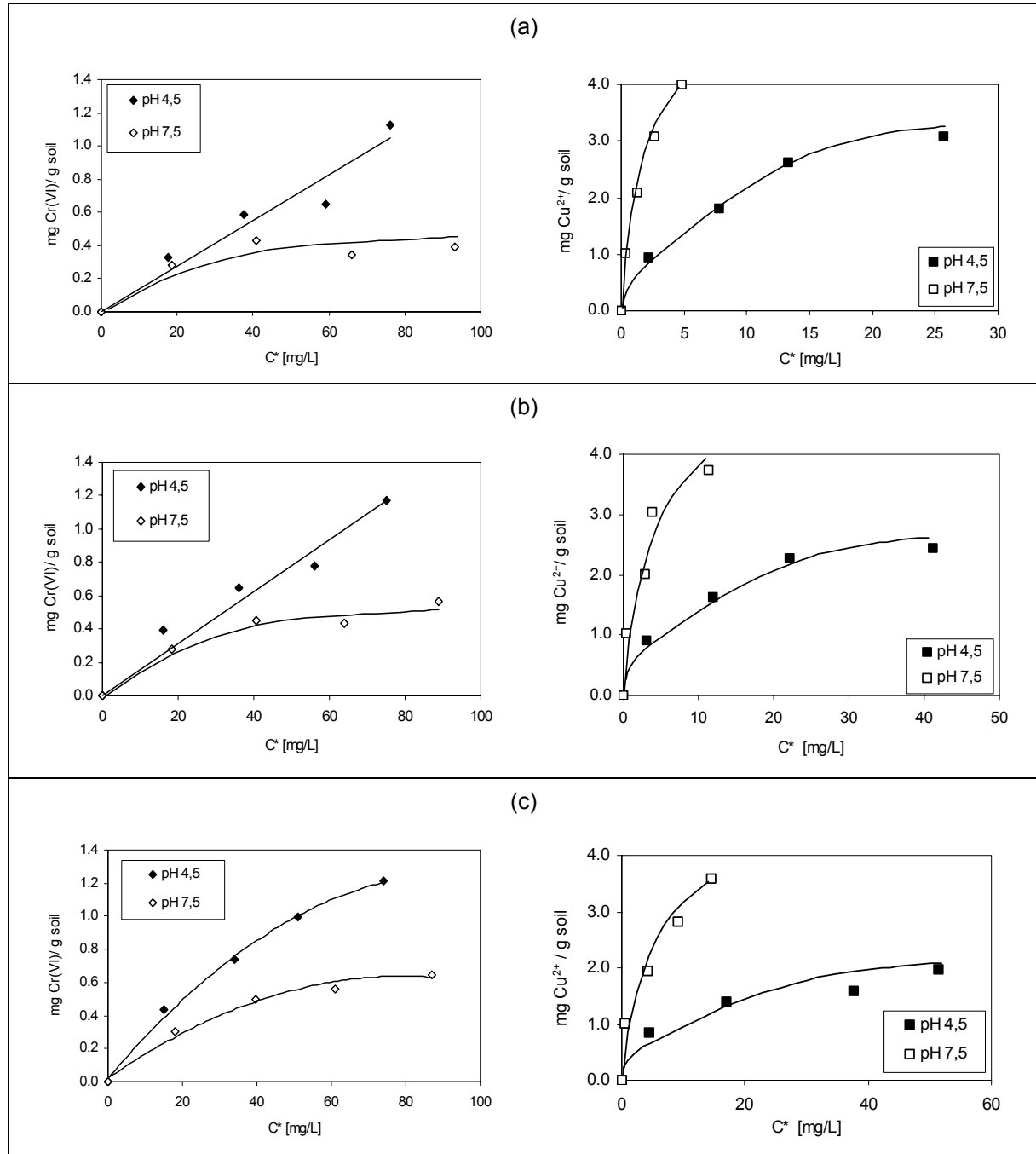
Figure 59: Cr(VI) (as CrO_4^{2-}) and Cu^{2+} adsorption isotherms as a function of pH for the different soil profiles (a: 5-20 cm; b: 20-40 cm and c: 40-60 cm)

The maximum Langmuir *b* value for Pb^{2+} uptake was determined to be 7.44 mg/g. Natural Croatian zeolites do adsorb maximum Pb^{2+} amounts between 88.5 and 89.7 mg/g [23], but in real clay landfill liners the sorption of Pb^{2+} reaches maximum values of 0.8 mg/g only [14]. Moreover, the Pb^{2+} uptake in different loams ranges between 0.2 and 9.7 mg/g [107].

The relative order of the volcanic soil heavy metals uptake seemed therefore to be: Pb^{2+} >> Zn^{2+} > Cu^{2+} >> Cr(VI) The Freudlich parameter k_F confirms this trend, as k_F is an empirical indicator for how much solution (L) is possible to treat with 1 g of adsorbent material. Only between Cu^{2+} and Zn^{2+} there could be little doubt, as both cations have a very similar adsorption capacity onto the three different volcanic soil profiles.
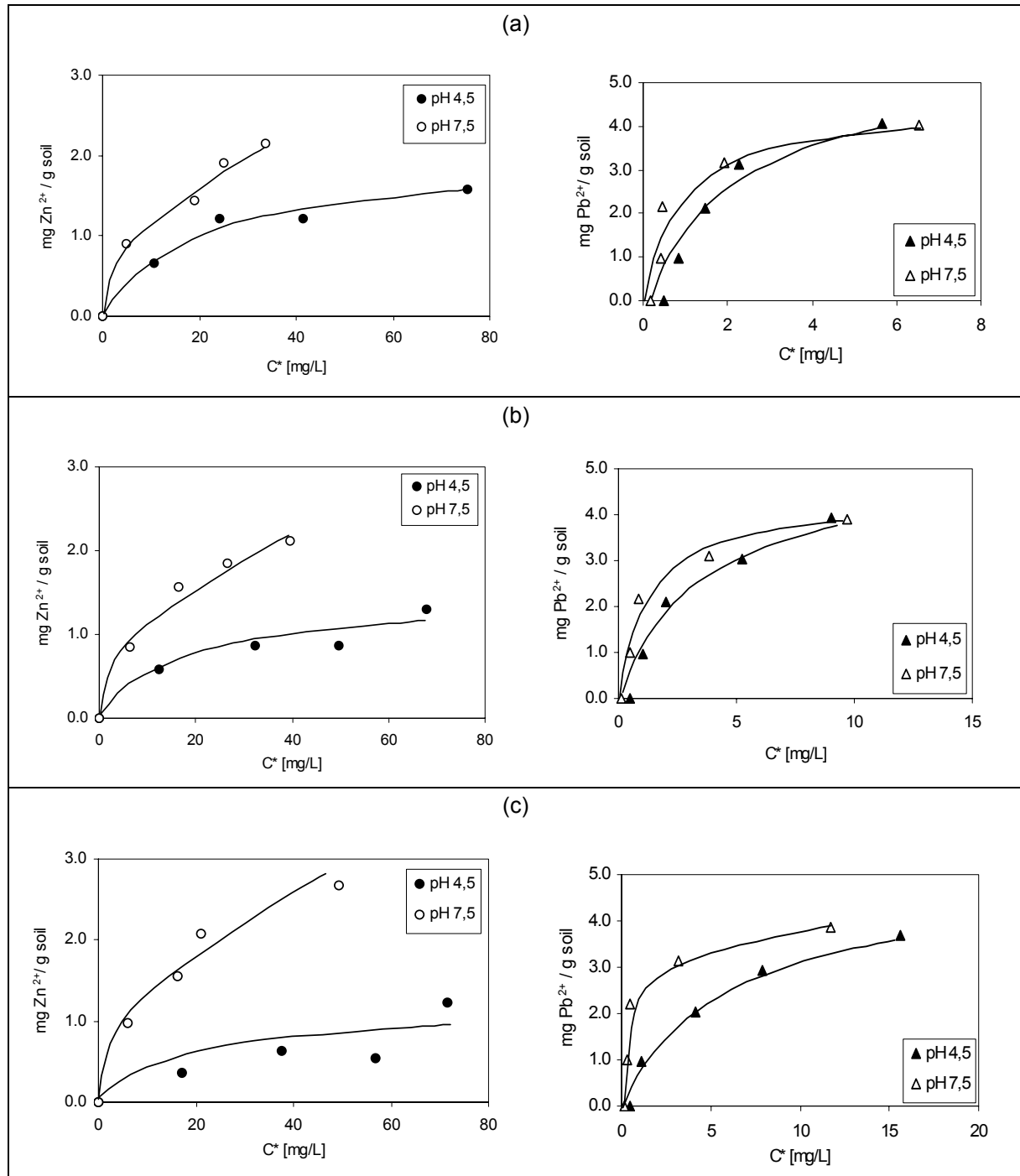
Figure 60: Zn^{2+} and Pb^{2+} adsorption isotherms as a function of pH for the different soil profiles (a: 5-20 cm; b: 20-40 cm and c: 40-60 cm)

Table 31: Langmuir and Freundlich parameters for heavy metal adsorption isotherms (see Figure 59 and Figure 60)

Pollutant	Volcanic soil profile	pH	Langmuir			Freundlich		
			b [mg/g]	k_L [L/mg]	R^2	n [-]	k_F [(L/mg)$^{(1/n)}$*(mg/g)]	R^2
Cr(VI) as (CrO$_4^{2-}$)	5-20 cm	4.5	2.74	0.007	0.355	1.32	0.037	0.914
		7.5	0.40	0.205	0.966	5.99	0.189	0.400
	20-40 cm	4.5	2.28	0.012	0.713	1.50	0.060	0.963
		7.5	0.70	0.036	0.929	2.49	0.091	0.884
	40-60 cm	4.5	2.30	0.015	0.983	1.53	0.074	0.998
		7.5	0.90	0.029	0.995	2.08	0.078	0.972
Cu^{2+}	5-20 cm	4.5	4.06	0.124	0.986	2.00	0.652	0.982
		7.5	5.32	0.583	0.986	1.90	1.813	0.997
	20-40 cm	4.5	2.88	0.136	0.993	2.51	0.598	0.973
		7.5	4.30	0.523	0.964	2.61	1.530	0.955
	40-60 cm	4.5	2.19	0.111	0.967	3.03	0.520	0.971
		7.5	4.03	0.146	0.944	2.82	1.298	0.985
Zn^{2+}	5-20 cm	4.5	1.95	0.051	0.973	2.38	0.266	0.888
		7.5	5.30	0.029	0.379	1.73	0.336	0.826
	20-40 cm	4.5	2.90	0.014	0.300	1.71	0.121	0.735
		7.5	5.86	0.023	0.659	1.50	0.243	0.960
	40-60 cm	4.5	4.18	0.005	0.038	1.19	0.030	0.635
		7.5	3.67	0.055	0.979	2.01	0.405	0.963
Pb^{2+}	5-20 cm	4.5	7.44	0.233	0.791	1.38	1.371	0.867
		7.5	4.63	1.030	0.981	1.66	2.106	0.729
	20-40 cm	4.5	5.90	0.218	0.963	1.64	1.107	0.932
		7.5	4.42	0.735	0.993	2.01	1.719	0.855
	40-60 cm	4.5	4.79	0.205	0.992	5.65	0.771	0.845
		7.5	4.11	1.223	0.997	5.19	1.963	0.770

The pH values selected for the elaboration of the isotherms (i.e., 4.5 and 7.5) are related with typical pH values of landfill leachates. In fact, pH 4.5 may be reached during the so-called acidogenic phase, which occurs shortly (within months) after dumping of fresh wastes in landfills. Usually, the pH value of the leachate is in the neutral or slightly alkaline region (around pH = 7.5), during the so-called methanogenic phase.

Nevertheless, the solubility of heavy metals in water is dependent on the pH value, as shown in Figure 61 [190]. For the heavy metals investigated in this work, only a precipitation of Cu^{2+}

and Zn^{2+} cations at pH 7.5 was expected to occur. On the one hand, the solubility of Cu^{2+} at pH 7.5 is only about 0.4 mg/L, compared to about 18 mg/L at pH 6.0. On the other hand, the solubility of Zn^{2+} decreases to about 20 mg/L at pH 7.5. In addition, CrO_4^{2-} is known to be soluble in the wide pH range and therefore its precipitation was not expected at the pH values used for the isotherms. In the case of Pb^{2+}, as shown in Figure 61, a decrease in the solubility can only be produced in the pH range between 8.8 and 11.0. Therefore no precipitation of lead was expected at the pH values of the isotherms.
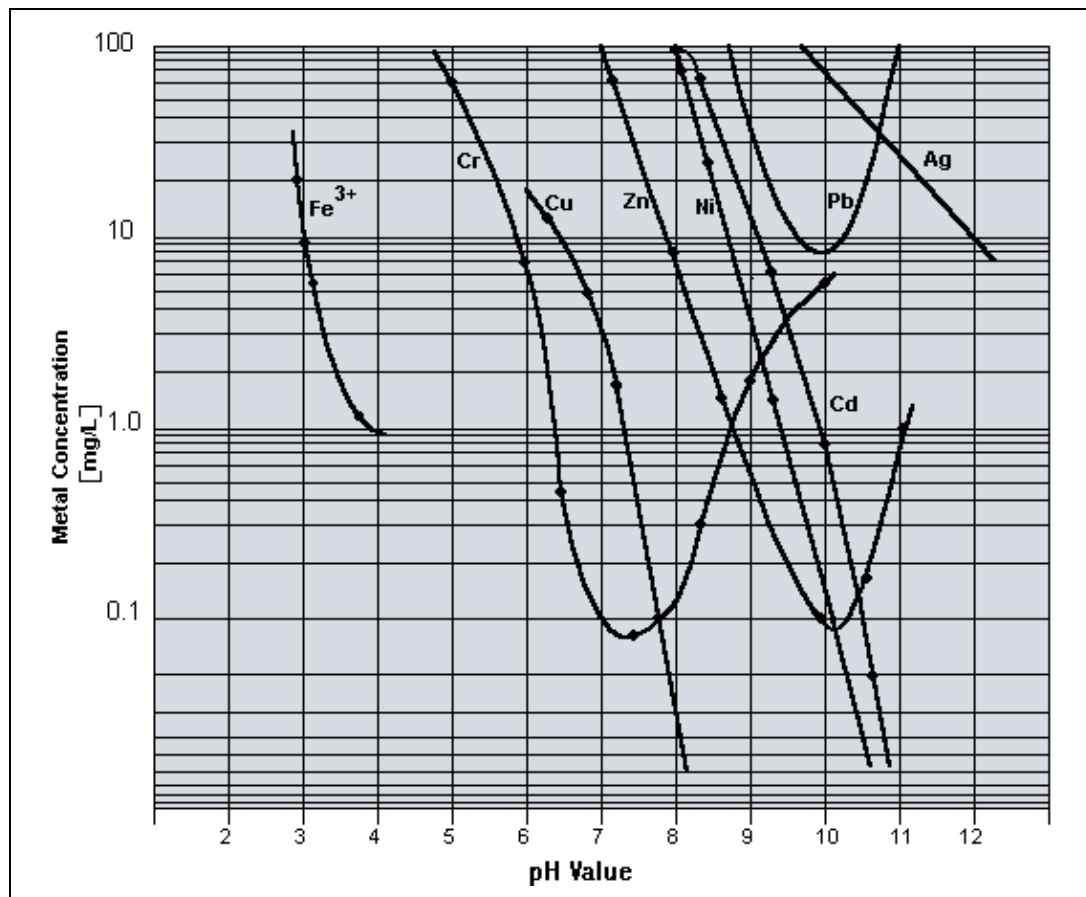
Figure 61: Heavy metals solubilitlity in water in dependence of the pH-value

This analysis indicates that for the isotherms performed at pH 4.5 (see Figure 59, Figure 60 and Table 31), only adsorption was responsible for the heavy metals retention on volcanic soil only. For the isotherms performed at pH 7.5, a combined precipitation-adsorption process was expected to occur for Cu^{2+} and Zn^{2+}. The maximum adsorption yields calculated for the isotherms of Cu^{2+} onto volcanic soil at pH 4.5 were found to range between 50 and 75%, compared to a range between 90 and 99% at pH 7.5. This increment in the adsorption yield can be related to the effect of the negative soil surface charge at pH 7.5 (as discussed previously) but also to a possible precipitation of Cu^{2+}. For Zn^{2+}, the maximum adsorption yields calculated for its isotherms onto volcanic soil at pH 4.5 were found to range between 30 and 40%, compared to a range between 55 and 68% at pH 7.5. The same forementioned explanation is feasible for the increment in the adsorption yield for Zn^{2+} at pH 7.5.

In order to determine the influence of precipitation on the obtained results, Cu^{2+} and Zn^{2+} solutions were prepared according to the observed concentration ranges in landfill leachates and identically as the isotherms solutions used (see Chapter 3.3.3). The solutions were tested for precipitation at pH 7.5. The results indicate that more than 90% of the dissolved Cu^{2+} and Zn^{2+} precipitated. Therefore, it was assumed, that the retention of these two heavy metal cations onto volcanic soil is effectively a combined precipitation-adsorption process.

4.4.2 Heavy metal diffusion through a mineral liner

The used heavy metal diffusion model (HMDM) was based on the Fick's second law (Equation 52). As shown in Figure 62 and Annex IV, the heavy metals diffusion through a compacted volcanic soil column was calculated.
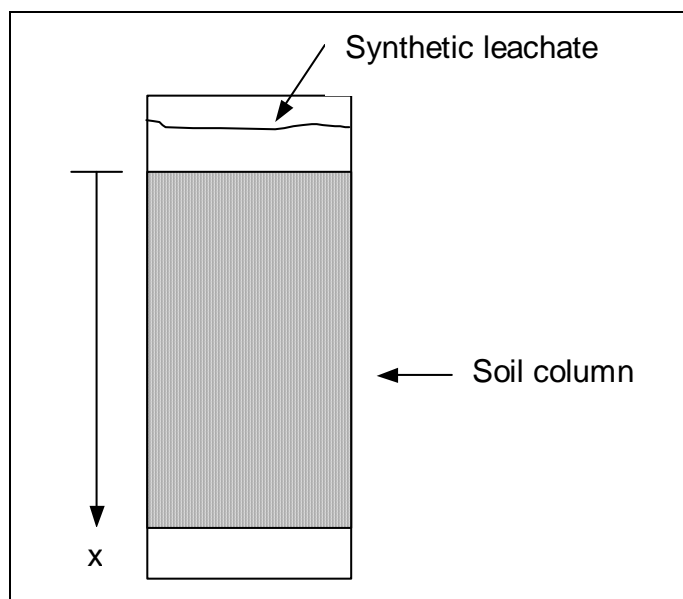
Figure 62: Schematic representation of the diffusion column for heavy metals

The mobility of heavy metals in the volcanic soil barrier can be described by a migration term, that includes advective and diffusive transport, and by a retardation term, that describes the reversible or irreversible fixation of heavy metal ions on the soil components. These processes are summarized in the advective/dispersive transport equation. For the one-dimensional case it may be written in the form [107]:

$$R_A * \frac{\partial c}{\partial t} = D_h * \frac{\partial^2 c}{\partial x^2} - u_a * \frac{\partial c}{\partial x} ,$$
(51)

where c is the heavy metal concentration [mg/L], t is the time [s], x [cm] is the distance from the contaminant source (the top of the column in this case), R_A is the retardation coefficient, D_h is the hydrodynamic dispersion coefficient [cm^2/s] and u_a is the average seepage velocity [cm/s].

As discussed in Chapter 2.7, the advective and dispersive processes can be clearly separated. In non-compacted and non-clayed soils with hydraulic conductivities (K_f) higher than $3*10^{-6}$ m/s, the liquid flow (or the linear velocity of the liquid phase) will be the variable that controls the contaminant mobility through the soil [15],[106]. On the other hand, in compacted and clayed soils with a K_f value lower than $3*10^{-6}$ m/s, the molecular diffusion will be the main process controlling the mobility of pollutants through the soil matrix [14], [15],[107]. Therefore, the fundamental transport equation can be simplified for u_a = 0 to a pure diffusion equation, which has the form of the Fick's second law (Equation 52). The hydrodynamic dispersion coefficient D_h, composed by the mechanical dispersion (D_m) and effective diffusion (D_e), becomes the effective diffusion coefficient D_e.

$$R_A * \frac{\partial c}{\partial t} = D_e * \frac{\partial^2 c}{\partial x^2} \tag{52}$$

Defining the term D_e/R_A as the apparent diffusion coefficient of a heavy metal ion in the volcanic soil liner (D_a), Equation 52 can be re-written as:

$$\frac{\partial c}{\partial t} = D_a * \frac{\partial^2 c}{\partial x^2} \tag{53}$$

Under specific boundary conditions, a homogeneous semi-infinite medium for the initial condition that all diffusants are concentrated in the top of the column (t = 0, x = 0, $c(0) = \infty$ and t = 0, x > 0, $c(x)$ = 0), Equation 53 can be solved analytically, and the general value of c is given by [153],[154]:

$$c = \frac{\int_0^\infty c(x,0)dx}{\sqrt{\pi * D_a * t}} * e^{\left(\frac{-x^2}{4D_a t}\right)} \tag{54}$$

The middle term of Equation 54 is in fact a constant term. Defining this term as M_c and applying natural logarithm, Equation 55 is obtained.

$$\ln(c) = \ln(M_c) - \frac{x^2}{4D_a t} \tag{55}$$

The total concentration (in soil and soil pores) of each heavy metal ion was measured at five different depths in each column (Annex IV) for a determined total time. In that way, M_c and D_a were calculated adjusting the obtained data to Equation 55. The intercept of the linear regression will be $\ln(M_c)$ and the negative slope will be $1/(4 D_a * t)$. With D_a, the breakthrough times for each heavy metal was calculated in a hypothetical 1 m deep volcanic soil liner using Equation 54. In addition, the effective diffusion coefficient D_e was calculated. For such

purposes, diffusion experiments with Cl⁻ were performed, knowing that this anion does not adsorb onto clay mineral surfaces [14]. Therefore, for the Cl⁻ anion $D_a = D_e$, as in this case no retardation (factor R_A) exists. In addition, as shown in Equation 56, the effective diffusion coefficient (D_e) is a function of the tortuosity of the soil column (ξ) and the free-solution diffusion coefficient (D_0).

$$D_e = \xi * D_0 \qquad\qquad (56)$$

The ξ value was obtained from the Cl⁻ anion experiment, as the obtained diffusion coefficient from Equation 55 was assumed to be D_e, while D_0 was obtained from the literature (see Table 34). For each heavy metal, the D_e coefficient was then calculated from Equation 56, while each retardation factor R_A was obtained from the expression $R_A = D_e/D_a$.

The average natural Pb, Cu and Zn content in the volcanic soil samples analyzed are presented in Table 32. No Pb was found in the volcanic soil profiles, while Cu and Zn were present in an important amount in all investigated soil profiles. These metal contents were considered (as blanks) when measuring the metals content in each diffusion experiment, and were discounted from all the obtained values.

Table 32: Natural Pb, Cu and Zn content (blanks) in the volcanic soil samples analyzed

Volcanic soil profile	Heavy metal content [mg/kg]		
	Pb	Cu	Zn
5-20 cm	0	60.4	97.9
20-40 cm	0	64.5	98.5
40-60 cm	0	63.9	99.3

The pH value of 4.5 was selectedinn the sense of the worst-case scenario, for analyzing the diffusion coefficients and transport of Pb^{2+}, Cu^{2+} and Zn^{2+} through a volcanic soil column, knowing that at this pH, the cations will adsorb only moderately as discussed before. This fact will promote maximum leaching of the selected cations in a volcanic soil landfill liner. Equation 55 was used for calculating the D_a and M_c coefficients.

The graphical results obtained for the diffusion of Pb^{2+}, Cu^{2+} and Zn^{2+} through a volcanic soil column filled with the 5-20 cm profile after 50 days at ph 4.5 are shown in Figure 63. In addition, the Cu^{2+} diffusion data from Figure 63 was plotted as indicated in Equation 55 (see Figure 64). The intercept with the ln(c) axis (i.e., 3.7547) will be ln(M_c) and the slope (i.e., -0.0359) will be equal to $1/(4 D_a t)$. As the time t from the diffusion experiment was known (50 days), D_a was easily calculated. All the calculated D_a and M_c coefficients at pH 4.5 and after 50 days diffusion experiments are presented in Table 33 for the different volcanic soil profiles. In addition, the Cl⁻ D_a and M_c coefficients were also calculated and included in Table 33.
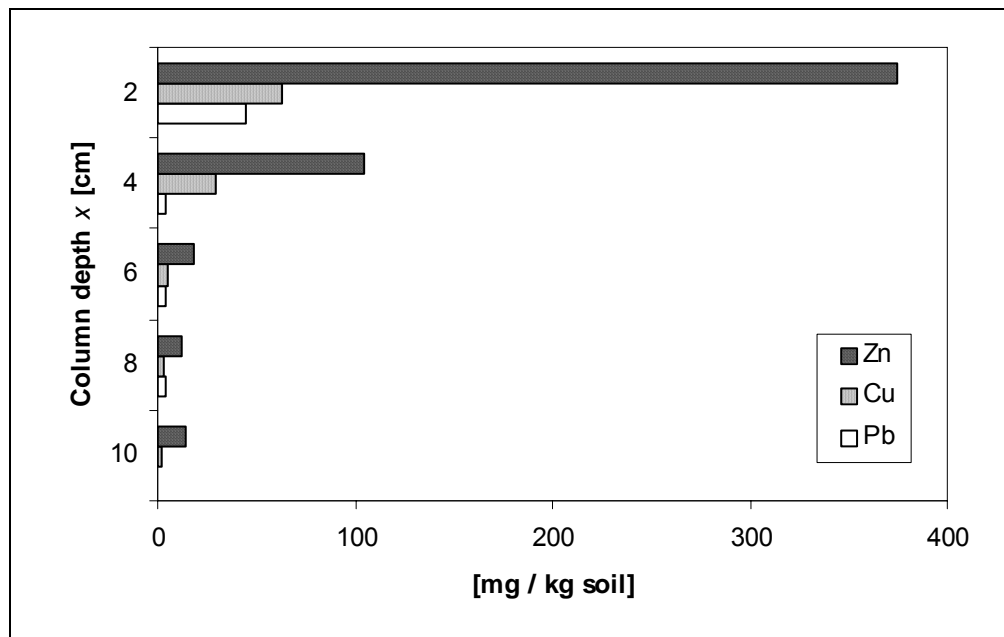
Figure 63: Diffusion of metal cations through a volcanic soil column filled with the 5-20 cm profile after 50 days at pH 4.5
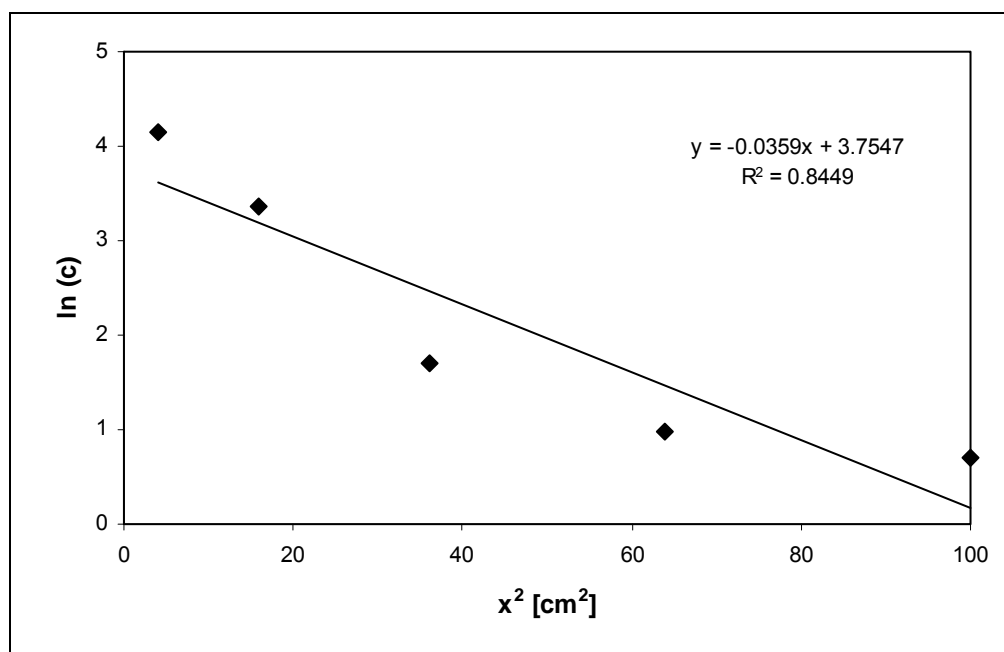
Figure 64: Cu^{2+} diffusion data plotted as indicated in Equation 55 (5-20 cm profile, pH 4.5, 50 days)

It can be clearly stated that, as expected, the average apparent diffusion coefficients (D_a) (for the three different soil profiles) are having the following order: $Cl^- > Cu^{2+} > Zn^{2+} > Pb^{2+}$. These results are in perfect agreement with the results presented in the heavy metals adsorption isotherms (see Figure 59 and Figure 60), where the Pb^{2+} cation was found to be the most adsorbable tested heavy metal onto the different volcanic soil profiles. In addition, previous results of heavy metals and chloride diffusion experiments through other mineral liners presented apparent diffusion coefficients of $1.2*10^{-7}$ and $5.6*10^{-7}$ cm^2/s, for Pb^{2+} and Zn^{2+}

respectively, while the Cl^- apparent diffusion coefficient was found to be $8.0*10^{-6}$ cm^2/s [14]. It seemed that the Pb^{2+} and Zn^{2+} apparent diffusion coefficients were about 10 times higher in the case of volcanic soil, although the Cl^- apparent diffusion coefficient was in the same order of magnitude.

The average D_a and M_c coefficients were used to estimate the breakthrough times of the different heavy metal cations and chloride through a 1 m deep volcanic soil liner using Equation 54, considering c = 1 mg/kg as the breakthrough initial concentration in the liner output. The breakthrough times are presented in Figure 65 and are clearly indicating that Pb^{2+} was the cation with the highest breakthrough time (i.e., 21.6 a).

Table 33: Calculated D_a and M_c coefficients at pH 4.5 and after 50 days of diffusion experiments with volcanic soil profiles

Pollutant	Volcanic soil profile	D_a [cm^2/s]	M_c [mg/kg]	R^2
Pb^{2+}	5-20 cm	$1.132 * 10^{-6}$	29.4	0.819
	20-40 cm	$1.022 * 10^{-6}$	36.0	0.920
	40-60 cm	$1.090 * 10^{-6}$	24.5	0.963
	Average	$1.082 * 10^{-6}$	30.0	
	SD	$5.549 * 10^{-8}$	5.7	
Cu^{2+}	5-20 cm	$1.612 * 10^{-6}$	42.7	0.845
	20-40 cm	$2.549 * 10^{-6}$	47.5	0.792
	40-60 cm	$3.233 * 10^{-6}$	24.0	0.608
	Average	$2.465 * 10^{-6}$	37.4	
	SD	$8.138 * 10^{-7}$	11.7	
Zn^{2+}	5-20 cm	$1.797 * 10^{-6}$	164.0	0.681
	20-40 cm	$1.072 * 10^{-6}$	345.1	0.891
	40-60 cm	$1.318 * 10^{-6}$	269.0	0.967
	Average	$1.396 * 10^{-6}$	259.4	
	SD	$3.689 * 10^{-6}$	90.9	
Cl^-	5-20 cm	$3.507 * 10^{-6}$	1769.8	0.962
	20-40 cm	$3.307 * 10^{-6}$	2044.5	0.969
	40-60 cm	$3.326 * 10^{-6}$	1827.1	0.957
	Average	$3.380 * 10^{-6}$	1880.5	
	SD	$1.106 * 10^{-7}$	144.9	

SD: Standard deviation

Zn^{2+} and Cu^{2+} presented similar breakthrough times from 10.2 and 8.9 a, respectively. These results are also in agreement with the adsorption isotherms data previously obtained, where no significant difference in the volcanic soil adsorption uptakes of Zn^{2+} and Cu^{2+} were found. In addition, the Cl^- breakthrough time was found to be 3.1 a, and as expected, was the lowest time, as no Cl^- adsorption occurred onto the volcanic soil. It clearly should be mentioned that pH 4.5 in landfill leachate may only be reached during the so-called acidogenic phase, which

occurs shortly (within months) after dumping of fresh waste containing biodegradables. Usually, the pH value of leachate is in the neutral or slightly alkaline region.
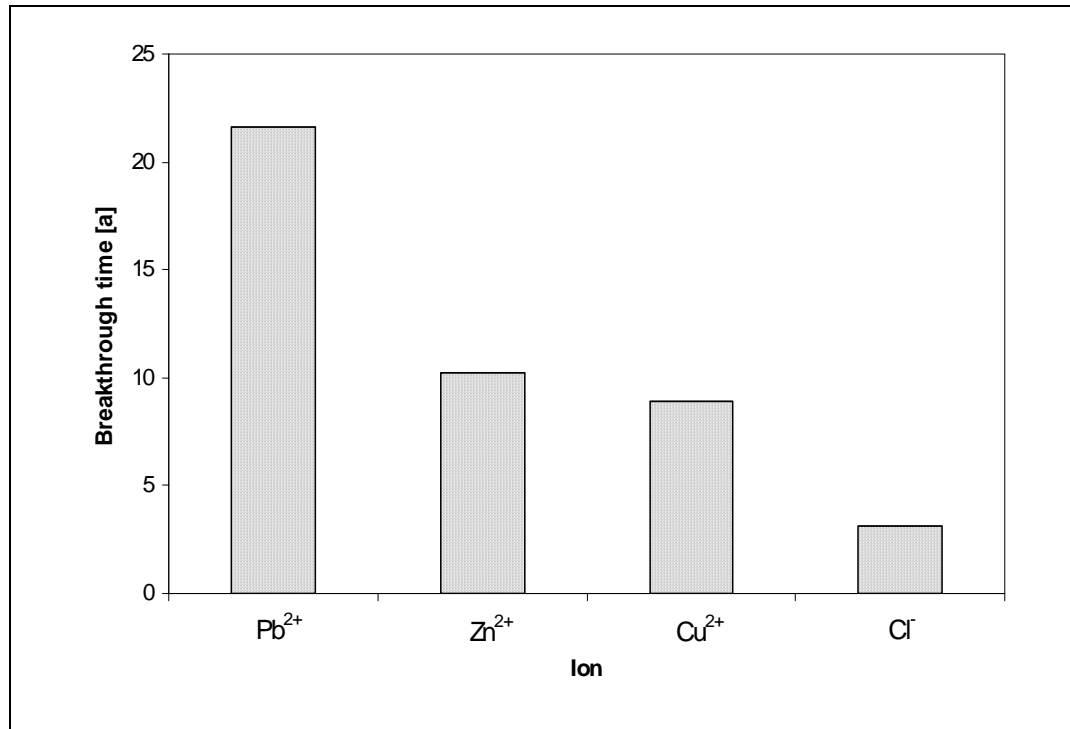
Figure 65: Ion breakthrough times for a 1 m deep volcanic soil liner at pH 4.5

The average tortuosity (ξ) of the volcanic soil columns was evaluated using Equation 56. The obtained average D_a coefficient for Cl⁻ was assumed to be the average D_e coefficient. Thus, knowing that the free-solution diffusion coefficient (D_0) for Cl⁻ is equal to $1.44*10^{-5}$ cm^2/s [191], the average tortuosity (ξ) for the volcanic soil columns was calculated to be 0.235. With this tortuosity (ξ) and the D_0 coefficients for all the heavy metal cations, the average R_A values were estimated as D_e/D_a, as shown in Table 34. As expected, the R_A factor was higher in the case of Pb^{2+} and was very similar while comparing the values for Cu^{2+} and Zn^{2+}. This fact corroborated the trend obtained with the adsorption isotherms, where Pb^{2+} was found to adsorb significantly more onto the volcanic soil profiles, compared with Cu^{2+} and Zn^{2+}.

Table 34: Average R_A factors for heavy metal diffusion onto a volcanic soil liner (D_0 coefficients obtained from [14],[192],[193])

Heavy metal	D_0 [cm^2/s]	D_e [cm^2/s]	D_a [cm^2/s]	R_A
Pb^{2+}	$1.799 * 10^{-5}$	$4.228 * 10^{-6}$	$1.082 * 10^{-6}$	3.91
Cu^{2+}	$1.220 * 10^{-5}$	$2.867 * 10^{-6}$	$2.465 * 10^{-6}$	1.16
Zn^{2+}	$7.179 * 10^{-6}$	$1.687 * 10^{-6}$	$1.396 * 10^{-6}$	1.21

4.5 Development of a stable ceramic adsorption material from volcanic soil

4.5.1 The foaming/sintering process

The volcanic soil investigated was collected in the surroundings of Temuco, in the south of Chile. The sample used in this work was the 20-40 cm soil profile. The natural soil was separated into two samples: the normal soil with a particle size fraction < 2 mm (Sample A, 76% of the total) and the particle size fraction < 63 µm (Sample B, 24% of the total). After preliminary trials, Sample B was selected for this study because of its excellent mixing properties while preparing the polyurethane foam and the excellent quality of the formed rigid foam. The foam produced when using the Sample A did not become compact, probably because of the large particle size range of the soil sample, and was therefore not considered for further experiments.

The selected volcanic soil fraction was mixed with the specific reagents presented in Annex V to form a volcanic soil-polyurethane foam. This compact and stable foam was then cut into slices (Figure 66) previous to the sintering process. The foam slices entered the sintering oven and were thermally treated using different temperature programs (Figure 67). These temperature programs were determined based on the flowing point temperature of the volcanic soil (i.e., 1415°C, see Annex VI) as the highest possible oven temperature. The thermal treatment was performed in the sintering oven Carbolite, type HTF 18/3, serial Nr. 4/01/1008 with a maximum possible temperature of 1800°C (Annex V).

Table 35: Volcanic soil foam mixtures (formulations) tested in this work

Compounds	Unit	E1	E2	E3	E4	E5	E6
Volcanic soil< 63 µm	[g]	48	72	48	60	48	60
Polyol P260	[g]	48	48	48	48	48	48
PC-Cat NP 40	[g]	0.15	0.15	0.15	0.15	0.15	0.15
DMEA	[g]	0.15	0.15	0.15	0.15	0.15	0.15
Tegostab B8433	[g]	0.15	0.15	0.15	0.15	0.15	0.15
Water	[g]	1.05	1.05	1.05	1.05	1.05	1.05
Lupranat M 20 A	[g]	60	60	60	60	60	60
Total mass	[g]	157.5	181.5	157.5	169.5	157.5	169.5
Volcanic soil recovery after thermal treatment	[%]	-	81.7	82.5	84.7	79.9	83.6

E: Experiment

Six different experiments with various volcanic soil foam-mixtures (E1-E6) were accomplished (Table 35). Related to the Polyol 260 mass, 100, 125 and 150% of volcanic soil was used in the foam formulations. The volcanic soil was mixed for 10 s with the reactants. The "foaming start time" occurred between 43 and 65 s in all of the experiments,

while the "free glue time" ranged between 105 and 136 s. Previous results for a zeolite-polyurethane foam also indicated mixing times of about 10 s, start times between 16 an 18 s, and free glue times between 90 and 95 s for foam formulations with zeolite in the range of 250, 400, 500 and 600% in relation to the used polyol mass [194]. These results indicate that the volcanic soil-polyurethane foam forms more slowly than the zeolite-polyurethane foam, although the rigidity of the final foam is very similar. The obtained compact and stable foam samples were cut into slices as shown in Figure 66, previous to their introduction in the sintering oven and their treatment under the selected temperature program.
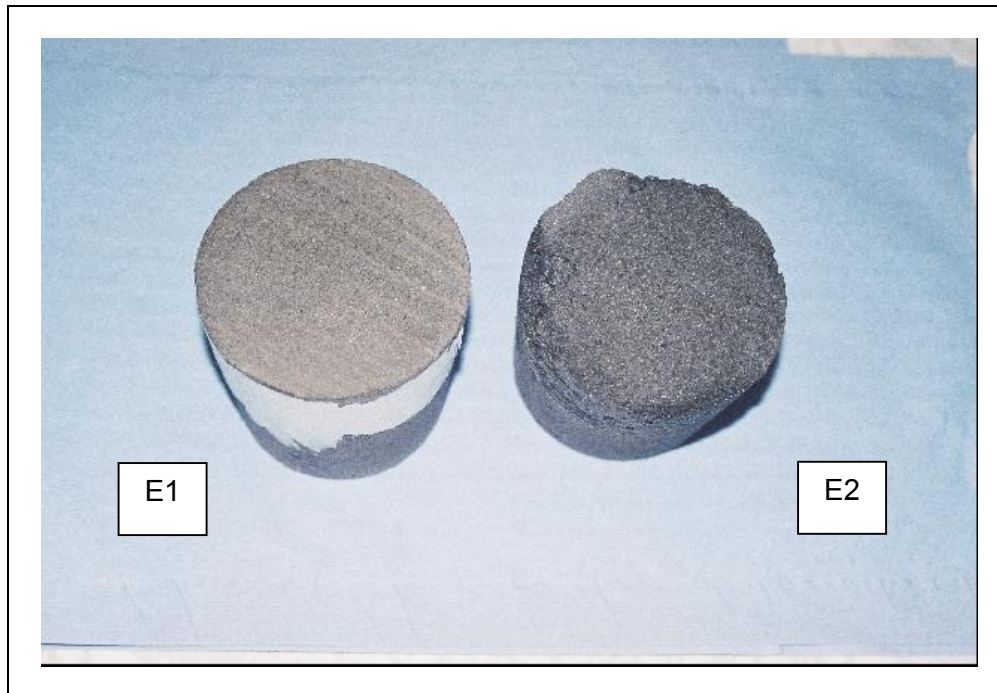
Figure 66: Foam cuts prior to thermal treatment in the sintering oven from the experiments E1 and E2

The first selected temperature program rapidly achieved the flowing temperature point of the volcanic soil (1415°C) during the treatment of the first foam mixture (E1), maintaining this temperature for one hour in the oven. As shown in Figure 68 (E1), this first experiment did not result successfully. In fact, no ceramic structure was obtained at this high temperature as the entire sample melted in the oven, suggesting that the selected maximum temperature was too high.

The second foam sample (E2) was then thermally treated at 1320°C for one hour, with a stop time of 15 min at 700°C. It is well known that polyurethane foams burn in the range between 150-600°C [194]. Therefore, the 700°C stop was thought of for a proper combustion of the polyurethane foam. The resulting ceramic sample is shown in Figure 68 (E2). A better porous ceramic structure was obtained, but its form was still different to the original foam sample slice, which suggests that the thermal treatment was still done at too high temperature.

The third foam sample (E3) was treated at 1250°C for one hour, with a 15 min stop at 700°C. A very much stable ceramic form was obtained (Figure 68, E3), suggesting that the maximum treatment temperature should be near 1200°C.
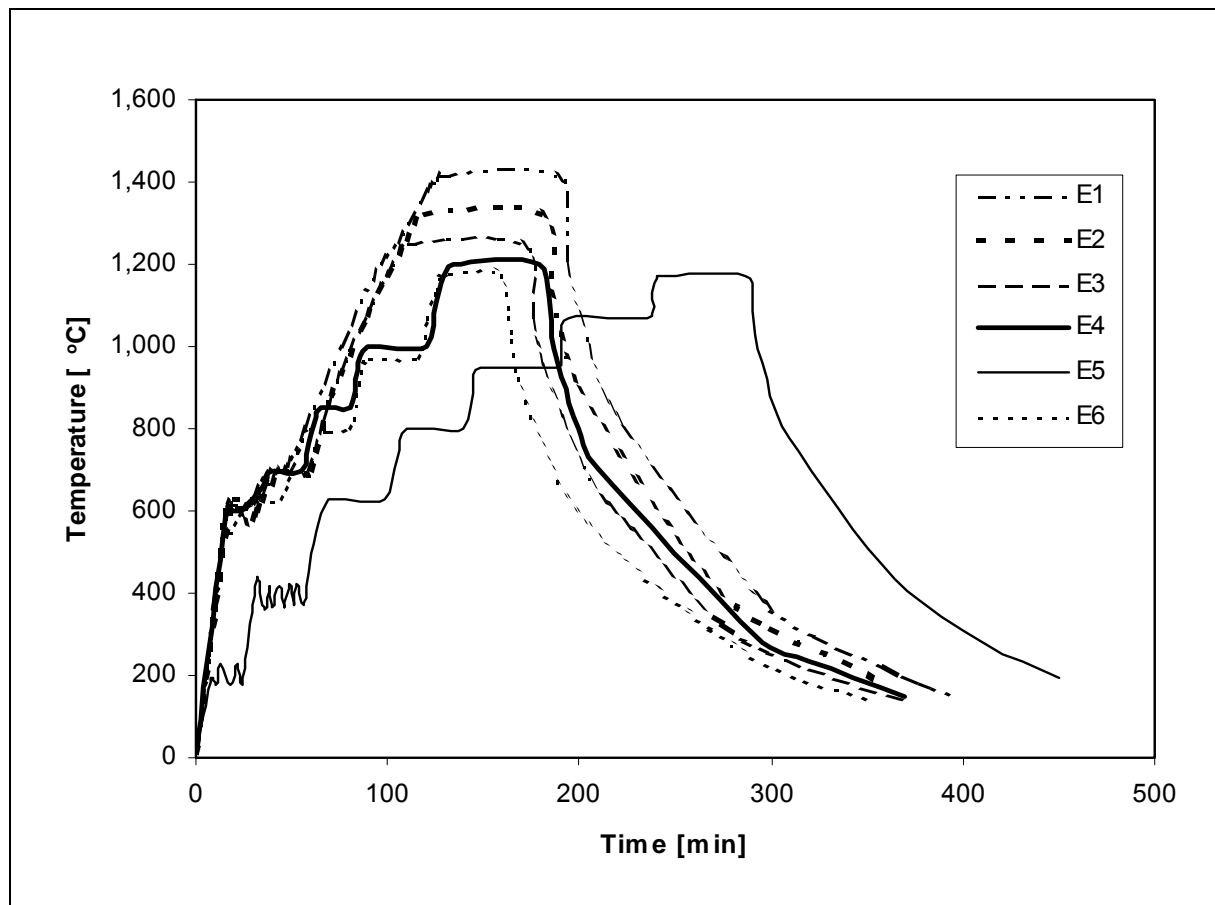
Figure 67: Sintering temperature programs for the experiments with volcanic soil (E: Experiment)

The fourth foam sample (E4) was then treated with a different temperature program. Stops at 700°C (15 min), 850°C (15 min), 1000°C (15 min) and 1200°C (45 min) were employed (see Figure 67). The resulted ceramic sample is shown in Figure 68 (E4). This was the most stable porous ceramic material obtained comparing all the performed trials done and the volcanic soil recovery was the highest of all the experiments (84.7%) (see Table 35).

In the fifth experiment (E5), the selected temperature of the program was slowly increased compared to E4. Therefore, a temperature program with stops at 200°C (15 min), 400°C (30 min), 630°C (30 min), 800°C (30 min), 950°C (40 min), 1070°C (40 min) and 1170°C (45 min), with 1170°C being the maximum temperature, was selected. The 200°C stop was thought to slow down burning of the organic matter of the soil and to properly conserve the resulting ceramic structure. The obtained ceramic material (Figure 68, E5) however clearly shows that the sample was treated for too long time in the sintering oven (300 min until starting the cooling process), which made the formed ceramic structure unstable.
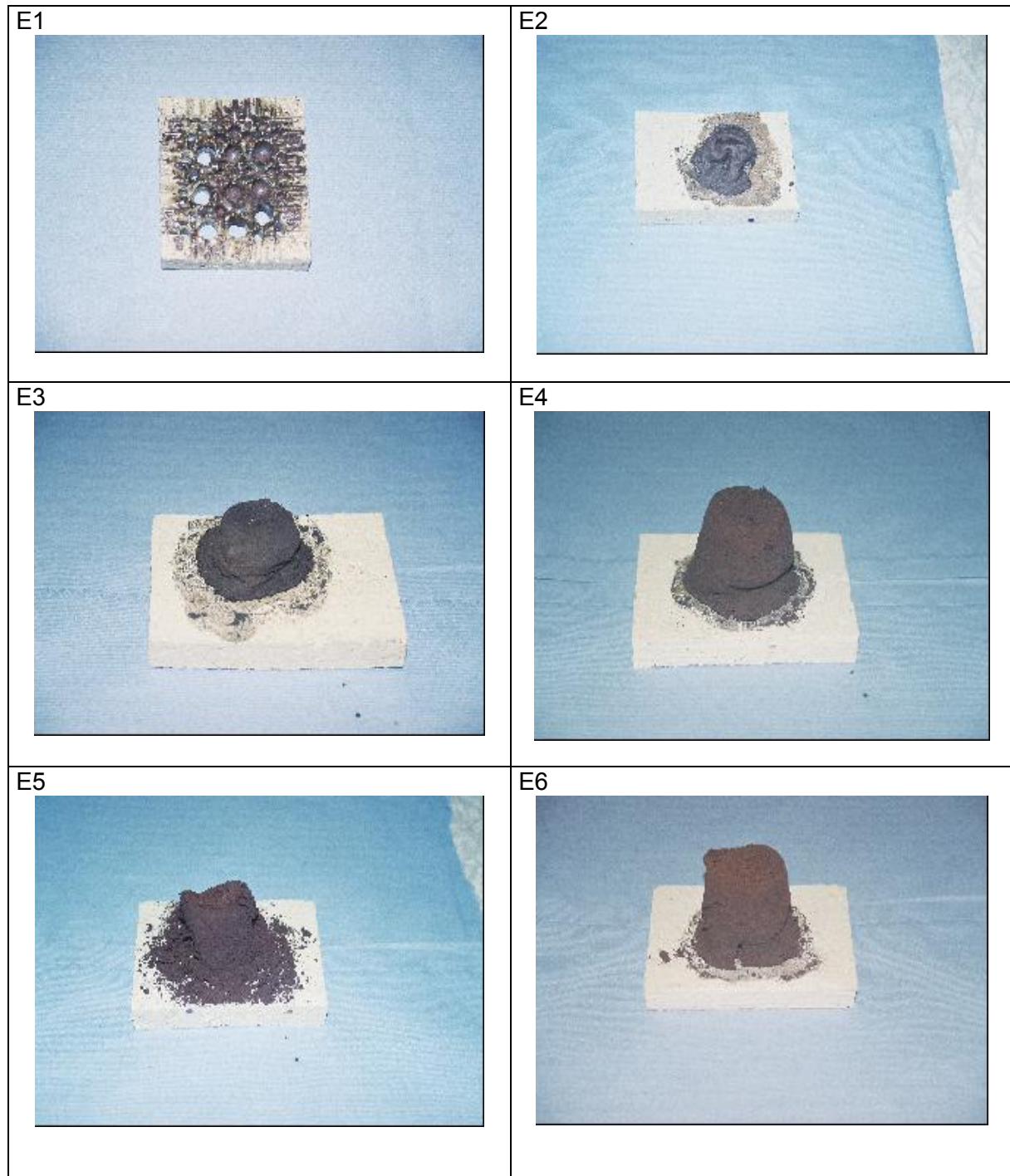
Figure 68: Porous ceramic material obtained from the experiments (E1-E6) with volcanic soil

The last experiment (E6), basically was a repetition of E4 but with a lower temperature profile. The temperature stops were made at 630°C (15 min), 800°C (20 min), 970°C (25 min) and 1170°C (30 min) as the maximum temperature. The total heating time was 159 min, almost half of the time compared with experiment E5. The ceramic structure obtained was comparable with E4. As the temperature programs apllied were almost the same, a reproducible ceramic product was achieved by both experiments. In both successful experiments (E4 and E6), 60 g of volcanic soil were used in the foam mixture (i.e., 125%

related to the polyol mass). It seems that this foam formulation (with 35.4% volcanic soil) is the most suitable and reproducible one for the thermal treatment proposed.

For industrial use of volcanic soil as a natural adsorbent in advanced or tertiary wastewater treatment facilities, it is necessary to aplly the soil in a compact and stable solid form to prevent dissolution, attrition losses and sludge formation. With the suggested process, a porous ceramic material is obtained, were the Si and Al sites of the original volcanic soil should be activated during the thermal treatment, because of the combustion and elimination of the organic matter in the soil. Comparing the obtained volcanic soil ceramic material with previous works that used zeolites and aluminum oxide as raw material (Figure 69), it is shown that the porous ceramic structure obtained in this work is comparable, and in some cases even better structures were developed with volcanic soil.

It is interesting to note that the used zeolite had an Al_2O_3 content of 11.5 to 13.1% [194] (compared to 20.8% in the volcanic soil), a situation that could be responsible for the higher temperature program needed in this work to sinter the sample in the oven. This fact would affect of course the energy consumption in a full scale sintering process. Nevertheless, the cost of the zeolites in the European market is around € 80/ton in its natural form (not milled), while the volcanic soil main natural size fraction is already smaller than 2 mm. Due to the fact that the zeolite particle size used in the development of a ceramic material was less than 70 μm [194], the milling cost will raise the total energy costs of the process (milling and sintering). This is not the case for volcanic soil, where the low sieving costs for recovering the < 63 μm fraction, buffer the total energy costs of the process when comparing them with zeolites.
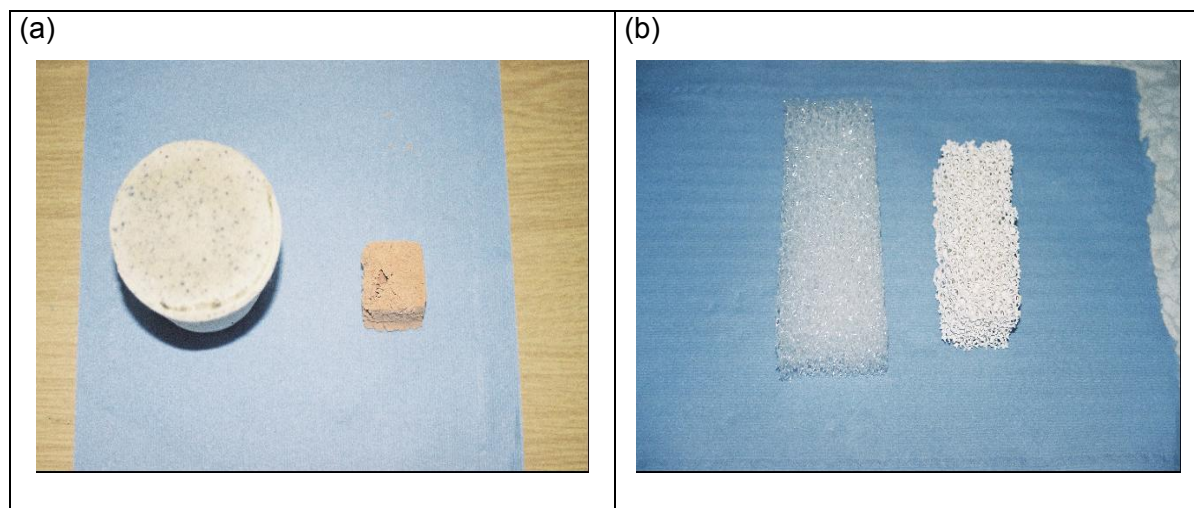
Figure 69: Foam and ceramic material obtained with zeolite (a) and aluminum oxide (b)

The proposed foaming-sintering process of volcanic soil based on recycled PET-polyols is an interesting as well as promising method to produce stable porous ceramic adsorption material with a possible use in advanced or tertiary wastewater treatment facilities as well as filling material in reactive walls (funnel & gate systems) for cleaning up groudwater. Particularly, an application in pulp and paper mills or leather tanneries effluent treatment, as

well as in landfill leachates depuration should be carefully studied. Moreover, the foaming process based on recycled PET-polyols will positively affect the process costs and partially may help to manage PET residues.

4.5.2   Adsorption isotherms for selected pollutants on ceramic material

2,4-dichlorophenol (2,4-DCP), pentachlorophenol (PCP) and Cu^{2+} were the selected pollutants to perform the adsorption isotherms with ceramic volcanic soil, for comparison purposes. Regarding the adsorption capacity of the ceramic material, it is clearly stated that there was a significant improvement in the adsorption capacity for both chlorophenols selected (2,4-DCP and PCP). In fact, as shown in Figure 70 and Figure 71, using the ceramic volcanic soil there was an increase in the adsorption capacities for both chlorophenols, from 0.2 to 0.8 mg DCP/g soil and from 0.5 to 1.2 mg PCP/g soil, respectively, compared to natural volcanic soil as adsorbent. Moreover, the maximum Langmuir adsorption values b increased from 0.736 to 4.570 mg/g for 2,4-DCP and from 2.81 to 33.90 mg/g for PCP (Table 36). The adsorption capacity of PCP onto natural and ceramic volcanic soil is higher than that of 2,4-DCP. As discussed in Chapter 4.3.1, the higher log K_{ow} value of PCP compared to that of 2,4-DCP makes PCP to have a greater affinity for the organic matter present in the natural soil, increasing its adsorption capacity through this mechanism. Moreover, the lower solubility of non-ionic PCP compared to that of non-ionic 2,4-DCP, would also indicate an affinity of 2,4-DCP to remain in the liquid phase, decreasing its adsorption capacity. Another simple reason is the higher molecular weight of PCP (MW = 266.3 g/mol), compared to 2,4-DCP (MW = 163.1 g/mol). In the case of the ceramic volcanic soil, the adsorption increment for both chlorophenols can probably be related with the liberation of active sites originally coated by the burned organic matter. Another reason may be due to the chlorophenols pK_a values. In fact, for PCP (pK_a = 4.7) at pH 6.0 the anionic form (phenolate) would be the most important. On the other hand, in the case of 2,4-DCP (pK_a = 7.9), at pH 6.0 the non-ionic form will still be the most important fraction. As the increment in the PCP adsorption capacity is higher than that of DCP, and there is no organic matter in the ceramic material after the sintering process, only electric charges would explain this behavior. It is supposed that at pH 6.0 the ceramic soil surface would be slightly positive charged, suggesting that for the PCP anion electrical charges would enhance the adsorption capacity onto the ceramic volcanic soil. This would indicate a change of the original average zero point charge pH (pH_{ZPC}) of the natural soil (i.e 5.5), suggesting a pH_{ZPC} value higher than 6.0 for the ceramic material. The inverse phenomenon has already been described to occur when coating synthetic allophanic materials with humic acids, reducing the isoelectric point from 8.6 to near 3.0 [32].

As discussed before, the total phenolic compounds uptake in volcanic soil can range between 4.5 and 14.5 mg/g for natural and acidified volcanic soil in fixed bed trials, respectively [11]; while in batch trials the Langmuir b values ranged between 10.8 and 18.8 mg/g (see Table 28). The chlorophenols uptake obtained onto the volcanic ceramic material was comparable to these results. As already discussed, the adsorption of PCP onto activated

carbon is around 160 mg/g at pH 8.5 for *C** values around 10 mg/L [19], which is a very high value compared with the ceramic volcanic soil. Nevertheless, the sorption of phenol and *p*-chlorophenol onto different cheaper adsorption materials (coal, shell, wood and rubber) can range between 20 – 80 mg/g and 30 – 110 mg/g, respectively, for *C** values around 10 mg/L [3], which are comparable to those of PCP adsorption onto the ceramic volcanic soil.
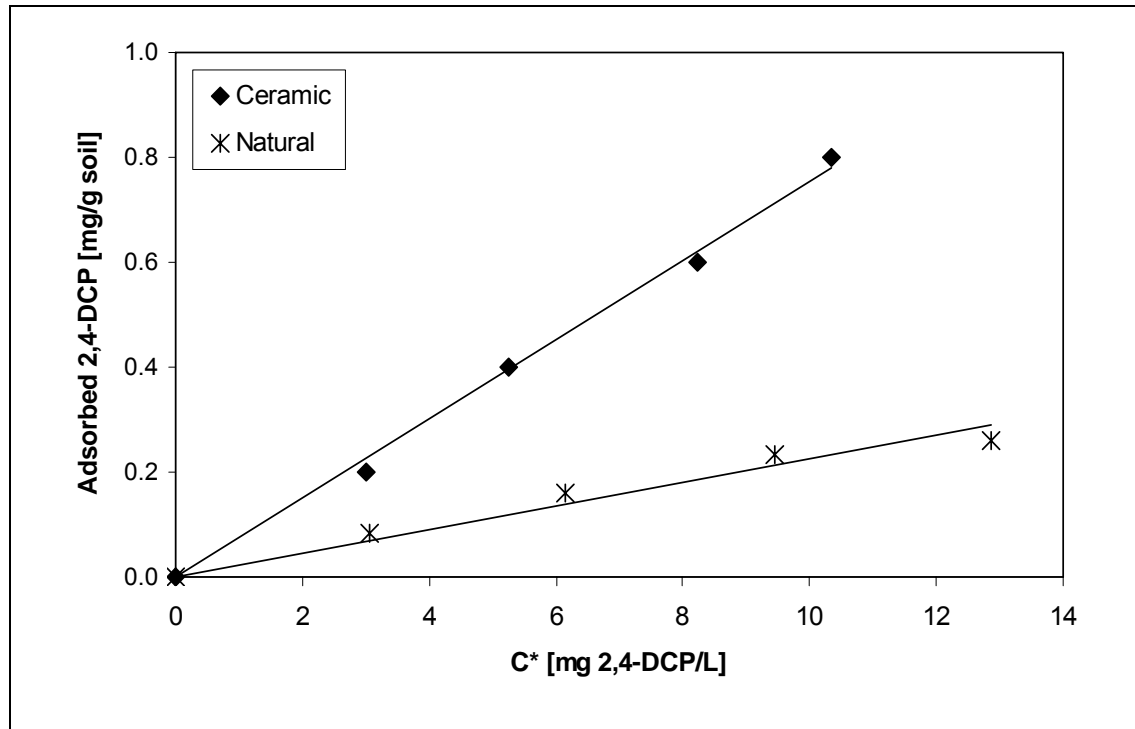

Figure 70: 2,4-DCP adsorption isotherms onto natural and ceramic volcanic soil
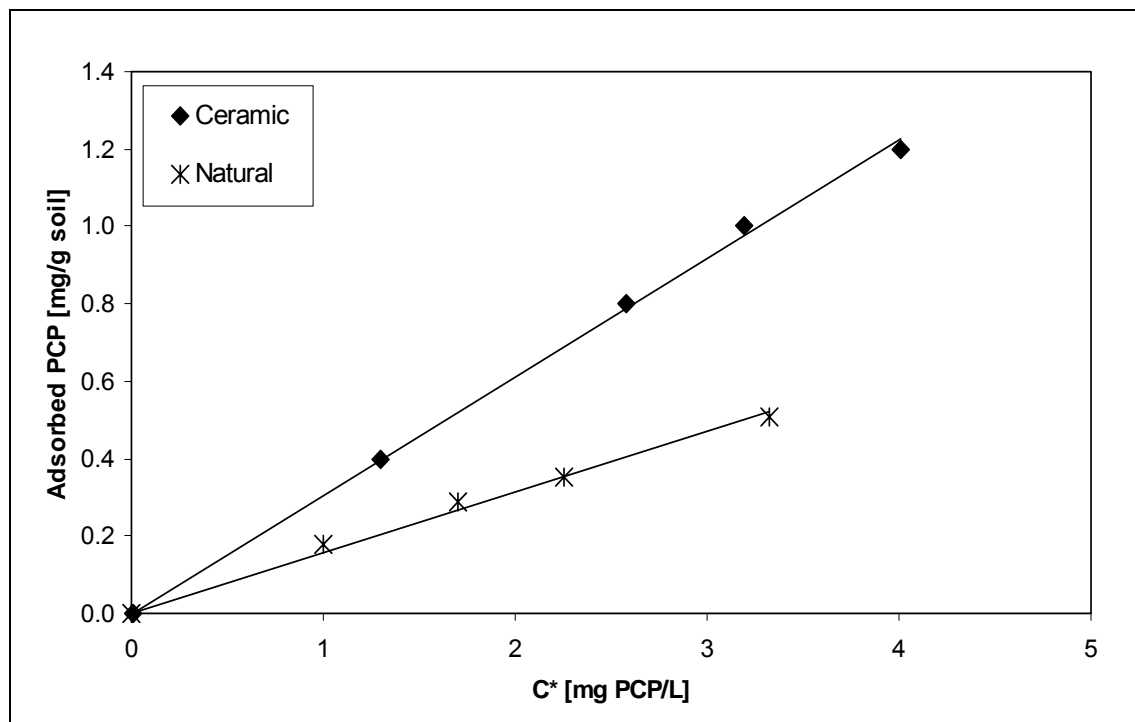
Figure 71: PCP adsorption isotherms onto natural and ceramic volcanic soil

The Freundlich model seems to fit the experimental data of Figure 70 and Figure 71 properly (see Table 36). As discussed in Chapter 4.3.1, for the adsorption of different substituted phenols onto activated carbon, the Freundlich model k_F constant varies between 0.3 and 2.2, which u is an empirical indicator for how much solution (L) is possible to treat with one gram of adsorbent material, while the n constant varies between 0.06 and 0.3 [18]. In our case the Freundlich k_F value moved in the lower range of the activated carbon. In addition, although there was a low R^2 for some Langmuir fits in the case of PCP (Table 36), it is clearly shown that the b values increased significantly for the ceramic volcanic soil, suggesting also that the increment in the adsorption capacity is at least 6 times for 2,4-DCP and 12 times for PCP compared to natural volcanic soil.

In the case of the Cu^{2+} adsorption, no significant enhancement effect could be observed in the adsorption capacity of the ceramic volcanic soil compared with the natural one (Figure 72 and Table 36). The adsorption values obtained under the experimental conditions used were about 4.0 mg Cu^{2+}/g soil for both, natural and ceramic soil, indicating that the novel ceramic material does not clearly adsorb more Cu^{2+} than the natural sample tested. The adsorption process of heavy metals in mineral soils is mainly regulated by electrical charges and cationic exchange capacity (CEC). An elimination of the organic matter in the sintering process should in principle liberate some more active mineral sites and enhance the cation exchange capacity. Nevertheless, as suggested before, a slightly movement in the pH_{ZPC} of the ceramic soil compared to the natural sample would have a negative effect on the adsorption capacity, as the ceramic soil surface would be only moderately negative charged at pH 7.5. On the other hand, at pH 7.5 the natural soil surface would be strongly negative charged, being capable to adsorb more heavy metal cations.
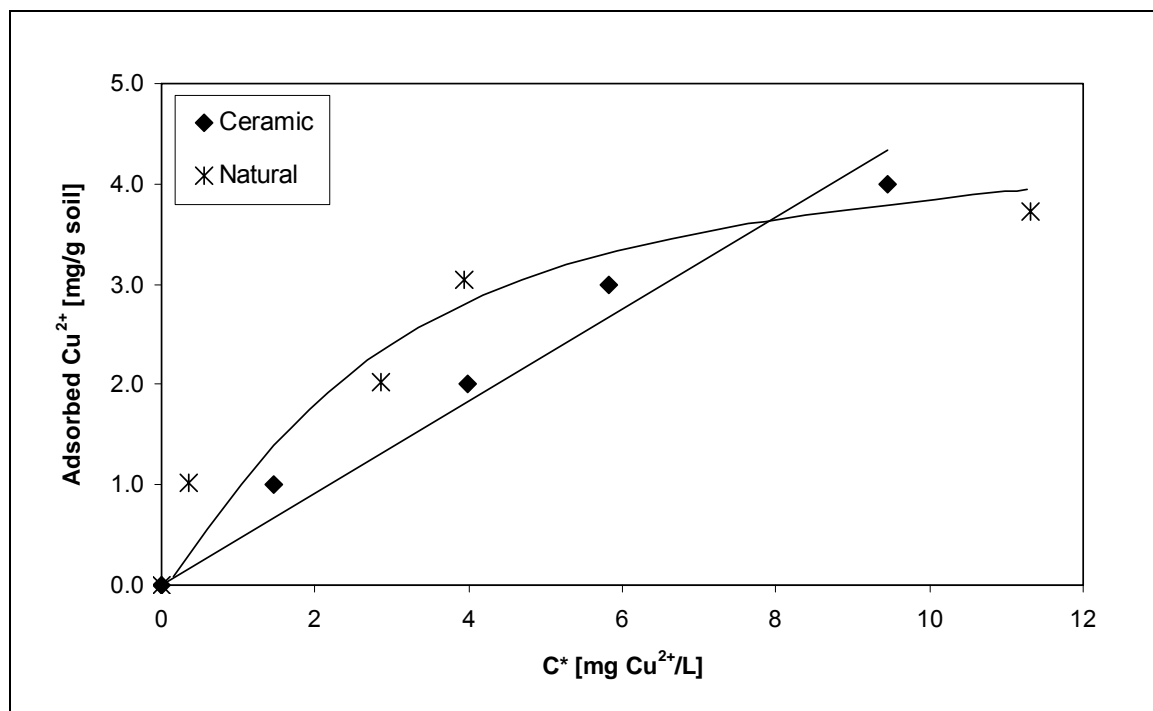
Figure 72: Cu^{2+} adsorption isotherms onto natural and ceramic volcanic soil at pH 7.5

As already discussed in Chapter 4.4.1, the maximum Cu^{2+} uptake on natural Croatian zeolite clinoptilolite was 26.0 mg/g [23]. In addition, values of the Langmuir model b parameter of 5.91 and 50.5 mg/g were obtained for natural and synthetic zeolites for Cu^{2+} uptake [24]. All these values are comparable to those of natural and ceramic volcanic soil. In fact, in our case Langmuir b values of 4.30 and 9.51 mg Cu^{2+}/g were obtained for natural and ceramic volcanic soil respectively, which would indicate a slight increment in the adsorption capacity of the ceramic material (about 2 times) compared with natural soil and zeolites. In addition, Cu^{2+} uptakes onto different activated carbons between 20.33 and 27.32 mg/g have been reported by [18] and are in the same order of magnitude as that of volcanic soil.

Table 36: Derived Langmuir and Freundlich model parameters for the adsorption processes onto the ceramic material

Pollutant / Adsorbent	Langmuir			Freundlich		
	b	k_L	R^2	n	k_F	R^2
	[mg/g]	[L/mg]		[-]	$[(L/mg)^{(1/n)}*(mg/g)]$	
2,4-DCP						
Natural soil	0.736	0.084	0.953	1.395	0.066	0.984
Ceramic material	**4.570**	**0.014**	**0.577**	**1.100**	**0.061**	**0.996**
PCP						
Natural soil	2.810	0.111	0.648	1.161	0.280	0.981
Ceramic material	**33.90**	**0.009**	**0.250**	**0.984**	**0.313**	**0.998**
Cu^{2+}						
Natural soil	4.30	0.523	0.944	2.608	1.530	0.985
Ceramic material	**9.51**	**0.076**	**0.892**	**0.753**	**0.748**	**0.993**

4.6   Possible adsorption mechanisms in volcanic soil

Different adsorption mechanisms are supposed to be involved in the color (lignin and polymerized tannins), phenolic compounds, chlorophenols and heavy metals uptake onto volcanic soil.

In the case of persistent or recalcitrant organic pollutants (like lignin and polymerized tannins, phenolic compounds and specific chlorophenols), several studies indicate that they can be incorporated into the soil organic matter (SOM) or dissolved humic materials after treatment with various oxidoreductases or metal oxides [195],[196],[197],[198]. As the products of lignin decomposition, i.e., humic constituents, are aromatic and posses a variety of functional groups they may be involved in the formation of covalent bonds between pollutants and organic matter [52],[199],[200]. In addition, fulvic acids contain stable free radicals that can also contribute to the incorporation of xenobiotics. The formation of free radicals involves hydroxyl groups of phenolic moieties that are present in humic materials, as well as the quinone and amine components of humus. Nevertheless, the low concentration of free radicals occurring in fulvic acids can hardly contribute to an extensive binding observed in

most studies [198]. This fact indicates, in the case of chlorophenols, additional free radicals can be transferred to humic materials from phenoxy radicals generated by enzymatic oxidation of the substrates [201]. For instance, a free radical reaction between 2,4-dichlorophenol (2,4-DCP) and humic acid resulted in the formation of C-C and O-C linkages [202], while the 4-chlorophenol transformation was enhanced at low humic acid concentrations [198]. Therefore, it seems that the adsorption process of chlorophenols (and maybe also other substituted phenolic and lignin compounds) onto the soil surface is not only a chemical but also a biochemical process, always under the presence of an important SOM fraction. Oxido-reductive processes involving enzymes like peroxidase, laccase, tyrosinase and oxigenase in the presence of humic acid will produce the oligomerization of the pollutants or their binding to the SOM [198]. Recently, the soil enzymatic presence and activity of laccase, manganese peroxidase, dehydrogenase and acid phosphatase in the studied volcanic soil under different chlorophenols contamination was established [203]. The soil presented enzymatic activity for all the mentioned enzymes; nevertheless, the enzyme activities had different responses to different chlorophenols contamination level. The long-term experiments pointed out that the enzymatic activities were affected in a different way, according to the concentration of PCP added. No inhibitory effect on the manganese peroxidase specific activity was observed during all the incubation period at different contamination levels of PCP (1, 10 and 100 mM), whereas the acid phosphatase specific activity was not affected only at a contamination level of 1 mM PCP. Moreover, laccase and dehidrogenase specific activities were negatively affected even at the smallest concentration of PCP [203]. These preliminary results are indicating that the manganese peroxidase specific activity is able to play an important role during the adsorption process of chlorophenols onto the studied volcanic soil.

In addition, a simple analytical test was performed in order to appreciate any difference in the spent volcanic SOM (saturated with the Kraft mill effluent pollutants) compared with a fresh non-contaminated volcanic SOM. Humic and fulvic acids were extracted from a spent acidified volcanic soil column after 1 year of finishing the adsorption breakthrough experiments described in Chapter 3.4.1. For comparison purposes, the same procedure was done with a fresh acidified volcanic soil column (not-contaminated). Several authors indicate that the humic and fulvic acids absorbances at 400 to 465 nm (E_4) and 600 to 665 nm (E_6) are a characteristic parameter for both compounds [32],[204],[205],[206],[207]. Generally, the E_4/E_6 ratio is expected to decrease with increasing the density and condensed aromatic rings content of the acids. In addition, the ratio is expected to increase with an increase in oxygen content and acidity [205],[207]. Therefore, the absorbances of the purified humic and fulvic acids from the contaminated and non-contaminated volcanic soil columns were measured at 440 nm (E_4) and 640 nm (E_6) and expressed as the E_4/E_6 ratio. For the non-contaminated volcanic SOM, average E_4/E_6 ratios of 3.66 ± 0.10 and 10.73 ± 0.65 were found for the humic and fulvic acids, respectively. In the case of the contaminated volcanic SOM, E_4/E_6 ratios of 4.21 ± 0.15 and 12.15 ± 0.73 were determined. It seems that there is a weakly increase in the E_4/E_6 ratios for humic and fulvic acids present in contaminated SOM. This fact could indicate a slight oxygen increase, maybe caused by the adsorbed phenolic compounds and

the subsequent decrease in the specific density, caused by the adsorbed pollutants. Therefore, it is possible to suggest, that the sorption process onto the dissolved organic matter of different phenolic compounds can be expressed as presented in Equation 57, as a function of the dissolved organic carbon concentration (DOC) [208].

$$DOC + PC \underset{k_2}{\overset{k_1}{\leftrightarrow}} DOC - PC \tag{57}$$

Where *DOC* is the dissolved organic carbon present in the volcanic soil, *PC* are the phenolic compounds to be adsorbed, *DOC-PC* is the complex formed after adsorption, and k_1 and k_2 are the adsorption and desorption rate constants, respectively. In the case of equilibrium, the adsorption coefficient is expressed by the ratio of the rate constants (Equation 58), where K_{oc} is the carbon-normalized partition coefficient.

$$K_{oc} = \frac{k_1}{k_2} \tag{58}$$

For 4-fluorophenol, 4-bromophenol, 4-iodophenol, 3-methoxyphenol and different chlorophenols, methylphenols, ethylphenols and chloromethylphenols, the log K_{oc} values were determined to range between 2.0 and 3.0 in the case of the adsorption process onto pure humic acid, while higher log K_{oc} values between 2.3 and 5.9 were obtained for the adsorption of the same pollutants onto protein bovine serum albumin. These results indicated that the K_{oc} value, interpreted as the adsorption rate/desorption rate ratio, reached a minimum value of 100 (3-methoxyphenol) and a maximum value of 1,000,000 (pentachlorophenol) for all the phenols studied, at an acid pH value where the main compounds were in their non-ionic form [208].

In the case of heavy metals, metal cations can adsorb onto the SOM, as well as onto the clay mineral fraction of the volcanic soil. The metal ion becomes adsorbed onto a complex-forming group in the soil surface (mostly onto organic coatings). Normally six extraction steps have been used to define the phases retaining heavy metals. The stability of bonds increases and the mobility of metals decreases in the following order: 1) water soluble phase, 2) exchangeable cations, 3) carbonatic fraction, 4) oxidic fraction, 5) organic fraction and 6) residual fraction [14],[107]. In the case of volcanic soil, the exchangeable (2), oxidic (4) and organic fractions (5) were expected to be the most important fractions involved in the adsorption process of heavy metal cations. As no carbonate was measured in the volcanic soil, no carbonatic fraction (3) is expected. Moreover, as the adsorption process of the metal cation is pH dependent, a simple adsorption model involving clay (oxides and exchangeable cations) and organic matter (SOM) is proposed. Adsorption equilibrium that is in principle similar to oxide surfaces can describe the extent of metal affinity to soil surfaces. As proposed by [209], an adsorption competition between protons (H^+) and metal cations (Me^{2+}) will occur onto the soil surface (Equation 59 and 60).

$$S + H^+ \leftrightarrow S\text{-}H \tag{59}$$

$$S + Me^{2+} \leftrightarrow S\text{-}Me \text{ or } 2S + Me^{2+} \leftrightarrow 2S\text{-}Me \tag{60}$$

Where S are the free, $S\text{-}H$ are the proton occupied, $S\text{-}Me$ and $2S\text{-}Me$ are the metal occupied soil sites. As there is a competition involving protons, the adsorption process will be dependent on the pH value. According to Equation 59 and 60, the corresponding equilibrium constants K_H (proton affinity) and K_{me} (metal affinity) can be defined, under the assumption that the affinities of hydrogen ion and metal ions toward all sites are identical (Equations 61 and 62) [209].

$$K_H = \frac{[S-H]}{[S][H^+]} \tag{61}$$

$$K_{me} = \frac{[S-Me]}{[S][Me^{2+}]} \tag{62}$$

For Cu^{2+} adsorption onto humus-kaolin complexes, it was observed that for a constant pH value, a higher log K_{me} (i.e., 5.2) was obtained for a synthetic soil composed of low molecular humic acids and kaolin. The log K_{me} for the Cu^{2+} adsorption onto pure kaolin was only 4.3, the same value obtained for a synthetic soil composed of a reference fulvic acid and kaolin [209]. These results indicate that although there is an adsorption affinity of Cu^{2+} with kaolin (clay fraction), the presence of humic acid (as occurs in natural volcanic soil) can enhance up to ten times the measured adsorption yield.

4.7   Practical aspects for large-scale industrial use of volcanic soil

4.7.1   Wastewater treatment considerations

In principle, acidified but also natural volcanic soil can be considered for industrial use in bleached Kraft mill effluent treatment, as the adsorption rates have only one order of magnitude difference. For an average water consumption of 30 m³/ton pulp and an average pulp production of 1,000 ton pulp/day in Chilean facilities, water consumption (and discharge) of 20,833 L/min will be achieved. Dividing this water flow rate by the adsorption rates for volcanic soil (last column in Table 29), the volcanic soil amounts per day, presented in Table 37, will be necessary. Moreover, considering that with an acid wash 31% of the adsorption capacity of the spent volcanic soil can be recovered, the real volcanic soil necessary amount will be reduced significantly (Table 37). If we select, for example, the scenario of experiment 3 and consider the use of acidified volcanic soil with acid washing after the volcanic soil exhaustion with color and phenolic compounds, a minimum of 8 ton/d of volcanic soil, as well as 8 ton/d of sand as support material will be necessary. As the pulp industry is one of the most water consuming Chilean industries, this example could be considered as an extreme scenario. Other industrial sectors like chemical industries need and discharge less water and will need significantly smaller amounts of volcanic soil as an adsorbent material. Moreover, as the pulp industry has normally a positive energy balance, the effluent stream could be

concentrated by simple evaporation stage. A clean condensed water stream would be recovered and a volcanic soil column adsorber or pile could then treat a concentrated effluent stream.

The calculated maximum amount of exhausted volcanic soil that can be used in the selected cement plant as an alternative clay material was found to be 278 ton/d (see Chapter 4.8.2, Table 45); suggesting that the resulting amount of spent volcanic soil which comes from wastewater treatment in the pulp industry could be satisfactorily managed in such facilities. It is supposed that no contamination will take place in the sand surface; therefore the sand could be sieved and reused in the same process. In addition, a biological natural attenuation process of the spent volcanic soil will be also possible (see Chapter 4.8.1) coupled with a sanitary landfill disposal. Preliminary results indicate that not more than 15% of the adsorbed phenolic compounds and color from bleached Kraft mill effluent can be desorbed from volcanic soil with water even at temperatures up to 60°C [143], suggesting that no leaching problems will affect a landfill disposal of the exhausted volcanic soil.

Table 37: Necessary volcanic soil amounts for a full scale Kraft mill wastewater treatment plant. Estimates based on experiments described in Chapter 3.4.1, Table 13 and Chapter 4.2.3.3, Table 29

Experiment (from Chapter 3.4.1, Table 13)	Pollutant	Type	Volcanic soil	
			Necessary amount [ton/d]	
			Without acid washing	With acid washing
1	Color	Natural	158	109
		Acidified	8	5
1	Phenolic Compounds	Natural	81	56
		Acidified	9	6
2	Color	Natural	86	59
		Acidified	5	3
2	Phenolic Compounds	Natural	40	28
		Acidified	12	8
3	Color	Natural	89	61
		Acidified	8	5
3	Phenolic Compounds	Natural	65	45
		Acidified	11	8

Considering the use of the porous ceramic adsorption material (see Chapter 4.5) for pulp industry wastewater treatment, the necessary amounts will be comparable to that for the acidified volcanic soil or even smaller. In fact, the adsorption capacity of this material is at least 6 times (for 2,4-DCP) or 12 times (for PCP) higher compared to the natural volcanic soil, and no sand will be required as structure material. The contaminated ceramic material managing options will have to be studied carefully.

4.7.2   Groundwater treatment considerations

Typical reactive wall funnel and gate process engineering is described in Annex VII. In the case of a volcanic soil reactive wall for groundwater remediation, it is of most importance that the system manages to treat the entire contaminated plume. Since groundwater flow directions can vary, it is extremely important that these fluctuations be accounted for. Secondly, the residence time of all the pollutants in the reactive wall must be sufficient to achieve the desired reduction in the contaminant concentration. Lastly, the ratio of cutoff walls to reactive walls in a funnel and gate system should be optimized to minimize costs [210]. One of the most critical factors in reactive wall design is the relationship between residence time of contaminated groundwater in the reactor and the rate of contaminant degradation that occurs within the reactor. Typical reactive wall K_f values are about $4*10^{-5}$ m/s. This value could be reached by mixing the volcanic soil with sand, as structure material, or by using the developed volcanic soil ceramic material as the filling reactive structure. Moreover, considering a flow gradient (i) of 0.02 m/m and a volcanic soil/sand mixture porosity (ε) of 0.5, the internal pore filter velocity (u_f) will be given by Equation 63.

$$u_f = \frac{K_f * i}{\varepsilon} \text{ [m/s]}$$ (63)

An internal pore filter velocity (u_f) of $1.6*10^{-6}$ m/s will be obtained. Therefore, a reactive wall flow rate of $1.6*10^{-3}$ L/s will be achieved per square meter volcanic soil cross-section of the gate. "Normal" chlorophenol groundwater contamination levels are about 200 µg/L; considering a 2,4-DCP and PCP concentration of 100 µg/L each in the groundwater stream input, and a desired retention yield of 99% in the volcanic soil, an output concentration of 1 µg/L of each chlorophenol will leave the reactive wall gate. The 2,4-DCP and PCP rate to be adsorbed will be $1.58*10^{-4}$ mg/s*m^2 for each chlorophenol. As the maximum uptake capacity of volcanic soil to retain 2,4-DCP and PCP is 0.736 and 2.812 mg/g, respectively (see Table 30), a total usage rate of $2.71*10^{-4}$ g/s*m^2 (g volcanic soil per second and square meter gate section) will be needed. This corresponds to a necessary amount of 8.55 kg volcanic soil per m^2 gate section and year. The final design of the reactive wall will involve the total cross-section of the gate and the volcanic soil exchange. Considering a gate cross-section of 10 m^2, the needed volcanic soil will be $2.71*10^{-3}$ g/s (or 85.5 kg/a). Defining a volcanic soil change-out of 10 years, 855 kg will be needed initially, and considering a volcanic soil average bulk density of 1.2 kg/L, the equivalent volcanic soil gate width will be 7.1 cm. A calculated average hydraulic residence time of 0.5 days will be obtained, which is appropriate, considering that the chlorophenols adsorption kinetics onto volcanic soil needs only a few minutes.

4.7.3   Mineral landfill liner considerations

Typical sanitary landfill engineering is described in Annex VIII. A slow permeable geological barrier, able to retain leachate pollutants, will be needed in the design of a landfill mineral

basal sealing. For this purpose, natural clays have been widely used. The main technical requirements in Austria for these mineral basal sealings are described in Table 38 [211].

Table 38: Mineral basal sealing technical requirements for landfills and comparison with volcanic soil

Parameter	Requirements	Volcanic soil
Hydraulic conductivity (K_f)	$5*10^{-10}$ m/s (laboratory test)	$5.16*10^{-9}$ - $6.48*10^{-9}$ m/s
	$5*10^{-9}$ m/s (in-situ test)	(laboratory test)
	Residual waste landfills	
Particle size distribution	Fines (< 2 µm): 20% w/w	Fines (< 2 µm): 1 - 23% w/w
	Clay minerals (from fines): 50% w/w	(see Annex IX)
Total organic carbon (TOC)	< 5% w/w	2.6 - 8.5% w/w

The volcanic soil characteristics seemto be near all the requirements presented in Table 38. For a possible use of volcanic soil in a sanitary landfill construction in the Temuco surroundings, several sites were analyzed (Annex IX) [175]. In the south of Temuco, Fundo El Castillo (Gorbea) and Fundo Huilquilco (Quepe) were investigated. Gorbea and Quepe are about 44 and 19 km southerly of Temuco. To the east, Fundo Cuatro Volcanes (in San Patricio, near Vilcún), about 87 km from Temuco was also inspected. Finally, in Temuco, Estación Las Encinas was explored as well. It was found, that the particle size distribution of the volcanic soil was very similar in all of these fields. Especially the Fundo Huilquilco (Quepe) tested soil presented excellent properties (i.e, particle size distribution) for its use as a sanitary landfill liner. All soils were found to have acid pH values, suggesting the same buffering capacity as presented before for the specific volcanic soil samples investigated in this work (Figure 30).

As an example for preliminary costs estimation, a sanitary landfill construction in Temuco, with a capacity of 500,000 m^3 was simulated (see Table 39 and Table 40). The volcanic soil was considered as the mineral basal sealing material.

This calculated average volcanic soil price of 45 €/ton is comparable to the zeolite price in the European market (about 80-90 €/ton). Moreover, considering a similar landfill construction in Santiago de Chile (700 km southerly from Temuco), the transport costs will rise and become more significant, reaching 840,000 €. The total costs will rise up to 5,080,000 € in this case, i.e., 85 €/ton volcanic soil for Case 1, when no reuse of the exploited volcanic soil site is feasible. In Case 2, a volcanic soil price of 30 €/ton is obtained, achieving an average price of 58 €/ton volcanic soil. Therefore, a landfill construction in the area of Santiago will still present a competitive volcanic soil price, 27% cheaper compared to the average zeolite price in the European market.

Table 39: Simulated landfill characteristics and estimation of necessary volcanic soil area for recovering the mineral landfill liner

Landfill characteristics	
Landfill volume	500,000 m^3
Waste body height	10 m
Landfill area	50,000 m^2 (i.e., 5 ha)
Volcanic soil bottom liner depth	1 m
Volcanic soil in-situ bulk density	~ 1.2 g/cm^3
Volcanic soil mass	50,000 m^2 * 1 m * 1.2 ton/m^3 = 60,000 ton
Necessary volcanic soil area	
Volcanic soil free bulk density	~ 1.0 g/cm^3 (1 ton/m^3)
Volcanic soil mass	60,000 ton / (1 ton/m^3) = 60,000 m^3
Usable volcanic soil depth (tested sites)	0.9 m
Necessary area	60,000 m^3 / 0.9 m = 66,667 m^2 = 6.7 ha

Table 40: Preliminary costs estimation for volcanic soil

Costs		
Volcanic soil site price	About 50 €/m^2 → 66,667 m^2 * 50 €/m^2 = 3,333,350 €	
Excavation costs	About 15 €/m^2 → 60,000 ton * 15 €/ton = 900,000 €	
Transport costs	About 20 ton/truck → 60,000 ton / 20 = 3,000 truck journeys	
Gasoline consumption	40 L/100 km	
Gasoline price	0.5 €/L	
Distance to the volcanic soil site	~80 km	
Gasoline costs	80 km * 40 L / 100 km * 0.5 €/L * 3,000 journeys * 2 (return) = 96,000 €	
Total costs	3,333,350 + 900,000 + 96,000 = 4,329,350 ~ **4,350,000 €**	
Reuse of the exploited site	**Case 1:** No reuse → **0 €**	**Case 2:** Recovery of the full price → **3,333,350 €**
Volcanic soil price	**(4,350,000 – 0 €) / 60.000 ton = 72.5 € / ton**	**(4,350,000 – 3,333,350 €) / 60,000 ton = 17.0 € / ton**
Average price	**45 € / ton volcanic soil**	

4.8   Spent volcanic soil management

It is of great importance to elaborate final management options for the spent (contaminated) volcanic soil, which has been used as large scale adsorbent. A regeneration/reactivation process of the volcanic soil has already been reported and studied, but this procedure is only intended to facilitate the reuse of the volcanic soil, after being saturated [147]. In this procedure, an acid wash was used for reactivating the spent volcanic soil. After 2 months of use, the volcanic soil columns were washed with a 0.01 M H_2SO_4 solution, using a volume of about 10% of the total effluent volume cleaned before. Then, a fixed bed adsorption system of reactivated volcanic soil was implemented (identically with the acidified soil columns described previously) for breakthrough curves and performance parameters determination. The results showed that, with the spent soil reactivation process, about 31% of the soil's original adsorption capacity could be reestablished. Nevertheless, the final spent contaminated volcanic soil will have to be managed independent of its reuse. In this Chapter, the natural attenuation of chlorphenols-contaminated soil will be dealt and discussed as a bioremediation tool. In addition, the possible use of contaminated volcanic soil (with chlorophenols and heavy metals) in the clinker and cement industry will be discussed, based on industrial process conditions, mass balances, and final product requirements.

4.8.1   Bioremediation of soil for specific chlorophenols

The biological natural attenuation properties of chlophenols-contaminated volcanic soil were investigated and discussed as a possible bioremediation tool.

No additional C, N and P were added to the soil consortium (biostimulation process), as well as no additional microorganisms were introduced in the system (bioaugmentation process). Both processes were described recently as useful procedures for remediating lindane-contaminated soil [212].

The toxic chlorophenols level for microorganisms in soil is 200 mg/kg [106],[111]. Therefore, the used 2,4-DCP and PCP contamination levels were 40 (M1), 4 (M2) and 0.4 (M3) mg 2,4-DCP or PCP per kg soil, respectively. The soil respirometric tests indicate clearly that there was a growing microbial activity during the entire incubation period of the assays (Figure 73). Moreover, there was a clear difference for PCP (Figure 73b) between the M1 (40 mg/kg) and the M3 (0.4 mg/kg) experiment. In fact, it seems that the soil microorganisms are able to produce more CO_2 when they are affected by a smaller PCP contamination, with an average difference of around 40 mg CO_2/100 g soil for day 60. In the case of the 2,4-DCP contamination, no clear difference in the CO_2 production was established between the M1, M2 and M3 experiments (Figure 73a). It is well known that the toxicity grade of 2,4-DCP is lower than that of PCP because of the fewer chlorine atoms substitution. This is probably the fact that didn't promote a difference in the measured respirometric response. Figure 74 shows the degradation kinetics of 2,4-DCP and PCP added to the soil during the incubation period. The expected soil initial concentrations of 2,4-DCP and PCP were not reached. The volcanic soil works as a dual adsorbent material; the organic matter present in the soil (SOM)

has a great affinity with pollutants that have a high log K_{ow} value, because of the presence of humic and fulvic acids (i.e. –COOH and phenolic –OH reactive groups).
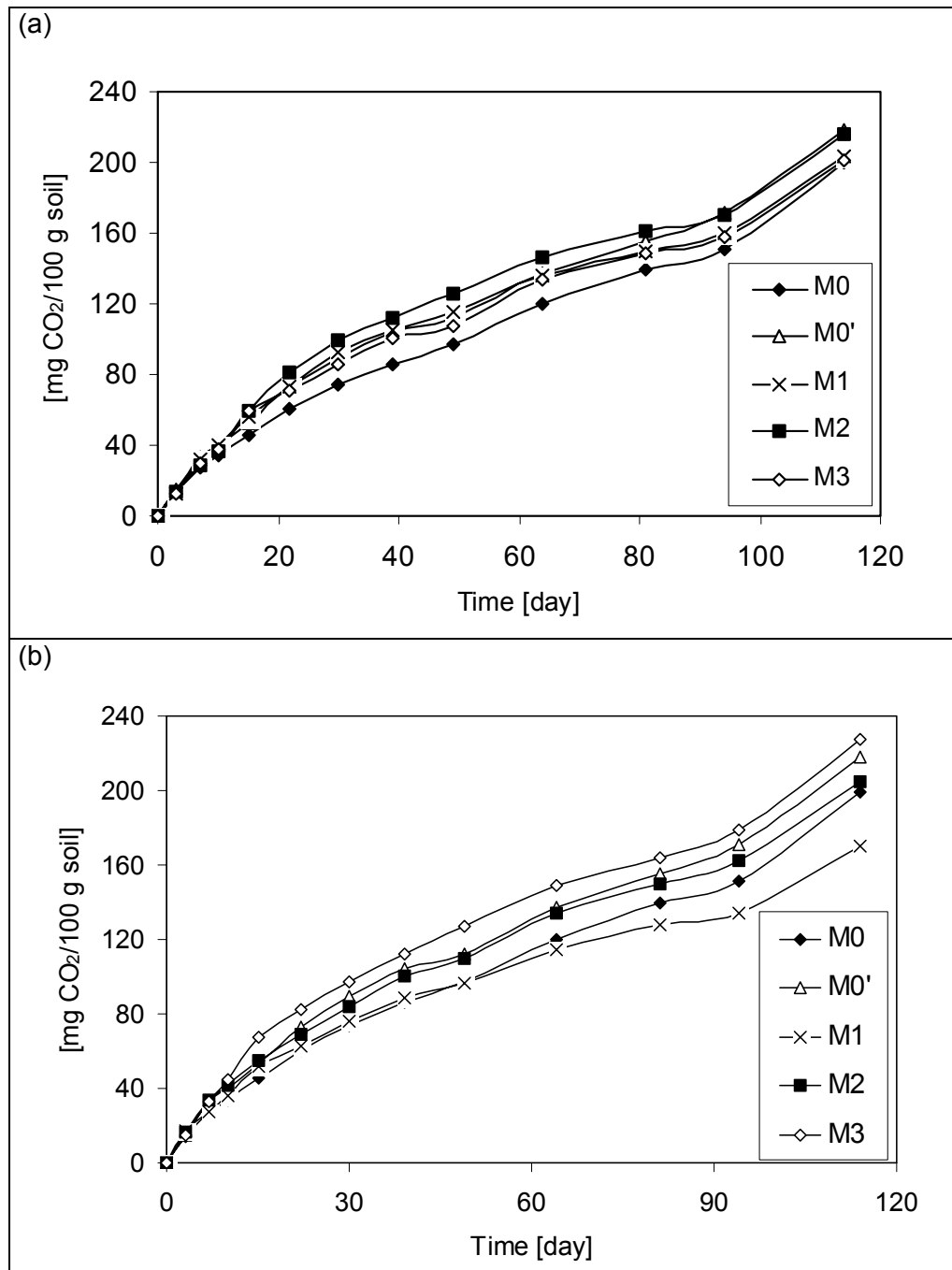
Figure 73: Respirometric response of the volcanic soil to the contamination with (a) 2,4-DCP and (b) PCP at three different initial levels M1, M2 and M3 (M0 and M0` defined in Chapter 3.6.1)

On the other hand, the clay-activated sites (metal oxides/hydroxides) are also involved in fixing organic pollutants in the soil matrix. In fact, it is known that the organic matter adsorption in clay occurs by ligand exchange with the surface hydroxyl groups, and therefore it follows that the Fe-humate and Al-humate complexes can influence the soil reactivity [32]. The adsorption of chlorophenols onto the SOM can be produced by the oligomerization of

the pollutants or their binding to the SOM. This phenomenon could probably contribute to the determination of a smaller quantity of 2,4-DCP and PCP in the initial time samples (3 and 4 mg/kg, respectively, compared to 40 mg/kg as expected), as both pollutants may be already bond to the humic and fulvic acids of the SOM. As described in Chapter 4.2.3.3, degradation of phenolic compounds within the fixed bed soil columns even at 1.7 days was observed for natural volcanic soil. In this case, after 15 and 60 days, the microorganisms present in the most contaminated soil sample (M1) were able to biodegradate the 2,4-DCP and PCP pollutants.
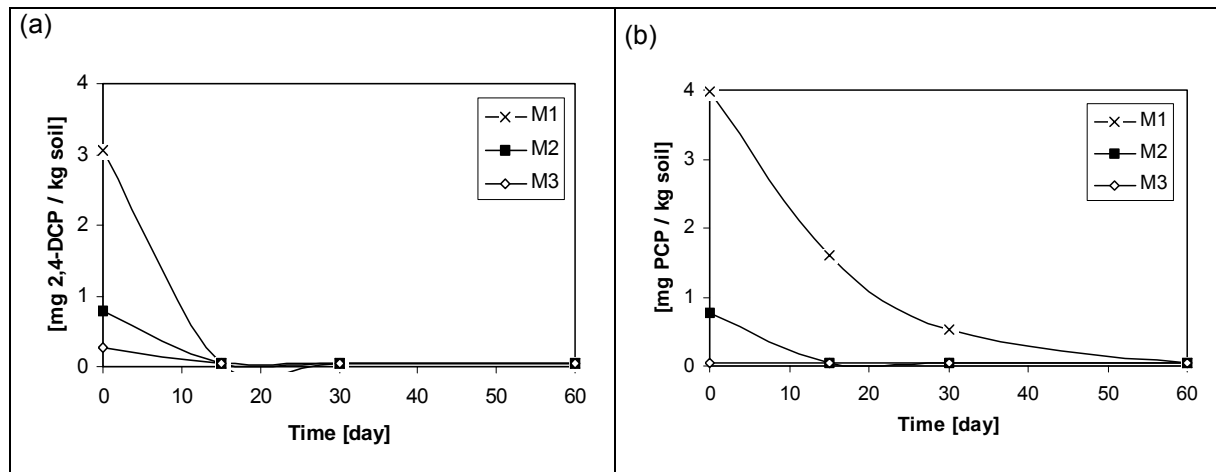
Figure 74: (a) 2,4-DCP and (b) PCP concentration in soil through the time at three different initial levels of contamination M1, M2 and M3
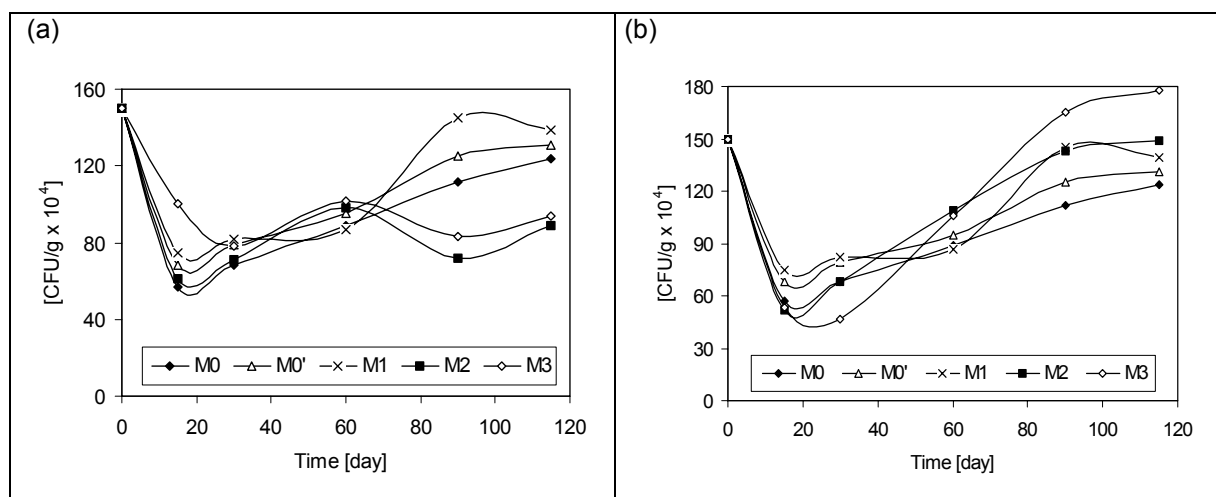
Figure 75: Bacteria count for (a) 2,4-DCP and (b) PCP contamination at three different initial levels M1, M2 and M3 (CFU: Colony forming units, M0 and M0` defined in Chapter 3.6.1)

Regarding the microorganisms count (Figure 75 to Figure 77), it seems that initially the bacteria population tends to decrease in the first 20 days. Soil bacteria are known to be very sensitive regarding different pollution levels and are normally used as indicator in toxicity bioassays. Under the particular conditions of this experience, it can be clearly stated that the population of bacteria is able to grow again in a chlorophenol-contaminated soil, after day 20 (Figure 75a and b). Actinomicetes and fungi seem to be more adaptable to the experimental

conditions used, as in fact, their concentration tends to grow with the time. Moreover, it is well known that fungi (and some actinomicetes) can survive in very strongly contaminated as well as in acidic environments. It appears that this microorganism's consortium is able to work in an optimized form. It seems that in the first 20 days only actinomicetes and fungi are able to biodegradate the 2,4-DCP and PCP pollutants, and after that bacteria are able to grow again in a less contaminated environment.
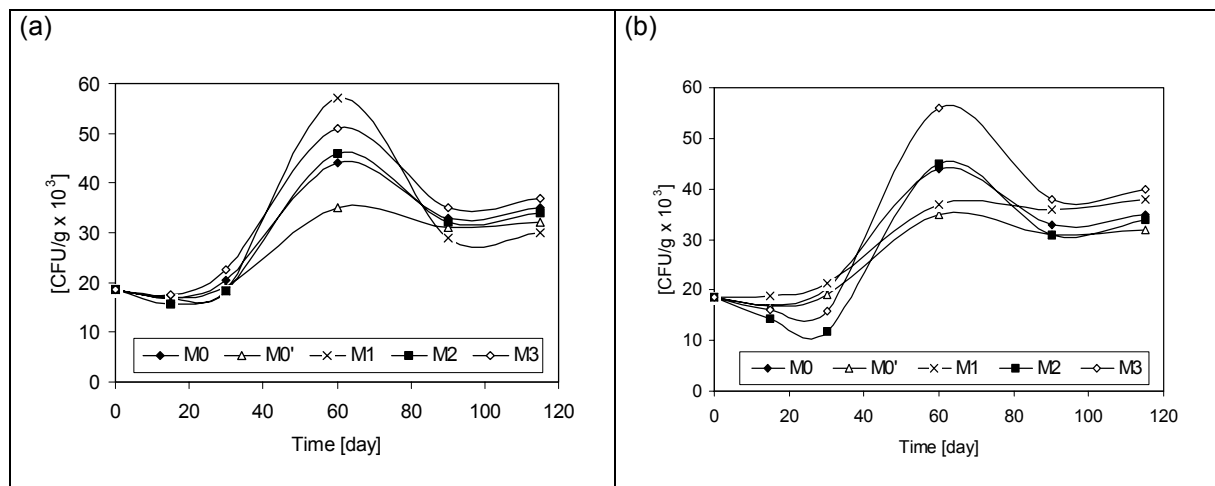
Figure 76: Actinomicetes count for (a) 2,4-DCP and (b) PCP contamination at three different initial levels M1, M2 and M3 (CFU: Colony forming units, M0 and M0` defined in Chapter 3.6.1)
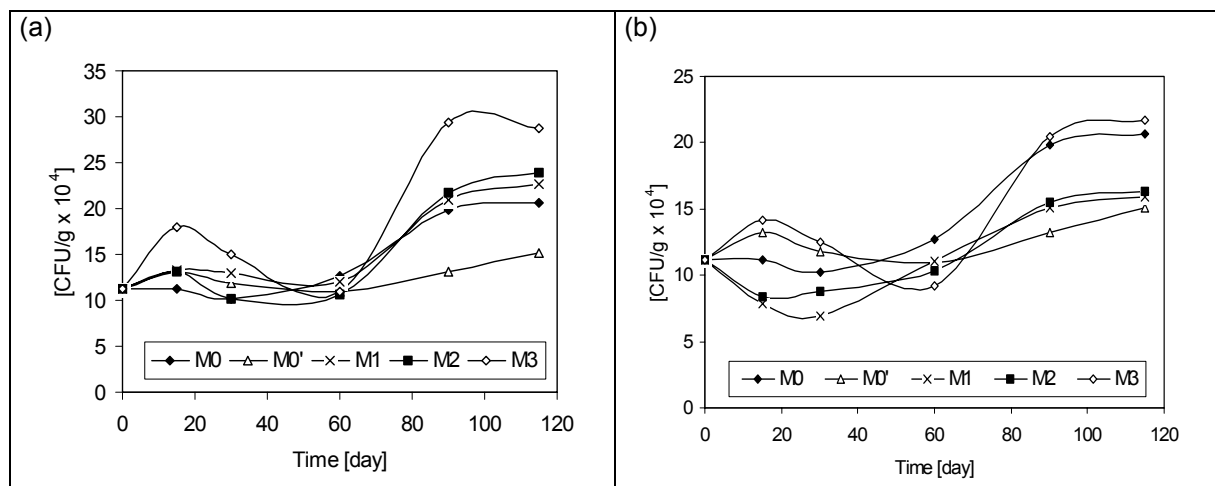
Figure 77: Fungi count for (a) 2,4-DCP and (b) PCP contamination at three different initial levels M1, M2 and M3 (CFU: Colony forming units, M0 and M0` defined in Chapter 3.6.1)

Looking at Figure 74 (a and b), at day 20 there is no more 2,4-DCP contamination in the soil left and the PCP contamination reaches a level of only 1 mg/kg, which would allow bacteria to grow again. Although these are only indigenous microorganisms, it seems that they can adapt themselves to the conditions of the experiments described before.

The volcanic soil biological activity and bioremediation capacity indicate that the micro-organisms present in this soil are able to degrade the adsorbed chlorophenols, being its

respiratory activity not significantly affected by the contamination levels studied. As already mentioned, actinomicetes and fungi are the most adaptable microorganisms in respect to the strength of the pollution conditions studied and are responsible for the initial biodegradation of chlorophenols. After this initial process, bacteria are able to grow again in a less contaminated environment and can participate in the bioremediation process of the volcanic soil as well.

4.8.2   Utilization as alternative raw material in the clinker/cement industry

Over thirty years have passed since the beginning of the systematical waste management in the clinker and cement industries all over the world. This management has allowed cost reductions in cement production and developed a more sustainable way to manage the utilization of important amounts of all types of residues, mainly alternative fuels.

The clinker/cement process contains three main stages: raw materials milling, pyroprocessing (clinkerization) and final milling of the clinker mixed with gypsum and other additive materials for obtaining cement as a final product. Limestone rock (75-80%) and clays (20-25%) are the main raw materials in the clinker production. Limestone rock supplies the necessary $CaCO_3$, which is present in limestone rocks, up to 95%. SiO_2 (45-65%), Al_2O_3 (10-15%), Fe_2O_3 (6-12%) and CaO (4-10%) are the main clay components. In addition, depending on the limestone rock and clay compositions, correction materials could be needed. High-purity limestone, silica and iron-rich clays are the most used corrections materials [213],[214]. The mixture is then milled to a final particle size of less than 300 μm, obtaining a fine powder called crude or raw meal, that goes through the clinkerization process [215]. In the clinkerization process, the crude is treated thermally in the kiln at temperatures up to 1450°C bed temperature corresponding to a gas temperature of about 2000°C, obtaining finally a transformed vitreous material. The first step in the clinkerization process is the precalcination or dehydratation stage, which eliminates the absorbed water and preheats the crude to temperatures up to 900°C. The calcination is the second step of the clinkerization process. The dehydrated crude reacts under temperatures between 600 and 900°C in the rotary kiln inlet-zone, where the $CaCO_3$ is thermally decomposed in CaO and CO_2 (decarbonatation reaction). In addition, the formed CaO reacts endothermically with the SiO_2 forming dicalcium silicate ($2CaO \cdot SiO_2$). All these reactions occur in the precalcinator or in the kiln inlet-zone, as well as the dehydratation step. The third step is the clinkerization itself. This stage occurs in semi-liquid phase and demands the highest energy charge of the whole process. Temperatures between 1250 and 1450°C are responsible for the formation of tricalcium silicate ($3CaO \cdot SiO_2$) from the reaction of $2CaO \cdot SiO_2$ with CaO. Moreover, tricalcium aluminate ($3CaO \cdot Al_2O_3$) and tetracalcium ironaluminate ($4CaO \cdot Al_2O_3 \cdot Fe_2O_3$) are also formed. The cooling step of the clinker (from 1450 to 200°C) is needed to stop the reactions and to promote the calcium compounds final crystallization. After that, the clinker (80%) is mixed with gypsum and other additive materials (20%) and milled to produce the final cement. The different additional materials (e.g. high-purity limestone, puzzolane,

siderurgical and glass slag, fly ashes from thermal power stations) can give the final cement the required character and mechanical properties [213],[214],[216].

Table 41: Main possible utilization of wastes as raw material and fuel in the cement industry [217]

Waste reuse as	Introduction in/as	Waste type
Fuel	Primary combustion	Used oil
	Secondary combustion	Reffinery/destillation residues
	Precalcinator	Chlorine-free solvents
	Gasification and combustion	Dried sludge
		Chlorine-poor plastic residues
		Wood residues and sawdust
		Swarfs
		Scrap-tires
		Rubber residues
		Used paper
Partial crude substitution	Milled limestone substitute	Foundry sand
	Clay substitute	Ashes
	Correction materials substitute	Contaminated soil
		Milled glass slag
		Clay and silt from soil-washing
Additive material	Cement mixture previous to milling	Fly-ashes
		Puzzolane
		Glass slag
		Dried gypsum sludge
		Lime sludge
Auxiliary material	DENOX reagent	Photography wastewaters
		Ammonia-containing wastewaters

The waste reuse in the cement industry is not only a waste management option, but also a cost reduction possibility. For instance, it is well established that one of the key points in the clinker/cement industry is the energy consumption and the reuse or utilization of wastes, as alternative fuel has become a common practice. In Table 41, the main possible waste utilizations as raw materials in the cement industry are shown. Regarding contaminated soil use, a soil with a high content of $CaCO_3$ will be useful as milled limestone substitute. Moreover, a soil with a high SiO_2, Al_2O_3, Fe_2O_3 and CaO content will be very useful as clay substitute or as correction material. In addition, a contaminated soil could be also useful as additive material, depending on its composition.

Table 42: Projects presented to the SEIA regarding the Chilean cement industry (since 1997)

Project title	Company	Presentation date	Status
Use of alternative fuel in the kiln Nr. 8 from La Calera plant of Cementos Melón	Melón	17/12/1997	Approved
Partial substitution of conventional by alternative fuels in the kiln Nr. 1 from Cemento Polpaico S.A.	Polpaico	24/07/1998	Withdrawn
Partial substitution of conventional by alternative fuels in the kiln Nr. 1 from Cemento Polpaico S.A. (second presentation)	Polpaico	25/01/2000	Approved
Use of oil pet-coke in the clinker kiln of Cementos Bío-Bío S.A.C.I.	Bío-Bío	07/02/2000	Approved
Conversion to natural gas	Inacesa*	07/07/2000	Approved
Use of pet-coke in the kiln Nr. 9 of the industrial plant of Cementos Melón	Melón	05/09/2000	Withdrawn
Use of alternative liquid fuel in the clinker kiln of the Industria Nacional de Cementos S. A., Curicó Division	Inacesa*	28/09/2000	Rejected
Use of mineral carbon in the clinker kiln of the Industria Nacional de Cementos S. A.	Inacesa*	15/01/2001	Approved
Use of natural gas in the process equipments of Cementos Bío-Bío S.A.C.I.	Bío-Bío	04/09/2001	Approved
Use of scrap-tires as an alternative fuel in the kiln Nr. 9 from La Calera plant of Cementos Melón	Melón	16/11/2001	Approved
Increment in the pet-coke used in the clinker kiln of Cementos Bío-Bío S.A.C.I.	Bío-Bío	18/12/2001	Approved
Combined use of alternative liquid fuel and mineral carbon in the clinker kiln of the Industria Nacional de Cementos S. A., Curicó Division	Inacesa*	23/01/2002	Approved
Use of pet-coke in the clinker kiln	Inacesa*	25/03/2002	Approved
Use of a pet-coke/coal mixture in the Cerro Blanco plant	Polpaico	30/05/2002	Approved
Use of pet-coke in the kilns Nr. 8 and 9 from La Calera plant of Cementos Melón	Melón	25/10/2002	Approved**
Enlargement of the substitution fuels and alternatives raw materials use in the Cerro Blanco plant	Polpaico	30/04/2003	Approved

* Inacesa is at present part of the Cementos Bío-Bío S.A.C.I. Company, ** with restrictions

In the year 2003, the total Chilean cement production reached 3.6 million ton, distributed in the three main production companies: Melón (36.4%), Polpaico (35.2%) and Bío-Bío (28.4%). The Chilean cement production has increased continuously since 1992 (2.6 million ton) with only one production fall in the year 1999. The Chilean yearly cement consumption in the period 1993-2001 increased from 218 to 234 kg/inhabitant, comparable to Brazil (217

kg/inhabitant), United Kingdom (235 kg/inhabitant), Canada (266 kg/inhabitant) and Mexico (278 kg/inhabitant), but is still far away from highly developed economies like Germany (370 kg/inhabitant), U.S.A. (408 kg/inhabitant), Austria (545 kg/inhabitant), Switzerland (607 kg/inhabitant), Italy (682 kg/inhabitant) and special cases like Taiwan (749 kg/inhabitant), Saudi Arabia (818 kg/inhabitant), South Korea (951 kg/inhabitant) and Spain (1,051 kg/inhabitant) [218]. These figures indicate that the Chilean cement consumption rate is likely to continue to grow. This projection is close to a possible future reality, as the Chilean economy has continuously grown in the last 13 years.

The environmental impact assessment system (SEIA) was introduced in Chile to implement the Law 19.300 about the general fundamentals of environmental issues (see Annex X). The purpose of the SEIA, applied to projects and/or activities performed by the public and private sectors is to assure the environmental sustainability of said undertakings. The Law 19.300 provides that certain projects or activities capable to generate environmental impacts must be subjected to a SEIA.

In Table 42, all the projects ingressed to the SEIA regarding raw materials and waste reuses in the cement industry are shown [214],[219]. Since 1997, 16 projects regarding the use of alternative fuel (liquids and scrap-tires), pet-coke, natural gas and mineral carbon were entered to the SEIA from Chilean cement production companies. From these 16 projects, the National Environmental Commission (CONAMA) approved 13 and rejected 1, while the responsible companies withdrew other 2 projects. In addition, and to our knowledge, only the most recent project (presented to the SEIA on the 30/04/2003 by Polpaico and approved by CONAMA) dealed also with the use of alternative raw materials in the cement process; this situation could be an indicator of future projects in the Chilean cement industry. This was the main reason to make a technical analysis of the possibility of using contaminated soil (spent volcanic soil contaminated with chlorinated phenolic compounds and/or heavy metals in this case) in the Chilean cement industry.

The Cementos Melón Company plant La Calera was selected for this preliminary study as in the last ten years it has been the company with main market participation. Moreover, the industrial facility of La Calera has an active environmental policy for the incorporation of alternative raw materials in the cement process and has also the ISO 14001 certification. The La Calera facility has two clinker kilns in operation (Nr. 8 and Nr. 9) and the main restrictions in the kilns operations concern magnesium, sulphur, phosphor, heavy metals, chlorine and chlorinated compounds content [214],[216]. A magnesium concentration under 2% of the principal phases of the clinkerization process has to be achieved. A higher content will lead to MgO formation that reacts with the settling water forming $Mg(OH)_2$. This reaction is normally very slow and since the $Mg(OH)_2$ occupies more volume than the MgO, it can produce some fissures in the final product. The sulphur content is also subjected to some operational restrictions. Sulphur could be present in the fuel and can be transformed into sulphate, which is retained in the clinker. The excess of sulphur can cause incrustation of the kiln, creating some operational problems. The maximum SO_3 content in the final cement has

to be less than 3-4%. P_2O_5 also has to be limited to less than 0.5%. Higher contents can cause a strong decrease in the cement initial resistance characteristics.

Table 43: Maximum retention factors of heavy metals in the clinker

Metal	Von Seebach [%] [214]	Roth [%] [216]
Sb	99.79	99.89
As	99.89	99.91
Ba	99.88	99.97
Be	99.87	99.99
Cd	99.56	99.88
Zn	99.79	99.97
Cr	99.86	99.97
Hg	**61.30**	**88.39**
Ni	99.96	99.93
Ag	99.84	99.96
Pb	99.85	99.91
Se	**95.40**	**92.56**
Tl	**90.12**	**99.80**
V	99.99	88.37

In addition, the behavior of heavy metals in cement kilns has been widely studied. In general, the heavy metals are retained in the clinker, because in the higher temperature zone of the kiln, the metals tend to form complex silicates. These complex silicates are included in the crystalline structure of the clinker and can affect it, if they exceed a certain concentration. During the cement hydration, and with the presence of alkali in the cement paste, the remaining and integrated metals can precipitate as unsoluble hydroxides. These hydroxides are then absorbed by the cement hydrosilicates. The maximum heavy metal retention factors in the clinker are presented in Table 43 [214],[216] and are around 99.9%, except for the most volatile metals Hg and Tl. This fact would indicate that only the use of Hg and/or Tl contaminated soil as an alternative raw material could affect the process emissions negatively.

Finally, chlorine may also affect the clinker process negatively, as chloride will be formed in an alkaline environment and transported with the off-gas stream, precipitating in the heat exchanger, returning with the material and vaporized in the sintering zone again. This closed internal cycle will continue until the crust formation will stop the operation of the clinker kiln. This is the main reason why the total chlorine content in the input materials of the clinker kiln has to be less than 1.0%. In addition, chlorine promotes corrosion (cement must have less than 0.1% chlorine), as well as mobilization of heavy metals, and can promote the formation of dioxins and furans, but due to the operational conditions of the clinker kilns, these reactions are minimized. In fact, the US EPA uses an equivalent dioxins emission factor in

clinker kilns of 0.29 ng/kg clinker under normal operation, but in the case of using hazardous wastes as alternative fuel; this factor may increase up to 24.34 ng/kg clinker [220],[221].

Table 44: Average contents of main oxides in limestone L-N and L-E, crude and volcanic soil

Oxide	Unit	L-N (70%)	L-E (30%)	Pimary Mixture	Crude with correction materials	Volcanic soil*
$CaCO_3$	[%]	72.0	88.2	76.9	77.0	0
SiO_2	[%]	17.2	7.3	14.2	13.5	43.4
Al_2O_3	[%]	4.8	1.5	3.8	5.0	20.3
Fe_2O_3	[%]	2.1	0.7	1.7	1.8	11.5
Rest	[%]	3.9	2.3	3.4	2.7	24.8
Total	[%]	100	100	100	100	100

*Average values from Table 17

$CaCO_3$, SiO_2, Al_2O_3 and Fe_2O_3 (Σ97.3%, see Table 44) are the main components of the crude average formulation in La Calera facility. The rest fraction corresponds mainly to MgO, K_2O, Na_2O, SO_3 and H_2O.

The Melón cement plant uses their limestone from the Navío mine (L-N) and external limestone mixtures (L-E) for its crude formulation. The normal limestone consumptions are 70% of L-N and 30% of L-E. The main imbalance produced under these conditions is due to Al_2O_3 content in the primary mixture; thus, correction clay materials rich in Al_2O_3 are often required. The total crude production previous to the clinkerization process at the plant is about 4,077 ton/d. 25.9% of the crude are processed in kiln Nr. 8, while the remaining 74.1% are processed in kiln Nr. 9. The total amount of different oxides required is 3,139 ton/d $CaCO_3$, 550 ton/d SiO_2, 204 ton/d Al_2O_3 and 73 ton/d Fe_2O_3. For a possible use of spent contaminated volcanic soil as an additive in crude mixing, a higher level of $CaCO_3$ in the primary mixture has to be achieved. For this, a 92% $CaCO_3$ content in the L-E seems to be a reasonable value considering all the limestone used in the plant as raw material. The recalculated contents of SiO_2, Al_2O_3 and Fe_2O_3 would then be 4.9, 1.0 and 0.5%, respectively. Moreover, depending on the "price of the contaminated volcanic soil" and its availability, La Calera facility would decrease its L-N consumption level for the crude preparation to a minimum of 35% of the final crude. In Table 45, the mass balance for the case of using 35% L-N and a L-E with 92% $CaCO_3$ content is presented for a total crude production of 4,077 ton/d. The L-E consumption is determined by the $CaCO_3$ balance, which means a consumption of 2,296 ton/d for L-E (56.3% of the crude). The imbalance indicates that SiO_2, Al_2O_3 and Fe_2O_3 are in a deficit condition, which requires the necessary volcanic soil consumption of 445 ton/d, 557 ton/d and 278 ton/d respectively. As the crude composition is based on a standard formulation, the maximum volcanic soil to be used in La Calera facility under these conditions will be 278 ton/d, closing the Fe_2O_3 balance and supplying 121 ton/d of SiO_2 and 56 ton/d of Al_2O_3. To close the imbalance for SiO_2 and Al_2O_3

also, correction materials are needed to provide the required SiO_2 and Al_2O_3 amounts (72 and 57 ton/d, respectively).

Table 45: Oxides consumption rates of L-N and L-E in the case of 35% L-N in the final crude

Oxide	Unit	L-N (35%)	L-E ($CaCO_3$ balance)	Crude Formulation	Raw materials imbalance	Necessary volcanic soil addition
$CaCO_3$	[ton/d]	1,027	2,112	3,139	0	0
SiO_2	[ton/d]	245	112	550	-193	445
Al_2O_3	[ton/d]	68	23	204	-113	557
Fe_2O_3	[ton/d]	30	11	73	-32	**278**

Table 46: Technical characteristics of kilns Nr. 8 and 9 from La Calera facility

	Kiln Nr. 8	Kiln Nr. 9
Installation	Long rotary kiln	Short rotary kiln with a 4-stage preheater and precalcinator
Process	Dry	Dry
Dimensions	3.6 m diameter	3.6 m diameter
	125 m length	51 m length
Fuel (% of thermal consumption)	50% pet-coke	80% pet-coke
	50% alternative liquid fuel	20% scrap-tires
Fuel consumption	46.7 ton/d pet-coke	152.3 ton/d pet-coke
	59.2 ton/d alternative liquid fuel	45.0 ton/d scrap-tires
Electrostatic filter 1	99.99% capture efficiency	98% capture efficiency
	(<30 mg/Nm^3 clean gas concentration)	(<100 mg/Nm^3 clean gas concentration)
Electrostatic filter 2	-	99.88% capture efficiency
		(<30 mg/Nm^3 clean gas concentration)
Crude consumption	1,057 ton/d (25.9%)	3,020 ton/d (74.1%)
Clinker production	700 ton/d	2,000 ton/d
Thermal consumption	4,598 kJ/kg clinker	3,620 kJ/kg clinker
Gas flow rate	66,795 Nm^3/h	153,379 Nm^3/h

In order to determine the tolerable pollutant content in the volcanic soil, a complete mass balance for each kiln was performed under the studied situation, considering the addition of 278 ton/d of contaminated volcanic soil as an alternative raw material. The maximum chlorine content (present in phenolic compounds like chlorophenols) in the contaminated soil

was estimated, considering the mass balance and the technical characteristics of kiln Nr. 8 and 9 (Table 46), as well as the requirement of having a chlorine content lower than 1% in all the input streams of the clinker kilns. In the input crude input, the volcanic soil input rate will be 72 and 206 ton/d to the kiln Nr. 8 and 9, respectively. Dividing, the total chlorine input rate is divided by the total input mass (see Table 47), the chlorine input content results. Considering that the chlorine input content should be less than 1%, the chlorine input rates in the volcanic soil in kiln Nr. 8 (W1) and kiln Nr. 9 (W2) were obtained. With the obtained values for W1 and W2, the theoretical (permissible) chlorine content in the contaminated volcanic soil were found to be 122 and 155 mg/g for kiln Nr. 8 and 9, respectively. Both values are higher than the maximum adsorption capacities obtained for phenolic compounds and chlorophenols onto volcanic soil (Table 28 and Table 30), indicating that no possible problems regarding the chlorine content in the volcanic soil have to be expected for the clinker kiln process.

Regarding heavy metals content in the contaminated volcanic soil, the balance was made for Cr, Pb and Zn. The maximum permissible heavy metal content in the contaminated soil was estimated by establishing the mass balance and considering the technical characteristics of kiln Nr. 8 and 9 (Table 46). In Table 48, the heavy metals content [g/ton] in all of the input streams of the clinker kilns are shown, as well as the heavy metal input rates [kg/d] as the result of each input mass flow analysis. Moreover, considering the clinker process retention factors for Cr, Pb and Zn (Table 43), the heavy metals emissions from each clinker kiln were estimated, depending on the heavy metal content of soil. These assessed heavy metal emissions then were compared with the maximum allowed emmission values of the draft project for the new Chilean "*Emission law for the incineration and co-incineration of wastes*" (Annex X), obtaining the maximum theoretical (permissible) heavy metal input rates in the contaminated volcanic soil to be introduced in the clinker kiln process.

Table 47: Total chlorine content in input and chlorine input rate

	Chlorine content [g/ton]		Chlorine input rate [kg/d]	
	Kiln Nr. 8	Kiln Nr. 9	Kiln Nr. 8	Kiln Nr. 9
Crude (without volcanic soil)	19.3	19.3	19.0	54,310
Volcanic soil	t.b.d	t.b.d	t.b.d	t.b.d
Pet-coke	1,000	1,000	46.7	152.3
Alternative liquid fuel	30,000*	-	1,776	-
Scrap-tires	-	1,000	-	45.0
Total chlorine input rate			1,842 + W1	251.6 + W2
Total input mass (ton/d)			1,063	3,217

*Maximum allowed content, t.b.d: to be determined, W1 and W2: Chlorine input rate contained in the volcanic soil in kiln Nr. 8 and 9, respectively

Table 48: Heavy metals content of input and input rates in the clinker kilns

Input stream	Heavy metal content					
	Cr [g/ton]		Pb [g/ton]		Zn [g/ton]	
	Kiln Nr. 8	Kiln Nr. 9	Kiln Nr. 8	Kiln Nr. 9	Kiln Nr. 8	Kiln Nr. 9
Crude (without volcanic soil)	23	23	56	56	140	140
Volcanic soil	t.b.d	t.b.d	t.b.d	t.b.d	t.b.d	t.b.d
Pet-coke	510	510	80	80	210	210
Alternative liquid fuel	2,000	-	1,000	-	527	-
Scrap-tires	-	500	-	760	-	20,500
	Heavy metal input rate					
	Cr [kg/d]		Pb [kg/d]		Zn [kg/d]	
	Kiln Nr. 8	Kiln Nr. 9	Kiln Nr. 8	Kiln Nr. 9	Kiln Nr. 8	Kiln Nr. 9
Crude (without volcanic soil)	22.6	64.7	55.2	157.6	137.9	394.0
Volcanic soil	t.b.d	t.b.d	t.b.d	t.b.d	t.b.d	t.b.d
Pet-coke	23.8	77.7	3.7	12.2	9.8	32,0
Alternative liquid fuel	118.4	-	59.2	-	31.2	-
Scrap-tires	-	22.5	-	34.2	-	922.5
Total input rate (kg/d)	164,9 + W3	164.9 + W4	118.1 + W5	204.0 + W6	178.9 + W7	1,348 + W8

t.b.d: to be determined, W3-W8: Respective heavy metal input rates with the volcanic soil in each kiln

With the resulting total input rates (Table 48, W3 to W8), the permissible heavy metal contents in the volcanic soil were determined.

In the case of Chrome, the calculated permissible content is 77.2 and 63.0 mg/g volcanic soil for kiln Nr. 8 and 9, respectively. These values are higher than the maximum adsorption capacities obtained for Cr onto volcanic soil (Table 31), suggesting that no emission problems regarding Cr have to be expected when volcanic soil is used.

In the case of Pb and Zn, the draft project for the new Chilean legislation indicates maximum emission values for the addition of both pollutants (i.e., Pb + Zn < 1 mg/Nm^3). A kind of worst-case scenario analysis was made assuming maximum Pb input rate values without the presence of Zn and fassuming maximum Zn input rate values without the presence of Pb in the volcanic soil, respectively. All the realistic situations in between these both extreme cases will result in lower Pb and Zn input rates. The calculated values are presented in Table 49. For clinker kiln Nr. 8, a maximum content for Pb and Zn in the volcanic soil input of 14.6 and 10.4 mg/g was estimated. As both values are clearly higher than the maximum adsorption capacities obtained for Pb and Zn onto volcanic soil (Table 31), no problems regarding Pb and Zn emissions should affect the clinker kiln Nr. 8 during its operation.

Table 49: Estimated maximum permissible heavy metal inputs with the contaminated soil

	Cr		Pb		Zn	
	Kiln Nr. 8	Kiln Nr. 9	Kiln Nr. 8	Kiln Nr. 9	Kiln Nr. 8	Kiln Nr. 9
Input rate [kg/d]	5,560	12,982	1,050	543	750	388
Content in kiln input [g/ton]	77,228	63,019	14,587	2,638	10,419	1,884

For clinker kiln Nr. 9, maximum permissible Pb and Zn contents in the input volcanic soil of 2.6 and 1.9 mg/g were calculated. As both values are smaller than the maximum adsorption capacities obtained for Pb and Zn onto volcanic soil (Table 31), in this case emission problems could actually affect the clinker kiln Nr. 9 during the operation with spent volcanic soil contaminated with a maximum Pb or Zn content. The contents of Cr, Pb and Zn in natural volcanic soil were found to be irrelevant for all the calculations done. In addition, as the natural volcanic soil has average SOM and TOC contents of 14.6% and 4.6%, respectively, a total diminution in the clinker production of 40.6 ton/d will occur when using this soil in the cement plant, as well as an enhancement in the CO_2 emissions of 7,550 mg/Nm^3 and 9,450 mg/Nm^3 in kiln Nr. 8 and 9, respectively.

5   Summary

In the **introduction** (Chapter 1), the problematic of the need of new cheaper and selective adsorption materials for their use in wastewater treatment facilities, groundwater remediation processes and in sanitary landfills (as mineral clay liners) is presented. In this sense, the objective of this work was to evaluate the possible use of volcanic soil (of Southern Chile) as natural and competitive adsorption material in the mentioned technical fields. Additionally, the development of a ceramic adsorption material based on the volcanic soil, for its use in wastewater and groundwater treatment was also a goal of this work; coupled with the evaluation of the most suitable waste management options for spent contaminated volcanic soil, especially regarding bioremediation or its possible use in clinker/cement facilities as an alternative raw material.

In the **theoretical background** (Chapter 2), the adsorption phenomenon is explained and selected properties and uses of the main adsorption materials (i.e., activated carbon, zeolites, clay minerals, waste-derived adsorbents, zero-valent metals and natural soils) are described. Moreover, the main parameters affecting sorption of contaminants to natural soil are analyzed, being the most importants soil organic matter (SOM) and clay content, surface area and cationic exchange capacity (CEC), as well as soil pH value. In addition, a general description of (Chilean) volcanic soils and andisols is presented, being andisols separated and described as allophanic and non-allophanic.

The main chlorophenols present in the environment are also described in Chapter 2 as well. Their main physico-chemical properties and fate in the surrounding environment are presented. Important physico-chemical properties of chlorophenols are their high water solubility (decreasing with chlorine substitution), their different pK_a values (decreasing with chlorine substitution), which are responsible for the presence of chlorophenols in their ionic or non-ionic form, and their varaible log K_{OW} values (increasing with chlorine substitution), which represent the affinity chlorophenols for binding with organic matter.

The main heavy metals present in the environment, their sources and toxic effects are also described in Chapter 2. Heavy metals are mainly produced in the metal finishing, fertilizer and plating industry. Regarding their toxicity, Cadmium (Cd^{2+}) and chromium (in the hexavalent oxidation state) show high toxicity to humans as well as to animals, while copper, nickel and zinc show moderate toxicity to humans and animals. All these metals are also toxic to plants, being nickel and cadmium the strongest phytotoxic elements. Moreover, hexavalent chromium is known to have also a potential carcinogenic effect.

The state of the art in the pulp and paper industry wastewater treatment is also analyzed in Chapter 2. The pulp wastewater stream can produce three kinds of impacts: biological oxygen demand (BOD), toxicity (attributed to wood resin, chlorinated phenols and tannins) and color (from the presence of lignin or polymerized tannins). Aerated lagoons and activated sludge remove about 50% and 60% of the chlorinated phenolic compounds, respectively. Nevertheless, both treatments are not able to remove the color present in the Kraft pulp industry effluent.

The most recent bleaching technologies, known as total chlorine free (TCF), have the advantage that no chlorinated organic compounds are produced in the bleaching step. Nevertheless, biological processes can poorly degrade their mainly used chelating agent (ethylenediamine tetraacetic acid, EDTA).

The main groundwater remediation processes are also analyzed in Chapter 2. For chlorophenols-contaminated water, biological and physico-chemical processes are analyzed. Particularly, the novel in-situ process known as reactive wall is explained and the possible application of this technology for chlorophenols-contaminated water remediation is discussed. The main reactive materials (i.e., activated carbon, zero-valent iron and minerals) are also presented and compared.

Design concepts used for mineral liners in sanitary landfills are also described in Chapter 2. The multibarrier design is introduced, in which clay mineral layers play an important role as constituents of landfill barriers, by preventing the breakthrough of hazardous contaminants like heavy metals or organic pollutants.

Contaminated soil waste managent options are presented and anlayzed in Chapter 2 as well. The geohydrological soil properties are analyzed regarding possible in-situ or ex-situ remediation, being soil particle size distribution, hydraulic conductivity (K_f) and organic matter content (SOM) the main parameters involved. For chlorophenols–contaminated soil remediation, different possible technologies are discussed. Biological (aerobic and anaerobic), as well as physico-chemical (soil wash, mechanical and thermal) processes are presented and analyzed. For heavy metals-contaminated soil remediation, isolation and containment, mechanical separation, pyrometallurgical separation, chemical treatment, permeable treatment walls, electrokinetics, biochemical processes, phytoremediation, soil flushing and washing, among others, are analyzed.

The possible development of a ceramic adsorption material (from volcanic soil) is also discussed in Chapter 2. For a possible large-scale industrial application of natural soils, clays and minerals as adsorbent materials, a stable form or matrix would be necessary, capable to resist hydraulic loads and to prevent attrition losses and sludge formation. For this purpose, a novel process was used. It basically consists on the foaming of the raw material (i.e. the natural volcanic soil) mixed with reactants for forming compact polyurethane foam, and a subsequent thermal treatment of the foam at the sintering temperature range of the raw material. The main foam reactants are aromatic polyester-polyols obtained by the glycolysis of recycled polyethylene terephthalate (PET) bottles.

In the **materials and methods** section (Chapter 3), all the used materials and techniques are described. First, the origin of the volcanic soil samples (Temuco, IX Región, Chile) is stated. Then, the methodology for the estimation of the adsorption kinetics data for color and phenolic compounds onto volcanic soil is described, as well as for the adsorption isotherms of different pollutants groups (i.e, color and phenolic compounds, chlorophenols and heavy

metals) onto volcanic soil. The Langmuir and Freundlich models were used to fit the experimental adsorption isotherms data.

The Kraft mill effluent trials methodology is also described in Chapter 3. The Kraft mill wastewater characterization and the experimental conditions for breakthrough curves determination are presented in this section. Moreover, the molecular weight distribution (MWD) technique used for the effluent pollutants characterization is described, as well as the fixed bed adsorption rate calculation method, which involves the use of a fixed bed phenomenological model.

The heavy metals diffusion trials are also described in Chapter 3. The layout of the column diffusion trials is described, and the calculation of the diffusion coefficient of pollutants through a mineral liner is also explained. A column diffusion model based on Fick's second law was used for the determination of the heavy metals diffusion coefficients and breakthrough times in a volcanic soil landfill liner.

The bioremediation of soil contaminated with specific chlorophenols methodology is described in Chapter 3 as well. The techniques of the respirometric assays; bacteria, actinimicetes and fungi plate counts and chlorophenol concentration measurement in soil through time are presented.

All the used analytical methods are also described in Chapter 3. The techniques used for the determination of the total organic carbon (TOC), soil organic matter (SOM), effective cationic exchange capacity (CEC_{eff}), echangeable cations, heavy metals and metal oxides content, anionic exchange capacity (AEC), pH value, buffer capacity, particle size distribution, loss on ignition (LOI), Proctor density, hydraulic conductivity (K_f), X-Ray fluorescence spectrometry, X-Ray diffractometry, light microscopy and scanning electron microscopy of the investigated volcanic soil and selected zeolites of the European market are described. In addition, the methodology for the determination of specific chlorophenols by high performance liquid chromatography (HPLC), color and phenolic compounds, humic and fulvic acids, tannins and lignins is also described in this Chapter.

The **results and discussion** section is presented in Chapter 4. First, the **volcanic soil characterization and comparison with zeolites** is presented and analyzed in Chapter 4.1. Regarding the particle size distribution of volcanic soil profiles and zeolites, it was found that the clay and silt fractions, which are the most reactive ones, ranged for volcanic soil between 38% (40-60 cm profile) and 54% (5-20 cm profile), while for zeolites these values reached only 13% for Agro Clino and 38% for Nat Min 9000.

The total organic carbon content in the volcanic soil profiles investigated ranged between 2.6% and 8.5%, while for the analyzed zeolites the TOC content was < 0.08%. The volcanic soil organic matter (SOM) was found to range between 11.1% (40-60 cm profile) and 20.2% (5-20 cm profile), while for analyzed zeolites the obtained values (lost on ignition (LOI) in this case) were 6.7% and 7.0% for zeolite Agro Clino and Nat Min 9000, respectively.

The main metal oxides determined by XRFS in the volcanic soil profiles samples were SiO_2 (41.6-45.0%), Al_2O_3 (18.6-21.6%), Fe_2O_3 (10.5-12.4%) and CaO (3.3-3.6%). For zeolite Nat Min 9000, the main metal oxides found were SiO_2 (71.5%), Al_2O_3 (12.3%), CaO (2.0%) and Fe_2O_3 (1.4%).

The effective cationic exchange capacity (CEC_{eff}) in volcanic soil ranged between 5.2 (40-60 cm profile) and 6.5 cmol+/kg (5-20 cm profile). For zeolite Agro Clino, the CEC_{eff} value obtained was 11.4 cmol+/kg, while for zeolite Nat Min 9000 the CEC_{eff} value was 9.7 cmol+/kg. The main exchangeable cations measured were Ca^{2+}, Mg^{2+}, K^+ and Mg^+ for both, volcanic soil profiles and zeolites. In addition, the anionic exchange capacity (AEC) of the volcanic soil samples ranged between 0.5 (40-60 cm profile) and 2.7 cmol/kg (5-20 cm profile). For zeolite Agro Clino and Nat Min 9000, the obtained AEC values were 0.5 and 0.6 cmol/kg, respectively.

The pH values (in water) of the volcanic soil profiles ranged between 5.9 (5-20 cm profile) and 6.8 (40-60 cm profile). For zeolite Agro Clino and Nat Min 9000, the obtained pH values were 7.6 and 7.3, respectively. Moreover, the buffer capacities of the three volcanic soil profiles were higher than those of the zeolite samples. For the volcanic soil profiles the pH value changed up to a maximum value of only 9.6 (40-60 cm profile), while the zeolites pH changed up to 11.2 (Agro Clino), when adding 22 mL of a 0.1 M NaOH solution. On the other hand, when adding 16 mL of a 0.1 M HCl solution, the volcanic soil profiles pH values decreased to a minimum of 3.0 (5-20 cm profile), while the zeolite samples reached a minimum pH value of 2.1 (Agro Clino). In addition, the shape of the zeolites buffering capacity curves showed a strong change when adding only small amounts (< 2 mL) of the acid and the alkaline solutions.

The Proctor densities of the volcanic soil profiles ranged between 1.11 (5-20 cm profile) and 1.15 g/mL (40-60 cm profile). For zeolite Agro Clino and Nat Min 9000, the obtained Proctor densities were 1.19 and 1.34, respectively. Additionally, the hydraulic conductivity values (K_f) of the volcanic soil profiles ranged between $6.48*10^{-9}$ (40-60 cm profile) and $5.16*10^{-9}$ m/s (5-20 cm profile). For zeolite Nat Min 9000, the obtained K_f value was $4.51*10^{-9}$ m/s.

X-Ray diffractograms indicated the main presence of plagioclase, quartz, magnetite and maghemite in the analyzed volcanic soil samples. The X-Ray diffractograms of zeolites showed the presence of clinoptilolite, cristobalite, tridymite, quartz, feldspars, illite, smectite and chlorite. Light microscopy pictures indicated the presence of organic matter, plagioclase, andesite and quartz in the volcanic soil samples. Moreover, the zeolite analyzed samples showed the presence of clinoptilolite, feldspars and quartz. In addition, scanning electron microscopy (SEM) showed the presence of andesine/labradorite, quartz, bytownite and allophane in the investigated volcanic soil. The zeolites samples showed the presence of sanidine, quartz, oligoclase and clinoptilolite.

In the section **adsorption of pollutants from bleached Kraft mill effluent** (Chapter 4.2), the color and phenolic compounds adsorption kinetic was determined to be about 30 min for

46% of color and 36% phenolic compounds adsorption yield. The adsorption isotherms for color and phenolic compounds onto volcanic soil showed a maximum Langmuir adsorption constant of 2,500 and 18.8 mg/g for color and phenolic compounds, respectively.

The volcanic soil fixed bed adsorption system trials showed a chemical oxigen demand (COD), tannins and lignins (T & L) removal efficiency between 60 and 70% for both. Moreover, the molecular weight distribution (MWD) performed to input and output effluent samples of a single volcanic soil column indicated that the fraction > 30,000 Da was the main adsorbed fraction onto the acified volcanic soil. In addition, the fixed bed adsorption rate was calculated using a phenomenological model. The maximum calculated adsorption rate for phenolic compounds and color onto acidified soil was $2.25*10^{-6}$ and $2.62*10^{-6}$ L/mg*min, respectively.

The **adsorption of chlorophenols from synthetic groundwater onto volcanic soil** (Chapter 4.3) was also evaluated in this section. Maximum Langmuir adsorption constants of 0.74 and 2.81 mg/g were obtained for 2,4-dichlorophenol (2,4-DCP) and pentachlorophenol (PCP), respectively.

The **adsorption of heavy metals from synthetic landfill leachate onto volcanic soil** (Chapter 4.4) showed maximum Langmuir adsorption constants of 2.74 mg/g for CrO_4^{2-} at pH 4.5, 5.32 mg/g for Cu^{2+} at pH 7.5, 5.30 mg/g for Zn^{2+} at pH 7.5 and 7.44 mg/g for Pb^{2+} at pH 4.5. For Cu^{2+} and Zn^{2+} at pH 7.5, adsorption coupled with precipitation was observed. In addition, the heavy metals diffusion coefficients calculated for a simulated 1 m deep volcanic soil liner showed in the worst-case scenario (i.e., landfill leachate pH of 4.5), breakthrough times of 21.6 a for Pb^{2+}, 10.2 a for Zn^{2+} and 8.9 a for Cu^{2+}.

The **development of a stable ceramic adsorption material from volcanic soil** (Chapter 4.5) indicates that the proposed foaming-sintering process based on the investigated volcanic soil and recycled polyethylene terephtalate (PET) is appropriate for producing a stable ceramic adsorption material. Moreover, an increment in the adsorption capacity of this ceramic material was established (for chlorophenols), compared to natural volcanic soil.

Regarding **possible adsorption mechanisms in volcanic soil** (Chapter 4.6), the results indicate the possible adsorption of color and phenolic compounds to the humic and fulvic acids present in the soil organic matter (SOM). In the case of heavy metals, cation exchange, oxidic fraction binding and adsorption to SOM, were found to be the most possible mechanisms.

The **practical aspects for large-scale industrial use of volcanic soil** (Chapter 4.7) indicate that for a full scale Kraft mill wastewater treatment plant, about 8 ton/d of volcanic soil are necessary. Moreover, for chlorophenols-contaminated groundwater remediation, 8.55 kg volcanic soil per year and m^2 gate section were estimated to be necessary. In addition, for the construction of a simulated 500,000 m^3 sanitary landfill, 60,000 ton volcanic soil were estimated as necessary with an average cost of 45 €/ton.

Finally, the investigated alternatives for the **management of spent volcanic soil** (Chapter 4.8) were the bioremediation of soil for specific chlorophenols and the utilization of the spent volcanic soil as alternative raw material in the clinker/cement industry.

In the first case (i.e., bioremediation of chlorophenols), the biological activity and bioremediation capacity of the volcanic soil indicate that the micro-organisms present in this soil are able to degrade the adsorbed chlorophenols, being its respiratory activity not significantly affected by the contamination levels studied. Actinomicetes and fungi are the most adaptable microorganisms in respect to the strength of the pollution conditions studied.

In the second alternative (i.e, alternative raw material in the clinker/cement industry), the metal oxides content of the volcanic soil (i.e., SiO_2, Al_2O_3 and Fe_2O_3) can be used for the substitution of clay and/or correction materials in primary clinker mixtures. The possible use of contaminated volcanic soil in La Calera cement production facility (Chile) could be 278 ton/d. In addition, only some minor emission problems for Pb and Zn would occur in the worst-case scenario, while using pet-coke and scrap-tires as alternative fuel in the clinker kilns.

6   Conclusions

The volcanic soil of Southern Chile seems to be an interesting natural adsorption material, comparable to natural zeolites. Environmental applications in advanced wastewater treatment (adsorption), groundwater remediation (reactive walls) and as mineral landfill liner appear to be very interesting as well as competitive.

The volcanic soil characterization indicates the presence of SiO_2, Al_2O_3, Fe_2O_3, CaO and other oxides; which may be partially responsible for the environmental pollutants adsorption and ionic exchange capacity. In addition, the presence of organic matter in the soil (SOM) may enhance these adsorption and ionic exchange capacities, suggesting a possible binding mechanism between the environmental pollutants and the humic substances present in the soil organic matter. The particle size distribution of the volcanic soil presents a fine fraction (< 2 µm) between 1 and 23%, which is the most reactive soil fraction. In addition, all the volcanic soil samples at the various investigated sites analyzed presented an acid pH value, toghether with a high buffering capacity, even in the alkaline pH range. The Proctor densities of the analyzed volcanic soil samples are in the lower range compared to typical clay minerals, while the hydraulic conductivity (K_f value) is similar to clay minerals like zeolites. Regarding the mineralogical composition of the volcanic soil, plagioclase (andesine and bytownite), quartz, magnetite and maghemite were found to be the main minerals present in the analyzed samples. In addition, allophane is also present in the volcanic soil, as expected.

Three possible environmental applications of this volcanic soil have been tested: adsorption of color and wastewater pollutants from bleached Kraft mill effluent, adsorption of chlorophenols from synthetic groundwater and adsorption of heavy metals from a synthetic landfill leachate.

In the first application test (Kraft mill effluent) the volcanic soil was capable to retain color and phenolic compounds present in these contaminated wastewaters, and even COD, tannins and lignins were adsorbed. The maximum batch adsorption capacities determined are 2,500 mg color/g and 18.8 mg phenolic compounds/g soil, which are comparable with zeolites adsorption capacity. In a fixed bed, maximum modeled adsorption rates of $3.94*10^{-6}$ and $2.25*10^{-6}$ L/mg*min, for color and phenolic compounds respectively, are obtained, which means in a real full-scale operation the use of 8 ton volcanic soil per day for the treatment of 30,000 m^3 Kraft mill effluent.

In the case of chlorophenols adsorption from synthetic groundwater, the maximum batch adsorption values are 0.74 and 2.81 mg/g soil for 2,4-DCP and PCP, respectively. This values are comparable to those of waste-derived adsorbents. A calculated full-scale groundwater treatment process will need about 8.55 kg volcanic soil per year and per m^2 gate section for an estimated contamination of 100 µg/L, 2,4-DCP and PCP each (assumed retention yield: 99%). Assuming a volcanic soil change-out period of 10 years for replacing the spent adsorbent, the equivalent volcanic soil gate will be 7.1 cm wide, resulting in an estimated hydraulic residence time of about 0.5 days.

In the case of adsorption of heavy metals from a synthetic landfill leachate, the maximum batch adsorption capacities are 2.74, 5.32, 5.86 and 7.44 mg/g for CrO_4^{2-}, Cu^{2+}, Zn^{2+} and Pb^{2+}, respectively. All these values are similar to those for heavy metals retention capacities onto zeolites. Moreover, the relative order of heavy metals uptake onto volcanic soil is Pb^{2+} >> Zn^{2+} > Cu^{2+} >> Cr(VI), which is also similar to other mineral clays.

In addition, the modeled heavy metals diffusion through a 1 m volcanic soil landfill bottom liner shows the same trend, having for Pb^{2+} under worst condition a breakthrough time of 22 a, compared to Cu^{2+} with only 9 a. In this case, assuming a 500,000 m^3 full-scale landfill, with a 1 m volcanic soil basal sealing, an average cost for the volcanic soil of 45 €/ton is obtained. This cost is comparable to that of European zeolites, with a current price between 80-90 €/ton.

For the case of wastewater and groundwater treatment, a porous ceramic material from volcanic soil was developed based on a patented foaming-sintering process that uses recycled PET polyols as the main raw material. This ceramic adsorbent material was developed to resist hydraulic loads, as well as to prevent attrition losses and sludge formation during treatment of contaminated water. The obtained ceramic material has a very stable structure and batch adsorption experiments show an enhanced adsorption capacity compared with the natural volcanic soil. An increment in the adsorption capacity of at least 6 times for 2,4-DCP and 12 times for PCP is observed for the ceramic adsorbent. This fact is explained by the possible pH_{ZPC} increment in the ceramic material compared to natural volcanic soil, enhancing the adsorption of negatively charged compounds, such as PCP at pH 6.0. In the case of Cu^{2+}, as expected, no clear adsorption increment was found comparing the ceramic material with the natural soil.

A sustainable management way for the spent volcanic soil (i.e., contaminated with chlorophenols or heavy metals) was also investigated. The main sound alternatives include bioremediation of soil (for chlorophenols) and immobilization (for heavy metals). Threfore, a natural attenuation process, including the chlorophenols-contaminated soil biological activity, and the possible use of the heavy metal-contaminated volcanic soil in the clinker/cement production were evaluated.

In the case of chlorophenols-contaminated soil, the soil biological activity and bioremediation capacity indicates that the microorganisms present in this soil are able to degrade the adsorbed chlorophenols, being its respiratory activity not significantly affected by the contamination levels studied. Actinomicetes and fungi are the most adaptable microorganisms to the strength pollution conditions studied and are responsible for the initial biodegradation of chlorophenols. After this initial process, bacteria are able to grow again in a less contaminated environment and can participate in the bioremediation process of the soil as well. In addition, the expected soil initial concentrations of 2,4-DCP and PCP were not reached. The volcanic soil works as a dual adsorbent material; the organic matter present in the soil (SOM) has a niticeable affinity to pollutants with a high log K_{ow} value, because of the presence of humic and fulvic acids (i.e. –COOH and phenolic –OH reactive groups). Therefore, the adsorption of chlorophenols onto the soil organic matter (SOM) can be

accomplished by the oligomerization of the pollutants or their binding to the SOM. This phenomenon probably contributes to the determination of a smaller quantity of 2,4-DCP and PCP in the initial time samples as expected, as both pollutants may already be bond to the humic and fulvic acids of the SOM.

In the case of spent contaminated soil use in clinker/cement production, the metal oxides content of the volcanic soil (i.e., SiO_2, Al_2O_3 and Fe_2O_3) can be used for the substitution of clay and/or correction materials in primary clinker mixture. As an example, the possible use of contaminated volcanic soil in La Calera cement production facility (Chile) could be 278 ton/d. In addition, only some minor emission problems would occur in the worst-case scenario, while using pet-coke and scrap-tires as alternative fuel in the clinker kilns. In this case, the Pb and Zn content in the flue gas may exceed the maximum level (or limit values) described in the draft project of the new Chilean emission law for incineration and co-incineration of wastes.

The use of volcanic soil as a cheap natural adsorption material seems to be an interesting alternative. For advanced wastewater and groundwater treatment processes, the developed ceramic adsorbent material will be the most suitable, one, enhancing the adsorption capacity and preventing material losses. On the other hand, the natural volcanic soil can be use as it is as mineral liner in landfill constructions due to the excellent properties of the soil for this matter.

7 Index

7.1 References

[1]   Suzuki, M. (1997) Role of adsorption in water environment processes. Water Science and Technology 35(3):1-11.

[2]   Gupta, V. K., Srivastava, S. K. & Tyagi, R. (2000) Design parameters for the treatment of phenolic wastes by carbon columns (obtained from fertilizer waste material). Water Research 34(5):1543-1550.

[3]   Streat, M., Patrick, J. W. & Camporro-Perez, M. J. (1995) Sorption of phenol and para-clorophenol from water using conventional and novel activated carbons. Water Research 29(2):467-472.

[4]   Karcher, S., Kornmüller, A. & Jekel, M. (2001) Cucurbituril for wastewater treatment. Part I: Solubility of cucurbituril and sorption of reactive dyes. Water Research 35(14):3309-3316.

[5]   Karcher, S., Kornmüller, A. & Jekel, M. (2001) Screening of commercial sorbents for the removal of reactive dyes. Dyes and Pigments 51:111-125.

[6]   Karcher, S., Kornmüller, A. & Jekel, M. (2002) Anion exchange resins for removal of reactive dyes from textile wastewaters. Water Research 36:4717-4724.

[7]   Genz, A., Kornmüller, A. & Jekel, M. (2004) Advanced phosphorus removal from membrane filtrates by adsortion on activated aluminum oxide and granulated ferric hydroxide. Water Research 38:3523-3530

[8]   Dentel, S. K., Bottero, J. Y., Kathib, K., Demougeot, H., Duguet, J. P. & Anselme, C. (1995) Sorption of tannic acid, phenol and 2,4,5-trichlorophenol on organoclays. Water Research 29(5):1273-1280.

[9]   Cox, M., Rus-Romero, J. R. & Sheriff, T. S. (2001) The application of montmorillonite clays impregnated with organic extractants for the removal of metals from aqueous solution. Part I. The preparation of clays impregnated with di-(2-ethylhexyl)phosphoric acid and their use for the removal of copper(II). Chemical Engineering Journal 84:107-113.

[10]   Diez, M. C., Mora, M. L. & Videla, S. (1999) Adsorption of phenolic compounds and color from bleached Kraft mill effluent using allophanic compounds. Water Research 33(1):125-130.

[11]   Navia, R., Levet, L., Mora, M. L., Vidal, G. & Diez, M. C. (2003) Allophanic soil adsorption system as a bleached Kraft mill effluent post-treatment. Water Air and Soil Pollution 148(1/4):321-331.

[12]   Stupp, H. D. (2000) Grundwasserreinigung von LCKW-Schäden durch Pump and Treat oder Reaktive Systeme? TerraTech 2:34-38.

[13]   Zorzi, M. & Hammer, S. (1998) In Situ-Filter-Reaktionswand zur Sanierung von KW- und LHKW-kontaminierten Grundwässern. In: Restabfallbehandlung, Deponietechnik, Entsorgungsbau und Altlastenproblematik, Hengerer et al. (Hrsg.), Balkema (Ed.), Rotterdam, 151-155.

[14]   Kugler, H., Ottner, F., Froeschl, H., Adamkova, R. & Schwaighofer, B. (2002) Retention of inorganic pollutants in clayey base sealings of municipal landfills. Applied Clay Science 21:45-58.

[15]   Mimides, T. & Perraki, T. (2000) Evaluation of the attenuating properties of selected Greek clays for toxic inorganic elements in landfill sites. The Science of the Total Environment 253:1-13.

[16]   Hillel, D. (1998) Environmental soil physics. Academic Press, San Diego, CA, USA.

[17]   Dabrowski, A. (2001) Adsorption - from theory to practice. Advances in Colloid and Interface Science 93:135-224.

[18]   Radovic, L. R., Moreno-Castilla, C. & Rivera-Utrilla, J. (2000) Carbon materials as adsorbents in aqueous solutions. In: Chemistry and physics of carbon, Radovic, L. R. (ed.), vol. 27, Marcel Dekker Inc., New York-Basel.

[19]   Mollah, A. H. & Robinson, C. W. (1996) Pentachlorophenol adsorption and desorption characteristics of granular activated carbon - I. Isotherms. Water Research 30(12):2901-2906.

[20]   Aksu, Z. & Yener, J. (2001) A comparative adsorption/biosorption study of mono-chlorinated phenols onto various sorbents. Waste Management 21:695-702.

[21]   Walker, G. M. & Weatherley, L. R. (1999) Kinetics of acid dye adsorption on GAC. Water Research 33(8):1895-1899.

[22]   Kesraou-Ouki, S., Cheeseman, C. & Perry, R. (1993) Effects of conditioning and treatment of chabazite and clinoptilolite prior to lead and cadmium removal. Environmental Science and Technology 27:1108-1116.

[23]   Peric, J., Trgo, M. & Vukojevic Medvidovic, N. (2004) Removal of zinc, copper and lead by natural zeolite - a comparison of adsorption isotherms. Water Research 38:1893-1899.

[24]   Alvarez-Ayuso, E., García-Sánchez, A. & Querol, X. (2003) Purification of metal electroplating waste waters using zeolites. Water Research 37:4855-4862.

[25]   Altin, O., Ozbelge, H. O. & Dogu, T. (1998) Use of general purpose adsorption isotherms for heavy metal-clay mineral interactions. Journal of Colloid and Interface Science 198:130-140.

[26]   Cincotti, A., Lai, N., Orru, R. & Cao, G. (2001) Sardinian natural clinoptilolites for heavy metals and ammonium removal: experimental and modeling. Chemical Engineering Journal 84:275-282.

[27]   Inglezakis, V. J., Loizidou, M. D. & Grigoropoulou, H. P. (2003) Ion exchange of Pb^{2+}, Cu^{2+}, Fe^{3+} and Cr^{3+} on natural clinoptilolite: selectivity determination and influence of acidity on metal uptake. Journal of Colloid and Interface Science 261:49-54.

[28]   Xu, Y. H., Nakajima, T. & Ohki, A. (2002) Adsorption and removal of arsenic (V) from drinking water by aluminum-loaded Shirasu-zeolite. Journal of Hazardous Materials B92:275-287.

[29]   Tuncan, A., Tuncan, M., Koyuncu, H. & Guney, Y. (2002) Use of natural zeolites as a landfill liner. Waste Management and Research 21:54-61.

[30]   Kaya, A. & Durukan, S. (2004) Utilization of bentonite-embedded zeolite as clay liner. Applied Clay Science 25(1/2):83-91.

[31]   García-Gutiérrez, M., Missana, T., Mingarro, M., Camper, J., Dai, Z. & Molinero, J. (2001) Solute transport properties of compacted Ca-bentonite used in FEBEX project. Journal of Contaminant Hydrology 47:127-137.

[32]   Mora, M. L. & Canales, J. (1995) Interactions of humic substances with allophanic compounds. Communications in Soil Science and Plant Analysis 26(17/18):2805-2817.

[33]   Mora, M. L., Escudey, M. & Galindo, G. (1994) Síntesis y caracterización de suelos alofánicos. Boletín de la Sociedad Chilena de Química 39:237-243.

[34]   Wada, K. (1980) Soils with variable charge. In: B.K.G. Theng (ed.), New Zealand Society of Soil Science, Lower Hutt, New Zealand.

[35]   Yaron, B., Calvet, R. & Prost, R. (1996) Soil pollution. Processes and dynamics. Springer-Verlag Berlin/Heidelberg, Germany.

[36]   Lehmann, M., Zouboulis, A. I. & Matis, K. A. (2001) Modelling the sorption of metals from aqueous solutions on goethite fixed-beds. Environmental Pollution 113:121-128.

[37]   Bright, M. I., Thornton, S. F., Lerner, D. N. & Tellam, J. H. (2000) Attenuation of landfill leachate by clay liner materials in laboratory columns, 1. Experimental procedures and behaviour of organic contaminants. Waste Management and Research 18:198-214.

[38]   Thornton, S. F., Bright, M. I., Lerner, D. N. & Tellam, J. H. (2000) Attenuation of landfill leachate by UK Triassic sandstone aquifer materials, 2. Sorption and degradation of organic pollutants in laboratory collumns. Journal of Contaminant Hydrology 43:355-383.

[39]   Lawrence, M. A. M., Kukkadapu, R. K. & Boyd, S. A. (1998) Adsorption of phenol and chlorinated phenols from aqueous solution by tetramethylammonium- and tetramethylphosphonium-exchanged montmorillonite. Applied Clay Science 13:13-20.

[40]   Stapleton, M. G., Sparks, D. L. & Dentel, S. K. (1994) Sorption of pentachlorophenol to HDTMA-Clay as a function of ionic strength and pH. Environmental Science and Technology 28:2330-2335.

[41]   Abollino, O., Aceto, M., Malandrino, M., Sarzanini, C. & Mentasti, E. (2003) Adsorption of heavy metals on Na-montmorillonite. Effect of pH and organic substances. Water Research 37:1619-1627.

[42]   Lenoble, V., Bouras, O., Deluchat, V., Serpaud, B. & Bollinger, J. C. (2002) Arsenic adsorption onto pillared clays and iron oxides. Journal of Colloid and Interface Science 255:52-58.

[43]   Gupta, V. K. & Ali, I. (2001) Removal of DDD and DDE from wastewater using bagasse fly ash, a sugar industry waste. Water Research 35(1):33-40.

[44]   Gupta, V. K., Jain, C. K., Ali, I., Sharma, M. & Saini, V. K. (2003) Removal of cadmium and nickel from wastewater using bagasse fly ash, a sugar industry waste. Water Research 37:4038-4044.

[45]   Sharma, D. C. & Forster, C. F. (1994) A preliminary examination into the adsorption of hexavalent chromium using low-cost adsorbents. Bioresource Technology 47:257-264.

[46]   Ko, D. C. K., Porter, J. F. & McKay, G. (2000) Optimised correlations for the fixed-bed adsorption of metal ions on bone char. Chemical Engineering Science 55:5819-5829.

[47]   Meunier, N., Blais, J. F. & Tyagi, R. D. (2002) Selection of a natural sorbent to remove toxic metals from acidic leachate produced during soil decontamination. Hydrometallurgy 67:19-30.

[48]   Magdy, Y. H. & Daifullah, A. A. M. (1998) Adsorption of basic dye from aqueous solutions onto sugar-industry-mud in two modes of operation. Waste Management 18:219-226.

[49]   Rozada, F., Calvo, L. F., García, A. I., Martín-Villacorta, J. & Otero, M. (2003) Dye adsorption by sewage sludge-based activated carbons in batch and fixed-bed systems. Bioresource Technology 87:221-230.

[50]   US EPA (1998) Permeable reactive barrier technologies for contaminant remediation. EPA/600/R-98/125, September.

[51]   Pignatello, J. J. (1998) Soil organic matter as a nanoporous sorbent of organic pollutants. Advances in Colloid and Interface Science 76/77:445-467.

[52]   Stevenson, F. J. (1994) Humus chemistry. 2nd edition, John Willey, New York, USA.

[53]   Mader, B. T., Goss, K. U. & Eisenreich, S. J. (1997) Sorption of non-ionic, hydrophobic organic chemicals to mineral surfaces. Environmental Science and Technology 31(4):1079-1986.

[54]   Rebhun, M., de Smedt, F. & Rwetabula, J. (1996) Dissolved humic substances for remediation of sites contaminated by organic pollutants. Binding-desorption model predictions. Water Research 30(9):2027-2038.

[55]   Providenti, M. A., Lee, H. & Trevors, J. T. (1993) Selected factors limiting the microbial degradation of recalcitrant compounds. Journal of Industrial Microbiology 12:379-395.

[56]   Zhou, J. L., Rowland, S. & Mantoura, R. F. C. (1995) Partition of synthetic pyrethroid insecticides between dissolved and particulate phases. Water Research 29(4):1023-1031.

[57]   Luther, S. M., Dudas, M. J. & Fedorak, P. M. (1998) Sorption of sulfolane and diisopropanolamine by soils, clays and aquifer materials. Journal of Contaminant Hydrology 2:159-176.

[58]   Summer, M. E. (2000) Handbook of soil science. CRC Press LLC, London, England.

[59]   Bezoaín, E. (1985) Suelos volcánicos de Chile. In: Tosso, J. (Ed.) Suelos volcánicos de Chile. Instituto de Investigaciones Agropecuarias, Ministerio de Agricultura, Santiago, Chile, pp. 25-95.

[60]   Borie, G., Peirano, P., Zumino, H. & Aguilera, S. M. (2002) N-pool in volcanic ash-derived soils in Chile and its changes in deforested sites. Soil Biology and Biochemistry 34:1201-1206.

[61]   Aguilera, M., Mora, M. L., Borie, G., Peirano, P. & Zunino, H. (2002) Balance and distribution of sulphur in volcanic ash derived soils in Chile. Soil Biology and Biochemistry 34:1355:1361.

[62]   Zech, W. & Hintermaier-Erhard, G. (2002) Böden der Welt - Ein Bildatlas. Spektrum Akademischer Verlag, Heidelberg, Deutschland.

[63]   Scheffer, F. & Schachtsschabel, P. (2002) Lehrbuch der Bodenkunde. 15. Auflage, Spektrum Akademischer Verlag, Heidelberg, Deutschland.

[64]   Shoji, S., Nanzyo, M. & Dahlgren, R. (1993) Volcanic ash soils - Genesis, properties and utilization. Elsevier, Amsterdam, Netherlands.

[65]   McKague, A. B. & Taylor, D. R. (2001) Isomer specific syntheses of chlorinated catechols and guaiacols relevant to pulp bleaching. Chemosphere 45:261-267.

[66]   Kerndorff, H. (1996) Chemische und humantoxikologische Grundlagen. In: Chemie und Biologie der Altlasten, Fachgruppe Wasserchemie in der GDCh (Hrsg.), VCH, Weinheim, Deutschland.

[67]   Jensen, J. (1996) Chlorophenols in the terrestrial environment. Reviews of Environmental Contamination and Toxicology146:25-51.

[68]   Shiu, W. Y., Ma, K. C., Varhanickova, D. & Mackay, D. (1994) Chlorophenols and alkylphenols: A review and correlation of environmentally relevant properties and fate in an evaluative environment. Chemosphere 29(6):1155-1224.

[69]   Schellenberg, K., Leuenberger, C. & Schwartzenbach, R. P. (1984) Sorption of chlorinated phenols by natural sediments and aquifer materials. Environmental Science and Technology 18:652-657.

[70]   Umweltbundesamt Berlin (1987) Umweltchemikalie Pentachlorphenol. Berichte 3/87, Erich Schmidt Verlag Berlin, Deutschland.

[71]   McLaughlin, M. J., Zarcinas, B. A., Stevens, D. P. & Cook, N. (2000) Soil testing for heavy metals. Communications in Soil Science and Plant Analysis 31:1661-1700.

[72]   Lackovic, J. A., Nikolaidis, N. P. & Dobbs, G. M. (2000) Inorganic arsenic removal by zero-valent iron. Environmental Engineering Science 17(1):29-39.

[73]   Namasivayam, C. & Ranganathan, K. (1995) Removal of Cd(II) from wastewater by adsorption on "waste" Fe(III)/Cr(III) hydroxide. Water Research 29(7):1737-1744.

[74]   Low, K. S. & Lee, C. K. (1991) Cadmium uptake by the moss *calympers delesertii*. Bioresource Technology 38:1-6.

[75]   Kawamura, Y., Yoshida, H., Asai, S. & Tanibe, H. (1997) Breakthrough curve for adsorption of mercury (II) on polyaminated highly porous chitosan beads. Water Science and Technology 35(7):97-105.

[76]   CEPI (2002) Annual Report. Confederation of European Paper Industries, Brussels.

[77]   Videla, S. & Diez, M. C. (1997) Experiences of wastewater treatment in Chilean forest industry. Water Science and Technology 35(2/3):221-226.

[78]   European Commission (2001) Integrated pollution prevention and control (IPPC). Reference Document on Best Available Techniques in the Pulp and Paper Industry.

[79]   Walden, C. C., McLeay, D. J. & McKeague, A. B. (1986) Anthropogenic compounds. In: O. Hutzinger (Ed.), The handbook of environmental chemistry, Vol. 3, Part D, Springer-Verlag, Berlin, 1-34.

[80]   Temmink, J. H. M., Field, J. A., van Haastrecht, J. C. & Merckelbach, R. C. (1989) Acute and sub-acute toxicity of bark tannins in carp (Cyprinus carpio L). Water Research 23:341-344.

[81]   Reeve, D. (1991) Organochloride in bleached Kraft pulp. Tappi Journal 74:123-126.

[82]   Briant, C. & Barkley, W. (1991) Biological dehalogenation of Kraft mill wastewater. Water Science and Technology 24(3/4):287-293.

[83]   Vidal, G., Navia, R., Levet, L., Mora, M. L. & Diez, M. C. (2001) Kraft mill anaerobic effluent color enhancement by a fixed-bed adsorption system. Biotechnology Letters 23:861-865.

[84]   Emilio, C. A., Wilson, F. J., Litter, M. I. & Mansilla, H. D. (2002) EDTA destruction using the solar ferrioxalate advanced oxidation technology (AOT). Comparison with solar photo-Fenton treatment. Journal of Photochemistry and Photobiology A: Chemistry 151:121-127.

[85]   Melin, E. S., Järvinen, K. T. & Puhakka, J. A. (1998) Effects of temperature on chlorophenol biodegradation kinetics in fluidized-bed reactors with different biomass carriers. Water Research 32(1):81-90.

[86]   Valo, R., Apajalahti, J. & Salkinoja-Salonen, M. (1985) Studies on the physiology of microbial degradation of pentachlorophenol. Applied Microbiology and Biotechnology 21:313-319.

[87]   Crawford, R. L. & Mohn, W. W. (1985) Microbial removal of pentachlorophenol from soil using Flavobacterium. Enzyme Microbiology and Technology 7:617-620.

[88]   Trudell, J. T., Marowitch, J. M., Thomson, D. G., Fulton, C. W. & Hoffmann R. E. (1994) In situ bioremediation at a wood-preserving site in a cold, semi-arid climate: feasibility and field pilot design. In: Hinchee et al. (Eds.), Bioremediation of chlorinated and polyaromatic hydrocarbon compounds, Lewis Publ., Boca Raton, FL, USA.

[89]   Li, D.-Y., Eberspächer, J., Wagner, B., Kuntzer, J. & Lingens, F. (1991) Degradation of 2,4,6-trichlorophenol by Azotobacter sp. strain GP1. Applied Environmental Microbiology 57:1920-1928.

[90]   Valo, R., Häggblom, M. M. & Salkinoja-Salonen, M. (1990) Bioremediation of chlorophenol containing simulated groundwater by immobilized bacteria. Water Research 24:253-258.

[91]   Järvinen, K. T., Melin, E. S. & Puhakka, J. A. (1994) High-rate bioremediation of chlorophenol contaminated groundwater at low temperatures. Environmental Science and Technology 28:2387-2392.

[92]   Hamby, D. M. (1996) Sites remediation techniques supporting environmental restoration activities-a review. The Science of the Total Environment 191:203-224.

[93]   Yak, H. K., Wenklawiak, B. W., Cheng, I. F., Doyle, J. G. & Wai, C. M. (1999) Reductive dechlorination of polychlorinated biphenyls by zerovalent iron in subcritical water. Environmental Science and Technology 33(8):1307-1310.

[94]   Cheng, I. F., Fernando, Q. & Korte, N. (1997) Electrochemical dechlorination of 4-chlorophenol to phenol. Environmental Science and Technology 31(4):1074-1078.

[95]   Kulikov, S. M., Plekhanov, V. P., Tsyganok, A. I., Schlimm, C. & Heitz, E. (1996) Electrochemical reductive dechlorination of chlororganic compounds on carbon cloth and metal-modified carbon cloth cathodes. Electrochimica Acta 41(4):527-531.

[96]   Morales, J., Hutcheson, R. & Cheng, I. F. (2002) Dechlorination of chlorinated phenols by catalyzed and uncatalyzed Fe(0) and Mg(0) particles. Journal of Hazardardous Materials B90:97-108.

[97]   Gillham, R. W. & O´Hannesin, S. F. (1994) Enhanced degradation of halogenated aliphatics by zero-valent iron. Ground Water 32(6):958-967.

[98]   Johnson, T. L. & Tratnyek, P. G. (1995) Dechlorination of carbon tetrachloride by iron metal: the role of competing corrosion reactions. 209th National Meeting American Chemical Society. Anaheim, CA. Preprint Extended Abstracts, Division of Environmental Chemistry, Vol. 35(1):699-701.

[99]   Matheson, L. J. & Tratnyek, P. G. (1994) Reductive dehalogenation of chlorinated methanes by iron metal. Environmental Science and Technology 28:2045-2053.

[100]   Orth, W. S. & Gillham, R. W. (1996) Dechlorination of trichloroethene in aqueous solutions using Fe^0. Environmental Science and Technology 30(1):66-71.

[101]   Novoszad, M. (2001) Abbau von chlorierten Kohlenwasserstoffen mit elementaren Eisen. Diplomarbeit, Institut für Entsorgungs- und Deponietechnik, Montanuniversität Leoben, Österreich.

[102]   Holzlöhner, U., Meggyes, T. & Seeger, S. (1999) Landfill technology in Germany. Land Contamination and Reclamation 7(2):109-119.

[103]   Pavlov, P., Navia, R., Draganov, L. & Lorber, K. E. (2002) Chemische Stabilität von Abfallteer und mögliche Anwendung als Dichtungsschichtkomponente von Deponien. Berg- und Hüttenmännische Monatshefte 147(11):370-372.

[104]   Fetter, C. W. (1993) Contaminant hydrogeology. Macmillan Publishing Company, NY, USA.

[105]   Voudrias, E. (2002) The concept of a sorption chemical barrier for improving effectiveness of landfill liners. Waste Management and Research 20:251-258.

[106]   Navia, R., Diez, M. C. & Lorber, K. E. (2002) Remediation of sites contaminated with chlorophenols. In: Altlastensanierung, Sanierung von Bergbaualtlasten, Thermische Verwertung von Abfällen, Managementsysteme, Ökobilanzierung und Prozessoptimierung, Lorber et al. (Hrsg.), Verlag Glückauf, Essen, Deutschland, 353-358.

[107]   Roehl, K. E. & Czurda, K. (1998) Diffusion and solid speciation of Cd and Pb in clay liners. Applied Clay Science 12:387-402.

[108]   Okx, J. P. & Stein, A. (2000) An expert support model for in situ soil remediation. Water Air and Soil Pollution 118:357-375.

[109]   DIN 4020 (2003) Geotechnische Untersuchungen für bautechnische Zwecke.

[110]   Bezama, A., Navia, R., Novak, J. & Lorber, K. E. (2004) Novel approaches for the management and redevelopment of contaminated sites. Osterreichischer Wasser- und Abfallwirtschafts Verein (ÖWAV), (in press)

[111]   Steinle, P., Stucki, G., Bachofen, R. & Hanselmann, K. W. (1999) Alkaline soil extraction and subsequent mineralization of 2,6-dichlorophenol in a fixed-bed bioreactor. Bioremediation Journal 3(3):223-232.

[112]   de Jong, E., Field, J. A., Spinnler, H., Wijnberg, J. & de Bont, J. (1994) Significant biogenesis of chlorinated aromatics by fungi in natural environments. Applied Environmental Microbiology 60:264-270.

[113]   Bouwer, E. J. & Zehnder, A. J. B. (1993) Bioremediation of organic compounds – putting microbial metabolism to work. Trends in Biotechnology 11:360-367.

[114]   Obst, U. & Seibel, F. (1996) Biologische und ökotoxikologische Grundlagen. In: Chemie und Biologie der Altlasten, Fachgruppe Wasserchemie in der GDCh (Hrsg.), VCH, Weinheim, Deutschland.

[115]   Cerniglia, C. E. (1984) Microbial metabolism of polycyclic aromatic hydrocarbons. Advances in Applied Microbiology 30:31-71.

[116]   Balfanz, J. (1991) Abbau von Phenol und chlorierten Phenolen durch eine immobilisierte Mischkultur im Modellboden. In: Biologischer Abbau von Chlorkohlenwassestoffen, Schriftreihe Biologische Abwasserreinigung, TU Berlin, Deutschland, 119-131.

[117]   Müller, R. (1997) Einfluss von Böden auf die Fähigkeit von Bakterien, chlorierte Kohlenwasserstoffe abzubauen. In: Reinigung kontaminierter Böden, TU Hamburg-Harburg Deutschland.

[118]   Reineke, W. & Knackmuss, H. J. (1988) Microbial degradation of haloaromatics. In: Ornston, L. N. et al. (eds.), Annual Review of Microbiology, Palo Alto, CA, USA.

[119]   Fam, S. (1996) Vapor extraction and bioventing. In: In situ treatment technology, Chap. 4, CRC Press Inc., USA.

[120]   Scholz, J. & Schwedes, J. (1999) Einfluss des Wassergehaltes auf biologische und physikalische Bodeneigenschaften bei der mikrobiologischen Bodenreinigung in Fesstoffreaktoren -1. Teil -. Altlasten Spektrum 1/99:34-39.

[121]   Scholz, J. & Schwedes, J. (1999) Einfluss des Wassergehaltes auf biologische und physikalische Bodeneigenschaften bei der mikrobiologischen Bodenreinigung in Fesstoffreaktoren -2. Teil -. Altlasten Spektrum 2/99:98-103.

[122]   DVWK (1996) Sanierung kontaminierter Böden. Schriftenreihe des Deutschen Verbandes für Wasserwirtschaft und Kulturbau, Heft 116, Bonn, Deutschland.

[123]   Falk, E., Kienberger, G. & Lugitsch, E. (1996) Konzept zur Unterfangung und Sanierung von Gebäuden auf Deponien am Beispiel Feldbach. In: Abfallbehandlung, Deponietechnik und Altlastenproblematik, Hengerer et al. (Hrsg.), Balkema, Rotterdam, Holland, 153-161.

[124]   Weissenbach, T. & Kaltenbrunner, W. (1998) Sanierung der Altdeponie Feldbach. In: Restabfallbehandlung, Deponietechnik, Entsorgungsbau und Altlastenproblematik, Hengerer et al. (Hrsg.), Balkema, Rotterdam, Holland, 157-163.

[125]   Anitzar-Ladislao, B. & Galil, N. I. (2002) Simulation of bioremediation of chlorophenols in a sandy aquifer. Water Research 37:238-244.

[126]   Eiermann, D. & Bolliger, R. (1996) Industiestandort Gaswerk: Neueste Erkenntnisse aus einer biologischen Langzeit-Bodensanierung. TerraTech 3:37-39.

[127]   Hackett, G. A. R., Easton, C. A. & Duff, S. J. B. (1999) Composting of pulp and paper mill fly ash with wastewater treatment sludge. Bioresource Technology 70:217-224.

[128]   Laine, M. M. & Jorgensen, K. S. (1996) Straw compost and bioremediated soil as inocula for the bioremediation of chlorophenol-contaminated soil. Applied and Environmental Microbiology 62(5):1507-1513.

[129]   Laine, M. M., Haario, H. & Jorgensen, K. S. (1996) Microbial functional activity during composting of chlorophenol-contaminated sawmill soil. Journal of Microbiological Methods 30:21-32.

[130]   Laine, M. M. & Jorgensen, K. S. (1997) Effective and safe composting of chlorophenol-contaminated soil in pilot scale. Environmental Science and Technology 31:371-378.

[131]   Reichert, J. K.& Roemer, M. (1996) Wasch- und Extraktionsverfahren. In: Chemie und Biologie der Altlasten, Fachgruppe Wasserchemie in der GDCh (Hrsg.), VCH, Weinheim, Deutschland.

[132]   Tähkälä, T. I. (1999) Mechanical treatment of chlorophenols contaminated site. M. Sc. Thesis, Helsinki University of Technology, Finland.

[133]   Mulligan, C. N., Yong, R. N. & Gibbs, B.F. (2001) Remediation technologies for metal-contaminated soils and groundwater: an evaluation. Engineering Geology 60:193-207.

[134]   US EPA (1994) Selection of control technologies for remediation of soil contaminated with arsenic, cadmium, chromium, lead or mercury. Revised Draft Engineering Bulletin, Jan. 31.

[135]   Evanko, C. R. & Dzombak, D. A. (1997) Remediation of metals-contaminated soils and groundwater. Technology Evaluation Report, TE-97-01. Ground-Water Remediation Technologies Analysis Center, Pittsburgh, USA.

[136]   Rodsand, T. & Acar, Y. B. (1995) Electrokinetic extraction of lead from spiked Norwegian marine clay. Geoenvironment 2000/2:1518-1534.

[137]   Baker, A. J. M., Reeves, R. D. & McGrath, S. P. (1991) In situ decontamination of heavy metal polluted soils using crops of metal-accumulating plants: A feasibility study. In: In situ bioreclamation, Hinchey, R. E. & Offenbach, R. S. (Eds.), Butterworth-Heineman, Boston, USA, 601-605.

[138]   Bolenz, S., Omran, H. & Gierschner, K. (1990) Treatments of water hyacinth tissue to obtain useful products. Biological Wastes 22:263-274.

[139]   Hunger, H. D., Langenstrassen, R., Schmidt, K. H & Behrendt, G. (2001) Poröse Sinterkeramikwerkstoffe und Verfahren zu ihrer Herstellung. DE-OS 19963554 (22.12.1999/05.07.2001).

[140]   Behrendt, G. & Pohl, M. (1999) Verfahren zur Herstellung von Polyole. DE-OS 19917932 (16.4.98/21.10.99).

[141]   Leppkes, R. (1993) Polyurethane: Werkstoff mit vielen Gesichtern. Verlag Moderne Industrie, Die Bibliothek der Technik, Bd. 91, Deutschland.

[142]   Oertel, G. (1993) Polyurethane Handbook. Carl Hanser Verlag, Munich, Vienna, New York.

[143]   Fuentes, B. (2003) Adsorción de compuestos fenólicos y color presentes en efluente de celulosa Kraft utilizando suelo alofánico. Tesis de Ingeniería Ambiental, Universidad de La Frontera, Temuco, Chile.

[144]   Navia, R., Lorber, K. E., Gallardo, F., Mora, M. L. & Diez, M. C. (2004) The capacity of volcanic soil to adsorb and bioremediate some specific chlorophenols present in contaminated water. 4th IWA World Water Congress and Exhibition, Sep. 19-24, Marrakech, Morocco.

[145]   Navia, R., Fuentes, B., Bezama, A., Lorber, K. E. & Diez, M. C. (2004) The use of volcanic soil as a sanitary landfill liner and its capacity to retain some specific heavy metals. ISWA World Environment Congress and Exhibition, Oct. 17-21, Rome, Italy.

[146]   Diez, M.C., Navia, R., Levet, L., Mora, M.L. & Vidal, G. (2001) Fixed bed adsorption system to color and phenolic compounds removal from Kraft mill aerobic effluent. 6th World Congress of Chemical Engineering, Sep 23-27, Melbourne, Australia.

[147]   Navia, R., Fuentes, B., Lorber, K. E., Mora, M. L. & Diez, M. C. (2004) In-series columns adsorption performance of Kraft mill wastewater pollutants onto volcanic soil. Chemosphere (submitted).

[148]   Rivero, M. J., Ibáñez, R. & Ortiz M. I. (2002) Mathematical modelling of styrene drying by adsorption onto activated alumina. Chemical Engineering Science 57:2589-2592.

[149]   Navia, R., Inostroza, X., Diez, M. C. & Lorber, K. E. (2004) Adsorption of bleached Kraft mill wastewater pollutants onto volcanic soil: fixed bed kinetic model. Journal of Environmental Management (submitted).

[150]   Annesini, M. C., Gironi, F. & Monticelli, B. (2000) Removal of oxygenated pollutants from wastewater by polymeric resins: data on adsorption equilibrium and kinetics in fixed beds. Water Research 34:2989-2996.

[151]   Bird, R. B., Stewart, W. E. & Lightfood, E. N. (1964) Fenómenos de transporte. Reverté S.A. (ed.), Barcelona, España.

[152]   American Public Health Association/American Water Works Association/Water Pollution Control Federation (1985) Standard Methods for the Examination of Water and Wastewater. 16th ed., Washington, USA.

[153]   Martín, M., Cuevas, J. & Leguey, S. (2000) Diffusion of soluble salts under a temperature gradient after hydration of compacted bentonite. Applied Clay Science, 17:55-70.

[154]   Nakashima, Y. (2000) The use of X-ray CT to measure diffusion coefficients of heavy ions in water-saturated porous media. Engineering Geology 56:11-17.

[155]   Alef, K. & Nannipieri, P. (1995) Methods in applied soil microbiology and biochemistry. Academic Press Ltd., San Diego, USA.

[156]   Thompson, I. P., Bailey, M., Ellis, R., Maguire, N. & Meharg, A. (1999) Response of soil microbial communities to single and multiple doses of an organic pollutant. Soil Biology and Biochemistry 31:95-105.

[157]   Alexander, M. (1980) Microbiología del suelo. AGT Editor S.A., Mexico.

[158]   Soto-Córdova, S. M., Baeza, J. & Freer, J. (2001) Soxhlet extraction of pentachlorophenol from soil with in situ derivatization. Boletín de la Sociedad Chilena de Química 46:179-185.

[159]   ÖNORM EN 13137 (2001) Charakterisierung von Abfall; Bestimmung des gesamten organischen Kohlenstoffs (TOC) in Abfall, Schlämmen und Sedimenten.

[160]   Schwedt, G. (1991) Taschenatlas der Analytik. 1. Auflage, Thieme Verlag, Stuttgart, Deutschland.

[161]   DIN ISO 11260 (1997) Bestimmung der effektiven Kationenaustauschkapazität und der Basensättigung unter Verwendung von Bariumchloridlösung.

[162]   Rowell, D. L. (1994) Bodenkunde - Untersuchungsmethoden und ihre Anwendungen. 1. Auflage, Springer Verlag Berlin, Deutschland.

[163]   EN 12176 (1998) Bestimmung des pH-Werts in Schlämmen.

[164]   DIN 18123 (1983) Untersuchung von Bodenproben - Korngrößenverteilung.

[165]   DIN E 18124 (1987) Versuche und Versuchsgeräte – Bestimmung der Korndichte, Kapillar- und Weithalspyknometer.

[166]   DIN EN 12879 (2001) Charakterisierung von Schlämmen – Bestimmung des Glühverlustes der Trockenmasse.

[167]   DIN 18127 (1993) Versuche und Versuchsgeräte – Proctorversuch.

[168]   DIN 18130 (1989) Versuche und Versuchsgeräte – Bestimmung der Wasserdurchlässigkeit, Laborversuche.

[169]   Institut für Allgemeine und Analytische Chemie (2003) Analysenprotokoll Röntgenfluoreszenzanalyse. Montanuniversität Leoben, Österreich.

[170]   Hahn-Weiheimer, P., Hirner, A. & Weber-Diefenbach, K. (1995) Röntgenfluoreszenzanalytische Methoden. Verlag Vieweg, Braunschweig/Wiesbaden, Deutschland.

[171]   Thurman, E. M. & Malcolm, R. L. (1981) Preparative isolations of aquatic humus substances. Environmental Science and Technology 15:463-466.

[172]   Reinert, G., Lotz, W., Fiedler, J., Bauer, T., Heidingsfelder, S., Neesse, T., Keller, U. & Breitner, R. (1999) Trennschnitt 5 µm für die Bodenwäsche-biologische Reinigung der Feinstfraktion. TerraTech 3:49-52.

[173]   DIN 4020 (2003) Geotechnische Untersuchungen für bautechnische Zwecke.

[174]   Joergensen, R. G. & Castillo, X. (2001) Interrelationships between microbial and soil properties in young volcanic ash soils of Nicaragua. Soil Biology and Biochemistry 33:1581-1589.

[175]   Schöffmann, E. (2004) Geologisch-mineralogische Charakterisierung einer Vulkanerde aus Chile zur umwelttechnischen Bewertung. Institut für Prospektion und Angewandte Sedimentologie, Montanuniversität Leoben, Österreich.

[176]   Hafner, G. (2004) Untersuchungen zur Charakterisierung einer Vulkanerde aus Chile in Hinblick auf umwelttechnische Anwendungen. Institut für nachhaltige Abfallwirtschaft und Entsorgungstechnik, Montanuniversität Leoben, Österreich.

[177]   Dubroeucq, D., Geissert, D., Barois, I. & Ledru, M. P. (2002) Biological and mineralogical features of andisols in the Mexican volcanic highlands. Catena 49:183-202.

[178]   Jongmans, A. G., Verburg, P., Nieuwenhuyse, A. & van Oort, F. (1995) Allophane, imogolite and gibbsite in coatings in a Costa Rican andisol. Geoderma 64:327-342.

[179]   Madeira, M., Auxtero, E. & Sousa, E. (2003) Cation and anion exchange properties of andisols from the Azores, Portugal, as determined by the compulsive exchange and the ammonium acetate methods. Geoderma 117:225-241.

[180]   Armas-Espinel, S., Hernández-Moreno, J. M., Muñoz-Carpena, R. & Regalado, C. M. (2003) Physical properties of "sorriba"-cultivated volcanic soils from Tenerife in relation to andic diagnostic parameters. Geoderma 117:297-311.

[181]   Döberl, G. (2004) Evaluierung von Modellen zur Bestimmung des langfristigen Verhaltens von Hausmülldeponien-Wissensdefizite und neue Ansätze. Dissertation, Institut für Wassergüte und Abfallwirtschaft, Fakultät für Bauingenieurwesen, Technische Universität Wien, Österreich.

[182]   Schwertmann, U., Süsser, P. & Nätscher. L. (1987) Protonenpuffersubstanzen im Boden. Zeitschrift für Planzenernährung und Bodenkunde 150:174-178.

[183]   Grazer, R. (2000) Technische Geologie. Vorlesungsskriptum, Institut für Prospektion und Angewandte Sedimentologie, Montanuniversität Leoben, Österreich.

[184]   Kolckmann, F. (1978) Lehrbuch der Mineralogie. 16. Auflage, Verlag Enke, Stuttgart, Deutschland.

[185]   Matthes, S. (1996) Mineralogie - Eine Einführung in die spezielle Mineralogie, Petrologie und Lagerstättenkunde. 5. Auflage, Springer Verlag, Berlin-Deutschland.

[186]   Levet, L. (2001) Estudio de condiciones operacionales para la remoción de color y compuestos fenólicos en columnas de adsorción rellenas con suelo alofánico. Tesis de Ingeniería Ambiental, Universidad de La Frontera, Temuco, Chile.

[187]   Navia, R., Fuentes, B., Mora, M. L. & Diez, M. C. (2001) Capacidad de retención de clorofenoles en suelo volcánico. XXIV Jornadas Chilenas de Química, Nov 28-30, Temuco, Chile.

[188]   Texier, A. C., Andres, Y., Faur-Brasquet, C. & La Cloirec, P. (2002) Fixed bed study for lanthanide (La, Eu, Yb) ions removal from aqueous solutions by immobilized Pseudomonas aeruginosa: experimental data and modelization. Chemosphere 47:333-342.

[189]   Christensen, T. H., Kjeldsen, P., Albrechtsen, H., Heron, G., Nielsens, P. H., Bjerg, P. L. & Holm, P. E. (1994) Attenuation of landfill leachate pollutants in aquifers. Critical Reviews in Environmental Science and Technology 24:119-202.

[190]   Hoffland Environmental Inc. (2004) http://www.hofflandenv.com

[191]   Perry, R. H. & Green, D. W. (1999) Perry`s Chemical Engineers` Handbook. 7th ed., McGraw-Hill Companies Inc.

[192]   Valente, A. J. M., Ribeiro, A. C. F., Lobo, V. M. M. & Jiménez, A. (2004) Diffusion coefficients of lead (II) nitrate in nitric acid aqueous solutions at 298 K. Journal of Molecular Liquids 111:33-38.

[193]   Motas, M. S., Hiskey, J. B. & Collins, D. W. (2000) The effect of copper, acid, and temperature on the diffusion coefficient of cupric ions in simulated electrorefining electrolytes. Hydrometallurgy 56:255-268.

[194]   Lorko, M., Oravec, P., Schmidt, K. H., Hunger, H. D. & Behrendt, G. (2003) Poröse Sinterkeramikformstoffe mit katalytischer Wirkung durch thermische Behandlung von mit Zeolithen hochgefüllten Schaumstoffen auf der Basis von Recyclaten. Wissenschaftliche Beiträge, Technische Fachhochschule Wildau, Deutschland, 41-45.

[195]   Jota, M. A. T. & Hasset, J. P. (1991) Effects of environmental variables on binding of a PCB congener by dissolved humic substances. Environmental Toxicology and Chemistry 10:483-491.

[196]   Bollag, J. M. (1992) Decontaminating soil with enzymes: An in situ method using phenolic and anilinic compounds. Environmental Science and Technology 26:1876-1881.

[197]   Park, J. W., Dec, J., Kim, J. E. & Bollag, J. M. (1999) Effect of humic constituents on the transformation of chlorinated phenols and anilines in the presence of oxidoreductive enzymes or birnessite. Environmental Science and Technology 33:2028-2034.

[198]   Park, J. W., Dec, J., Kim, J. E. & Bollag, J. M. (2000) Transformation of chlorinated phenols and anilines in the presence of humic acid. Journal of Environmental Quality 29:214-220.

[199]   Weber, E. J., Spidle, D. L. & Thorn, K. A. (1996) Covalent binding of aniline to humic substances: I. Kinetic studies. Environmental Science and Technology 30:2755-2763.

[200]   Thorn, K. A., Pettigrew, P. J. & Goldenberg (1996) Covalent binding of aniline to humic substances: II. ^{15}N NMR studies of nucleophilic addition reactions. Environmental Science and Technology 30:2764-2775.

[201]   Dec, J. & Bollag, J. M. (1994) Dehalogenation of chlorinated phenols during oxidative coupling. Environmental Science and Technology 28:484-490.

[202]   Hatcher, P. G., Bortiatynsky, J. M., Minard, R. D., Dec, J. & Bollag, J. M. (1993) Use of high resolution ^{13}C NMR to examine the enzymatic covalent binding of ^{13}C-labeled 2,4-dichlorophenol with humic substances.

[203]   Saavedra, G. (2003) Determinación de la actividad lacasa, manganeso peroxidasa, dehidrogenasa y fosfatasa del suelo para evaluar la detoxificación de un suelo andisol de la IX Región. Tesis de Ingeniería Ambiental, Universidad de La Frontera, Temuco, Chile.

[204]   Tsutsuki, K. & Kuwatsuka, S. (1992) Characterization of humin-metal complexes in a buried volcanic ash soil profile and a peat soil. Soil Science and Plant Nutrition 38(2):297-306.

[205]   Kang, K. H., Shin, H. S. & Park, H. (2002) Characterization of humic substances present in landfill leachates with different landfill ages and its implications. Water Research 36:4023-4032.

[206]   Chen, J., Gu, B., LeBoeuf, E. J., Pan, H. & Dai, S. (2002) Spectroscopic characterization of the structural and functional properties of natural organic matter fractions. Chemosphere 48:59-68.

[207]   Thomsen, M., Lassen, P., Dobel, S., Hansen, P. E., Carlsen, L. & Mogensen, B. B. (2002) Characterisation of humic materials of different origin: A multivariate approach for quantifying the latent properties of dissolved organic matter. Chemosphere 49:1327-1337.

[208]   Ohlenbusch, G., Kumke, M. U. & Frimmel, F. H. (2000) Sorption of phenols to disolved organic matter investigated by solid phase microextraction. The Science of the Total Environment 253:63-74.

[209]   Huang, C. & Yang, Y. L. (1995) Adsorption characteristics of Cu(II) on humus-kaolin complexes. Water Research 29(11):2455-2460.

[210]   Palmer, P. L. (1996) Reactive Walls. In: In-situ treatment technology, Nyer, E. K., Kidd, D. F., Palmer, P. L., Crossman, T. L., Fam, S., Johns II, F. J., Boettcher, G. & Suthersan, S. S. (eds.), CRC Press Inc., Lewis Publishers, Boca Raton, Florida, USA.

[211]   BGB1 1996/164 (2000) Verordnung des Bundesministers für Umwelt über Ablagerung von Abfällen. Deponieverordnung, Kodex Abfallrecht, Österreich.

[212]   Jiménez, A. (2004) Biorrecuperación de suelos contaminados con HCH mediante biorreactores anaerobios. Memoria de Ingeniero Técnico Industrial, Escuela Técnica Superior de Ingeniería, Universidad de Santiago de Compostela, España.

[213]   Cemento Cruz Azul (2004) http://www.cruzazul.com.mx

[214]   Valenzuela, R. & Reyes, C. (2004) Uso de suelo contaminado como materia prima alternativa en la industria cementera: análisis técnico. Tesis de Ingeniería Ambiental, Universidad de Valparaíso, Valparaíso, Chile.

[215]   AMBAR (2000) Evaluación de impacto ambiental: Utilización de neumáticos como combustible alternativo en el horno 9 de la planta industrial de La Calera de Empresas Melón S. A. CONAMA V Región, Chile.

[216]   AMBAR (2002) Evaluación de impacto ambiental: Uso de carbon en los hornos 8 y 9 de la planta industrial de La Calera de Empresas Melón S. A. CONAMA V Región, Chile.

[217]   Piller,   R.   (2001)   Herstellungsverfahren   in   der   Zementindustrie   aus abfallwirtschaftlicher   Sicht.   Studienarbeit,   Institut   für   Entsorgungs-   und Deponietechnik, Montanuniversität Leoben, Österreich.

[218]   Instituto del Cemento y del Hormigón de Chile (2004) http://www.ich.cl/estadistica/

[219]   Anónimo (2003) Sobre coincineración en hornos cementeros. Revista Ecoamérica 19, Junio de 2003.

[220]   US EPA (1998) The inventory of sources of dioxin in the United States. EPA/600/P-98/002Aa.

[221]   Chen, C. M. (2004) The emission inventory of PCDD/PCDF in Taiwan. Chemosphere 54:1423-1420.

7.2   Symbols

a	Year
a	Sieve passage mass fraction
a_1 to a_4	Regression constant
A	Cross section of the soil sample
Å	Angström (1 Å = 10^{-10} m)
A_C	Transversal area of the cylindrical test-tube
AAS	Atomic absorption spectrometry
AEC	Anionic exchange capacity
AOX	Adsorbable organic halides
b	Langmuir model empirical parameter (maximum amount that can be adsorbed)
bp	Break point
BOD	Biological oxygen demand
BTEX	Benzene, toluene, ethybenzene, xylene
c	Heavy metal concentration
cm	Centimeter
cmol+	Cation centimoles
C	Cl_2 bleaching stage
°C	Degrees Celsius
C	Pollutant concentration
C^*	Equilibrium concentration of the pollutant in the liquid phase
C_0	Concentration input value
C_1	Measured magnesium concentration in the sample
C_2	Corrected magnesium concentration in the sample
C_b	Magnesium concentration in the blank solution

C_{calc}	Calculated concentration value
C_E	Specific element concentration
C_{exp}	Experimental concentration value
C_m	Hydrometer's reading correction factor
C_T	Temperature correction factor
C_X	Cation concentration
CEC	Cationic exchange capacity
CEC_{eff}	Effective cationic exchange capacity
CEC_{pot}	Potential cationic exchange capacity
CFU	Colony forming units
Cm	Clay mineral
COD	Chemical oxygen demand
CONAMA	Chilean National Environmental Commission
d	Day
d	Soil particle diameter
d_g	grid surface distance in the crystal analyzer
D	ClO_2 bleaching stage
D_0	Free-solution diffusion coefficient
D_a	Apparent diffusion coefficient
D_e	Effective diffusion coefficient
D_h	Hydrodinamical dispersion coefficient
D_m	Mechanical dispersion coefficient
Da	Dalton
DENOX	NO_x treatment
DMEA	Dimethylethanolamine
DOC	Dissolved organic carbon present in the volcanic soil
$DOC\text{-}PC$	Complex formed after the phenolic compounds adsorption
e.g.	Exempli gratia
E	Optical density
E_4	Humic and fulvic acid absorbance value at 440 nm
E_6	Humic and fulvic acid absorbance value at 640 nm
ECF	Elemental chlorine free
EDTA	Ethylenediamine-tetraacetic acid
EDS	Energy dispersive spectra
EDXRF	Energy dispersive X-Ray fluorescence
EO	Oxygen-reinforced alkaline extraction stage
EOP	Oxygen and hydrogen-peroxide reinforced alkaline extraction stage
ES	Ex situ
E1 to E6	Experiment 1 to experiment 6
f_{oc}	Soil organic carbon fraction
FBAS	Fixed bed adsorption system

g	Acceleration of gravity
g	Gram
h	Hour
h	Height of the hydrometer's body until the begin of the rod
h₁	Distance between the beginning of the rod of the hydrometer and the reading level
h_p	Hydrometer's reading level
Hc	Hydrocarbon radical
HMDM	Heavy metals diffusion model
HPLC	High performance liquid chromatography
i	Groudwater flow gradient
i.e.	Id est
I	Measured intensity
I₀	Modified Bessel function from the first type and order 0
I_i	Initial intensity
I_n	Modified Bessel function from the first type and order n
IS	In situ
ISO	International Standards Organisation
J₀	Bessel function from the first type and order 0
J_n	Bessel function from the first type and order n
k₁	Adsorption rate constant
k₂	Desorption rate constant
k_F	Freundlich model empirical parameter
k_L	Langmuir model empirical parameter (affinity term)
kg	Kilogram
kJ	Kilojoule
km	Kilometer
kV	Kilovolts
K_a	Acidity constant
$K_c{}^* a$	Overall mass transfer coefficient
K_d	Global distribution coefficient
K_f	Hydraulic conductivity
K_{f10}	Hydraulic conductivity at 10°C
K_H	Proton affinity constant
K_{me}	Metal affinity constant
K_{oc}	Carbon-normalized partition coefficient
K_{ow}	Octanol/water partition coefficient
L	Liter
L	Total column/soil sample length
L-E	External limestones mixture
L-N	Limestone from the Navío mine
LOI	Loss on ignition

pK$_a$	- log [K$_a$]
PC	Phenolic compounds
PCBs	Polychlorinated biphenyls
PCP	Pentachlorophenol
PET	Polyethylene terephthalate
Q	Water flowrate
rpm	Revolutions per minute
R	Hydrocarbon radical
R	Corrected auxiliar value
R$_A$	Retardation coefficient
R`	Auxiliar value calculated from the hydrometer's reading
R^2	Regression factor
s	Second
sp	Saturation point
S	Free soil sites
°S	Latitude south degrees
S-H	Proton occupied soil sites
S-Me	Metal occupied soil sites
2*S-Me*	Metal occupied soil sites
SEIA	Chilean Environmental Impact Assessment System
SEM	Scanning electron microscopy
SOM	Soil organic matter
SWP	Soil wash process
t	Time
t´	Modified time variable
ton	Ton (1,000 kg)
T	Temperature
TC	Total carbon
TCE	Trichloroethene
TCF	Total chlorine free
TCP	Trichlorophenol
TIC	Total inorganic carbon
TOC	Total organic carbon
T & L	Tannins and lignins
u$_o$	Linear flow velocity through the column beds for breakthrough curves determination
u$_a$	Average seepage velocity
u$_f$	Filter velocity
US EPA	United States Environmental Protection Agency
v	Soil particle sedimentation velocity
vol.	Volume
V	Solution volume

V_b	Bulk volume occupied by the soil sample in the pycnometer
V_c	Volume of the pycnometer
V_H	Volume of the hydrometer's body
V_{MgSO4}	Added volume of the MgSO$_4$ solution
V_w	Water volume in the pycnometer
W	Total pollutant amount adsorbed
Wt.	Weight
W1	Chlorine input rate contained in the volcanic soil in kiln Nr. 8
W2	Chlorine input rate contained in the volcanic soil in kiln Nr. 9
W3 to W8	Respective heavy metal input rate in the volcanic soil in each kiln
x	Distance from the contaminant surce (column depth)
x/m	Adsorbed amount of pollutant onto the soil
X	Dimensionless liquid phase concentration variable
X_E	Measured specific element
X_C	Measured exchangeable cation
XRD	X-Ray diffractometry
XRFS	X-Ray fluorescence spectrometry
Y	Dimensionless liquid phase equilibrium concentration variable
z	Column length variable
2-CP	2-chlorophenol
3-CP	3-chlorophenol
2,4-DCP	2,4-dichlorophenol
2,6-DCP	2,6-dichlorophenol
2,4,5-TCP	2,4,5-trichlorophenol
2,4,6-TCP	2,4,6-trichlorophenol
2,3,4,6-TeCP	2,3,4,6-tetrachlorophenol
α	Volcanic soil fraction in the column beds for breakthrough curves determination
Δh	Water level difference in Darcy's law principle
ε	Porosity
η	Dynamic viscosity of the soil suspension
θ	Diffraction angle (Bragg law)
λ	X-Ray radiation wavelength
µm	Micrometer
ξ	Tortuosity of the soil column
ρ	Bulk density of the column beds for breakthrough curves determination
ρ_p	Soil particle density
ρ_w	Water density
$\rho\grave{}$	Hydrometer's reading
τ	Dimensionless time variable

Ø	Dimensionless length variable
Ω	Objective error function
]	Adsorptive bond
°	Degree
€	Euros

7.3   Tables

Table 1: Basic types of industrial adsorbents (adapted from [17])

Table 2: Typical properties of selected clay minerals (adapted from [16],[33])

Table 3: Definitions of SOM components of soil (adapted from [51],[52])

Table 4: Mechanisms of adsorption of organic (humic) compounds to clay surface in soil (adapted from [35])

Table 5: Parameters affecting sorption of contaminants to soil (adapted from [55])

Table 6: Physico-chemical properties of relevant chlorinated phenols (adapted from [68])

Table 7: Heavy metals produced in different industrial, agricultural and domestic activities

Table 8: Effect of low groundwater temperature in the mineralization of chlorophenols

Table 9: Organochlorinated compounds treatability with Fe0 as reactive wall (adapted from [50],[97])

Table 10: Fe0 and activated carbon as reactive barrier for cholorophenols reduction in groundwater remediation

Table 11: Geohydrological parameters of different soil types (adapted from [108],[109])

Table 12: Kraft mill wastewater characterization

Table 13: Breakthrough experiment conditions

Table 14: Description of soil in relationship to the particle size fractions

Table 15: TC, TIC, TOC and SOM content in volcanic soil and zeolite samples [176]

Table 16: Chemical characterization of volcanic soil and zeolite samples by flame-AAS. Content of metal oxides and elemental composition ( ) [176]

Table 17: Chemical characterization of volcanic soil and zeolite samples by XRFS. Content of metal oxides and elemental composition ( ) [176]

7.4   Figures

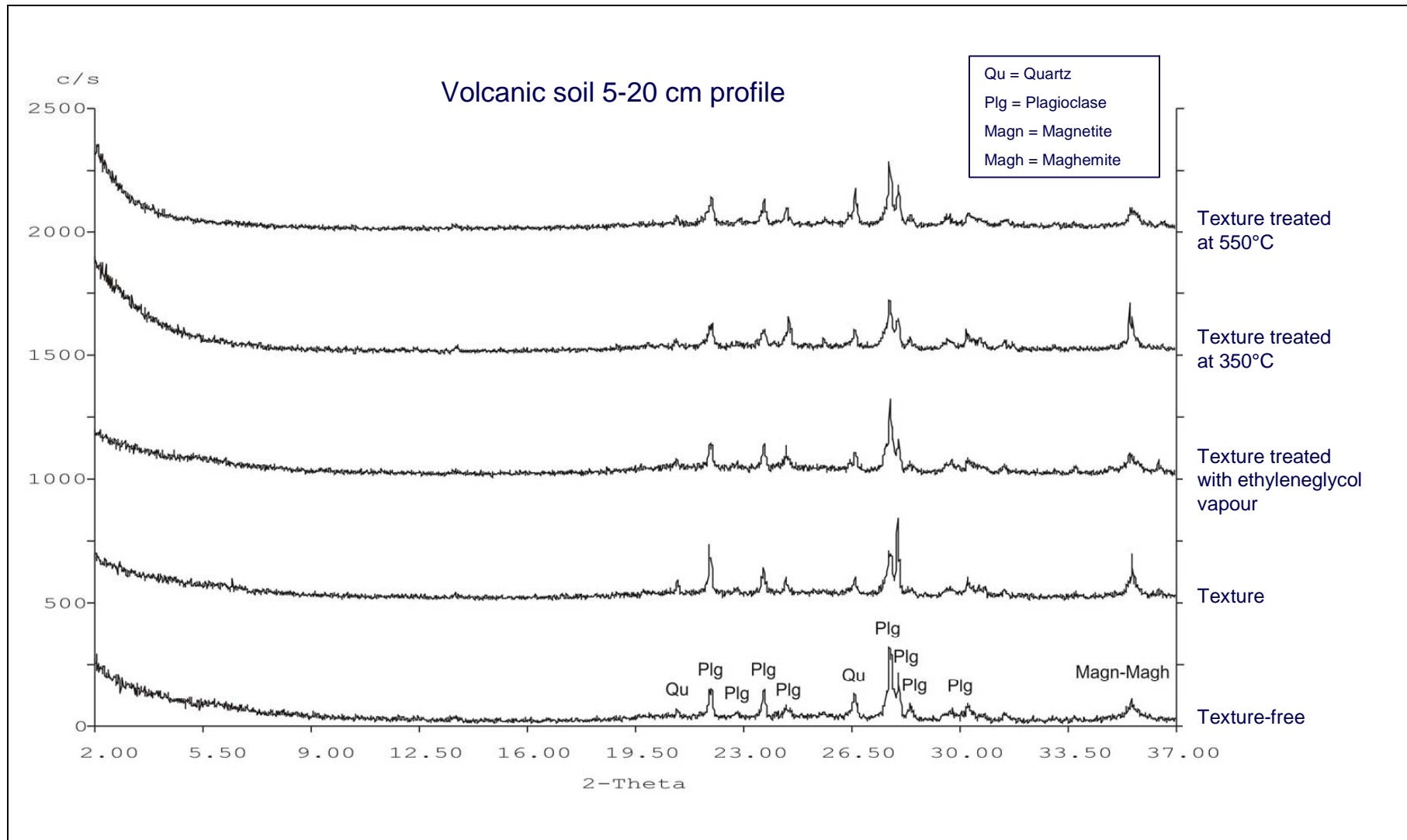## Annex I: Roentgen diffractograms (XRD-spectra)

Figure I-1: Roentgen diffractogram (XRD-spectra) of the volcanic soil 5-20 cm profile
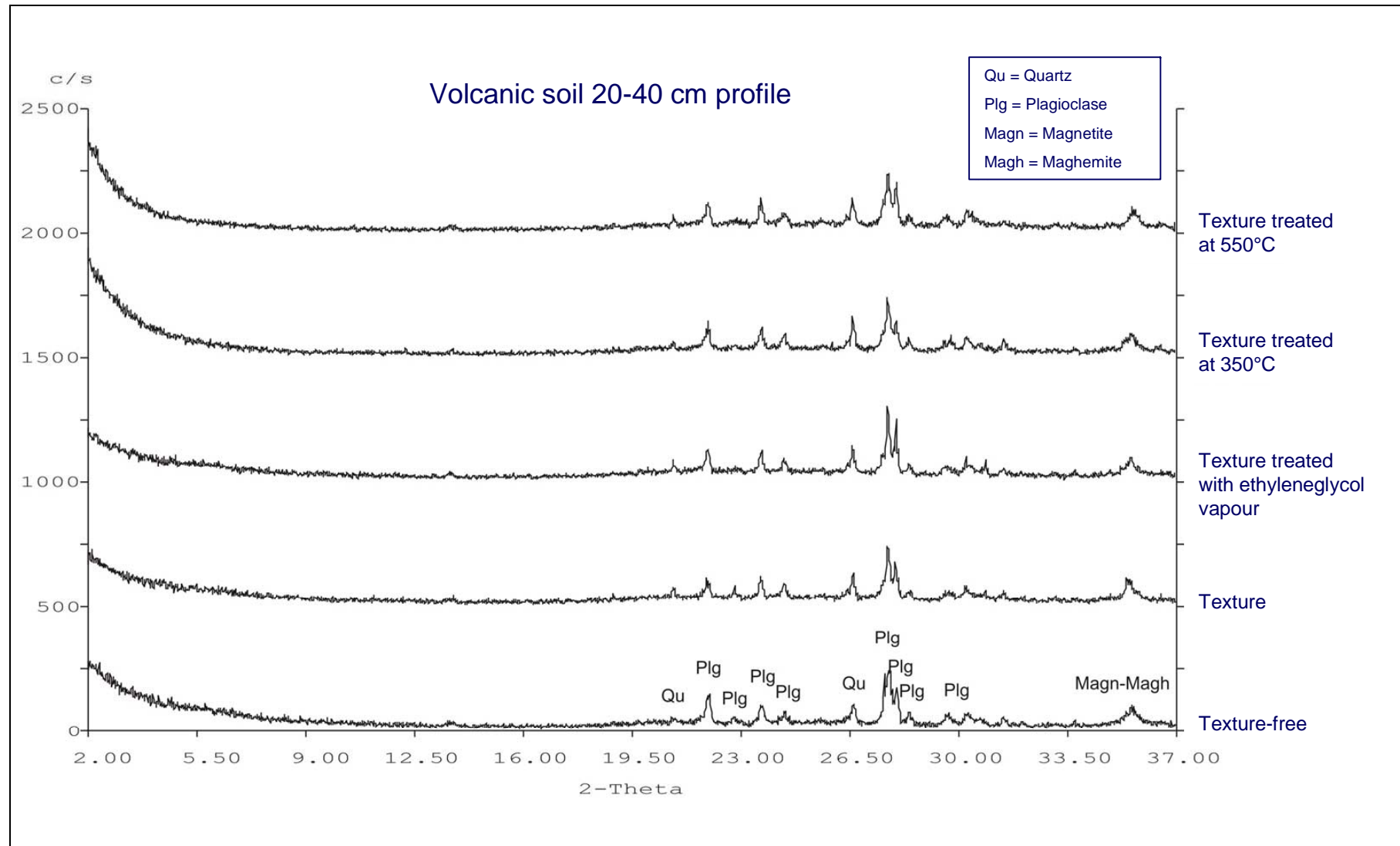
Figure I-2: Roentgen diffractogram (XRD-spectra) of the volcanic soil 20-40 cm profile
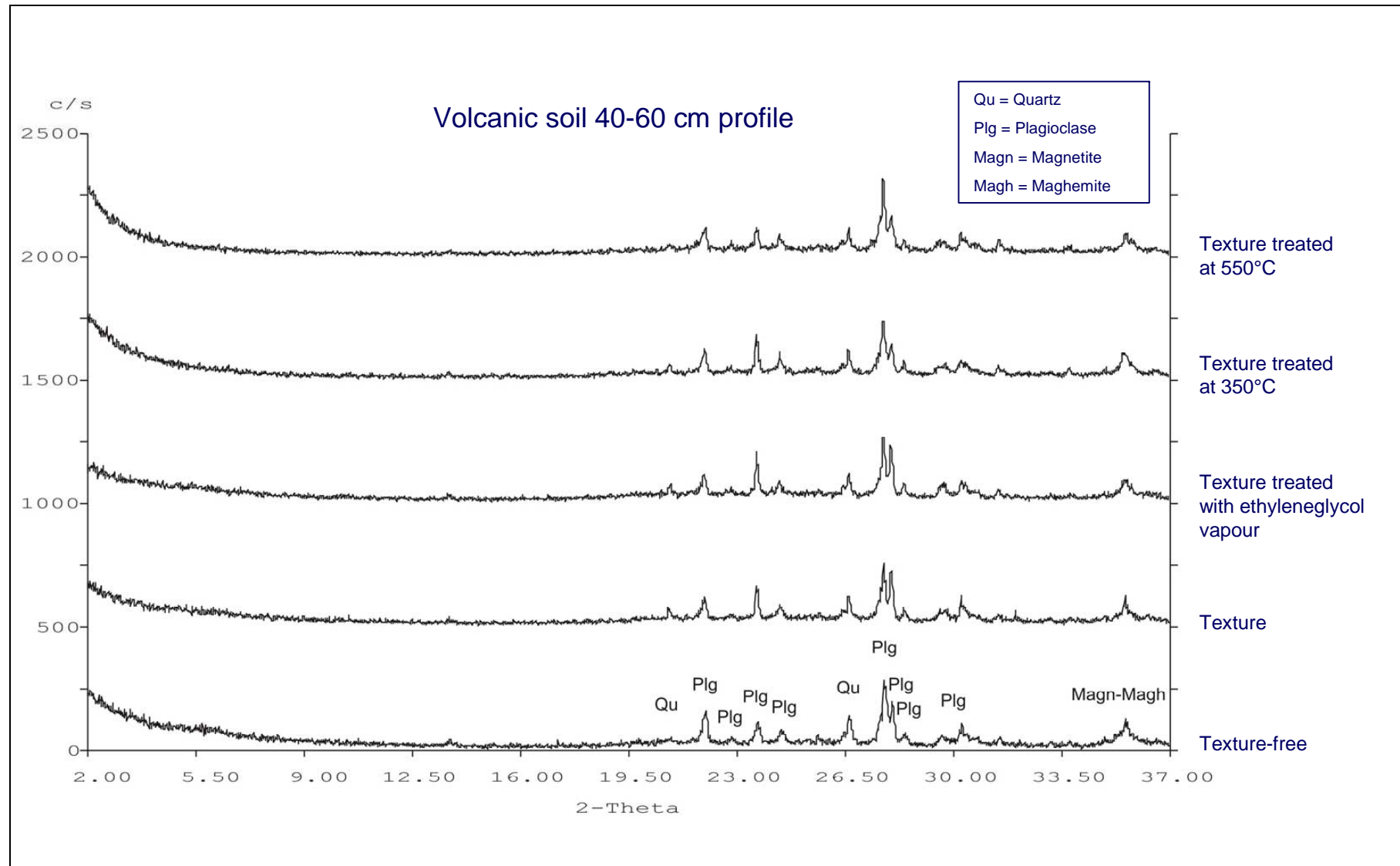
Figure I-3: Roentgen diffractogram (XRD-spectra) of the volcanic soil 40-60 cm profile
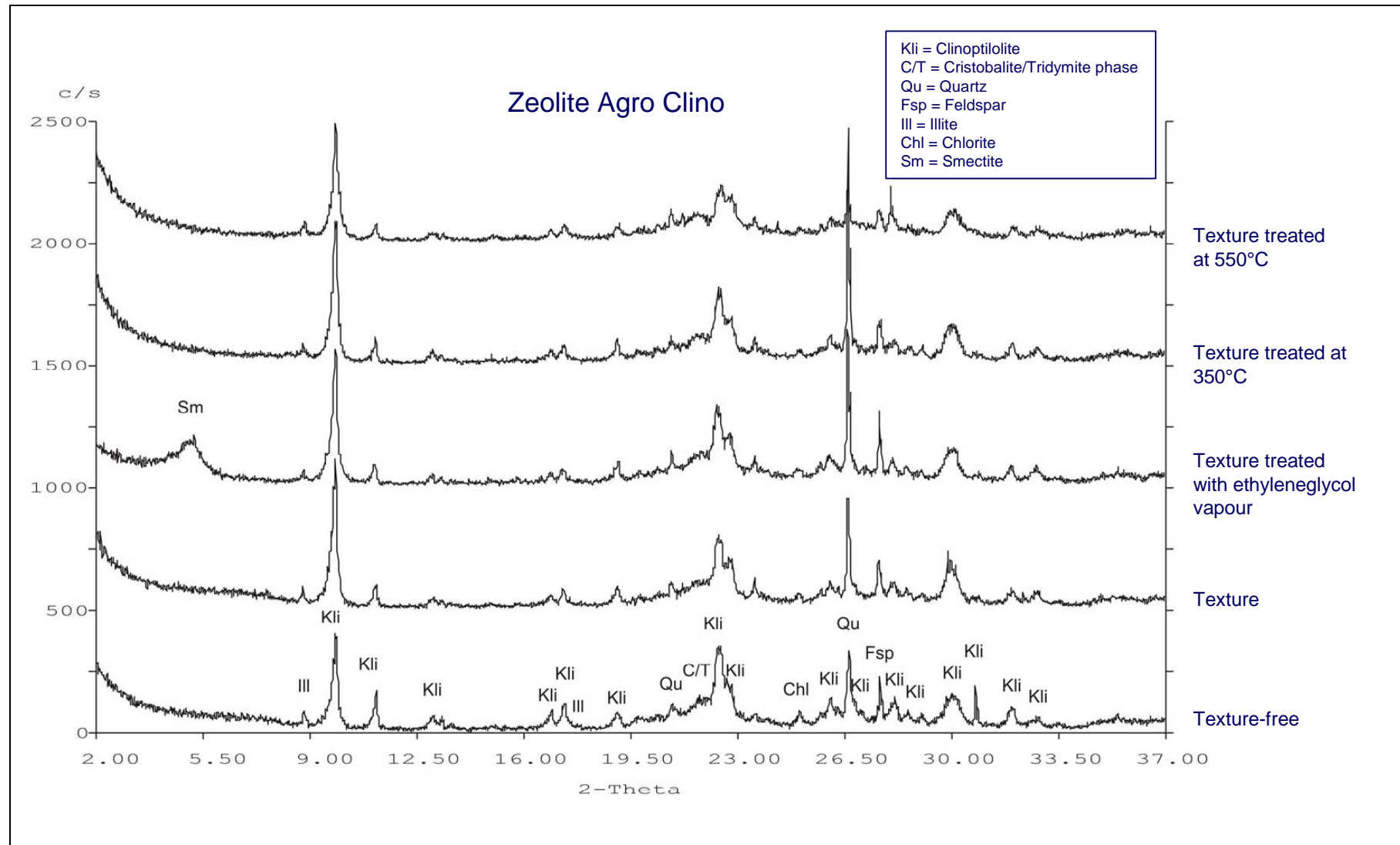
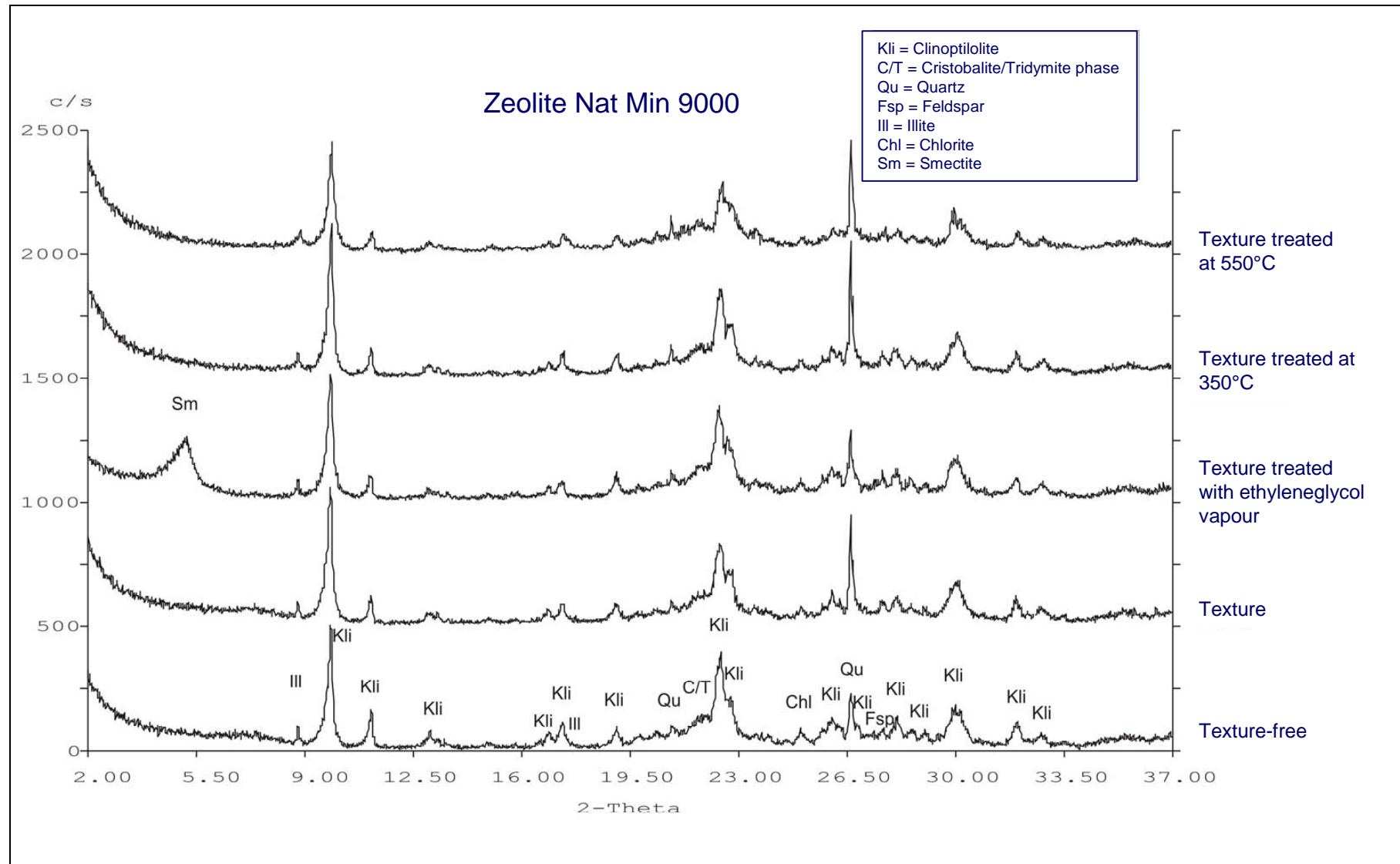Figure I-4: Roentgen diffractogram (XRD-spectra) of the zeolite Agro Clino

Figure I-5: Roentgen diffractogram (XRD-spectra) of the zeolite Nat Min 9000

Annex II: Scanning electron microscopy (SEM) analyses

The results of the scanning electron microscopy (SEM) analyses for volcanic soil (20-40 cm profile) and zeolite Agro Clino are summarized in Tables II-1 and II-2.

Table II-1: Summarized SEM analyses for volcanic soil profile 20-40 cm

Point	Composition [%]								Identified Mineral Phase
	SiO_2	Al_2O_3	Na_2O	CaO	K_2O	MgO	Fe_2O_3	TiO_2	
(1)	54.09	28.41	7.21	9.55	-	-	0.74	-	Andesine/Labradorite
(2)	Only Si and oxygen peaks								Quartz
(3)	57.75	9.66	4.98	2.04	2.38	8.87	12.13	2.19	Not identified
(4)	46.24	34.15	2.54	16.38	-	-	0.69	-	Bytownite
(5)	Similar to point (6)								Allophane
(6)	48.31	31.17	3.40	1.98	-	-	12.97	1.81	Allophane

Table II-2: Summarized SEM analyses for zeolite Agro Clino

Point	Composition [%]								Identified Mineral Phase
	SiO_2	Al_2O_3	Na_2O	CaO	K_2O	MgO	Fe_2O_3	TiO_2	
(1)	65.66	19.05	3.32	-	11.96	-	-	-	Sanidine
(2)	71.98	14.31	0.87	-	11.55	-	1.29	-	Sanidine
(3)	Only Si and oxygen peaks								Quartz
(4)	65.65	18.57	3.03	-	12.75	-	-	-	Sanidine
(5)	63.32	22.70	8.99	3.91	1.08	-	-	-	Oligoclase
(6)	63.43	22.82	8.54	4.12	1.09	-	-	-	Oligoclase
(7)	77.84	13.60	0.92	1.95	2.43	1.12	2.13	-	Clinoptilolite
(8)	79.92	12.07	0.95	2.02	3.02	0.60	1.42	-	Clinoptilolite
(9)	69.85	17.37	0.72	1.01	6.84	1.36	2.86	-	Clinoptilolite
(10)	77.90	14.29	0.80	1.78	1.23	1.48	2.52	-	Clinoptilolite

Annex III: Fixed bed adsorption system

For the breakthrough curves determination the following scheme was used (Figure III-1). The polluted effluent is passed through the volcanic soil column until no more adsorption takes place. M_s is the total pollutant adsorbed mass during the breakthrough curve determination, C_e is the pollutant concentration in the column output at any time or effluent volume passed through the column, C_b is the pollutant concentration in the column output at the break point, C_x is the pollutant concentration in the column output at the exhaustion or saturation point, C_o is the pollutant concentration in the column output at the moment in which no more adsorption takes place and is equal to the column input pollutant concentration. V_e is the total effluent volume passed through the column and V_b and V_x are the effluent volumes passed through the column at the break point and exhaustion point, respectively.
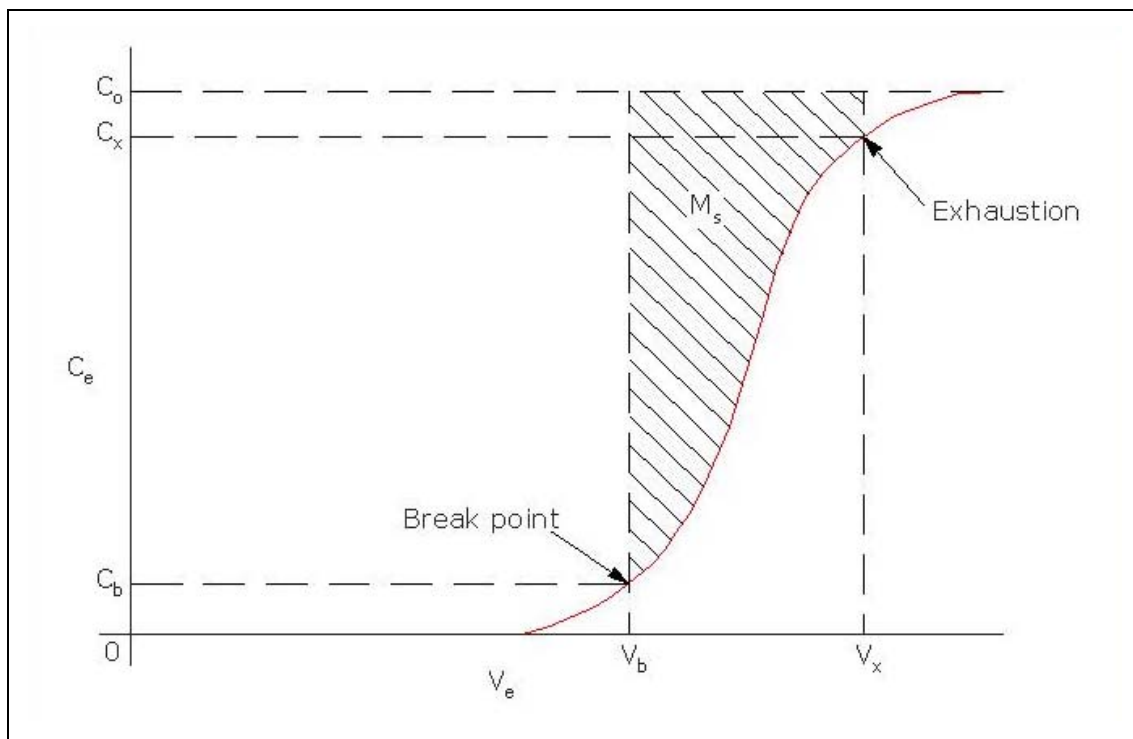
Figure III-1: Breakthrough curve determination in a column system

The complete fixed bed adsorption system is presented in Figure III-2. Four simultaneous columns were filled with volcanic soil as adsorbent material and sand as structure material. The brown-colored bleached Kraft mill effluent was pumped through the columns on the top, and was received and sampled at the bottom of each column. Initially, the effluent output was completely transparent (before the break point), as shown in Figure III-2. The four columns were operated simultaneously, filled with activated soil (acidified), natural soil and different mixture ratios with sand, for comparison purposes. The effluent at the column output was analyzed for color, phenolic compounds, tannins and lignins, COD, pH and total accumulated volume. One of the single columns is presented in Figure III-3. A 2 cm brown-colored Kraft mill effluent level (column input) is shown at the top of the column. The effluent color change during the breakthrough curve determination is presented in Figure III-4.

Figure III-2: Four simultaneous columns for breakthrough curves determination

Figure III-3: Single column with a level of brown-colored
Kraft mill effluent

Figure III-4: Effluent color change during the breakthrough curves determination

It can be clearly seen that initially, the effluent sampled at the column output was completely transparent (Figure III-4, flask 2), compared with the input brown-colored Kraft mill effluent (Figure III-4, flask 1). During the experience, the effluent at the column output was becoming a light brownish color, as shown for the breakpoint (Figure III-4, flask 3) and finally at the exhaustion point (Figure III-4, flask 4).

Annex IV: Heavy metal diffusion trials system

An overview of the volcanic soil columns used for heavy metal diffusion determination is presented in Figure IV-1. The different columns correspond to different pH-values, diffusion times and soil profiles studied.

Figure IV-1: Overview of the volcanic soil columns for heavy metal diffusion determination

Figure IV-2: Single column slices previous to heavy metal determination in soil

In Figure IV-2 and IV-3, a single column is presented after finishing its diffusion trial. The column was cut in slices for heavy metal determination in different depths of the volcanic soil column.
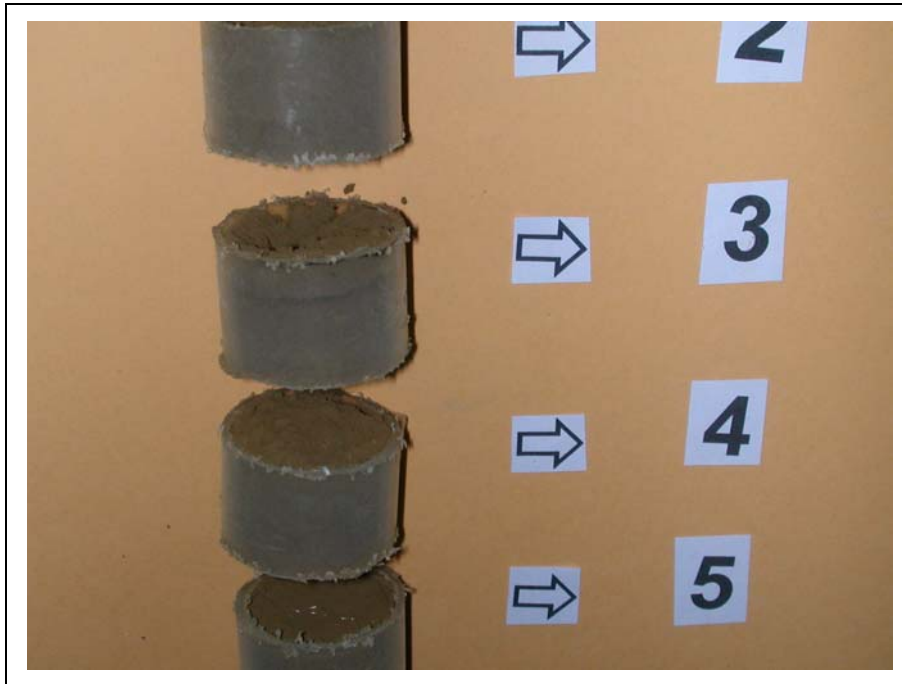
Figure IV-3: Single column slices close-up

Annex V: Foaming/sintering process reactives and materials
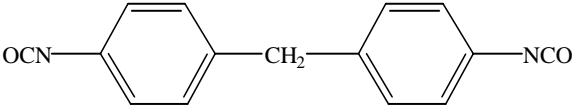
Table V-1: Specific reactives used in the foaming process
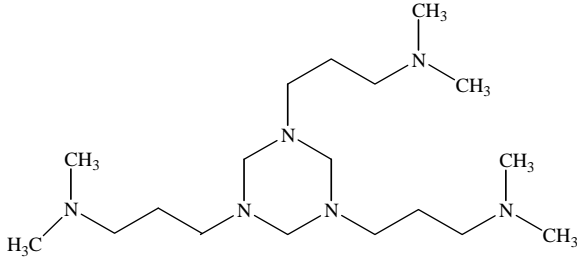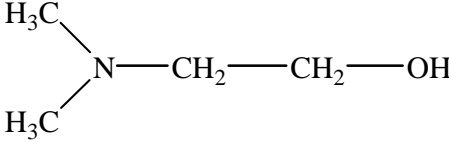
Reactant	Characteristics	Commercial name	Dose (g)
Polyol	Aromatic polyester-polyol obtained from recycled PET residues OH- Value 363 mg KOH/g Viscosity 2300 mPa s	Polyol 260	48
1,3,5-tris(dimethylaminopropyl) hexahydrotriazine	Catalyst 1	PC-Cat NP 40	0.15
Dimethylethanolamine	Catalyst 2	DMEA	0.15
Polyetersyloxan	Stabilisator	Tegostab B8433	0.15
Water	Blowing agent H_2O	-	1.05
Diphenylmethane-4,4`-diisocyanate		Lupranat M 20 A	60

Figure V-1: Carbolite sintering oven (general view)
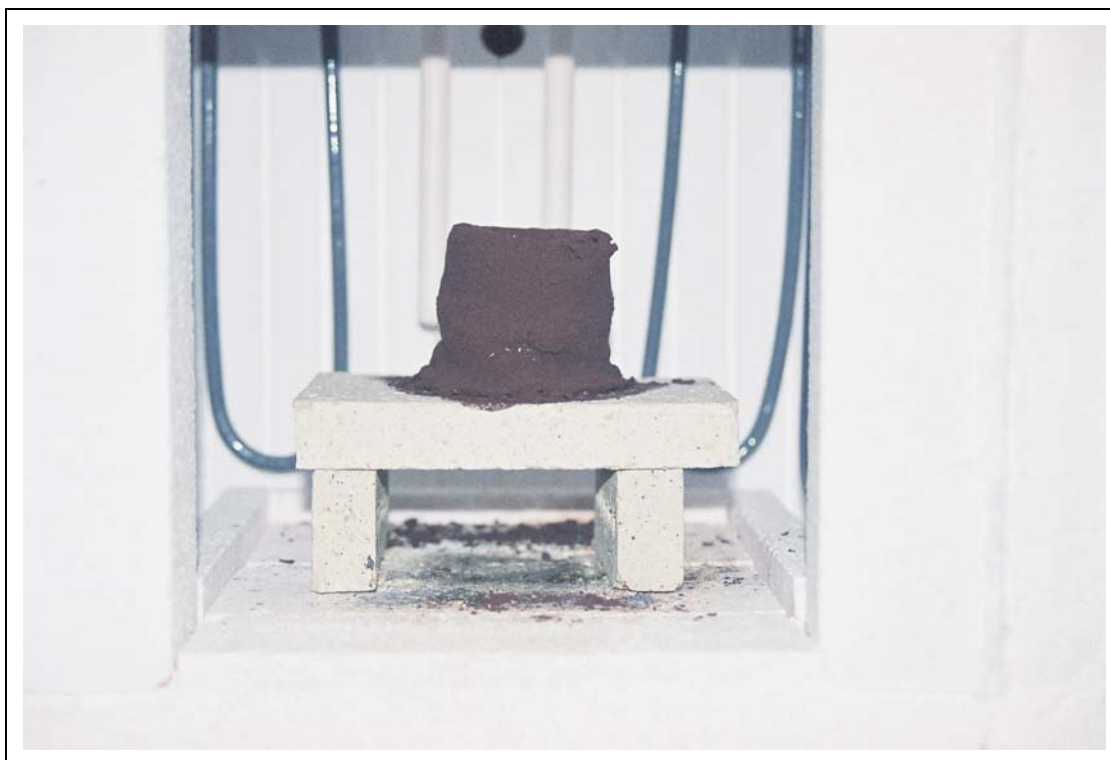
Figure V-2: Carbolite sintering oven (internal view)

Annex VI: Thermal behavior of the volcanic soil

The theoretical melting point of the volcanic soil was estimated from the Al_2O_3-FeO-SiO_2 ternary system diagram (Figure VI-1) and was compared with zeolite Nat Min 9000 (Table VI-1). As the other metal oxides (CaO, MgO, Na_2O, TiO_2, P_2O_5, K_2O and MnO, see Table 17) are only present in very small quantities, they were neglected for estimating the theoretical melting temperature. In practice, FeO from diagram has to be converted to Fe_2O_3, which is present in the volcanic soil.
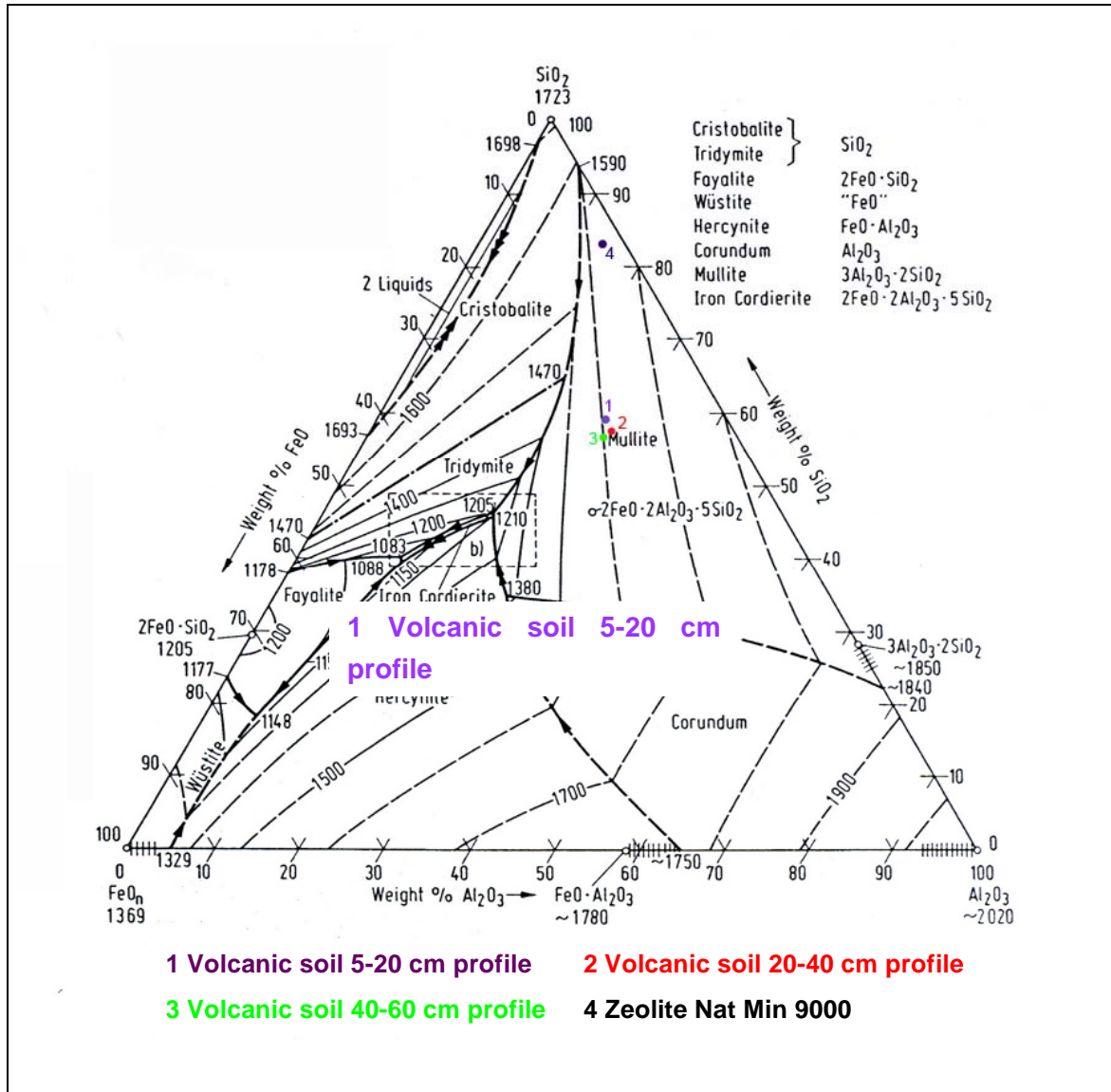

Figure VI-1: Al_2O_3-FeO-SiO_2 system diagram in equilibrium with iron (the FeO content was determined theoretically with the iron content previously determined in Table 17)

The values are in agreement with the performed thermal behavior test of the volcanic soil. In fact, ARP/ECV GesmbH, Leoben, Austria, according to DIN 51730 (ash thermal behavior), performed the thermal behavior of the volcanic soil. Two samples were analysed; the fine fraction of the volcanic soil determied by ARP/ERC (5068/analysefein) and a special sample

of volcanic soil with a particle size under 100 μm (5068/<100μm). The thermal behavior of the 5068/<100μm sample was considered for the development of the stable ceramic adsorption material from volcanic soil. In Table VI-2 the thermal behaviors of both samples are summarized.

Table VI-1: Theoretical melting points of volcanic soil and zeolite

|	Theoretical melting point (°C)
Volcanic soil 5-20 cm profile	1605
Volcanic soil 20-40 cm profile	1610
Volcanic soil 40-60 cm profile	1600
Zeolite Nat Min 9000	1620

Table VI-2: Thermal behavior of the volcanic soil samples analyzed by ARP/ERC GesmbH, Leoben

Melting behavior	ARP/ECV sample	
	5068/analysefein	5068/<100μm
Refractory deformation temperature (Erweichungstemperatur)	Not visible	Not visible
Hemispheric point (Halbkugelpunkt)	1370°C	1380°C
Flowing point (Fliesspunkt)	1385°C	1415°C

As example of the performed test, the thermal behavior of the 5068/analysefein is presented in the following picture series.
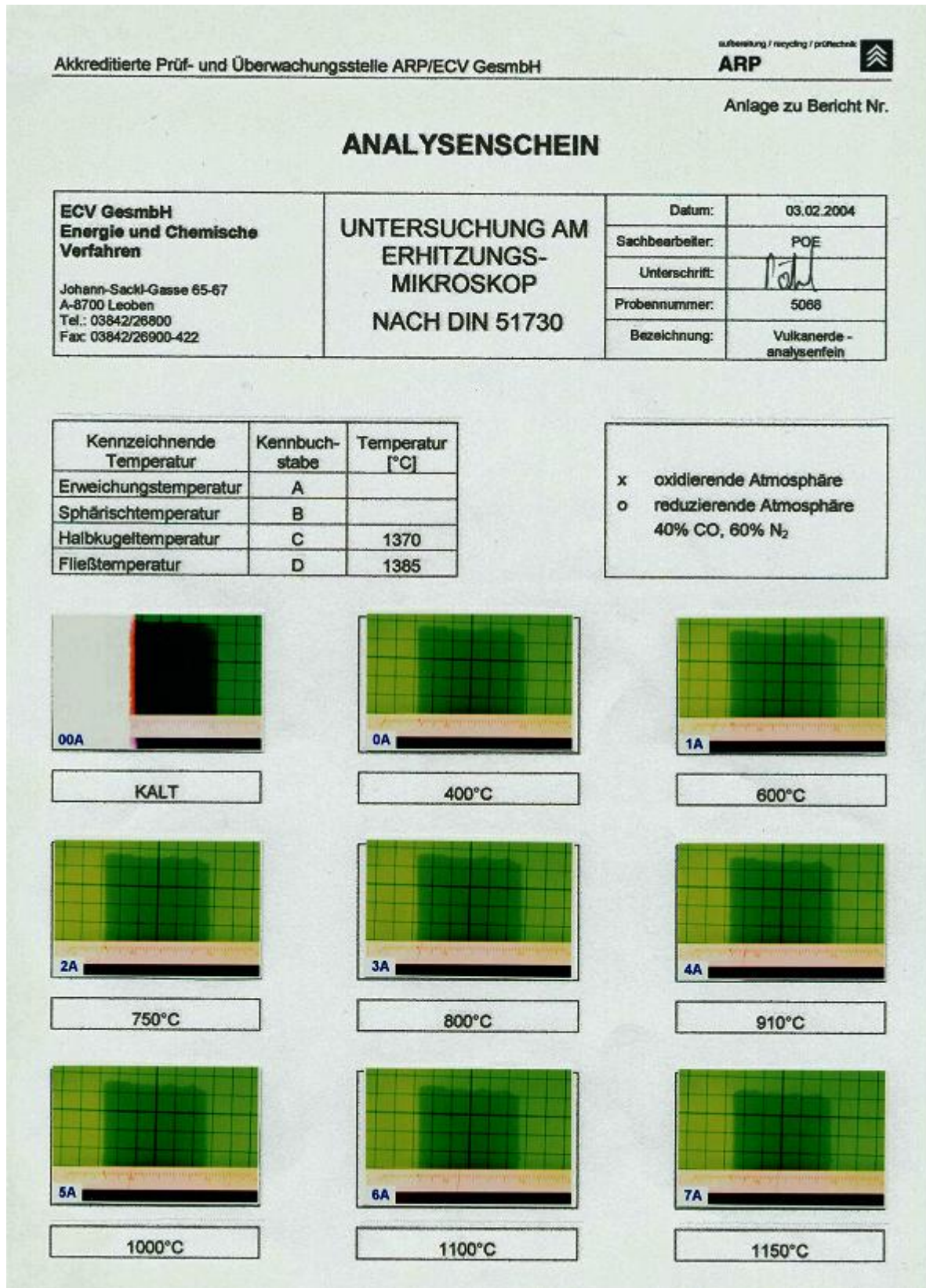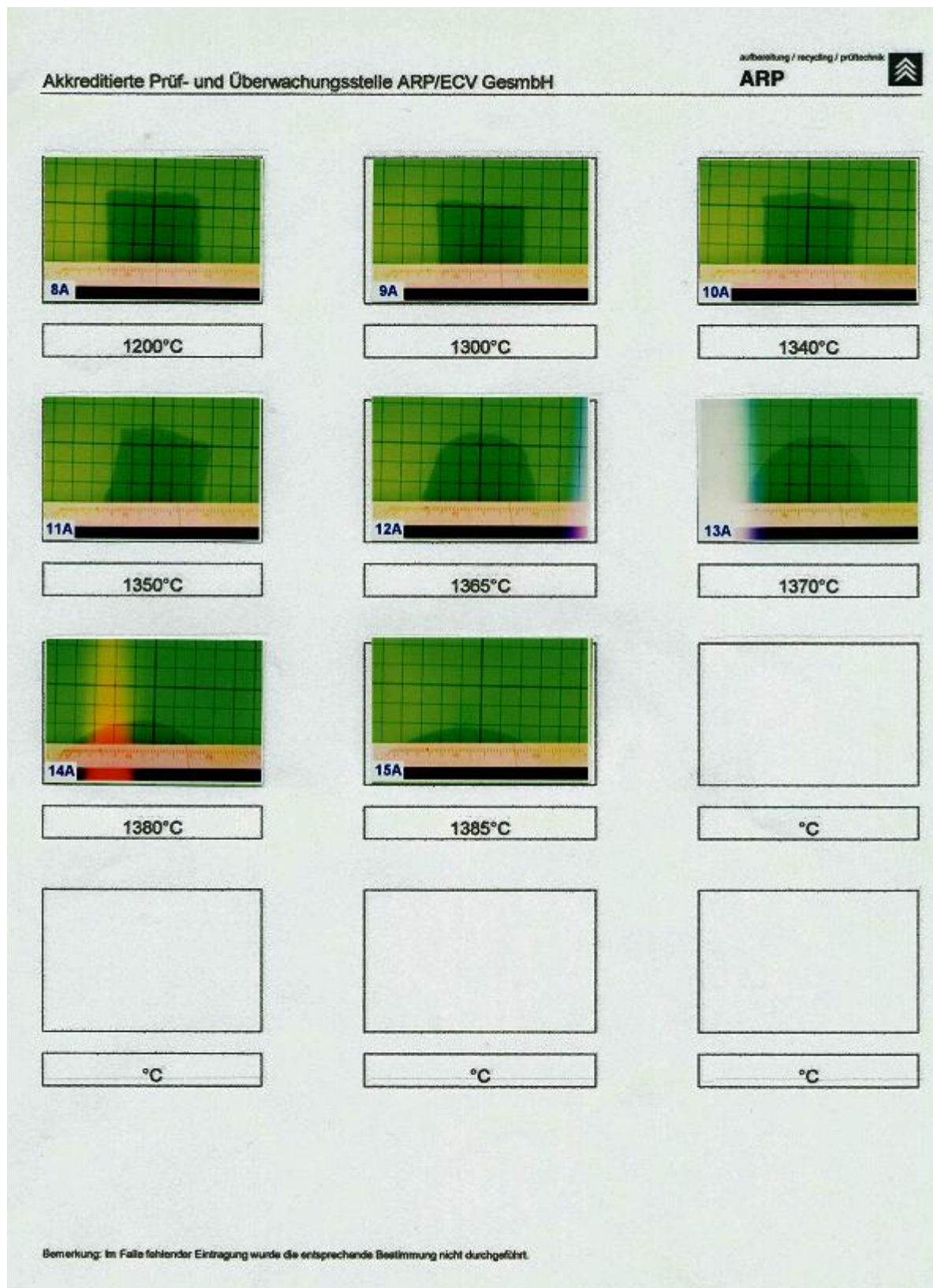
Annex VII: Reactive wall "funnel and gate"-engineering

The funnel and gate system is one of the most used configurations for the in-situ remediation of contaminated groundwater. The cutoff walls are normally made of steel and the reactor walls can be made of different materials depending on the pollutants and the associated costs. The cutoff walls can be constructed using different technologies (like sheet-pile walls, slurry trench walls and others) and materials depend principally on the depth of the walls and the desired hydraulic conductivity, respectively. Typical cutoff wall depths can vary between 15 and 100 m, while the hydraulic conductivities can vary between 10^{-8} and 10^{-10} m/s for bentonite and bentonite-cement mixtures and zero for steel walls.

The reactive wall reactors are mainly constructed as some kind of filter tubes that are then inserted in a special configuration into the gate. Typical reactive materials used are activated carbon, biocoal (carbon with a biological activity), zeolites and zero-valent metals.
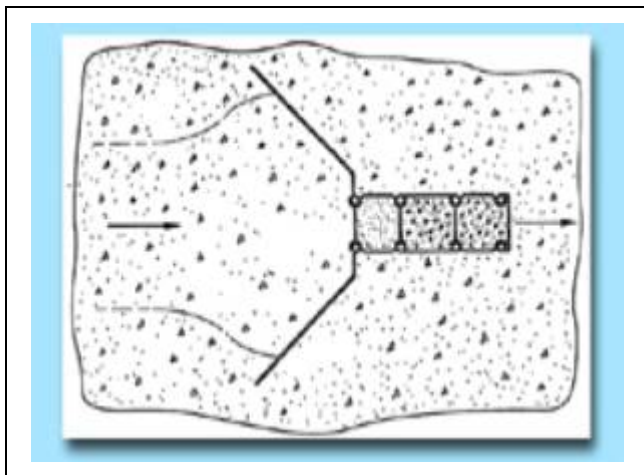

Figure VII-1: Typical funnel and gate configuration

Figure VII-2: Silet-piler method for building a sheet-pile cutoff wall
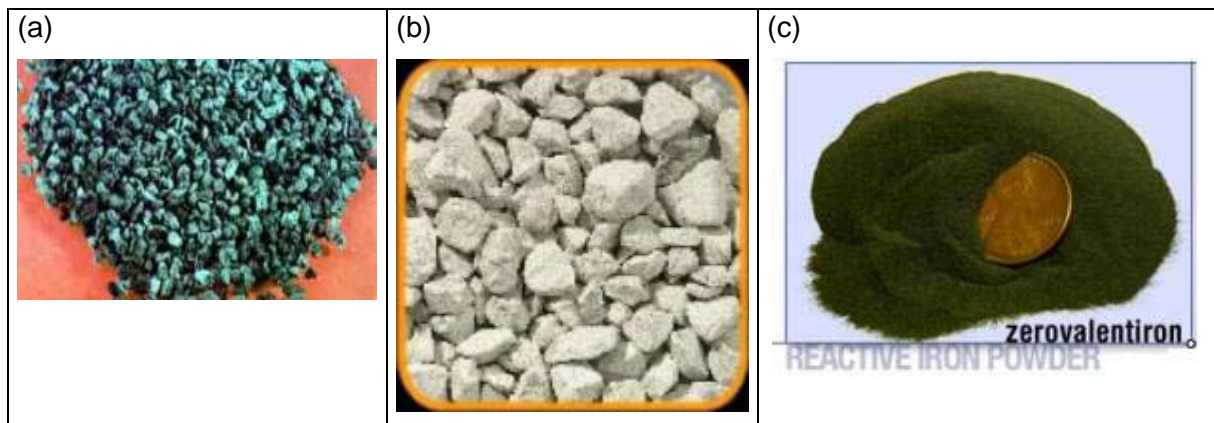
Figure VII-3: Reactive wall reactor modules

Figure VII-4: Reactive materials (a) biocoal, (b) zeolite and (c) zero-valent iron

Annex VIII: Sanitary landfill engineering

The typical landfill construction features are presented in this Annex. The base and cover sealing for non-hazardous wastes are presented in Figures VIII-1 and VIII-2. The volcanic soil studied could be used as a geological barrier, due to its excellent properties for retaining specific pollutants. Moreover, the hydraulic conductivity of the soil is near the EU normative values. Typical geomembranes and geotextiles used for landfill basal sealings are presented in Figure VIII-3 and typical landfill leachate pipes and pipeline configuration in the underground of the landfill base is presented in Figure VIII-4. The generated biogas is collected through a gas manifold and burned for energy recovery (Figure VIII-5), while the collected leachate of modern landfills is treated in a reverse osmosis plant (Figure VIII-6) or other facilities.
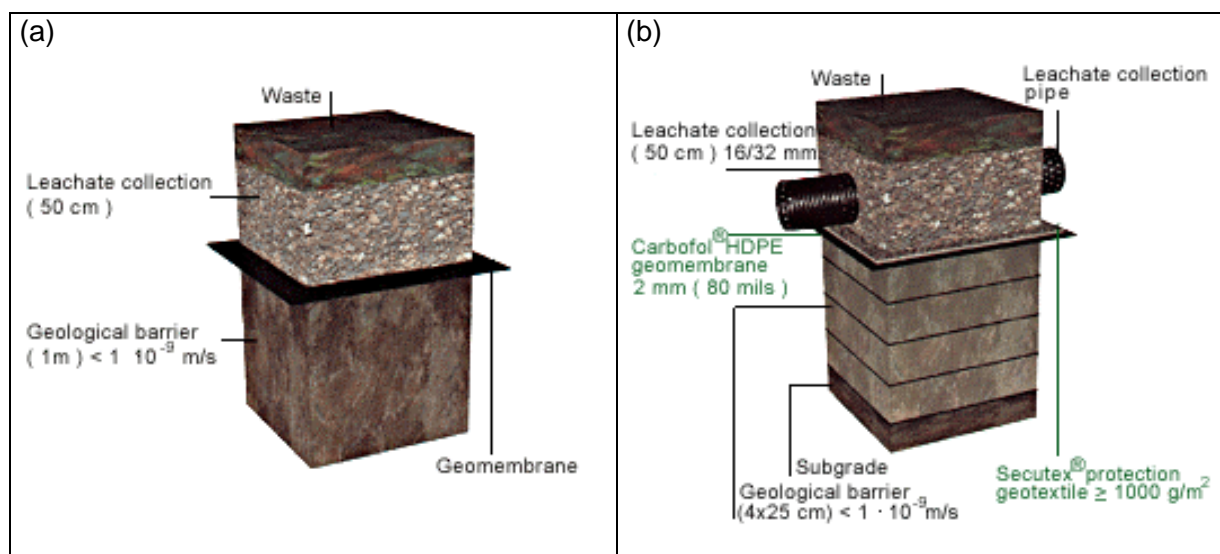

Figure VIII-1: Non-hazardous waste landfill basal sealing (a) EU normative (b) EU state of practice
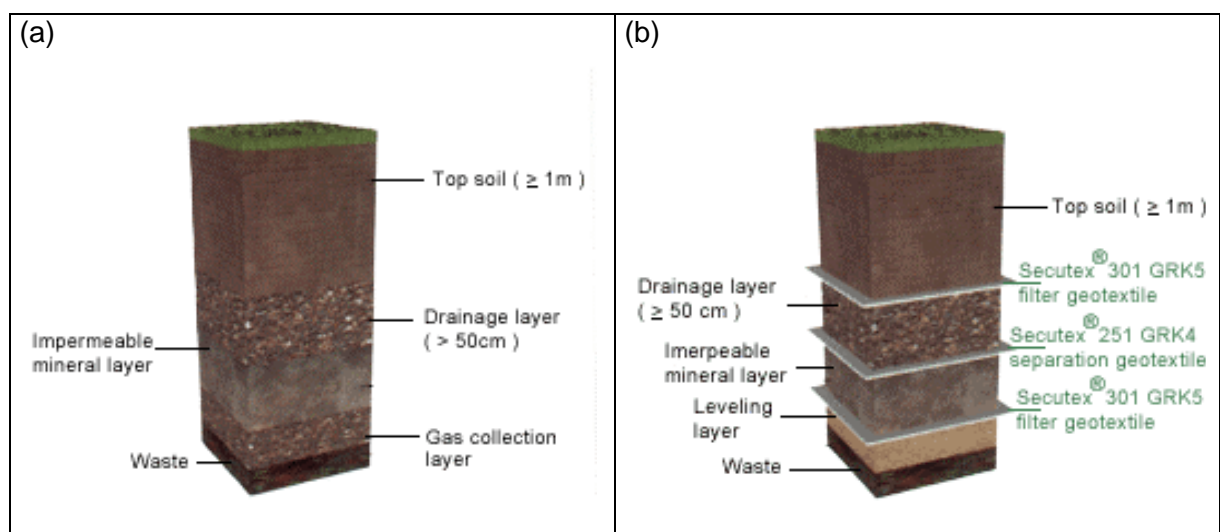

Figure VIII-2: Non-hazardous waste landfill cover sealing (a) EU normative (b) EU state of practice
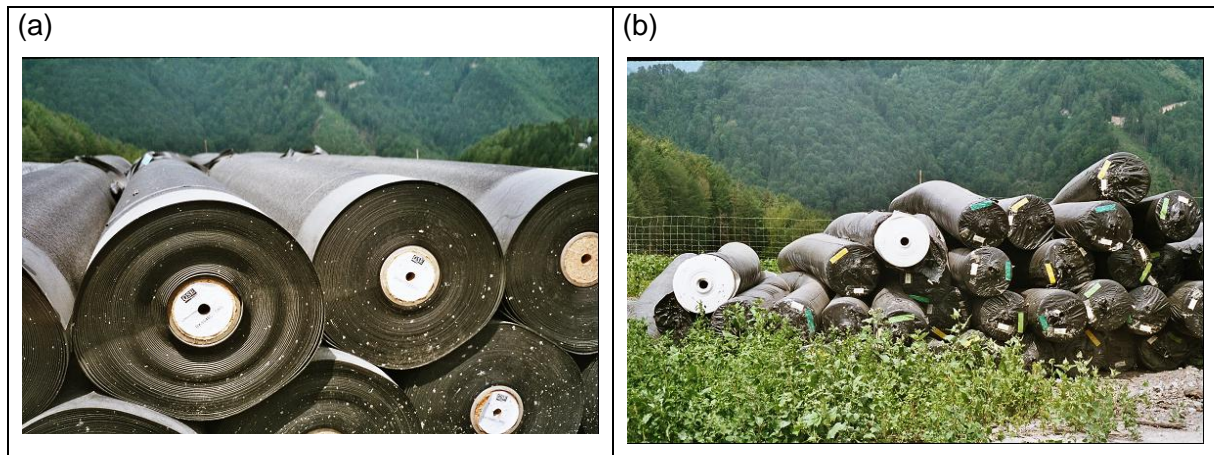
Figure VIII-3: (a) Geomembranes and (b) geotextiles used for landfill basal sealing

Figure VIII-4: Landfill leachate collection pipelines and pipeline configuration

Figure VIII-5: Biogas collection and energy recovery systems

Figure VIII-6: Landfill leachate reverse osmosis treatment plant

Annex IX: Volcanic soil sites in the Temuco surroundings

In the Temuco surroundings, four sites were explored, sampled and analyzed, with the final goal to assess possible volcanic soil sites availability in this region. As shown in Figure IX-1, sites in Gorbea (Fundo El Castillo), Quepe (Fundo Huilquilco), San Patricio, near Vilcún (Fundo Cuatro Volcanes) and Temuco (Estación Las Encinas) were selected for this field study.

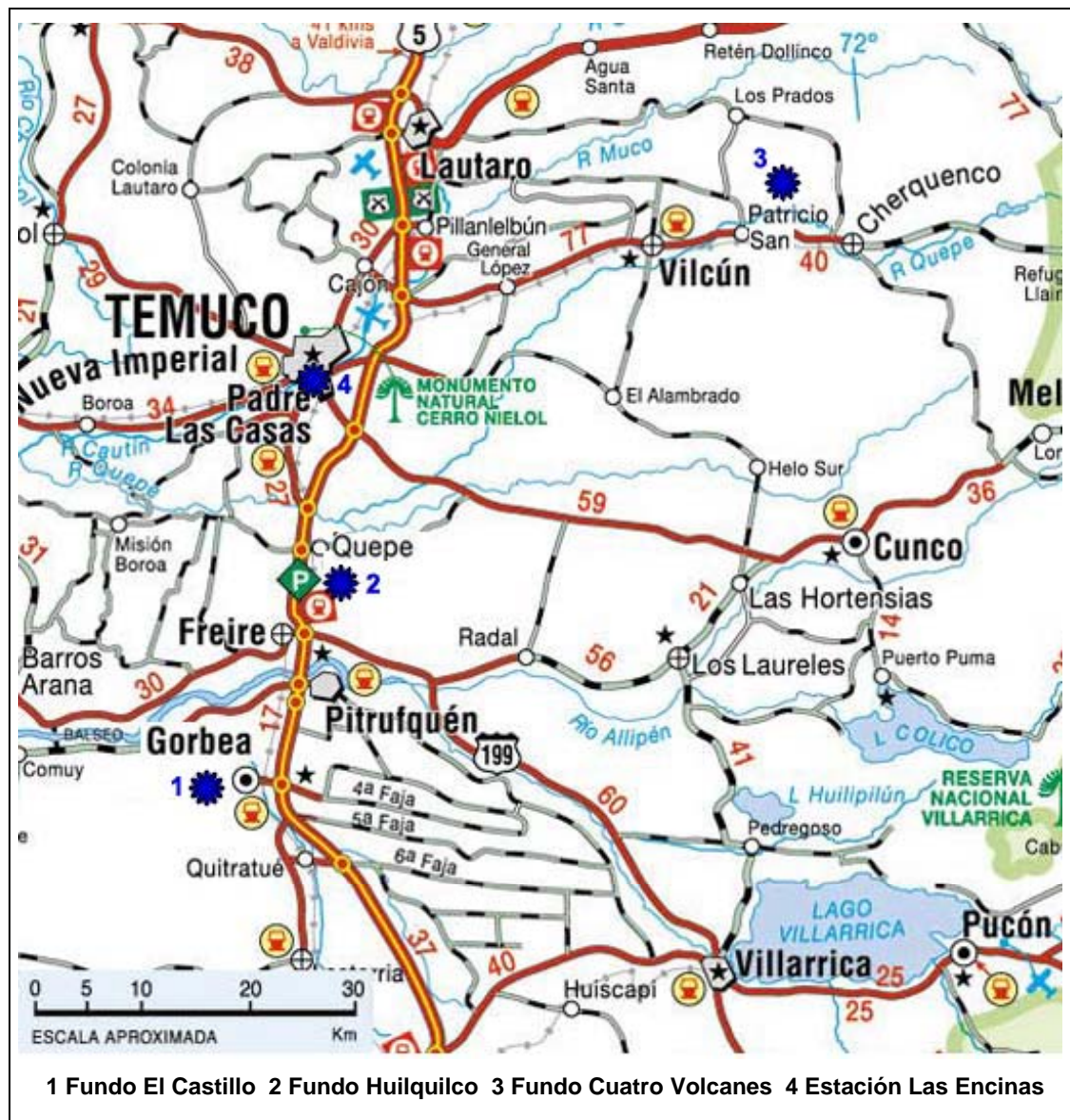**1 Fundo El Castillo 2 Fundo Huilquilco 3 Fundo Cuatro Volcanes 4 Estación Las Encinas**

Figure IX-1: Analyzed volcanic soil sites in the Temuco surroundings

Each site was explored and sampled with the help of Global Positioning System (GPS) equipment, which allowed exactitude of ± 10 m for each point. Sampling was done using a scanning method, dividing the test field in a grid as shown in Figures IX-2 to IX-5, with a 200 m distance between each sampling points. The total sampled area was about 100 ha per site (except for Las Encinas with only 3 ha). The samples were analyzed for particle size distribution, pH value and Roentgen diffractometry (XRD).
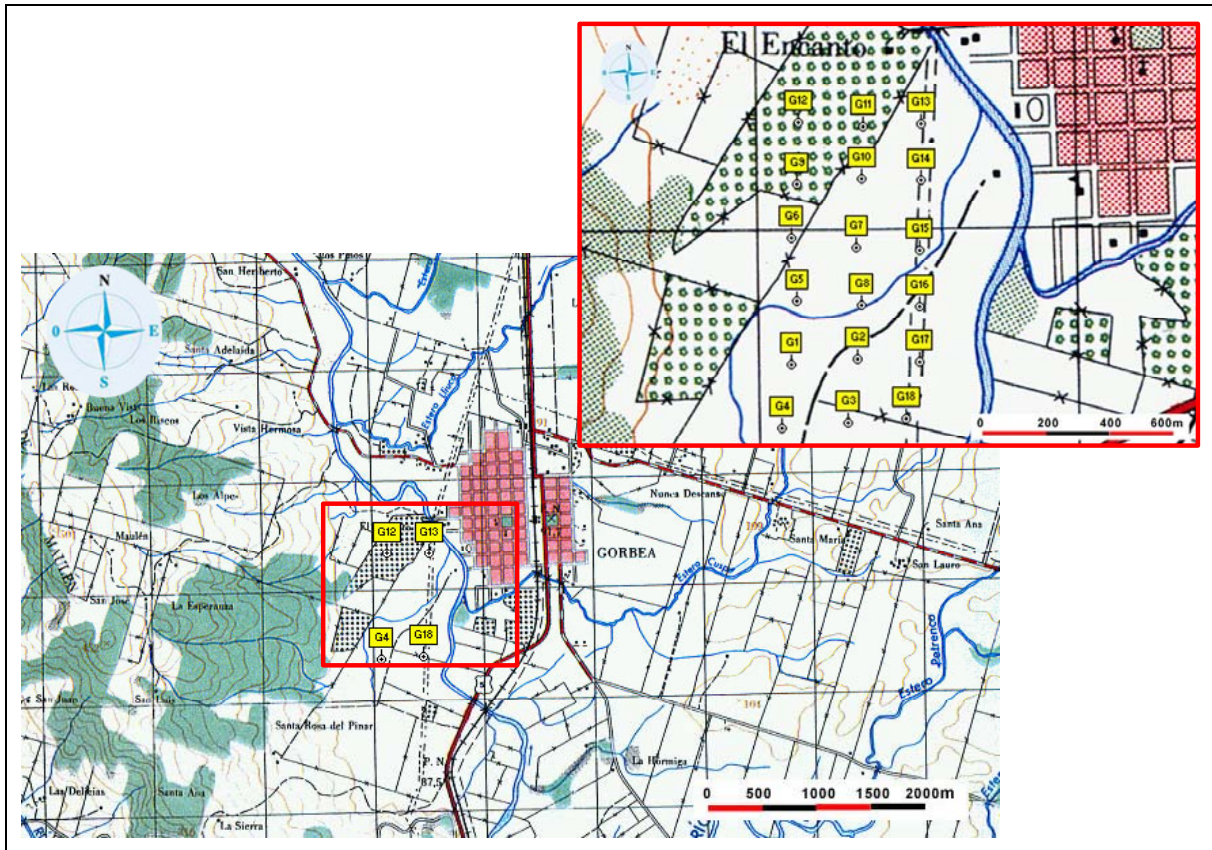
Figure IX-2: Gorbea overview and detail of the sampled area at Fundo El Castillo
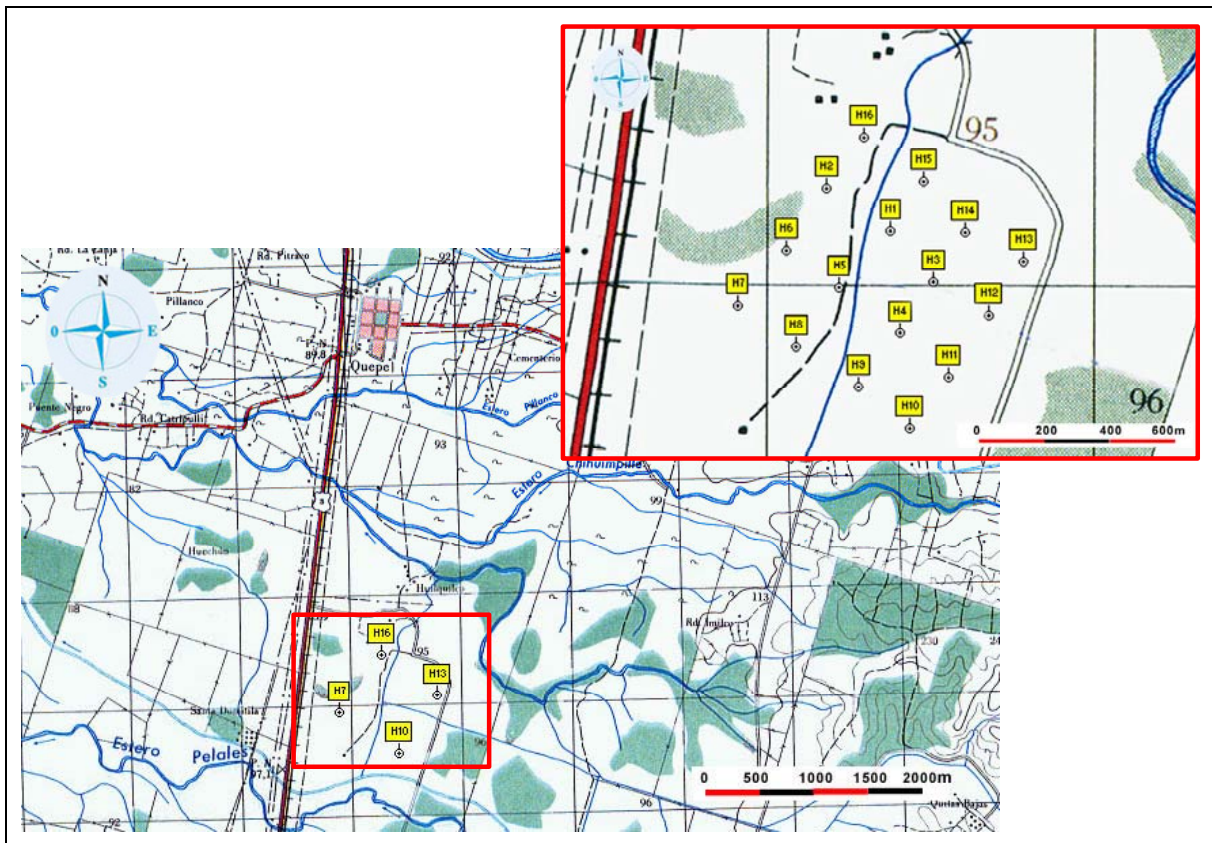

Figure IX-3: Quepe overview and detail of the sampled area at Fundo Huilquilco
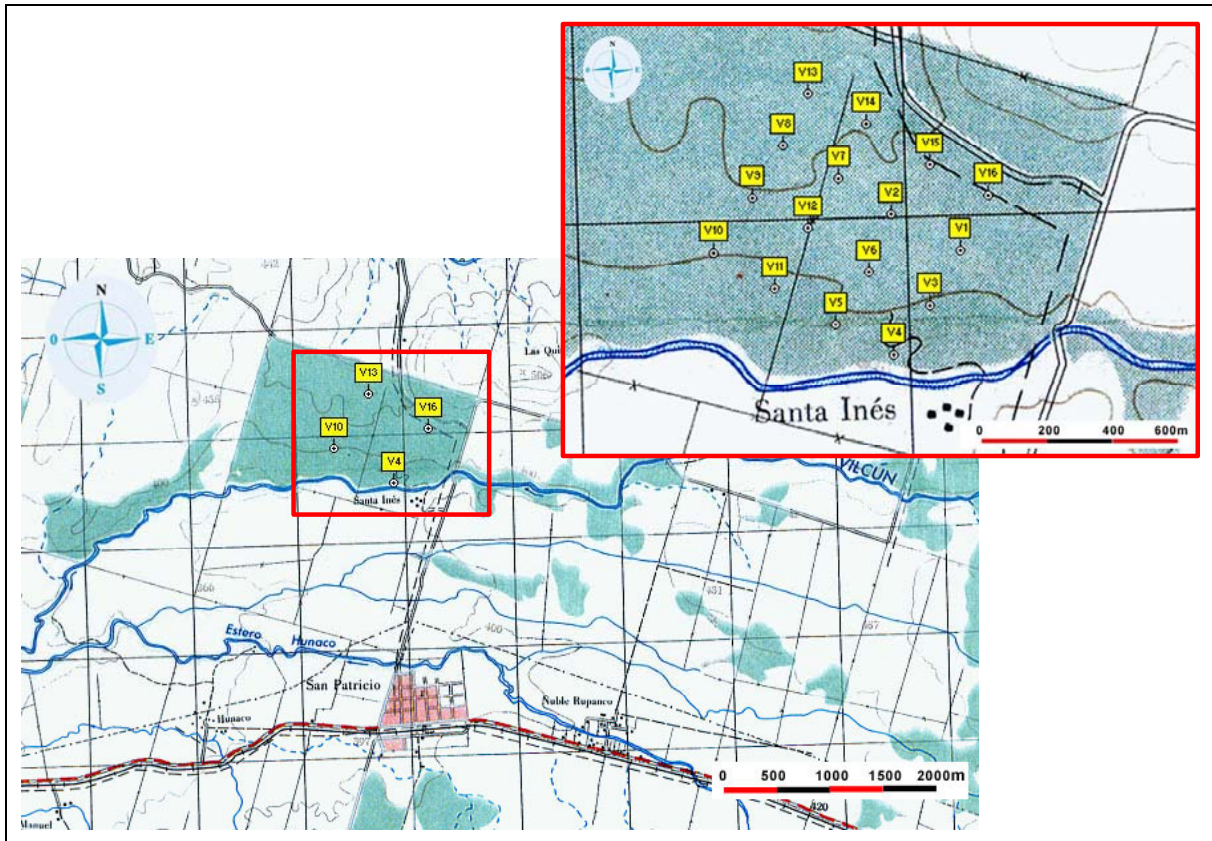
Figure IX-4: San Patricio overview and detail of the sampled area at Fundo Cuatro Volcanes
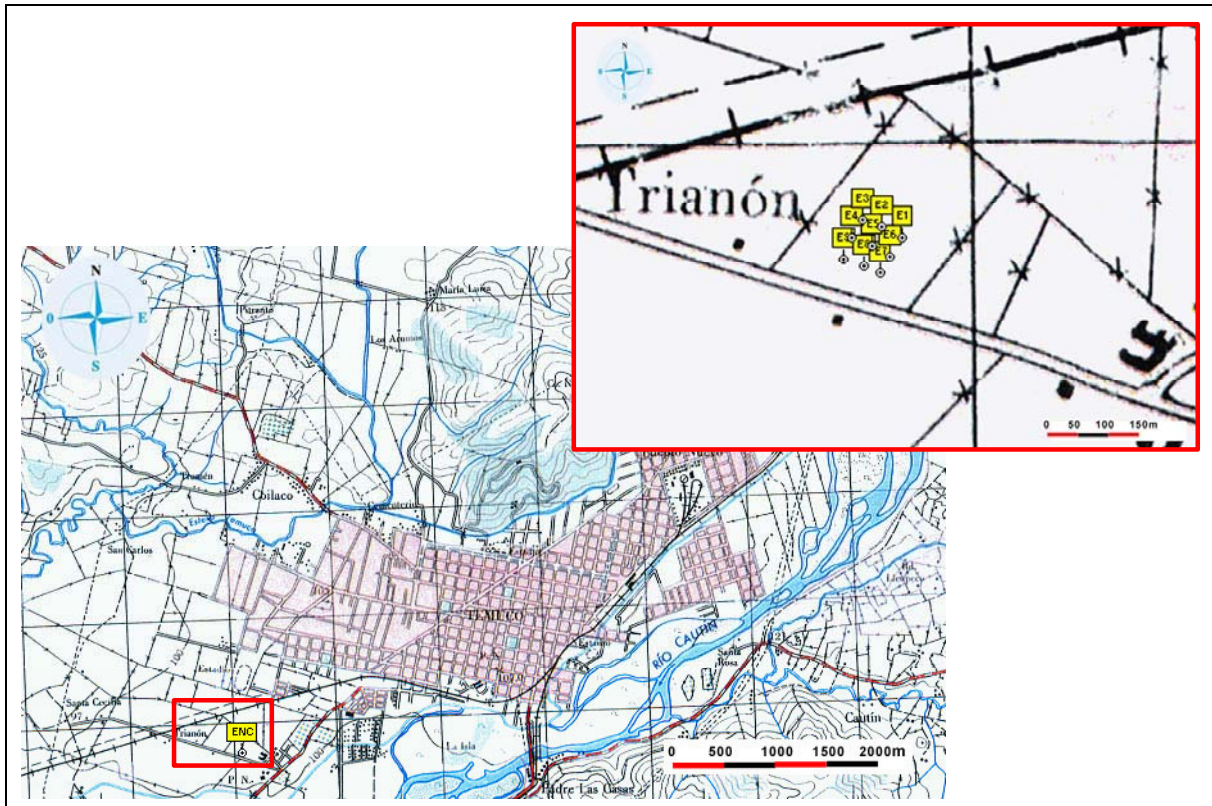
Figure IX-5: Temuco overview and detail of the sampled area at Estación Las Encinas

Figure IX-6: Particle size distribution of the volcanic soil sampled at Fundo El Castillo, Gorbea

Figure IX-7: Particle size distribution of the volcanic soil sampled at Fundo Huilquilco, Quepe

Figure IX-8: Particle size distribution of the volcanic soil sampled at Fundo Cuatro Volcanes, San Patricio

Figure IX-9: Particle size distribution of the volcanic soil sampled at Estación Las Encinas, Temuco

The particle size distribution of the four fields tested is presented in Figures IX-6 to IX-9. At Fundo El Castillo, Gorbea, 18 mixed samples (G1-G18) were taken from a soil profile between 5 and 80 cm, and three profile samples (G1 5-20 cm, G1 20-40 cm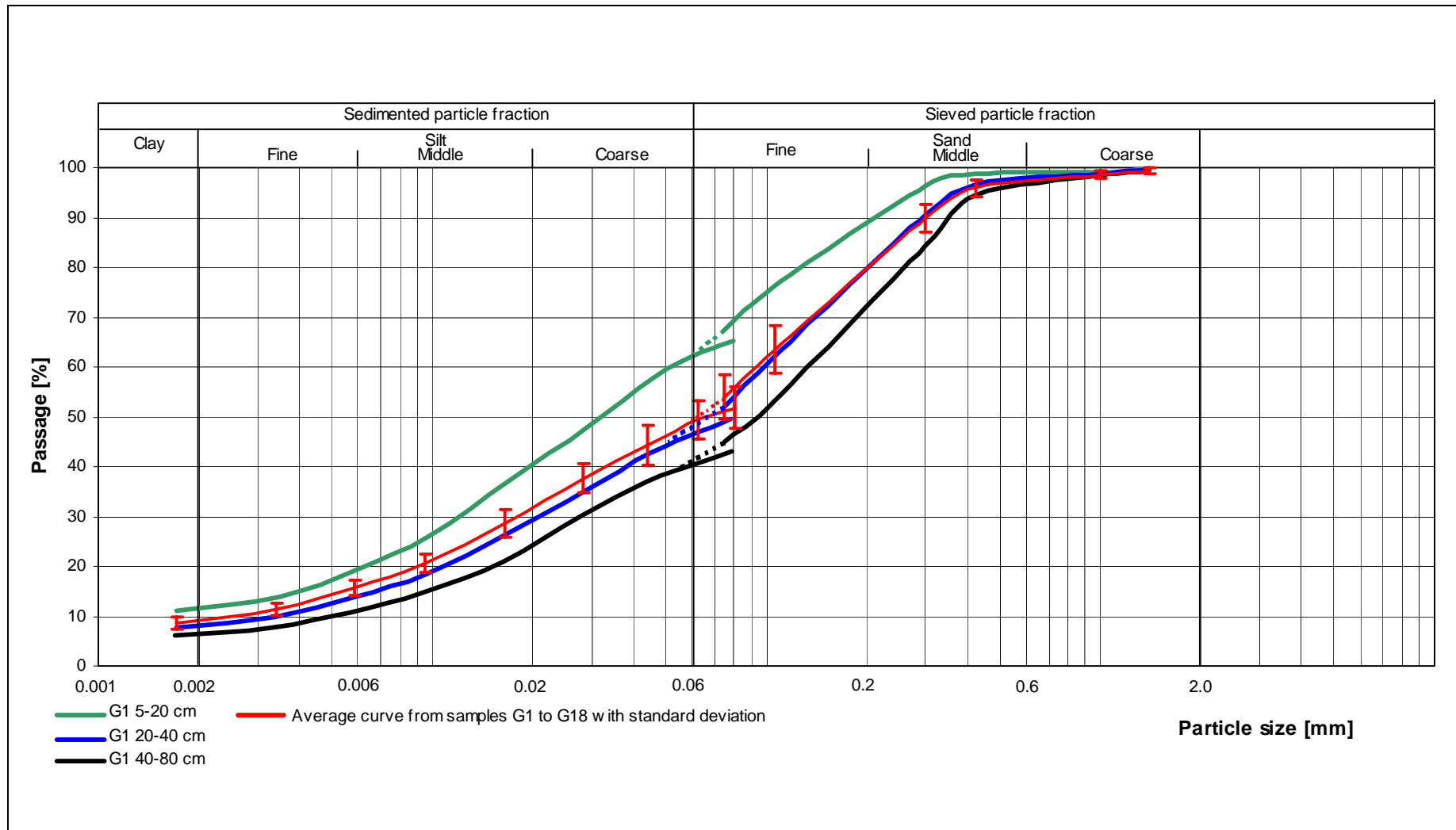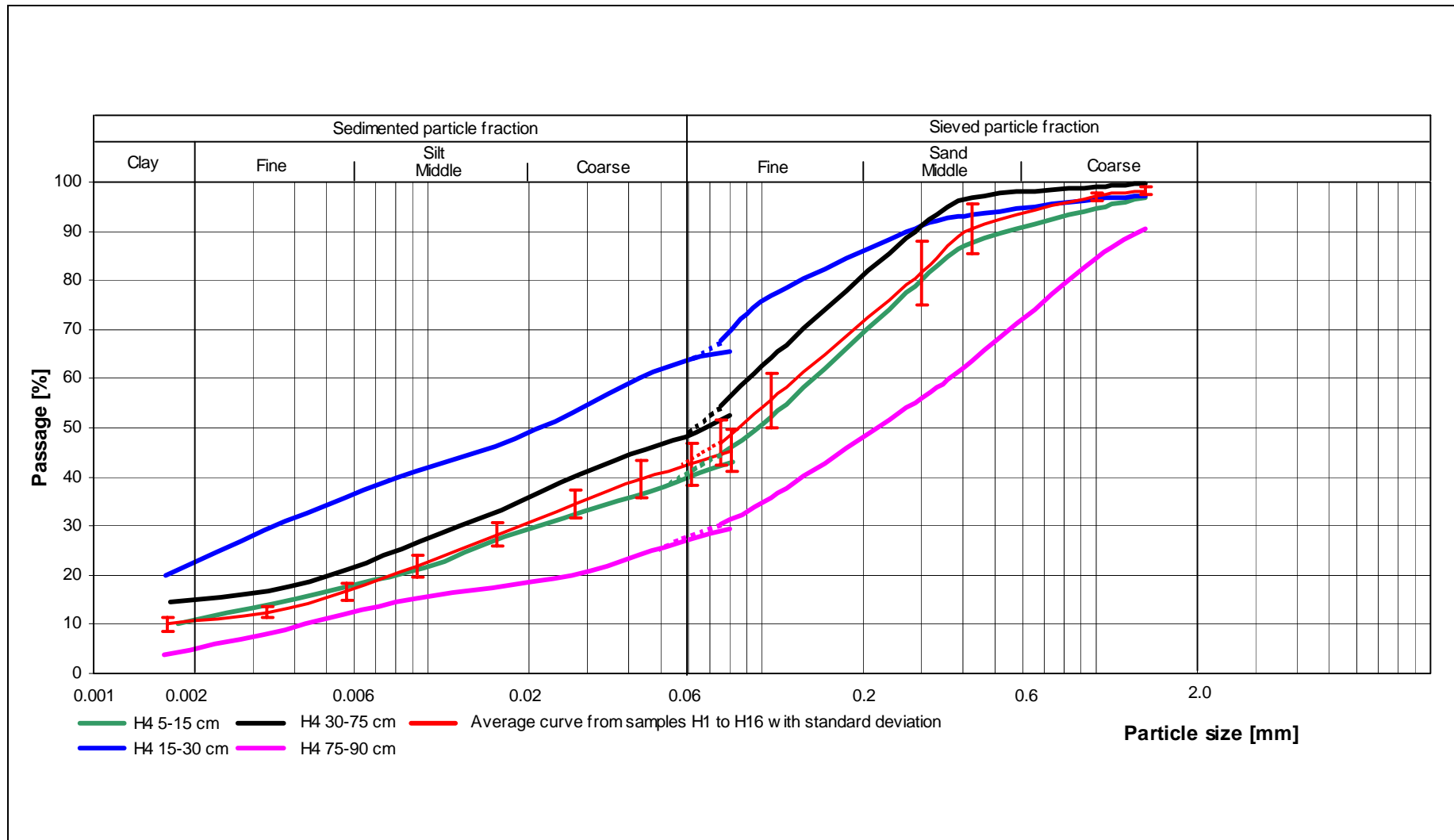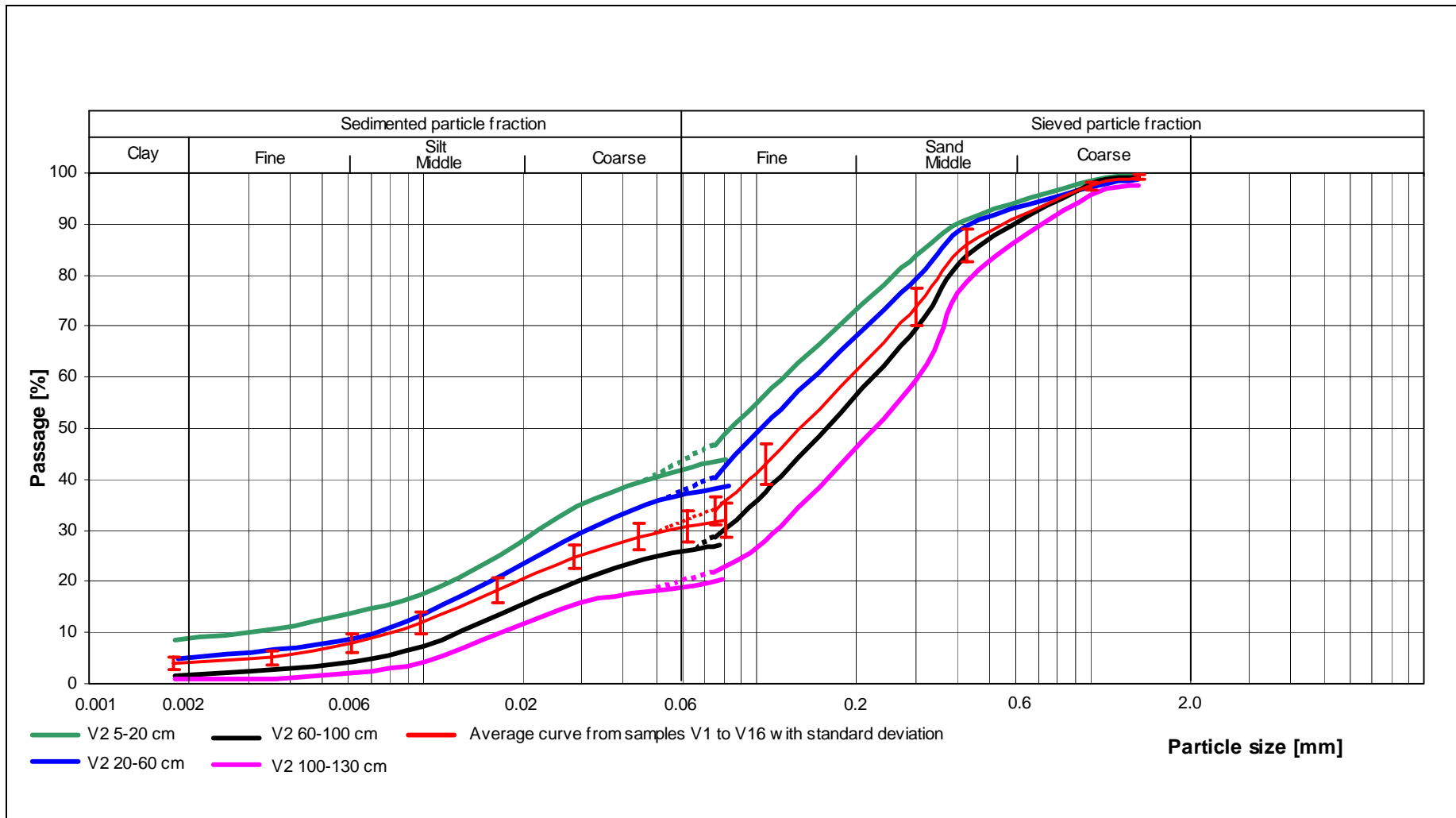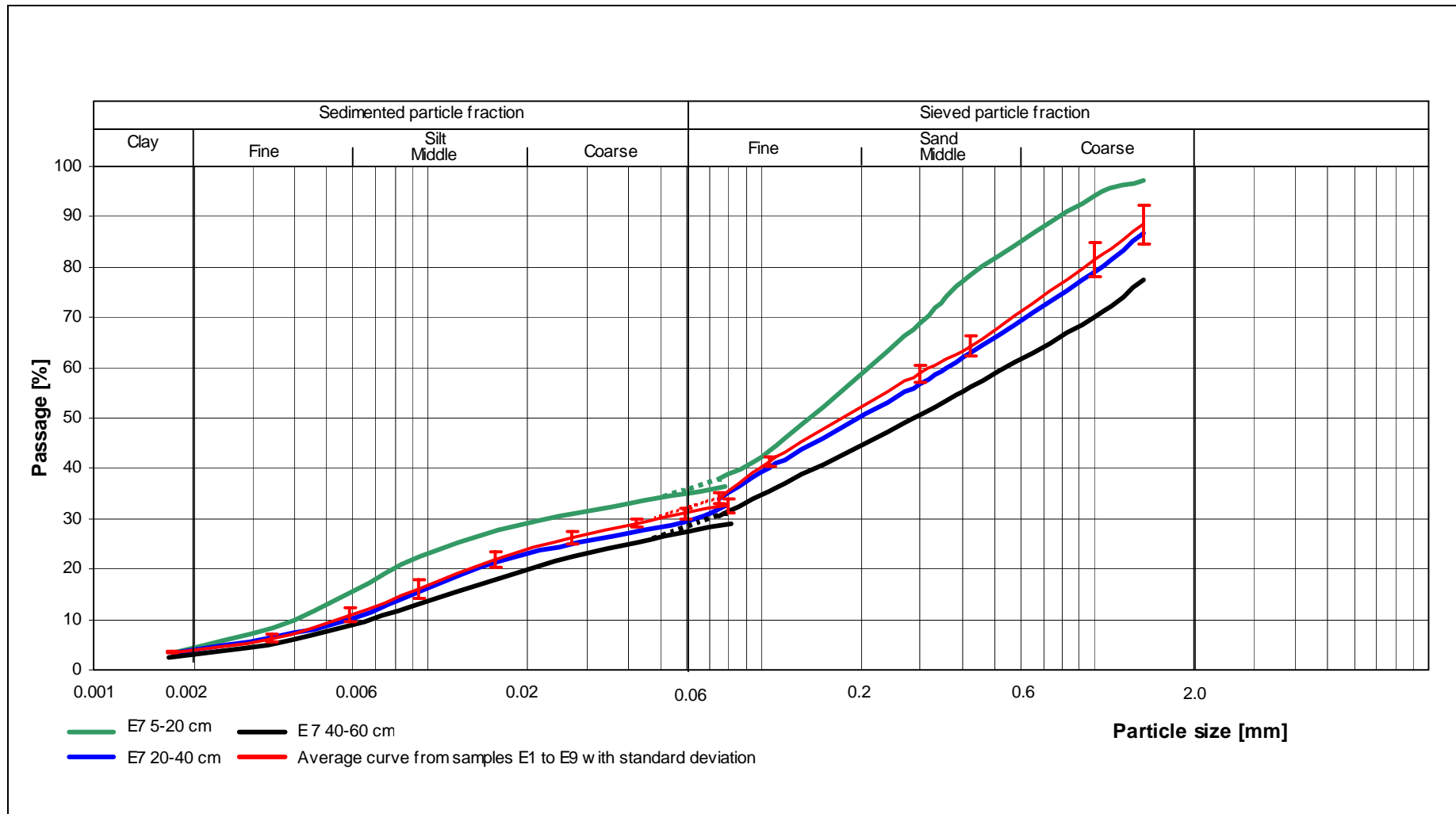 and G1 40-80 cm) were individually analyzed. At Fundo Huilquilco, Quepe, 16 mixed samples (H1-H16) were taken from a soil profile between 5 and 90 cm, and 4 profile samples (H4 5-15 cm, H4 15-30 cm, H4 30-75 cm and H4 75-90 cm) were individually analyzed. At Fundo Cuatro Volcanes, 16 mixed samples (V1-V16) were taken from a soil profile between 5 and 130 cm, and four profile samples (V2 5-20 cm, V2 20-60 cm, V2 60-100 cm and V2 100-130 cm) were individually analyzed. Finally, in Estación Las Encinas, 9 mixed samples (E1-E9) were taken from a soil profile between 5 and 60 cm, and 3 profile samples (E7 5-20 cm, E7 20-40 cm and E7 40-60 cm) were individually analyzed. In all the sites, the fine particle size fraction (< 2 µm) ranged between 1 and 23%, being Fundo Huilquilco the site with the largest fine particle size fraction.

The pH values (in distilled water) of all the samples analyzed in the four field tests were found to be acid (Table IX-1). Moreover, the soil profiles pH values increased with the soil depth. In fact, for G1, the pH value increased from 5.17 (5-20 cm profile) to 5.81 (40-80 cm profile), for H4 from 5.72 (5-15 cm profile) to 6.47 (75-90 cm profile), for V2 the pH value increased from 5.47 (5-20 cm profile) to 5.95 (100-130 cm profile) and for E7 from 5.58 (5-20 cm profile) to 6.15 (40-60 cm profile).

Table IX-1: pH values of all the samples analyzed in the four field tests

Sample	Volcanic soil site			
	El Castillo (G)	Huilquilco (H)	Cuatro Volcanes (V)	Las Encinas (E)
1	5.47	6.08	5.70	5.93
2	5.38	6.04	5.66	5.87
3	5.43	6.23	5.74	5.82
4	5.47	6.27	5.61	6.06
5	5.37	6.24	5.53	5.98
6	5.20	6.12	5.64	5.77
7	6.60	6.21	5.51	5.91
8	5.64	6.34	5.71	5.85
9	5.14	6.29	5.47	-
10	5.57	6.23	5.54	-
11	5.24	6.17	5.69	-
12	5.71	6.31	5.65	-
13	5.63	6.23	5.59	-
14	5.33	6.09	5.47	-
15	5.49	6.12	5.53	-
16	5.31	6.28	5.56	-
17	5.52	-	-	-
18	5.64	-	-	-
Average	**5.51**	**6.20**	**5.60**	**5.90**
S. D.	**0.32**	**0.09**	**0.09**	**0.09**

S. D. Standard deviation
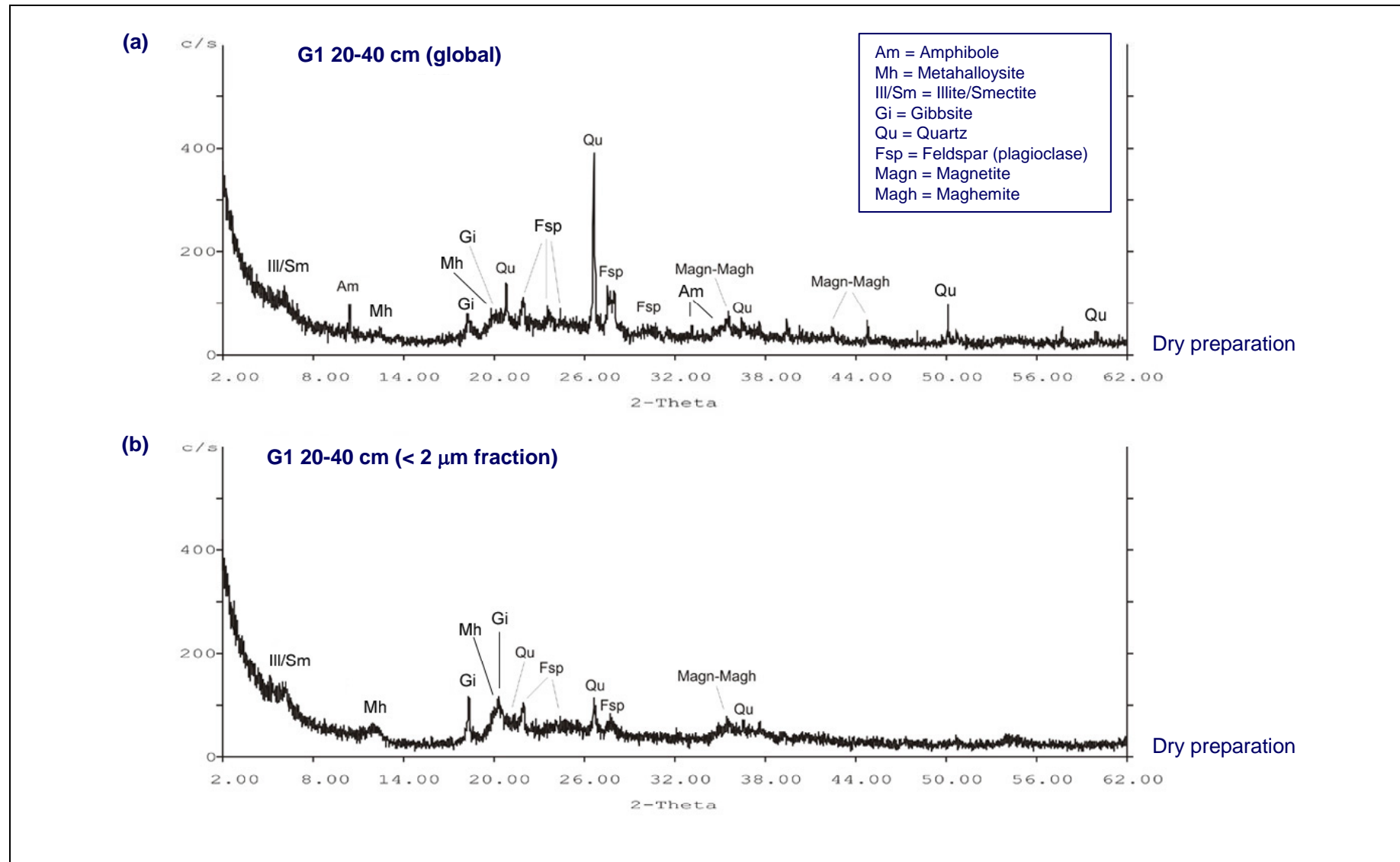
Figure IX-10: Roentgen diffractogram (XRD-spectrum) of the G1 20-40 cm (a) global and (b) < 2 µm sample, Fundo El Castillo, Gorbea
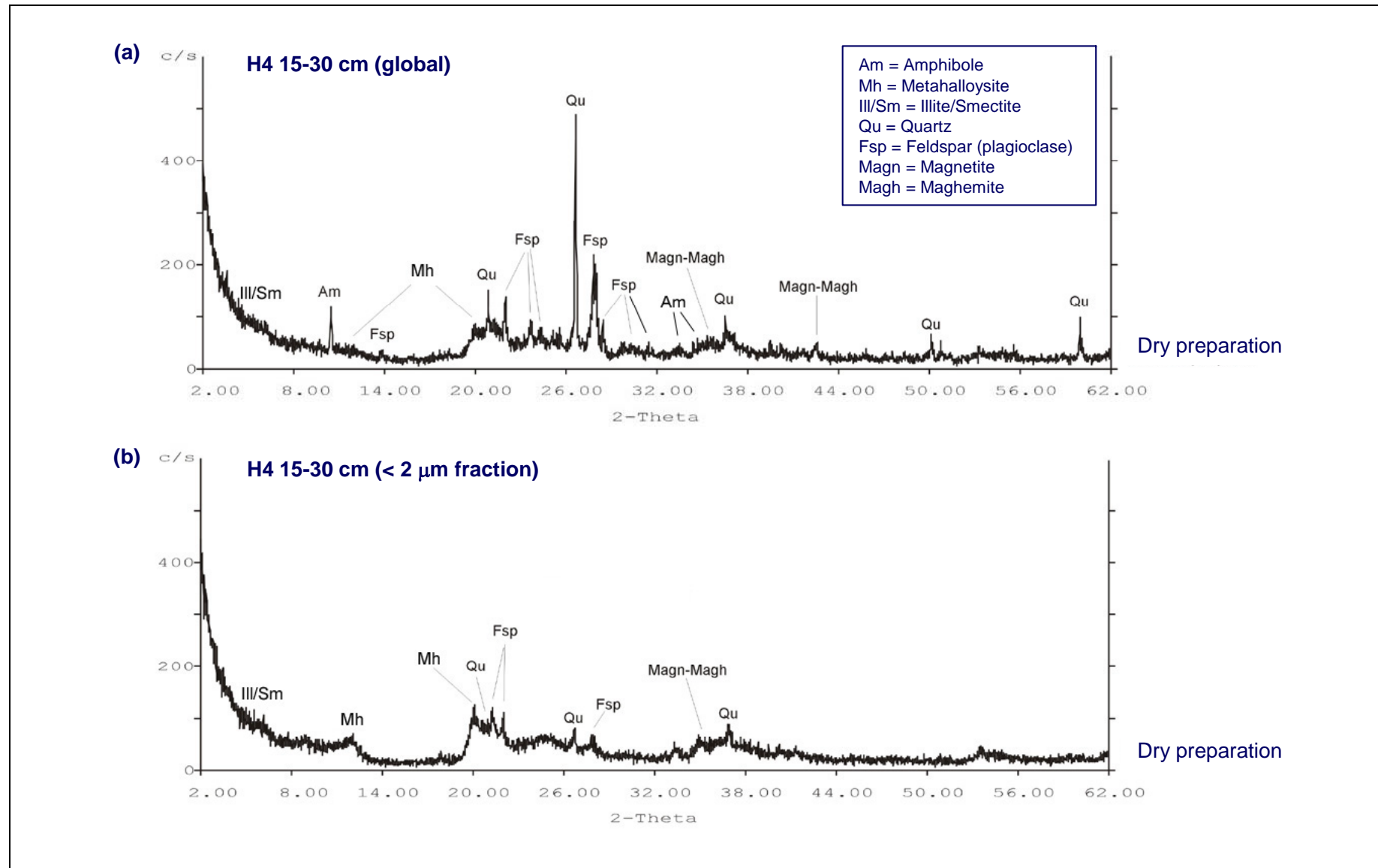
Figure IX-11: Roentgen diffractogram (XRD-spectrum) of the H4 15-30 cm (a) global and (b) < 2 µm sample, Fundo Huilquilco, Quepe
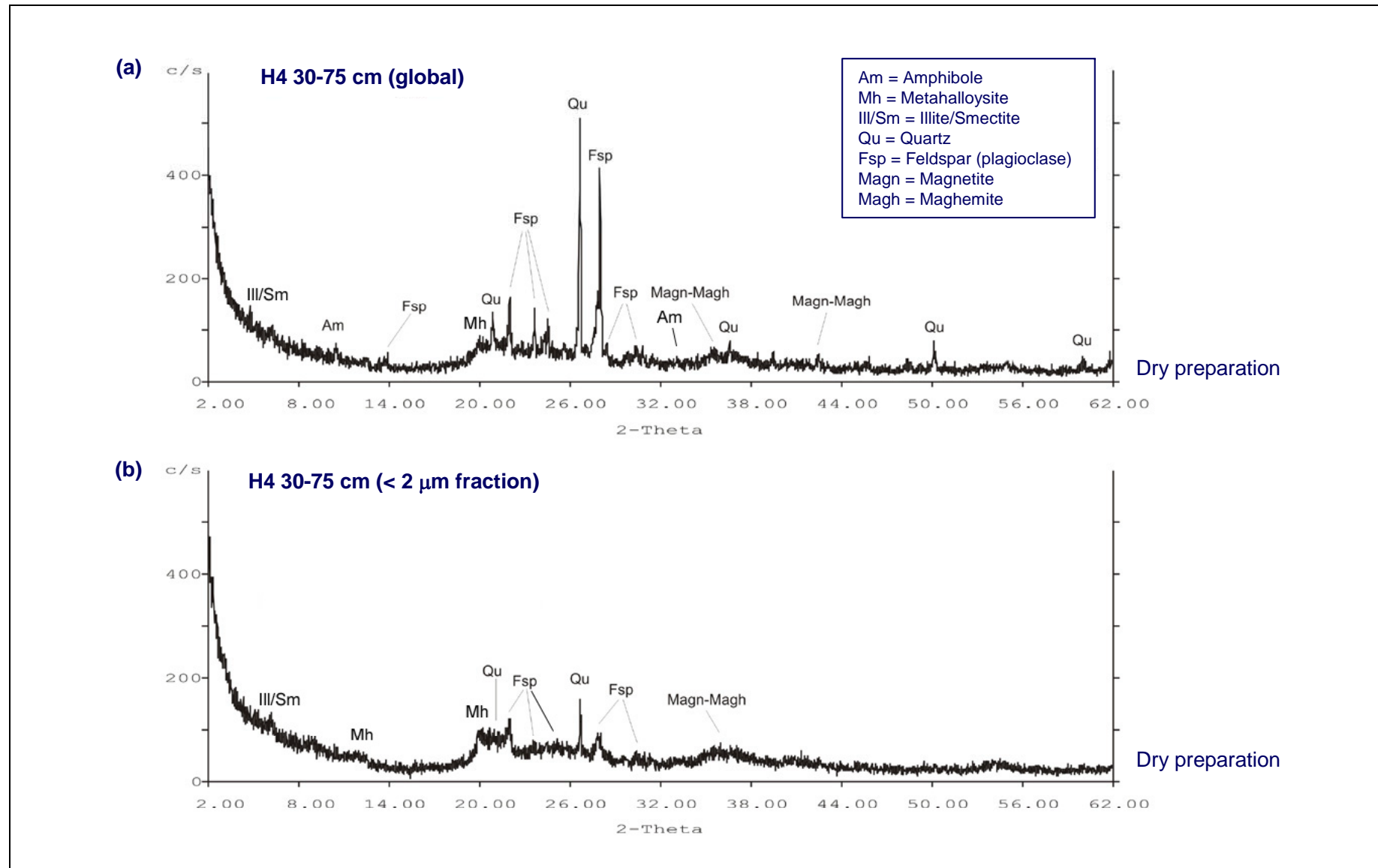
Figure IX-12: Roentgen diffractogram (XRD-spectrum) of the H4 30-75 cm (a) global and (b) < 2 µm sample, Fundo Huilquilco, Quepe
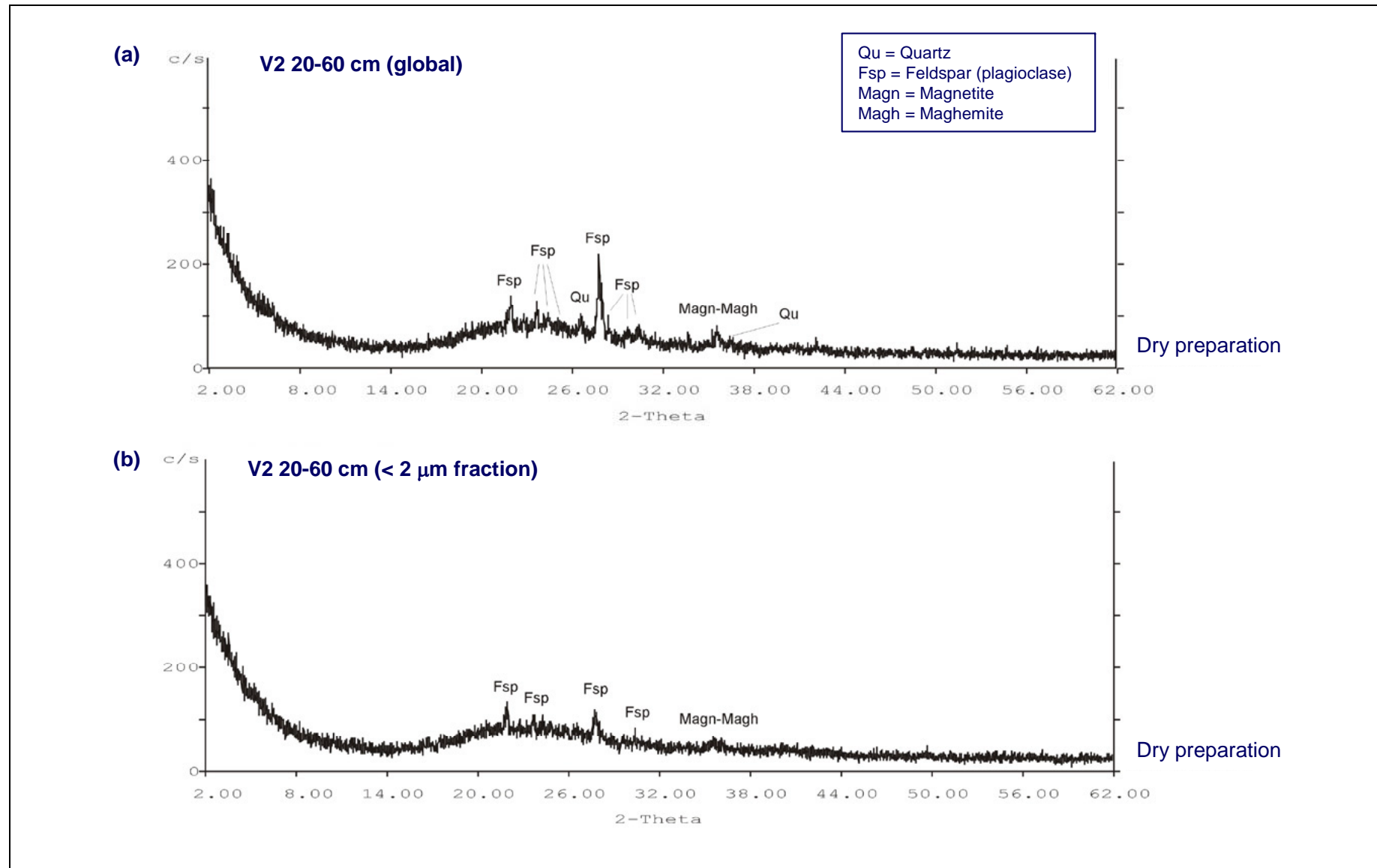
Figure IX-13: Roentgen diffractogram (XRD-spectrum) of the V2 20-60 cm (a) global and (b) < 2 µm sample, F. Cuatro Volcanes, San Patricio

Roentgen diffractograms (XRD-spectra) were also developed for selected samples of the tested fields (Figure IX-10 to IX-13). In fact, from Fundo El Castillo, Gorbea, sample G1 20-40 cm and its < 2 μm fraction were analyzed. From Fundo Huilquilco, Quepe, samples H4 15-30 cm and H4 30-75 cm with their respective < 2 μm fractions were analyzed, while from Fundo Cuatro Volcanes, San Patricio, sample V2 20-60 cm and its < 2 μm fraction were analyzed. As expected, the main minerals detected in the field tests were quartz, feldspars (plagioclase), magnetite and maghemite. In addition, amphibole, metahalloysite and illite/smectite were also detected in all samples. Moreover, particularly in the G1 20-40 cm sample, gibbsite was detected as well. All these minerals are known to be reactive and are partially responsible for the retention of environmental pollutants. The X-Ray diffractograms of the tested field samples are similar to those presented in Annex I for Estación Las Encinas.

Institut für nachhaltige
i a e
Abfallwirtschaft u. Entsorgungstechnik

Annex X: Summarized Chilean environmental normative

1) General Norms

They refer to the Political Constitution of the State, Organ Constitutional Laws, General Fundamentals in Environmental Issues, Navigation Law, Supreme Decreets, Law Decreets, Decreets with Law Force, Water Code, Sanitary Code and specific Resolutions.

- Political Constitution

The Political Constitution of the State in its Article 19, Nr. 8, guarantees all the persons to "*live in an environment free of contamination*" and that is "*an obligation of the State to watch for this right not to be affected and to preserve the natural surroundings*".

- Govern and Regional Administration Organ Constitutional Law Nr. 19.175

This law establishes that at a provincial level will exist a government that will be in charge of watching for the preservation and improvement of the environment.

- Municipalities Organ Constitutional Law 18.695

Establishes the role of the municipalities in the application of legal norms and techniques for preventing the environmental deterioration (Art. Nr. 20).

- Law Nr. 19.300 about General Fundamentals in Environmental Issues

This law, established in 1994, is aimed for establishing a sound relationship between economy, nature and the human population. It sets the base for a modern and realistic environmental management at a national level. In addition, the Environmental Impact Assessment System (SEIA) was introduced to implement the Law 19.300. The purpose of the SEIA, applied to projects and/or activities performed by the public and private sectors is to assure the environmental sustainability of said undertakings. The Law 19.300 provides that certain projects or activities capable to generate environmental impacts must be subjected to a SEIA. Their specific effects, characteristics or circumstances will determine if an Environmental Impact Statement or an Environmental Impact Study should be performed. The SEIA is to be conceptualized as a set of procedures designed to identify and evaluate positive and negative environmental impacts to be generated or presented by a given project or activity. The SEIA will assist in designing measures aimed for abating the negative impacts and enhancing any positive effects. An important part of these procedures depends on the involvement of State entities with environmental jurisdiction and/or in charge of issuing sectorial environmental permissions associated with the project or activity. The Law 19.300 has placed the burden of implementing and administrating the SEIA on the National Environmental Commission (CONAMA). Within this institutional framework, CONAMA and the Regional Environmental Commission (COREMAS) are in charge of coordinating the process whereby ratings are assigned to the Environmental Impact Study and Environmental

Impact Statements. The various different State bodies with environmental competences participate actively in this process.

- Navigation Law, Law Decreet Nr. 2.222

In Article 142, it is prohibited to throw residues or to spread oil and derivates, mineral tailing pond waters and other hazardous materials that produce damage to the water bodies under national jurisdiction, in ports, lakes and rivers.

- Supreme Decreet Nr.1 from the Ministry of Defense

This norm establishes the Rules for the Control of the Aquatic Contamination, derived from the Navigation Law.

- Resolution 12.600 from DIRECTEMAR

The resolution 12.600 of the General Administration of the Marine Territory and Merchant Navy (DIRECTEMAR) regulates the disposal of wastewaters into the juridical territory of this institution, namely seas and navigable continental water bodies.

- Water Code

Under the ruling principles of the water code a great quantity of specific legal instructions of different origin and character are in force. Their objectives vary from funding of water-connected activities to control of emissions and the delivery of environmental quality norms. The total of the norms related to contamination is formed by 61 dispersed juridical texts: international agreements, laws, decrees and resolutions. These texts are primarily aimed for prohibiting contamination of maritime and continental water.

- Drinking Water Law

The regulation of services for water destined for human consumption that was established in 1969; and lays down that water for human consumption may not contain elements, chemical substances, toxic or dangerous substances and pathogen organisms that possibly have not been eliminated by a common treatment in higher concentrations than the ones laid down. These waters also must be free of microscopic organisms and substances that can cause problems in the normal operation and efficiency of treatment processes. Furthermore, obligations for the drinking water providing enterprises are established in this law.

- Chilean Norm for Potable Water

The Chilean Potable Water Norm defines the physical, chemical, radioactive and bacteriological requirements with that waters destined for human consumption have to comply. This norm is applicable to potable water from every source. The tables in this norm define the maximum acceptable limit for each type of contaminant (substance or element, chemical or radio-active matter) that the water may contain. In the case of bacteriological

contaminations the norm requires that drinking water have to be totally free of microorganisms of faecal origin. Furthermore the norm establishes that the drinking water that is distributed by drinking water networks, has to be treated with a disinfection process that has a permanent effect. Chlorine, chlorinated compounds and iodine are authorized by the responsible Health Service. At the same time, the norm lays down that the minimum residual concentration of free chlorine has to be equal to or higher than 0,2 mg/L in every point of the net. No maximum concentration for free chlorine is set.

- Law 3.133 about Neutralization of Liquid Industrial Wastes

This is the first legislative text of Chile that was aimed for the protection and conservation of the waters against the contamination by industries. It came into force in 1916. Since its creation in 1989 it is the responsibility of the SISS (Sanitary Service Office) to implement it. This law establishes the obligation of all industries to neutralize and purify their liquid industrial wastes that are disposed in aqueducts, watercourses, and catchment areas of rivers, lakes or ponds. It lays down that factories and metallurgical complexes that dispose their wastewaters in sewage systems have to submit these waters to a special neutralizing treatment so that the piping of the sewage systems is not damaged. The sanitary company that owns the sewage system where the wastewater is disposed has to control the compliance with the law. The SISS has to authorize the type of treatment and to supervise its correct function.

- Supreme Decreet Nr. 351 from the Ministry of Public Building (MOP)

Establishes the prohibition of the discharge of industrial liquid wastewaters and other hazardous substances to the irrigation or the consume in any pipeline, artificial or natural drain and sewage system.

- Supreme Decreet Nr. 609/2000 from the Ministry of Public Building (MOP)

Is the emission norm for the regulation of contaminants associated with the disposal of liquid industrial wastewaters in the sewage system. It was elaborated and set into force in 1995 by the National Environmental Commission (CONAMA) in the implementation process of the Law 19.300 together with further emission norms and norms for environmental quality. This emission norm regulates the maximum quantity of contaminants that industries may feed into the public sewage systems. Its objective is to protect the sewage systems and networks of the enterprises that have to collect and dispose of their wastewaters, as well as protecting wastewater treatment plants and reducing eventual risks for the population.

- Supreme Decreet Nr. 90/2000 from the Ministry of the General Secretary of the Presidency

On the 3rd of September 2001, the emission norm for the regulation of contaminants associated with the disposal of liquid industrial wastewaters into marine and superficial continental waters came into force. The aim of this norm is to prevent the contamination of

these water bodies. It is applicable to all emitting entities – industrial as well as sanitary – that dispose their wastewaters into superficial water bodies (rivers, lakes, seas). For plants already existing when the norm came into force, the deadline for its implementation is established on the 3rd of September 2006.

- Supreme Decreet Nr. 46/2002

It is the emission norm for the regulation of contaminants to groundwater courses and bodies. It was elaborated by CONAMA and came into force in March 2002. Its objective is the prevention of contamination of groundwater bodies by the control of deposition of liquid industrial wastes that percolate into the water carrying layers. It determines the maximum allowed concentrations of the mentioned contaminants in the emitted liquid industrial waste that is emitted via the ground to the water carrying layers by operations that are aimed for the infiltration of these wastewaters. This norm does not touch infiltration due to irrigation.

- Chilean Water Quality Norm 1.333, Decreet Nr. 867

The Ministry of Public Building (MOP) elaborated this quality norm. It establishes the quality requirements for water for different types of applications, e.g. drinking water for human consumption, drinking water for animal consumption, irrigation, recreation, and aquatic life.

- Sanitary Code

Establishes in a general form that the Health Services are responsible for the approvement of projects related with any construction for the evacuation, treatment or disposal of wastewaters and industrial and mining solid wastes.

- Resolution Nr. 5.081 from the SESMA

The Metropolitan Environmental Health Service (SESMA) established a system for the declaration of industrial solid wastes managed in the Metropolitan Region of Santiago.

- Supreme Decreet Nr. 86 from the Ministry of Mining

Establishes the Rules for the Construction and Operation of Tailing Ponds

- Supreme Decreet Nr. 144 from the Ministry of Health

Establishes in its Article 10, that any "*gases, vapors, dust, emanations or contaminants of every nature*", produced by any industrial facility have to be collected and eliminated. In its Article 60 prohibits the incineration of wastes in the urban area of the cities.

- Decreet with Law Force Nr. 34

Establishes the environmental legislation of the fishing industry and its derivates.

- Supreme Decreet Nr. 474 from the Ministry of Foreign Relationships

International agreement for the prevention of seawater contamination by hydrocarbons.

- Supreme Decreet Nr. 476 from the Ministry of Foreign Relationships

International agreement for the prevention of seawater contamination by residues and other wastes.

2) Municipal Wastes

Correspond to Laws, Supreme Decreets and Resolutions that in general establish that the municipalities are the responsible organisms for the cleanliness of the cities.

- Law Decreet Nr. 3.557

In Article 9, it is established that any owner of an urban or rural ground is obligated to destroy, treat or process any wastes or waste mixtures dangerous to the agriculture.

- Resolution Nr. 2.444 from the Ministry of Health

Establishes the minimal sanitary norms regarding grounds, operation and abandonment of non-controlled landfills.

- Resolution Nr. 07077/76 from the Ministry of Health

Prohibits the incineration of municipal and industrial solid wastes in several communities of the Metropolitan Region and also prohibits the accidental or deliberated incineration in non-controlled landfills. In addition, obligates the industries that generate wastes to adopt the necessary measurements for the treatment (excluding incineration) and/or disposal.

3) Hazardous wastes

- Supreme Decreet Nr.1 from the Ministry of Defense (see General Norms)

- Law Decreet Nr. 3.557 (see Municipal Wastes)

- Sanitary Code (see General Norms)

- Supreme Decreet Nr. 685 from the Ministry of Foreign Relationships

Establishes the "Basel Agreement about the Control of Movements of Hazardous Wastes and their Elimination".

- Resolution Nr. 3.276/77 from the Ministry of Health

Establishes the norm for the transportation of organic residues from the food industry and that can be used in animals growing farms. It also specifies the kind of vehicles and storage to be used for the transportation.

- Decreet Nr. 298 from the Ministry of Transport and Telecommunications

It rules the transportation of hazardous cargos through the streets and gives some guidelines for the transference and transport operations

4) Draft project: Emission law for the incineration and co-incineration of wastes

Table X-1: Limit emission values for co-incineration

Contaminant	Maximum value (mg/Nm^3)
Total suspended particles (TSP)	100
Hg and its compounds (as Hg)	0.1
Cd and its compounds (as Cd)	0.1
Tl[1]	0.2
Pb + Zn and its compounds (as total metal)	1
As + Co+ Ni + Se + Te and its compounds (each element and as a total sum)	1
Sb + Cr + CN + F + Mn + Pd + Pt + SiO$_2$ + Rh + Sn + V CN and F only if are easily water soluble SiO$_2$ only in fine powders	5
Gaseous inorganic chlorinated compounds (as HCl)	30
Gaseous inorganic fluorinated compounds (as HF)	5
Benzo(a)pyrene (C$_{20}$H$_{12}$)	0.1
Benzene (C$_6$H$_{12}$)	5

[1]: Only in clinker kilns, CN and F

Table X-2: Operational conditions in incineration and co-incineration facilities[1]

Operational condition	Incineration	Co-incineration
Minimum gas temperature in the combustion zone	850°C (1100°C when wastes with more than 1 mass-% chlorine are combusted)	850°C (1100°C when wastes with more than 1 mass-% chlorine are combusted)
CO emission at the chimney output	50 mg/Nm^3	-
Temperature at the control equipment input after the gases cooling process	< 200°C	< 200°C

[1]: The dioxins and furans maximum permitted emission levels will be considered as exceeded when the operational conditions of Table X-2 are not accomplished and when the gases cooling time between 400 and 200°C is not minimized

Annex XI: Selected publications (journals & congresses)

<u>Journals</u>

Navia, R., Schmidt, K. H., Behrendt, G., Lorber, K. E., Rubilar, O. & Diez, M. C. (2004) Improving the adsorption capacity and solid structure of natural volcanic soil by a foaming-sintering process based on recycled PET. *Journal of Cleaner Production* (submitted).

Navia, R., Fuentes, B., Lorber K. E., Mora, M. L. & Diez, M. C. (2004) In-series columns adsorption performance of Kraft mill wastewater pollutants onto volcanic soil. *Chemosphere* (submitted)

Navia, R., Inostroza, X., Diez, M. C. & Lorber, K. E. (2004) Adsorption of bleached Kraft mill wastewater pollutants onto volcanic soil: fixed bed kinetic model. *Journal of Environmental Management* (submitted)

Diez, M. C., Quiroz, A., Ureta-Zañartu, S., Vidal, G., Mora, M. L., Gallardo, F. & Navia, R. (2004) Soil retention capacity of phenols from biologically pre-treated Kraft mill wastewater. *Water Air and Soil Pollution* (submitted)

Bezama, A., Navia, R., Novak, J. & Lorber, K. E. (2004) Novel approaches for the management and redevelopment of contaminated sites. *Osterreichischer Wasser- und Abfallwirtschafts Verein (ÖWAV)* (in press)

Pavlov, P., Bezama, A. & Navia, R. (2004) Improvement of clay impermeability by using cement as an additive. *Berg- und Hüttenmännische Monatshefte* 149(6), 223-224.

Navia, R., Levet, L., Mora, M. L., Vidal, G. & Diez, M. C. (2003) Allophanic soil adsorption system as a bleached Kraft mill effluent post-treatment. *Water Air and Soil Pollution* 148, 321-331.

Pavlov, P., Navia, R., Draganov, L. & Lorber, K. E. (2002) Chemische Stabilität von Erdölabfall und mögliche Anwendung als Dichtungsschichtskomponente von Deponien. *Berg- und Hüttenmännische Monatshefte*, 147(11), 370-372.

Vidal, G., Navia, R., Levet, L., Mora, M. L. & Diez, M. C. (2001) Kraft mill anaerobic effluent color enhancement by a fixed-bed adsorption system. *Biotechnology Letters* 23, 861-865.

Congress proceedings

Navia, R., Lorber, K. E., Schmidt, K. H. & Behrendt, G. (2004) Development of a porous ceramic material from natural volcanic soil and recycled PET. Depotech 2004, Nov. 24-26, Leoben, Austria.

Navia, R., Bezama, A., Lorber, K. E., Valenzuela, R. & Reyes, C. (2004) Contaminated soil as an alternative raw material in Chilean cement production facilities. Depotech 2004, Nov. 24-26, Leoben, Austria.

Navia, R., Fuentes, B., Bezama, A., Lorber, K. E. & Diez, M. C. (2004) The use of volcanic soil as a sanitary landfill liner and its capacity to retain some specific heavy metals. *ISWA World Environment Congress and Exhibition*, Oct. 17-21, Rome, Italy.

Navia, R., Lorber, K. E., Gallardo, F., Mora, M. L. & Diez, M. C. (2004) The capacity of volcanic soil to adsorb and bioremediate some specific chlorophenols present in contaminated water. *4th IWA World Water Congress and Exhibition*, Sep. 19-24, Marrakech, Morocco.

Navia, R., Inostroza, X. & Diez, M. (2003) Modelación matemática de la adsorción de contaminantes de efluentes de celulosa en suelo de origen volcánico. *XV Congreso de Ingeniería Sanitaria y Ambiental AIDIS-Chile*, Oct. 1-3, Concepción, Chile.

Navia, R., Diez, M. C. & Lorber, K. E. (2002) Remediation of sites contaminated with chlorophenols. In: *Altlastensanierung, Sanierung von Bergbaualtlasten, Thermische Verwertung von Abfällen, Managementsysteme, Ökobilanzierung und Prozessoptimierung*, Lorber et al. (Hrsg.), Verlag Glückauf, Essen, Deutschland, 353-358.

Navia, R., Fuentes, B., Mora, M. L. & Diez, M. C. (2001) Capacidad de retención de clorofenoles en suelo de origen volcánico. *XXIV Jornadas Chilenas de Química*, Nov. 28-30, Temuco, Chile.

Diez, M. C., Navia, R., Mora, M. L. & Gallardo, F. (2001) Efecto de la adición de efluente de celulosa Kraft sobre la actividad biológica de suelo volcánico. *XV Congreso Latinoamericano y V Cubano de la Ciencia del Suelo*, Nov. 11-16, Varadero, Cuba.

Diez, M. C., Navia, R., Levet, L., Mora, M. L. & Vidal, G. (2001) Fixed bed adsorption system to color and phenolic compounds removal from Kraft mill aerobic effluent. *6th World Congress of Chemical Engineering*, Sep. 23-27, Melbourne, Australia.

Navia, R., Levet, L., Vidal, G., Mora, M. L. & Diez, M. C. (2000) Adsorción de compuestos fenólicos y color de efluentes de celulosa Kraft en columnas rellenas con suelo alofánico. *XIV Congreso Chileno de Ingeniería Química*, Oct. 23-26, Santiago, Chile.